SANDIA REPORT
SAND87—0327 • UC—92a
Unlimited Release
Printed April 1987

Multiwell Experiment Final Report: I. The Marine Interval of the Mesaverde Formation

Multiwell Experiment Project Groups,
at Sandia National Laboratories and CER Corporation

Prepared by
Sandia National Laboratories
Albuquerque, New Mexico 87185 and Livermore, California 94550
for the United States Department of Energy
under Contract DE-AC04-76DP00789

SF2900Q(8-81)

Issued by Sandia National Laboratories, operated for the United States Department of Energy by Sandia Corporation.

Printed in the United States of America
Available from
National Technical Information Service
U.S. Department of Commerce
5285 Port Royal Road
Springfield, VA 22161

NTIS price codes
Printed copy: A12
Microfiche copy: A01

SAND87-0327
Unlimited Release
Category 92a

MULTIWELL EXPERIMENT FINAL REPORT:

I. THE MARINE INTERVAL OF THE MESAVERDE FORMATION

Compiled by the
Multiwell Experiment Project Groups
at
Sandia National Laboratories
Albuquerque, New Mexico 87185
and
CER Corporation
Las Vegas, Nevada 89109

April, 1987

ABSTRACT

The Department of Energy's Multiwell Experiment is a field laboratory in the Piceance Basin of Colorado which has two overall objectives: to characterize the low permeability gas reservoirs in the Mesaverde Formation and to develop technology for their production. Different depositional environments have created distinctly different reservoirs in the Mesaverde, and MWX has addressed each of these in turn. This report presents a comprehensive summary of results from the lowermost interval: the marine interval which lies between 7450 and 8250 ft at the MWX site. Separate sections of this report are background and summary; site description and operations; geology; log analysis; core analysis; in situ stress; well testing, analysis and reservoir evaluation; and a bibliography. Additional detailed data, results, and data file references are given on microfiche in several appendices.

CONTENTS

CONTENTS (Cont'd)

CONTENTS (Cont'd)

CONTENTS (Cont'd)

CONTENTS (Cont'd)

TABLES AND FIGURES APPEAR AT THE END OF EACH CHAPTER

1.0 BACKGROUND AND SUMMARY

David A. Northrop
Sandia National Laboratories

1.1 INTRODUCTION

New and improved technology is required to enhance natural gas production from the low permeability reservoirs of the United States. This is a large potential resource with an estimated maximum recoverable resource of over 600 TCF.[1] The U.S. Government's efforts to stimulate production from these reservoirs began in the mid-1960's. The early work evaluated the use of nuclear explosives for fracturing, but this technique was abandoned in 1973. Efforts then focused upon massive hydraulic fracturing and several government-industry projects were conducted. The results were disappointing and did not result in either an improved technology or confident, commercial production. The basic shortcoming was that these past field tests provided insufficient data to define the critical factors affecting gas production from this resource.

The Department of Energy's Multiwell Experiment (MWX) was conceived as a field laboratory to obtain sufficient information on the geologic and technical aspects to unlock this resource. A key feature of MWX is three wells between 110 and 215 ft apart. Detailed core, log and well test data from such close spacings provide a detailed characterization of the reservoir. Interference and tracer tests as well as the use of fracture diagnostics in offset wells, give additional, out-of-the-ordinary information on stimulation and production. A second key is the synergism resulting from a broad spectrum of activities: geophysical surveys, sedimentological studies, core and log analyses, well testing, in situ stress determinations, stimulation, fracture diagnostics, and reservoir analyses. All these activities are further enhanced by the closely spaced wells. Thus, the Multiwell Experiment provides a unique opportunity for understanding and developing economic production from tight gas reservoirs.

Further discussion of the rationale, plans, objectives and activities of MWX can be found in references 2-5. The intent of this report is to compile results from activities associated with one interval--the marine--at the MWX site. Similar final reports will be compiled for subsequent intervals.

1.2 GEOLOGIC SETTING

The Multiwell Experiment's focus is the Mesaverde Formation in the Piceance Basin of Northwest Colorado. This thick sequence was deposited during the late Cretaceous age over a broad region of the western United States and contemporaneous formations are found in the Green River, Wind River, Uinta, and San Juan basins. The great extent and thickness of these gas-containing deposits is the reason that this is a significant natural gas resource.

At the MWX site, the Mesaverde Formation lies at a depth of 4000 to 8250 ft, between the overlying Wasatch Formation and the underlying Mancos Shale (Figure 1.1). The Mesaverde is exposed in outcrop at Rifle Gap in the Grand Hogback, approximately 11 miles northeast of the MWX site, and the outcrops have allowed excellent insight into the subsurface geology at the site. The sandstones stand out clearly on outcrop and sedimentological studies have been performed on them. These studies show that the Mesaverde can be divided into five distinct intervals based upon different depositional environments and resulting sandstone morphologies.[6-7]

(1) The lowest interval (7450-8250 ft) was formed immediately on either side of an oscillating coastline and is composed of widespread shoreline-to-marine blanket sandstones, marine shales, and paralic coals. This interval contains the Corcoran, Cozzette and Rollins sandstones and it is the focus of this final report.

(2) The paludal interval (6600-7450 ft) lies above the Rollins sandstone and contains thick, abundant coal deposits. These are interspersed with lenticular, distributary channel and splay sandstones formed in a lower delta plain environment. The sand percentage in this zone is markedly lower (26%) than other intervals (~ 40%), and channel widths are probably 250-500 ft.

(3) The coastal interval (6000-6600 ft) is characterized by distributary channel sandstones deposited in an upper delta plain environment. Most of these sandstones are probably less than 200 ft in width and are interbedded with carbonaceous mudstones and siltstones.

(4) The fluvial interval (4400-6000 ft) consists of irregularly shaped, multistory, composite sandstones which were deposited by broad meandering stream systems. These sandstones have widths on the order of 1000-2500 ft and contain abundant internal discontinuities.

(5) The uppermost paralic interval (400-4400 ft) is a zone of returned marine influence with more widespread, uniform sandstones. The interval is water-saturated at the MWX site.

Specific sands in the shoreline/marine, paludal, coastal and fluvial intervals have been the focus of separate MWX investigations.

1.3 MWX DESCRIPTION

The Multiwell Experiment field laboratory is located in the Rulison Field in the southeastern portion of the Piceance Basin in Colorado. The site is located in the SW 1/4, NW 1/4, Sec. 34, T6S, R94W, Garfield County and it is seven miles southwest of Rifle and just south of the Colorado River. Agreements on the lease and landowners were obtained in mid-1981 and work at the site began in August of that year. A chronology of MWX activities is given in Figure 1.2.

Three wells were drilled: MWX-1 to a depth of 8350 ft in September-December 1981,[8] MWX-2 to a depth of 8300 ft in January-March 1982,[9] and MWX-3 to a depth of 7565 ft in June-August 1983.[10] Over 4100 ft of 4-in core, approximately 1135 ft of it oriented, were cut with a recovery of >99%. Numerous logging programs containing both standard and experimental logs were conducted. An overview of the coring and logging activities in all three wells in relation to the Mesaverde section at the site is given in Figure 1.3. The three wells are exceptionally straight as seen in Figure 1.4; relative separations are between 110 and 215 ft within the Mesaverde. Significant gas shows were encountered throughout the section in all three wells and mud weights as high as 15 lbs/gal were required to control the well.

The entire Mesaverde at the MWX site as seen by gamma ray logs in the three wells is shown in Figure 1.5.

1.4 THE MARINE INTERVAL

The initial MWX investigations were performed in the marine interval which lies between 7450 and 8250 ft and is shown in Figure 1.6. Note that only MWX-1 and MWX-2 penetrate this entire interval and were the only wells available in mid-1982 to mid-1983 for the well tests conducted in the Corcoran, lower Cozzette and upper Cozzette and for stress tests performed over the interval.

DOE decided in early 1983 that the Multiwell Experiment's most appropriate focus was the lenticular, nonmarine sandstones that comprise the majority (~85%) of the Mesaverde at the MWX site and elsewhere in the Piceance and other basins. One factor in this decision was the high, sustained production without stimulation from the upper Cozzette zone in MWX-1 which indicated a large, naturally fractured (jointed) reservoir. Other factors were the blanket, marine nature of these sandstones and that there is limited commercial production from them in parts of the basin. Thus, no stimulations were conducted in this interval.

MWX-3 was drilled specifically to provide better characterization of the nonmarine, lenticular portion of the Mesaverde. Thus, it was drilled only into the top of the Rollins sandstone, although a short open hole section was cored into the Rollins for specific in situ stress investigations.

1.5 ACTIVITY SUMMARIES

The results of the MWX activities conducted in the marine interval of the Mesaverde are presented in separate sections of this report, each authored by the principal investigator. Summaries from these sections are presented here.

1.5.1 GEOLOGY (Section 3.0)

The sandstones in the marine interval were deposited in environments which oscillated between shallow marine, shoreline, and lower delta plain. The main sandstones are shallow marine to wave-dominated shoreline deposits, the interbedded shales are predominately deep marine shales, and the associated carbonaceous mudstones, coals, and lenticular sandstones are nonmarine, lower delta plain deposits.

- The Corcoran sandstone has two parts. The lower is a shallow marine to shoreline sandstone of 30 ft thickness; the upper is a distributary channel sandstone with different thicknesses (30 and 15 ft) in each well. Carbonaceous, nonmarine lithologies separate the two sands.

- The Cozzette sandstone has two parts. Both are shallow marine to shoreline deposits which are thick (70 and 50 ft) and very continuous and uniform between the two wells. The top of the lower sandstone contains a shale break and a thin (8 in) coal seam, and has less marine character than the rest of the Cozzette.

- The Rollins sandstone is characteristic of a prograding, wave-dominated shoreline. It is 70 ft thick and very uniform between the wells.

- The deep-marine Mancos shale underlies this entire interval. Well-developed, uniform tongues of the Mancos shale abruptly overlie the upper Corcoran and upper Cozzette sandstone and distinctly separate the Corcoran, Cozzette and Rollins.

Sandstone petrology (grain size, composition, and diagenetic history) is the primary control on reservoir porosity and matrix permeability. Most of the sandstones are well-sorted and show little variation between the few cored intervals. The diagenetic sequence in the three sandstones has been interpreted to include at least two cycles of calcite cementation, dissolution of feldspar, authegenic clay formation, and recementation by calcite and/or quartz. Dissolution of feldspar and rock fragments leads to authegenic illite and illite-smectite which reduce the primary porosity and permeability. The absorbent clays may also contribute to the relatively high water saturations in these sandstones.

Natural gas in the marine section could have come from organic material in either deep marine or terrestrial sources. The levels of maturation are high: coal rank below 7800 ft is semi-anthracite and vitrinite reflectance levels range from 1.35 to over 2.15. Thus, the organic material produced hydrocarbons. Isotopic gas analyses indicate that most of the gas in this interval originated in marine rocks, although there are indications of nonmarine contributions as well. The top 20 ft of the upper Cozzette contains pyrobitumin (pyrolyzed oil) in the pores, which effectively reduces porosity and permeability.

Only five natural extension fractures were observed in Corcoran and Cozzette core. These are thin (hairline to 4 mm), vertical, and filled or partially filled with calcite and quartz. The importance of natural fractures is evident in the well test results for this interval.

1.5.2 LOG ANALYSIS (Section 4.0)

Extensive logging programs were conducted during the drilling of the MWX wells. However, the marine interval in MWX-1 and MWX-2 was logged only during the final open-hole logging program as the interval was at the bottom of each well. A variety of standard and experimental logs were run in the oil-based-mud-filled wells.

The well logs were analyzed with the tight gas sand log interpretation model called TITEGAS.[11] Computer-generated, two- and three-dimensional crossplots show relationships between the various reservoir parameters and shed light upon the various tool responses. The analysis of the marine interval used data from the dual induction/gamma ray log, the lithodensity/compensated neutron/gamma ray/caliper, the long-spaced sonic log, the cement bond log, and core measurements of porosity, permeability, grain-density and water saturation.

The model calculates various estimates of reservoir properties. The porosity, saturation and clay volume (Vcl), of both the flushed zone and virgin formation, are computed based primarily on the dual induction and lithodensity/compensated neutron logs. The model also computes volume carbonate from the photoelectric effect in the lithodensity log. The model then obtains the average flushed-zone saturation, S_{xo}, from corrected neutron porosity and gamma ray responses in order to derive porosity. R_w is computed in uninvaded sandstones by combining S_{xo}, porosity, and resistivity data. Finally the virgin formation water saturation, Sw, is calculated by the total shale relationship. Comparison of the flushed zone and virgin water saturations, ΔSw, indicates the amount of invasion and identifies permeable zones. Also a quantitative estimate of in situ permeability, kh, is made based on porosity, clay content and water saturation. A summary of the log analyses for the four Corcoran and Cozzette intervals is given in Figure 1.7. The plotted logs have been calculated by TITEGAS and give an estimate of the density and neutron response in an uninvaded, virgin formation. These results provide an overall reservoir evaluation for the four sandstone units. The two

Cozzette sandstones are good candidates for testing and stimulation. They are thick, uniform, and have reasonable reservoir properties. The two Corcoran sandstones are less viable candidates. The upper sandstone is very nonuniform and is the least attractive reservoir.

1.5.3 CORE ANALYSIS (Section 5.0)

Limited core was taken from the marine interval: 221 ft of 4-in core in MWX-1 and MWX-2 and 28 ft of 2 1/2-in core in MWX-3. Core samples were distributed to participants in a comprehensive core analysis program.[12] Both routine and special core analyses for reservoir properties were made at frequent intervals in the sandstones. Many analyses also extended above and below the sandstone so that properties are also available for the bounding lithologies.

A summary of the core-derived reservoir properties for the marine interval is given in Figure 1.8. (This compilation includes a diverse number of samples; many more samples were taken in the sandstones themselves.) Typical reservoir properties of the best reservoir, the upper Cozzette sandstone, show dry Klinkenberg permeabilities of 4-7 μd (at 1000 psi confining pressures), porosities of 6-8%, and water saturations of 25-50%. The permeabilities of these sandstones are a strong function of the net stress and water saturation. The dry Klinkenberg permeabilities of 4-7 μd should be reduced by at least an order of magnitude to obtain a more realistic estimate of the in situ matrix permeability. In addition, capillary pressures greater than 500 psi were found at the prevailing water saturations.

Other core analyses included vertical permeabilities, compressibility, caprock analysis, triaxial tests for compressive strength, modules, and Poisson's ratio, fracture toughness, and tensile strength. Core samples were also used in other MWX activities such as sedimentology, mineralogy/petrology, organic content and maturation, natural fractures, and estimates of in situ stresses.

1.5.4 IN SITU STRESS MEASUREMENTS AND ANALYSIS (Section 6.0)

Several different stress-related measurements were made in the marine interval. Cased-hole stress tests were conducted in MWX-2 at eleven depths in, between, and below the Rollins and Cozzette sandstones. These tests were repeated small volume hydraulic fractures (<100 gal) conducted through perforations under conditions where the instantaneous shut-in pressure is equal to the minimum in situ stress.[13] The measured minimum in situ stresses and frac gradients are summarized in Figure 1.9. Significantly different stresses were characteristic of the sandstones (0.85-0.90 psi/ft) and the confining shales (1.00-1.11 psi/ft). Different test behaviors were noted for the different lithologies where shales had low breakdown pressures and relatively constant injection pressures, and sandstones exhibited generally larger breakdown pressures and larger reopening pressures. One test, in a siltstone between the Cozzette sands, exhibited a repeatable dual shut-in which may be indicative of a thin silt or sandstone surrounded by higher stress shales. The measured stress distribution around the Cozzette sandstone is ideal for hydraulic fracture containment during stimulation; there are upper and lower stress contrasts of 2000 and 1300 psi, respectively. Fracture height calculations show excellent containment of a frac at treatment pressures less than 1000 psi over the minimum in situ stress.

Open hole stress tests were conducted in MWX-3 at two locations in the Rollins sandstone. As seen in Figure 1.9, there is good agreement with the cased hole tests in MWX-2. An estimate of the maximum horizontal in situ stress can be obtained from the breakdown and/or reopening pressures in open hole tests. The minimum and maximum horizontal in situ stresses in the Rollins were found to be 6800 and 7600 psi, respectively. An impression packer was run in the upper interval and gave indications of a hydraulic fracture orientation of N50-70°W.

Two stress-related analyses were made on oriented core: anelastic strain recovery (ASR)[14] and differential strain curve analysis (DSCA).[15] The primary ASR result is the direction of the maximum horizontal in situ stress, which is the azimuth of a hydraulic fracture. The measured azimuths for four sandstone core samples in each of the Rollins, Cozzette and Corcoran are given in Figure 1.10; three shale tests were unsuccessful. (A hydraulic fracture was subsequently conducted at 7100 ft. The frac azimuth was determined by the borehole seismic method to be N67±8°W.[16]) Stress magnitudes were also calculated from ASR data via a procedure that requires several basic assumptions[17]; only fair agreement with the hydraulic fracture data was obtained. Two Cozzette sandstone samples were analyzed via DSCA; these gave a frac azimuth estimate of N76°W and a minimum stress, assuming a 1.05 psi/ft overburden stress, of 6400 and 6930 psi.

1.5.5 WELL TESTING, ANALYSIS AND RESERVOIR EVALUATION (Section 7.0)

Several well tests of various kinds were conducted in the Corcoran and Cozzette sandstones. The overall results from these tests and analyses[18] indicate:

(1) Unstimulated production from these very tight sandstones with matrix permeabilities of the order of 0.1 μd can be substantial provided there exists an extensive, interconnected natural fracture system that is connected to the well.

(2) Damage surrounding the wellbore can mask the true productive capacity of a highly overpressured, naturally fractured reservoir. In all tests, a breakdown was required to initiate flow, and continually increasing relative gas permeabilities were observed during the test periods. Such continual cleanup suggests that prefrac testing be extended and carefully monitored and analyzed before considering any stimulation technique.

(3) Average reservoir permeabilities obtained from the production well (200-400 μd) do not reveal the large anisotropy of the natural fracture system or its high flow capacity.

(4) Well test data from the production well may indicate conventional production history and not exhibit, at least in a reasonable time, a slope change on semilog plots that would suggest a dual porosity system.

A production test was conducted in the Corcoran sandstone in MWX-1 over a perforated interval of 8110-8230 ft. After a breakdown and two weeks of various flow periods, the well flowed at 340-390 MCFD at a surface flowing tubing pressure of 225 psi. A modified isochronal test was conducted at rates of 125-135, 200-210, and 310-420 MCFD. However, rates continued to increase and a lower limit for deliverability of 620 MCFD was found at the end of the test period. This represents an estimated average permeability of 30-60 μd over the entire interval; this is a substantial increase over the measured matrix permeability of 0.1 μd measured in core.

Transient pressure tests were conducted in the lower Cozzette sandstone in MWX-1 over a perforated interval of 7940-7954 ft. Two flow and buildup tests were performed. The first buildup after a nine day flow period with rates increasing from 30 to 90 MCFD, gave Horner plots which indicated an average reservoir permeability of 6 μd. The second test was conducted at flow rates of 95 at first and then 150 MCFD; Horner plots of the subsequent buildup data gave an average reservoir permeability of 400 μd. These results suggest the presence of an interconnected natural fracture system with relatively high average permeability. Yet the pressure signatures from the well tests do not indicate the presence of a long singular fracture.

An interference test was conducted in the upper Cozzette sandstone with MWX-1, perforated from 7855 to 7892 ft, as the production well, and MWX-2, 123 ft away and perforated at three intervals between 7830 and 7885 ft, as the observation well. The test is shown schematically in Figure 1.11; a downhole shut-off tool was used in MWX-2 to isolate a small bottomhole volume and increase the sensitivity of the pressure response. After breakdown and a several day flow period at 300-400 MCFD in which interference was noted in MWX-2, a series of pulses were produced in MWX by alternating shut in periods with flow periods of 500, 600 and 1100 MCFD. The corresponding pressure transients in MWX-2 are small, but definite; the time lag is about 2.5 hrs. An analytic analysis of the pressure response provided a best match for an anisotropic natural fracture system with kx and ky of 120 md and 0.4 md and an average system permeability of 7 md. Several numeric analyses were performed with different simulators to study the relative effects and sensitivity of permeability, wellbore damage, nondarcy flow, and boundaries. As before, a comparison of data obtained in MWX-1 at the beginning and end of the tests in this zone showed an increase in average permeability from 75 to 225 μd and a reduction in skin from 2.6 to nearly zero.

After a three month shut-in, MWX-1 was flowed from the upper Cozzette interval into the pipeline at various times over a four month period. The average production rate was 550 MCFD with a cumulative produced volume of 35 MMCF. A Horner analysis of a buildup test at this end of this period gave a relative gas permeability of 380 μd, a 70% increase since the previous test seven months before. There was no evidence of boundaries or a decrease in the ability of the natural fracture system of this reservoir to produce gas over an extended period of time.

1.5.6 OTHER ACTIVITIES

Three geophysics-related experiments were conducted over the Mesaverde Formation at the MWX site: three-dimensional surface seismic,[19,20] vertical seismic profile,[19,20] and cross-well acoustic survey.[19,21] The primary focus for each of these experiments was the lenticular sands, but limited data include the marine interval. These are not specifically discussed in this report, but key references to each experiment are given above.

1.6 SIGNIFICANT ACCOMPLISHMENTS

We have drilled three wells which penetrate the Mesaverde Formation in the Piceance basin at a site near Rifle, Colorado. These establish the Multiwell Experiment as a field laboratory for the study of the tight gas resource in this formation. The Mesaverde has been subdivided into five distinct intervals based upon their depositional environments, which, in turn, strongly influence their reservoir characteristics. We have completed work for the deepest of these intervals--the marine--and this report is the culmination of that work.

We have conducted well tests in three zones of the marine interval which show that unstimulated Mesaverde sandstones may be more productive than generally recognized in standard practice. While these sandstones have matrix permeabilities on the order of 0.1 μd, average reservoir permeabilities were measured to be between 2 to 4 orders of magnitude higher, thus indicating that production is through an extensive, interconnected natural fracture system. Also, we observed that these sandstones required breakdown and continued to clean up with time under various flow and pressure conditions even at the end of each test. Flow rates as high as 1,100 MCFD for short periods, and of several hundred MCFD over four months, were found for the upper Cozzette sandstone interval tested.

We have developed a cased-hole stress test procedure, based on small volume hydraulic fracture, to determine the minimum in situ stress. Thirteen tests in the marine interval showed characteristic frac gradients of 0.85-0.90 and 1.00-1.11 psi/ft for the marine sandstones and shales, respectively. Thus, there are good stress contrasts (1000-1800 psi) between the sands and confining lithologies.

We have used the MWX logging data to aid in the development of TITEGAS, an improved log analysis program for tight gas sands.

We have compiled a comprehensive body of core, log and geologic data for this part of the Mesaverde Formation. These data are available publicly as a result of the Multiwell Experiment.

1.7 ACKNOWLEDGMENTS

A project of this magnitude is clearly the result of the efforts of a large number of people. The principal investigators express their appreciation for the assistance received from the MWX project personnel at Sandia National Laboratories and CER Corporation. Special thanks are extended to the CER field crew for their hard work and dedication in maintaining the site and conducting the various tests, often under difficult conditions.

We also acknowledge the contributions from many contractors and other participants in MWX who have helped us compile a unique, comprehensive set of data for this potential resource. The inputs of the U.S. Geological Survey have been particularly helpful.

The Multiwell Experiment is the major production technology project in the U. S. Department of Energy's Western Gas Sands Subprogram. DOE personnel responsible for MWX at various times have been C. H. Atkinson, A. B. Crawley, and J. K. Westhusing. The Western Gas Sands Subprogram is currently managed by K-H Frohne, Morgantown Energy Technology Center.

1.8 REFERENCES

1. National Petroleum Council, "Unconventional Gas Sources--Volume V: Tight Gas Reservoirs, Part I," Library of Congress Card Number 80-82488, December 1980.

2. C. H. Atkinson, A. B. Crawley, D. A. Northrop, A. R. Sattler, R. L. Mann, and J. C. Schillo, "The Department of Energy's Western Gas Sands Project Multi-Well Experiment," SPE/DOE 9891, Proceedings of the 1981 SPE/DOE Symposium on Low Permeability Gas Reservoirs, Denver, CO, May 27-29, 1981, pp 577-582.

3. A. B. Crawley, D. A. Northrop, and A. R. Sattler, "The Department of Energy's Western Gas Sands Project Multi-Well Experiment Update," SPE 11183, the 57th Annual Society of Petroleum Engineer's Technical Conference and Exhibition, New Orleans LA, September 26-29, 1982.

4. D. A. Northrop, A. R. Sattler, and J. K. Westhusing, "Multi-Well Experiment: A Field Laboratory for Tight Gas Sands," SPE/DOE 11646, Proceedings of the 1983 SPE/DOE Joint Symposium on Low Permeability Gas Reservoirs, Denver, CO, March 13-16, 1983, pp 393-398.

5. D. A. Northrop, A. R. Sattler, R. L. Mann, and K. H. Frohne, "Current Status of the Multiwell Experiment," SPE/DOE/GRI 12868, Proceedings of the 1984 SPE/DOE/GRI Unconventional Gas Recovery Symposium, Pittsburgh, PA, May 13-15, 1984, pp 351-358.

6. J. C. Lorenz, "Sedimentology of the Mesaverde Formation at Rifle Gap, Colorado and Implications for Gas Bearing Intervals in the Sub-Surface," Sandia National Laboratories Report, SAND82-0604, March 1982.

7. J. C. Lorenz, "Reservoir Sedimentology in Mesaverde Rocks at the Multi-Well Experiment Site," Sandia National Laboratories Report SAND83-1078, June 1983.

8. CER Corporation, "Multi-Well Experiment: MWX-1 As-Built Report," Sandia National Laboratories Contractor Report, SAND82-7201, July 1982.

9. CER Corporation, "Multi-Well Experiment: MWX-2 As-Built Report," Sandia National Laboratories Contractor Report, SAND82-7100, August 1982.

10. CER Corporation, "Multi-Well Experiment: MWX-3 As-Built Report," Sandia National Laboratories Contractor Report, SAND84-7132, February 1984.

11. G. C. Kukal, "A Systematic Approach for the Effective Log Analysis of Tight Gas Sands," SPE/DOE/GRI 12851, Proceedings of the 1984 SPE/DOE/GRI Unconventional Gas Recovery Symposium, Pittsburgh, PA. May 1984, pp 209-220.

12. A. R. Sattler, "The Multi-Well Experiment Core Program," SPE/DOE 11763, Proceedings of the 1983 SPE/DOE Joint Symposium on Low Permeability Gas Reservoirs, Denver, CO, March 13-16, 1983, pp 437-444.

13. N. R. Warpinski, P. Branagan, and R. Wilmer, "In Situ Stress Measurements at U.S. DOE's Multiwell Experiment Site, Mesaverde Group, Rifle, Colorado," Journal of Petroleum Technology, 37 (3), 527-536, March 1985.

14. L. W. Teufel, "Determination of In Situ Stress from Anelastic Strain Recovery Measurements of Oriented Core," SPE/DOE 11649, Proceedings of the 1983 SPE/DOE Joint Symposium on Low Permeability Gas Reservoirs, Denver, CO, March 13-16, 1983, pp 421-430.

15. F. G. Strickland and N-K Ren, "Predicting the In Situ Stress for Deep Wells Using the Differential Strain Curve Analysis," SPE8954, Proc. of the Unconventional Gas Recovery Symposium, Pittsburgh, PA, May 1980, pp 251-258.

16. L. W. Teufel, C. M. Hart, A. R. Sattler, and J. A. Clark, "Determination of Hydraulic Fracture Azimuth by Geophysical, Geological and Oriented Core Methods at the Multi-Well Experiment Site, Rifle, Colorado," SPE 13226, 59th Annual Technical Conference and Exhibition of the Society of Petroleum Engineers of AIME, Houston, TX, September 16-19, 1984.

17. T. L. Blanton, "The Relation Between Recovery Deformation and In Situ Stress Magnitudes," SPE11624, Proceedings of 1983 SPE/DOE Symposium on Low Permeability Gas Reservoirs, Denver, CO, March 1983, pp 213-218.

18. P. T. Branagan, G. Cotner, and S. J. Lee, "Interference Testing of the Naturally Fractured Cozzette Sandstone: A Case Study at the DOE MWX Site," SPE/DOE/GRI 12869, Proceedings of the Unconventional Gas Recovery Symposium, Pittsburgh, PA, May 1984, pp 359-366.

19. C. A. Searls, M. W. Lee, J. J. Miller, J. N. Albright, J. Fried and J. K. Applegate, "A Coordinated Seismic Study of the Multi-Well Experiment Site," SPE/DOE 11613 Proceedings of the 1983 SPE/DOE Joint Symposium on Low Permeability Gas Reservoirs, Denver, CO, March 13-16, 1983, pp 115-120.

20. C. A. Searls, "The Multiwell Experiment Geophysics Program; Final Report," Sandia National Laboratories Report, SAND85-1013, September 1985.

21. J. N. Albright, D. A. Terry, and C. R. Bradley, "Pattern Recognition and Tomography Using Crosswell Acoustic Data," SPE/DOE 13854, Proceedings of the 1985 SPE/DOE Joint Symposium on Low Permeability Reservoirs, Denver, CO March 1985, pp 55-64.

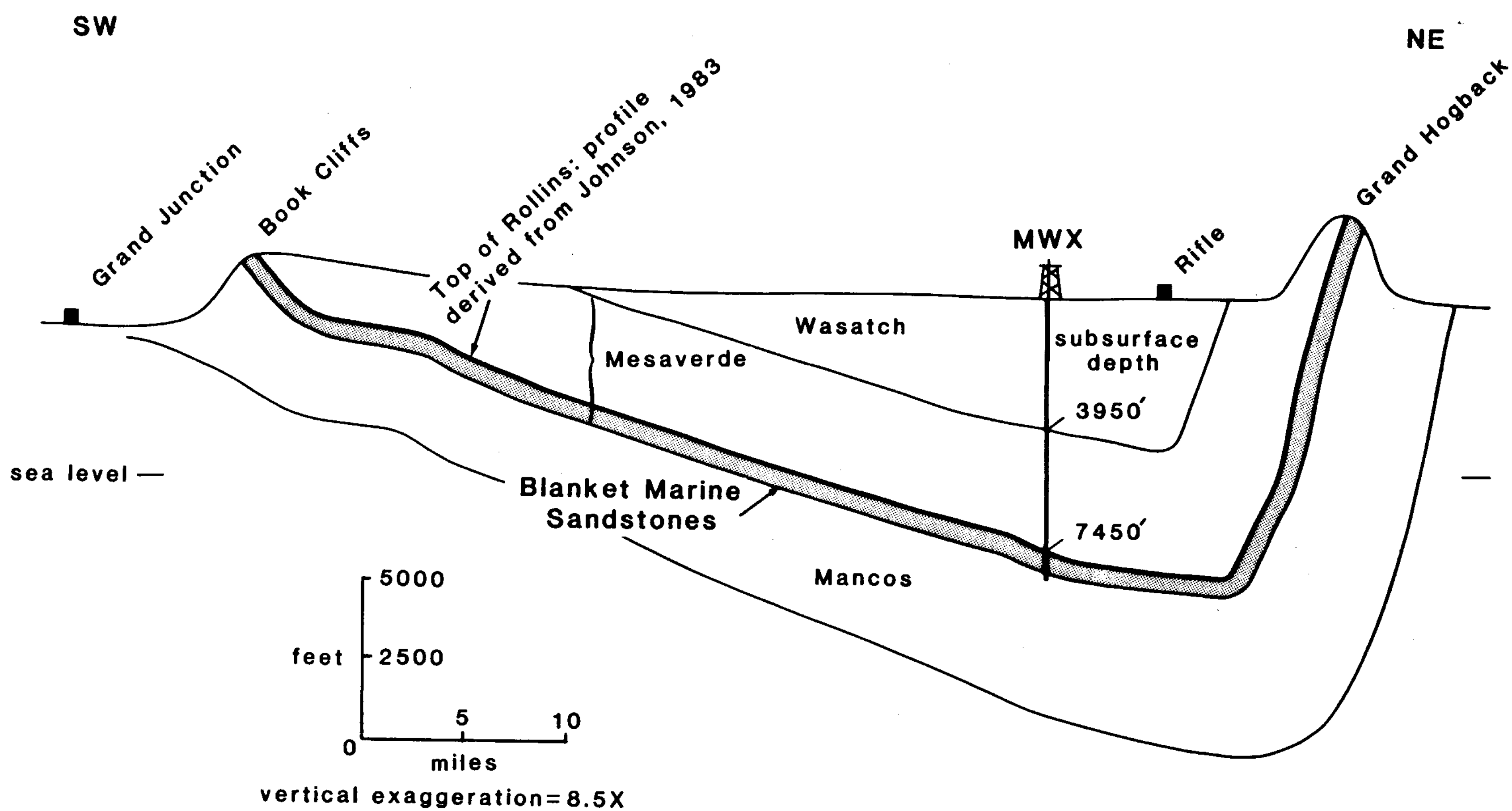

Figure 1.1 General Structure of the Mesaverde Formation in the Piceance Creek basin, Northwest Colorado.

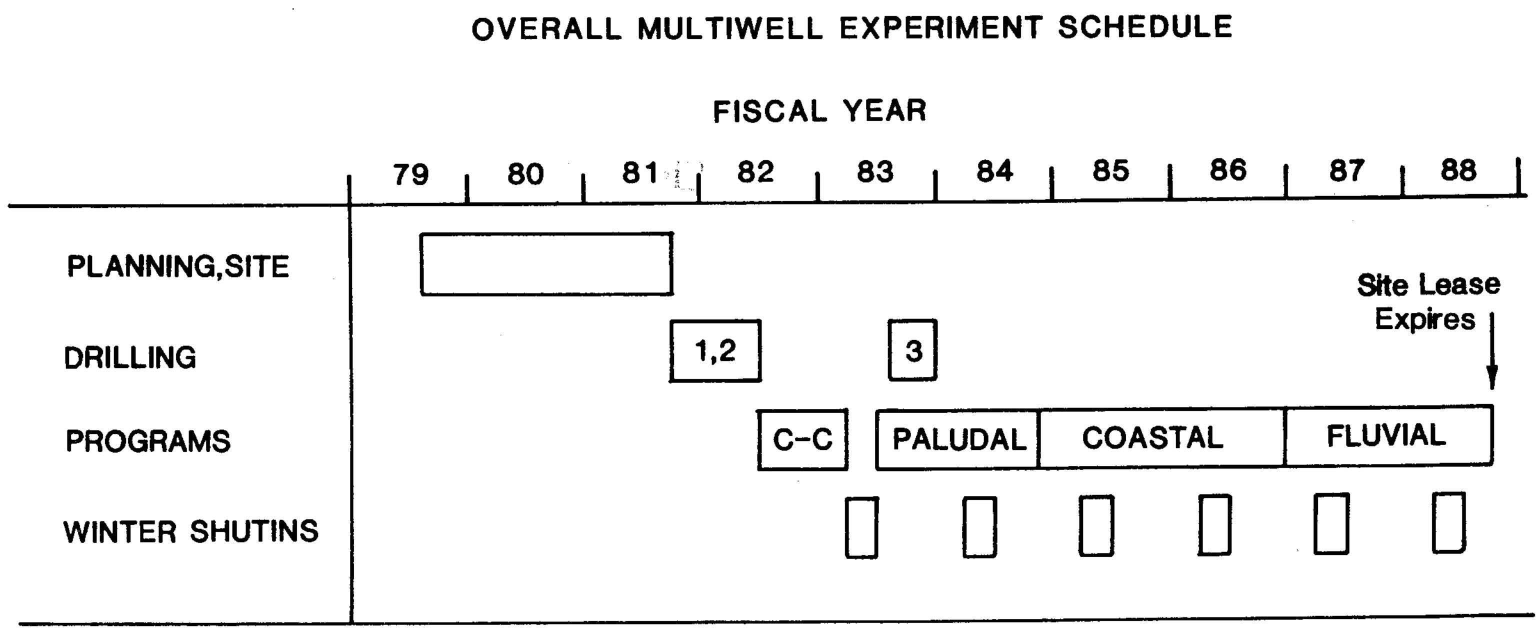

Figure 1.2 Overall Multiwell Experiment Schedule

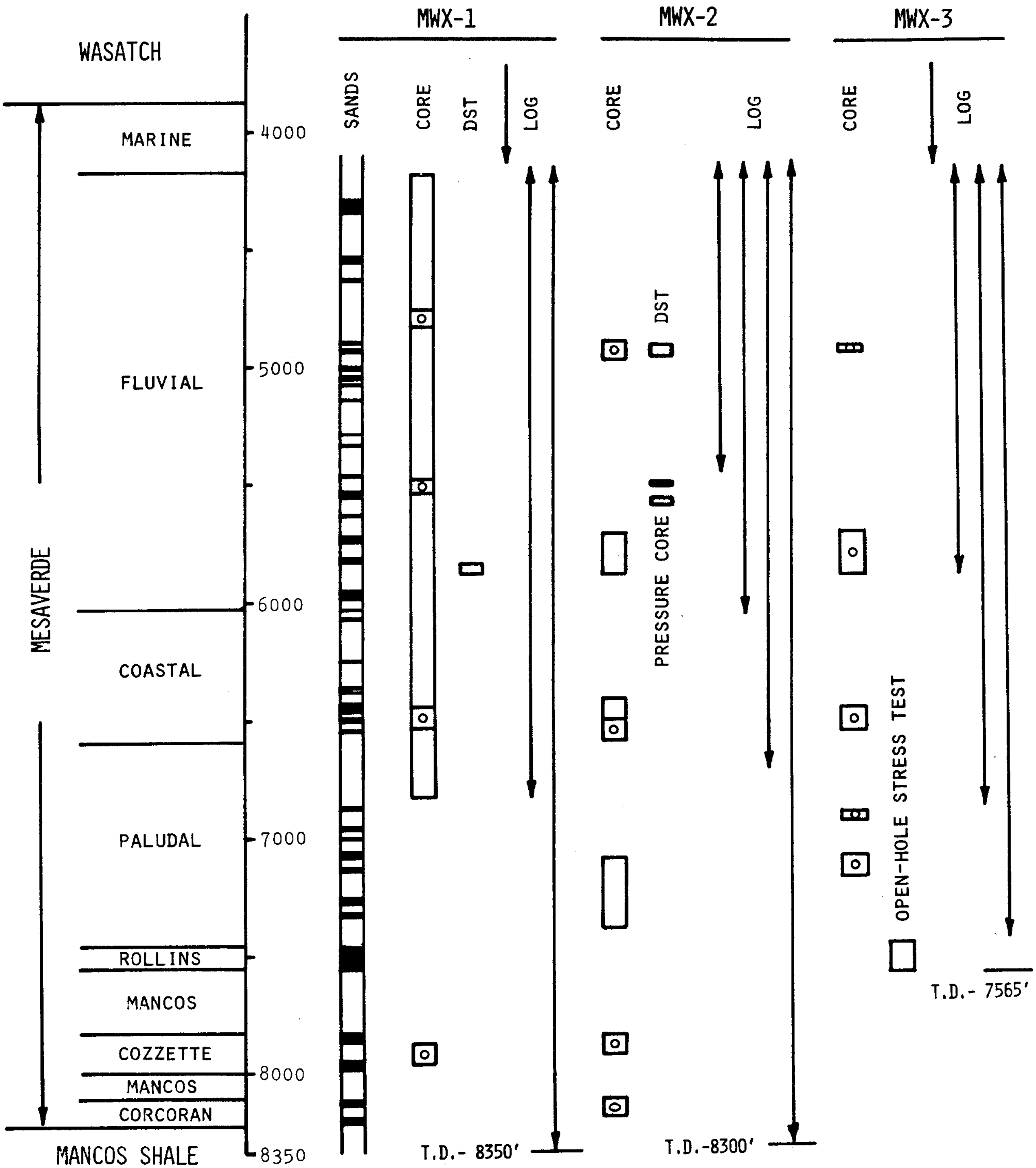

Figure 1.3 Summary of Coring and Logging Operations on the Three Multiwell Experiment Wells

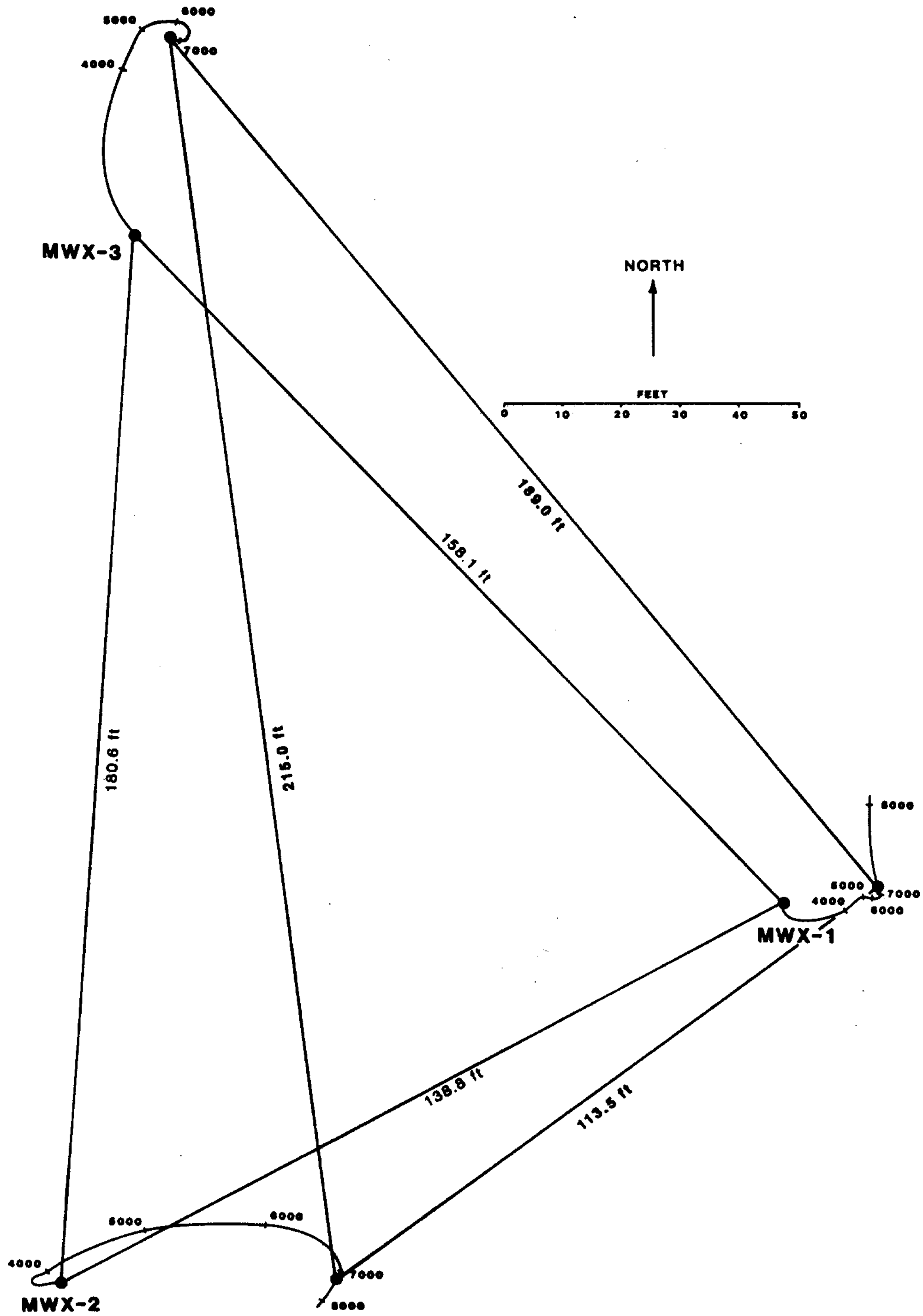

Figure 1.4 Relative Well Springs at Surface and 7300 ft (the deepest survey in all three wells)

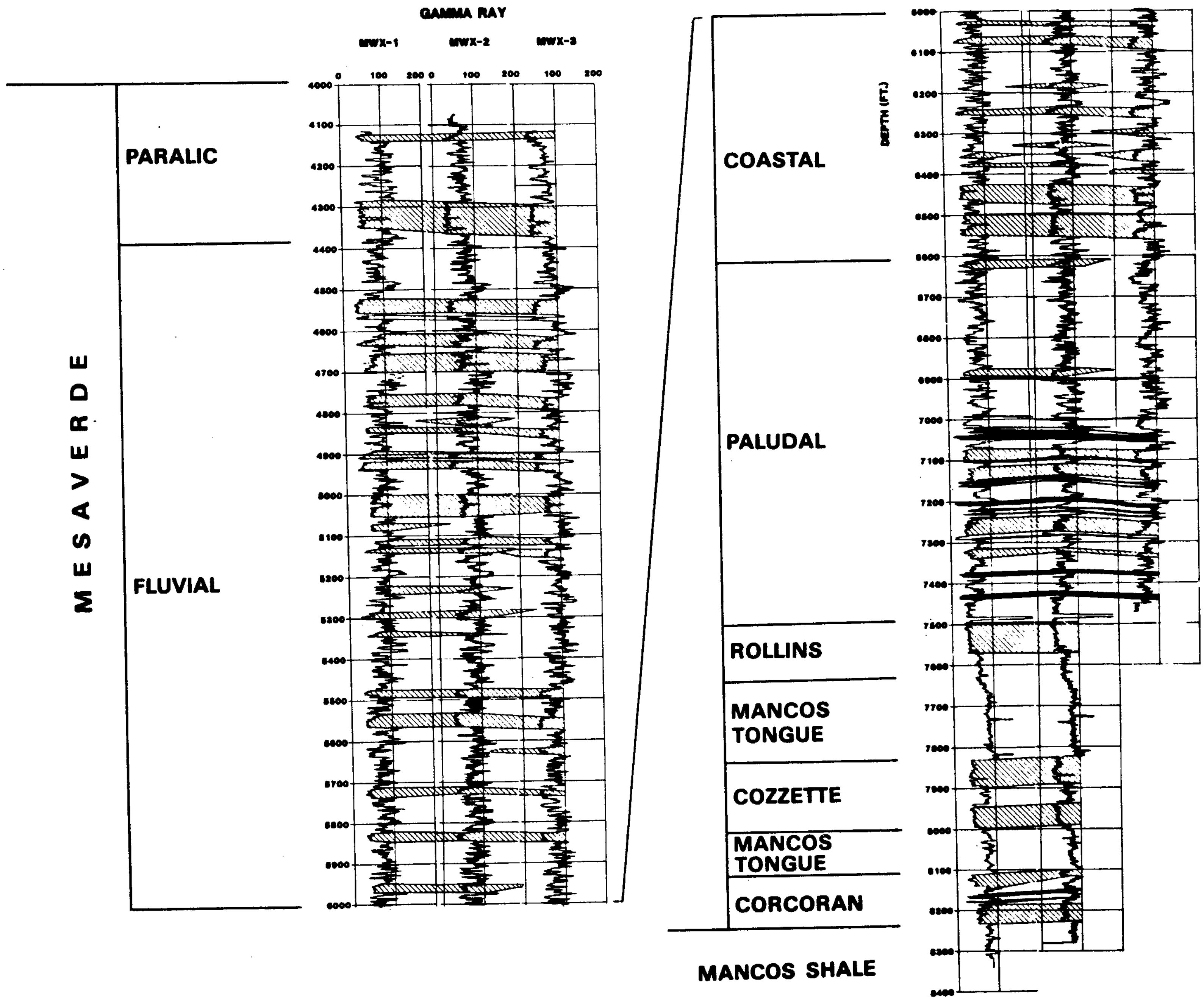

Figure 1.5 Gamma Ray Logs of the Three Multiwell Experiment Wells with Sands Identified

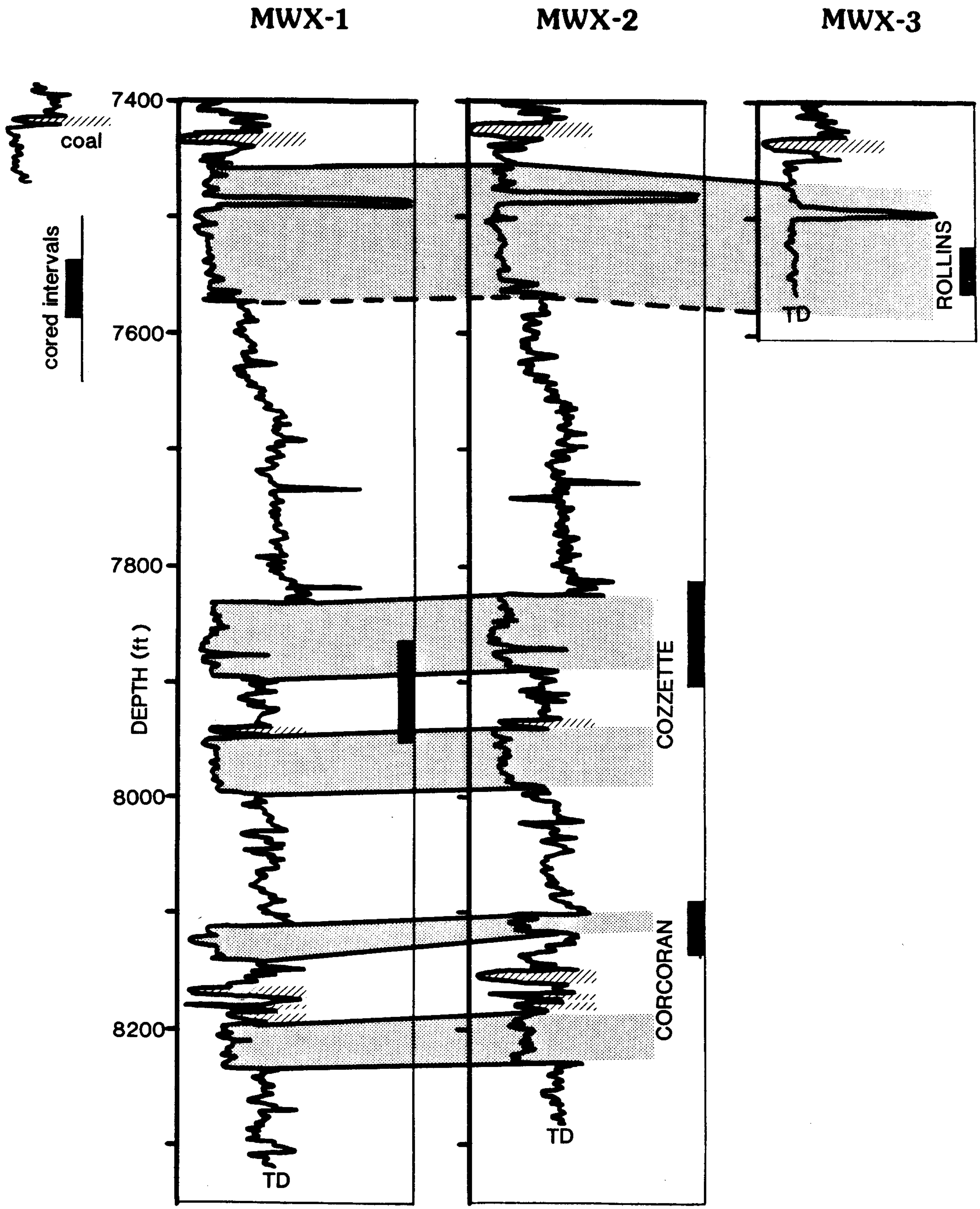

Figure 1.6 Gamma Ray Logs of the Marine Interval of the Mesaverde

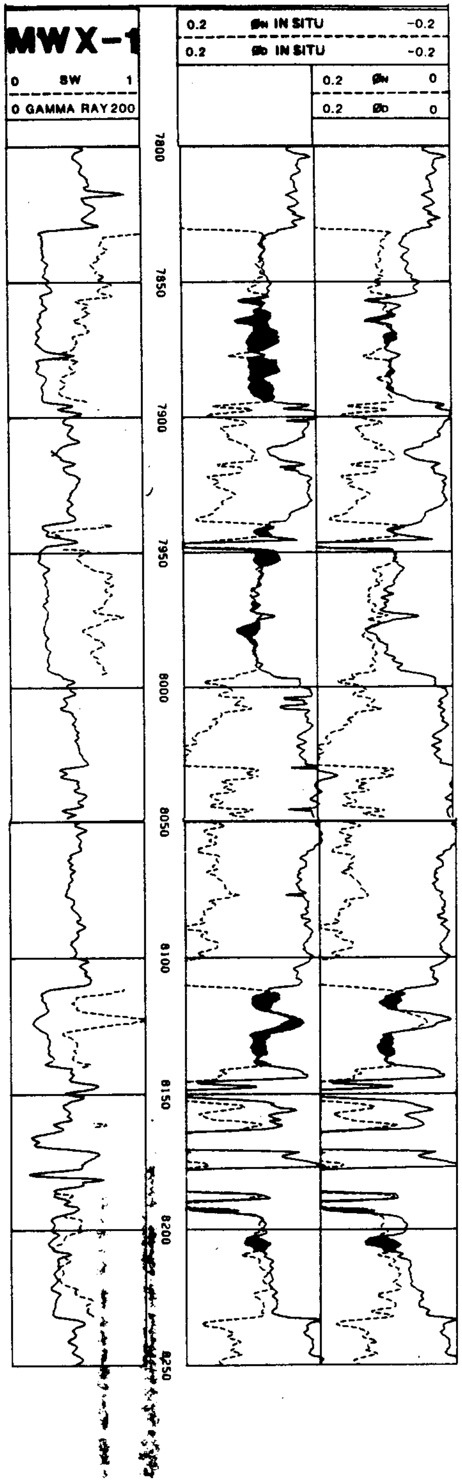

Figure 1.7
Log-Derived Reservoir Properties

	Well	Interval (ft)	Thickness (ft)	Vcl (fraction)	ϕ (fraction)	S_w (fraction)	Kh (md-ft)
Upper Cozzette*	MWX-1	7854.0-7894.5	39.5	0.079	0.073	0.511	0.37
	MWX-2	7845.5-7887.0	39.5	0.095	0.069	0.496	0.38
Lower Cozzette	MWX-1	7939.5-7995.0	52.0	0.110	0.075	0.647	0.29
	MWX-2	7933.0-7987.0	51.0	0.130	0.072	0.673	0.22
Upper Corcoran	MWX-1	8111.5-8140.0	29.0	0.094	0.067	0.575	0.20
	MWX-2	8100.5-8114.5	11.0	0.173	0.067	0.647	0.06
Lower Corcoran	MWX-1	8195.0-8232.0	35.5	0.183	0.059	0.449	0.30
	MWX-2	8185.0-8226.0	29.5	0.205	0.056	0.508	0.17

* Upper Cozzette excluding pyrobitumen zone. Gross sand thicknesses are 62.5 and 61.0 ft in MWX-1 and MWX-2, respectively.

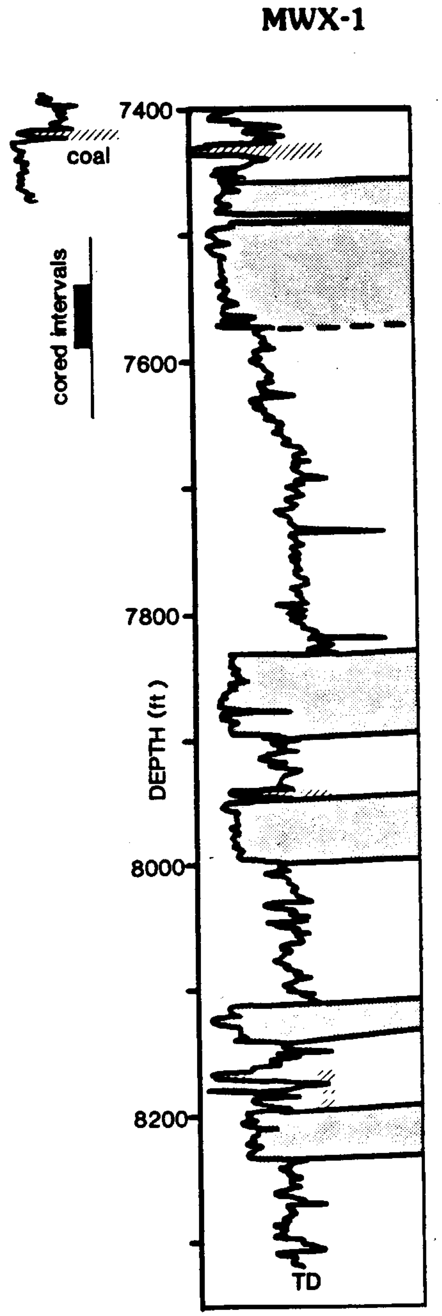

Figure 1.8
Core-Derived Reservoir Properties

		Permeability* (k, μd)	Porosity (ϕ, %)	Water Saturation (S_w %)	Young's Modulus** (E, GPa)	Poisson's Ratio (ν)	CEC (meq/100g)
Rollins	Sandstone	-	4-8	60-80	27-45	0.19-0.23	-
Mancos Tongue	Shale	-	-	-	19	0.23	-
Upper Cozzette	Pyrobitumen	$\leq$1	3	70-90	39	0.15	1.0-2.5
Upper Cozzette	Sandstone	4-7	6-8	25-50	35-40	0.21-0.23	0.5-0.1
Intermediate	Mixed	<1-3	2-6	30-60	28-36	0.15-0.22	0.1-2.5
Lower Cozzette	Sandstone	4	6	30-35	35	0.22	0.5
Mancos Tongue	Shale	<<1	2	75	17	0.21	>3
Upper Corcoran	Sandstone	2-7	4-6	25-60	33	0.18	0.5-1.5

* dry Klinkenberg permeabilities @ 1000 psi confining pressure
** at confining pressure of 20 MPa; secant modulus measured between 20% and 60% of 2900 psi ultimate stress

Figure 1.9
Minimum In Situ Stress Measurements
and Frac Gradient

Well	Depth (ft)	Lithology	ISIP (psi)	Frac Gradient (psi/ft)
MWX-2	7467	Sandstone	6800 ± 30	0.91
	7531	Sandstone	6590 ± 20	0.88
	7601	Siltstone	7610 ± 20	1.00
	7665	Shale	8150 ± 100	1.06
	7766	Shale	8590 ± 100	1.11
	7850	Sandstone	6645 ± 50	0.85
	7895	Siltstone	6830 ± 30	0.86
	7924*	Siltstone	6850 ± 50	0.86
		Shale	7800 ± 50	0.98
	7971	Sandstone	6885 ± 30	0.86
	8015	Shale	8150 ± 30	1.02
	8061	Shale	8230 ± 20	1.02
MWX-3	7510	Sandstone	6810 ± 30	0.91
	7543	Sandstone	6765 ± 30	0.90

*Dual closure stress

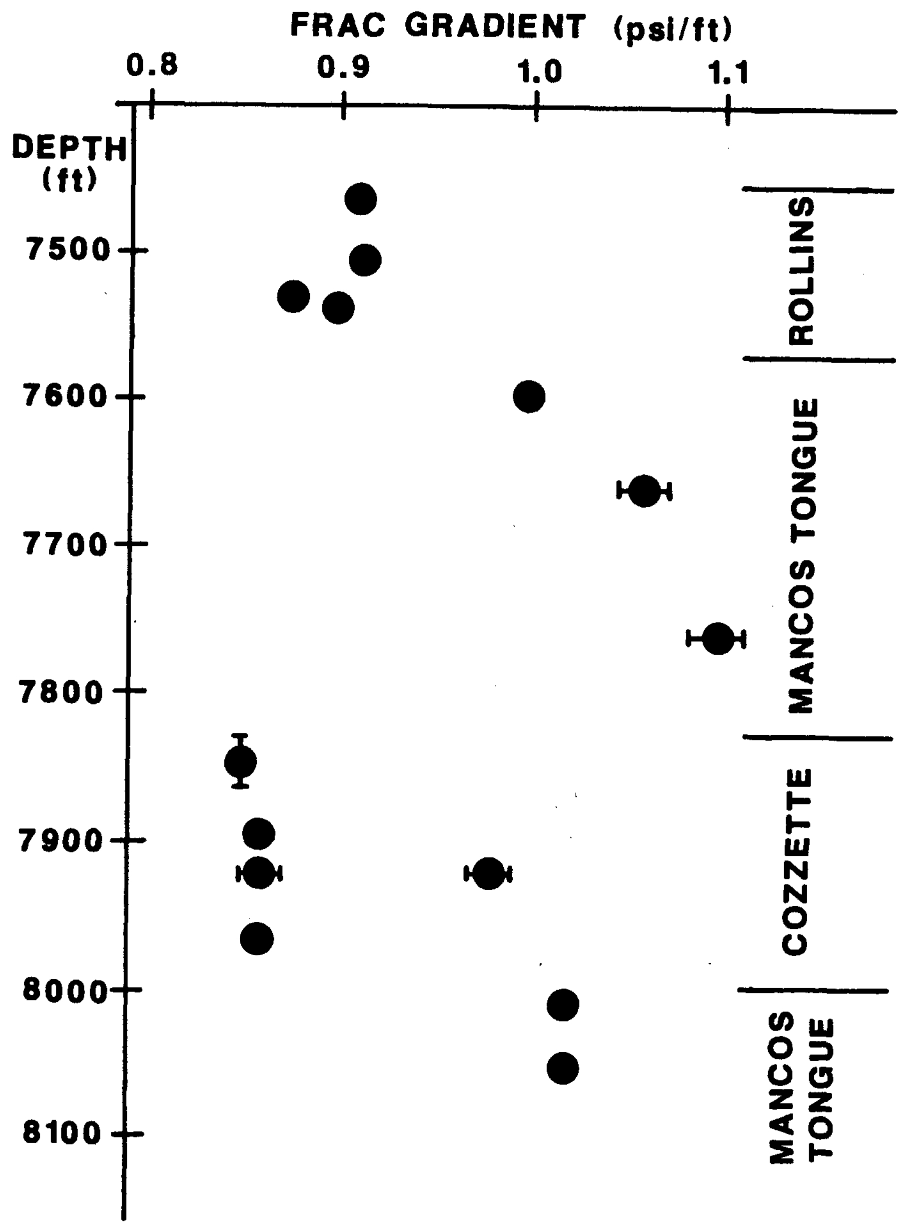

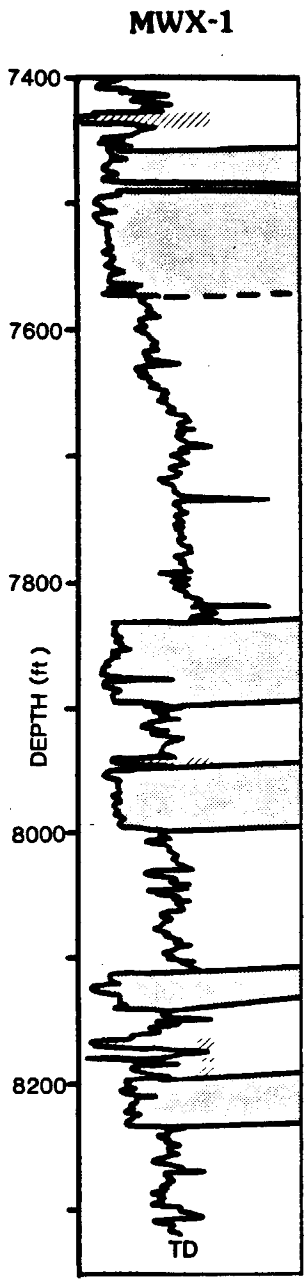

Figure 1.10
Anelastic Strain Recovery Results

Well/Interval	Depth (ft)	Azimuth*	Calculated Horizontal Stress (psi) Max	Min
MWX-3 Rollins	7560	N66W ± 4	7610	7260
	7561	N59W ± 3	7590	7235
	7562	N72W ± 6	7680	7365
	7564	N55W ± 4	7731	7183
Average		N61W ± 2		
MWX-2 Cozzette	7884	N49W ± 10	-	-
	7888	N60W ± 8	8365	8000
	7894	N74W ± 9	-	-
	7895	N69W ± 11	8340	7955
Average		N63W ± 5		
MWX-2 Corcoran	8118	N92W ± 9	-	-
	8119	N82W ± 11	8800	8340
	8120	N83W ± 7	-	-
	8121	N78W ± 8	8915	8370
Average		N83W ± 4		

* Maximum Horizontal Stress Direction

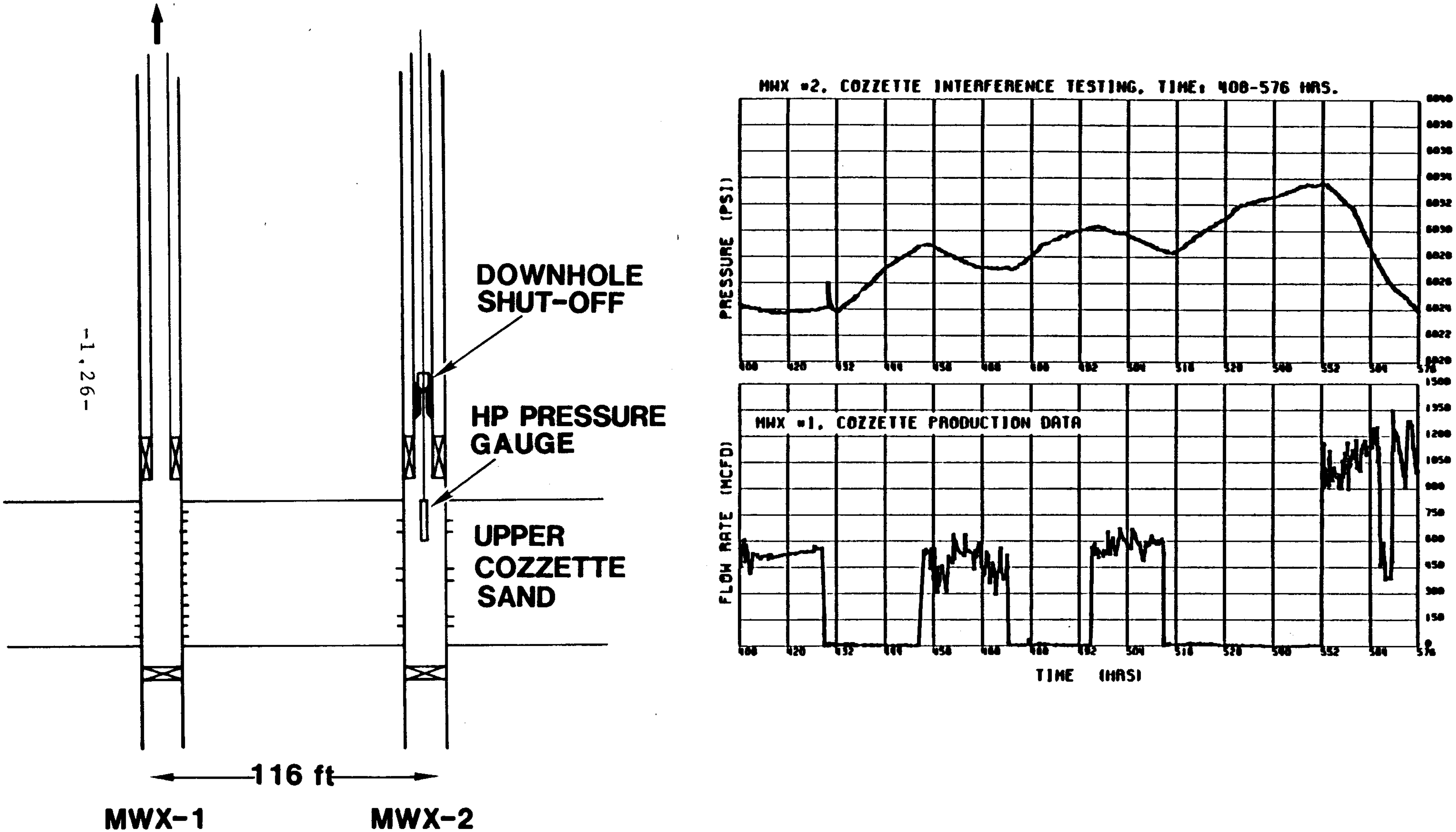

Figure 1.11 Configuration of the Cozzette Interference Test with Flow and Pressure Data

2.0 SITE DESCRIPTION AND OPERATIONS

Robert L. Mann
CER Corporation

2.1 WELL DRILLING AND WELL DESCRIPTIONS

As shown in Figure 2.1, the Multiwell Experiment (MWX) is located in the Rulison Field in the southeastern portion of the Piceance Basin in Colorado. The site is located in the SW1/4 NW1/4 Sec. 34, T6S, R94W, Garfield County, and is about 7 miles southwest of Rifle.

Site selection was based upon several factors, such as:

- The Mesaverde Group was at a reasonable depth in the area.
- The zones of interest were typical of the tight gas sands formations.
- The zones were also in an area of proven Mesaverde production.

An agreement was reached with Superior Oil Company in mid-1981 and all necessary drilling and operating permits were acquired. Drilling of MWX-1 began in mid-September 1981, achieving total depth at 8350 ft. The well was drilled through the blanket Mesaverde sections and 7-in, 29-lb N-80 casing was run and cemented. As shown in Figure 2.2, a total of 2747 ft of the Mesaverde group was cored and recoverd, including 470 feet of oriented core.

The rig was moved to the adjoining location and the second well was spudded on December 31, 1981. MWX-2 was also drilled through the blanket marine Mesaverde to a depth of 8300 ft with 915 ft of formation cored and recovered, as shown in Figure 2.3. The MWX-2 casing program was similar to the first well. The casing was run and cemented and the rig released on March 30, 1982.

The third well, MWX-3, was spudded on June 7, 1983, and was drilled to a depth of 7564 ft. As shown in Figure 2.4, it penetrated the Rollins Formation but not the Corcoran/Cozzette. "As-built" reports have been published on all three wells.[1,2,3]

Detailed geologic information is provided in other sections of this report, but a brief description of the formation tops and characteristics is appropriate here. A geologic section in MWX-1 is shown in Figure 2.5.

The top of the Rollins section of the marine Mesaverde was penetrated at 7488 ft KB in MWX-1. The Mancos Shale Tongue separated the Rollins sandstone from the lower marine Mesaverde Corcoran/Cozzette sandstone. The Mancos Tongue was penetrated at 7672 ft KB in MWX-1. The Mancos Tongue is approximately 150 ft thick and is a fairly uniform marine shale interfering in the lower Mesaverde section. In MWX-1, the top of the Cozzette was penetrated at 7830 ft and the Corcoran at 8110 ft KB. Both wells penetrated the massive Mancos Shale underlying the marine Mesaverde formations at approximately 8230 ft KB. Table 2.1 gives the formation tops for all three wells.

During the drilling of the three MWX wells, it was noted that a gradual increase of formation pressure was encountered starting at approximately 5600 ft. Mud weight had to be continually increased with depth from 9.0 lb/gal at 5600 ft to over 15.0 lb/gal at 8350 ft, as shown in Figure 2.6. The Cozzette required a pressure gradient of 0.71 psi/ft and the Corcoran 0.75 psi/ft to control the formation pressure during drilling. From these data and subsequent test data, it is apparent that the lower Mesaverde formations are substantially overpressured.

Complete logging suites were run on all three wells and the logs and detailed analyses of the Corcoran/Cozzette interval are presented in Section 4.0.

Detailed direction surveys were also run in the wells to determine the relative well spacing at various depths, as well as at the surface. The wells were drilled with very little directional deviation so the relative spacing with depth does not change significantly. Figure 2.7 shows the relative locations of the three wells at the surface and at 7300 ft.

2.2 OPERATIONS

After MWX-2 was drilled and cemented in early 1982, the test separator, flow lines, stress test equipment, wireline trailers and pressure test equipment were moved on to location, set up and tested.

In early July 1982, Los Alamos National Laboratory (LANL) ran cross-hole seismic surveys on both MWX wells. A temperature log run in conjunction with this operation is given in Figure 2.8. The survey was completed in mid-July and MWX-1 was shut in and remained shut in until mid-August. One interval in MWX-2 was perforated and stress tested in late July and four other intervals were perforated and stress tested in early August. MWX-2 was then shut in until late October. Detailed analyses of the stress test data are presented in Section 6.0 and elsewhere.[4,5]

After analysis of both core and log data, it was decided that the Upper Cozzette zone was the best candidate for testing and evaluation as the "blanket base case" reservoir. The zone was more uniform and similar in both wells and appeared to be continuous from well to well. The Lower Cozzette and Corcoran Formations showed large variations between the two wells. For thoroughness, however, it was decided to run brief production tests on both of the zones before conducting more extensive tests in the Upper Cozzette. The results of all well testing are given in Section 7.0.

The Corcoran zone in MWX-1 was perforated from 8100-8230 ft on August 15, 1982. The well was swabbed and flowed from August 15 to August 27. Because the zone was not producing, it was broken down on August 28. The zone was cleaned up and tested until September 11, at which time a bridge plug was run and set above the Corcoran.

The well was perforated in the Lower Cozzette zone from 7949-7954 ft on September 16, 1982. The zone was flowed and tested until October 19. A bridge plug was set above the Lower Cozzette at 7920 ft on October 21. This completed the brief production test of the two lowest zones.

The Upper Cozzette zone in MWX-1 was perforated from 7855-7892 ft on October 22, 1982. The perforations were broken down and then cleaned up and shut in in MWX-1 on October 25. The MWX-2 was then perforated in Upper Cozzette for interference testing from 7830-7840 ft , 7850-7860 ft and 7874-7884 ft.

MWX-1 was shut in for build-up while MWX-2 was worked on from October 25 to November 30. The interference tests were delayed due to a stuck packer in MWX-2 and instrumentation problems. The interference test was started November 30.

MWX-1 was flowed and shut in periodically from November 30 to December 13, at which time MWX-1 was killed with a $CaCl_2/CaCO_3$ solution to retrieve wireline tools and prepare the wells for winter shutdown. Both wells were flowed for cleanup and then shut in for winter. The site was closed from December 17, 1982, until March 1983.

On March 9, 1983, the MWX-1 well was turned over to Superior Oil Company and connected to the Western Slope Gas line for sales. It was produced for sales from the Upper Cozzette from March 9 through June 17, 1983, except for a 2-week period from May 1 to May 15 when CER took control of the well to run pulse tests on MWX-1 and MWX-2. During the period of March 9 to June 17, 30.6 MCF of gas was produced for sales from the Upper Cozzette.

At the completion of the pulse tests, stress tests were run in MWX-2 over the Upper Cozzette, the Mancos Tongue, the Rollins and the lower paludal section. Results of those tests are reported in Section 6.0. All work in MWX-2 in the blanket marine Mesaverde section was completed with the final stress test run on June 2, 1983.

During this same period, the drilling pad was being prepared for the third well. MWX-3 was spudded on June 7, 1983, and reached TD of 7,474 ft on August 3. After logging and running 7-in. casing, the well was deepened to a total depth of 7,564 ft where open-hole stress tests were performed on the open-hole section of the Rollins. After completion of these tests on September 10, a wireline bridge plug was set at 7350 ft and MWX-3 was no longer in communication with the blanket marine Mesaverde section.

CER took possession of MWX-1 on June 20, 1983, and pulled tubing and set a Model D packer at 7810 ft, above the Upper Cozzette. A new string of 2-7/8-in tubing was run and the final testing of Upper Cozzette was initiated. The well was flowed for cleanup and then shut in for final build-up tests until July 7, when a bridge plug was set a 7,777 ft above the Upper Cozzette Formation. With the setting of the bridge plug, MWX-1 was no longer in communication with the blanket marine Mesaverde formations.

Thus, all work was completed in the marine Mesaverde formations in MWX-1, MWX-2, and MWX-3 on July 7, June 2, and September 10, 1983, respectively.

2.3 REFERENCES

1. CER Corporation, "Multi-Well Experiment: MWX-1 As-Built Report," Sandia National Laboratories Contractor Report, SAND82-7201, July 1982.

2. CER Corporation, "Multi-Well Experiment: MWX-2 As-Built Report," Sandia National Laboratories Contractor Report, SAND82-7100, August 1982.

3. CER Corporation, "Multi-Well Experiment: MWX-3 As-Built Report," Sandia National Laboratories Contractor Report, SAND84-7132, February 1984.

4. CER Corporation, "Multi-Well Experiment Activities: July 1 1982-December 31, 1982," Sandia National Laboratories Contractor Report, SAND83-7465, December 1983.

5. N. R. Warpinski, P. Branagan, and R. Wilmer, "In Situ Stress Measurements at U.S. DOE's Multiwell Experiment Site, Mesaverde Group, Rifle, Colorado," Journal of Petroleum Technology, 37 (3), 527-536, March 1985.

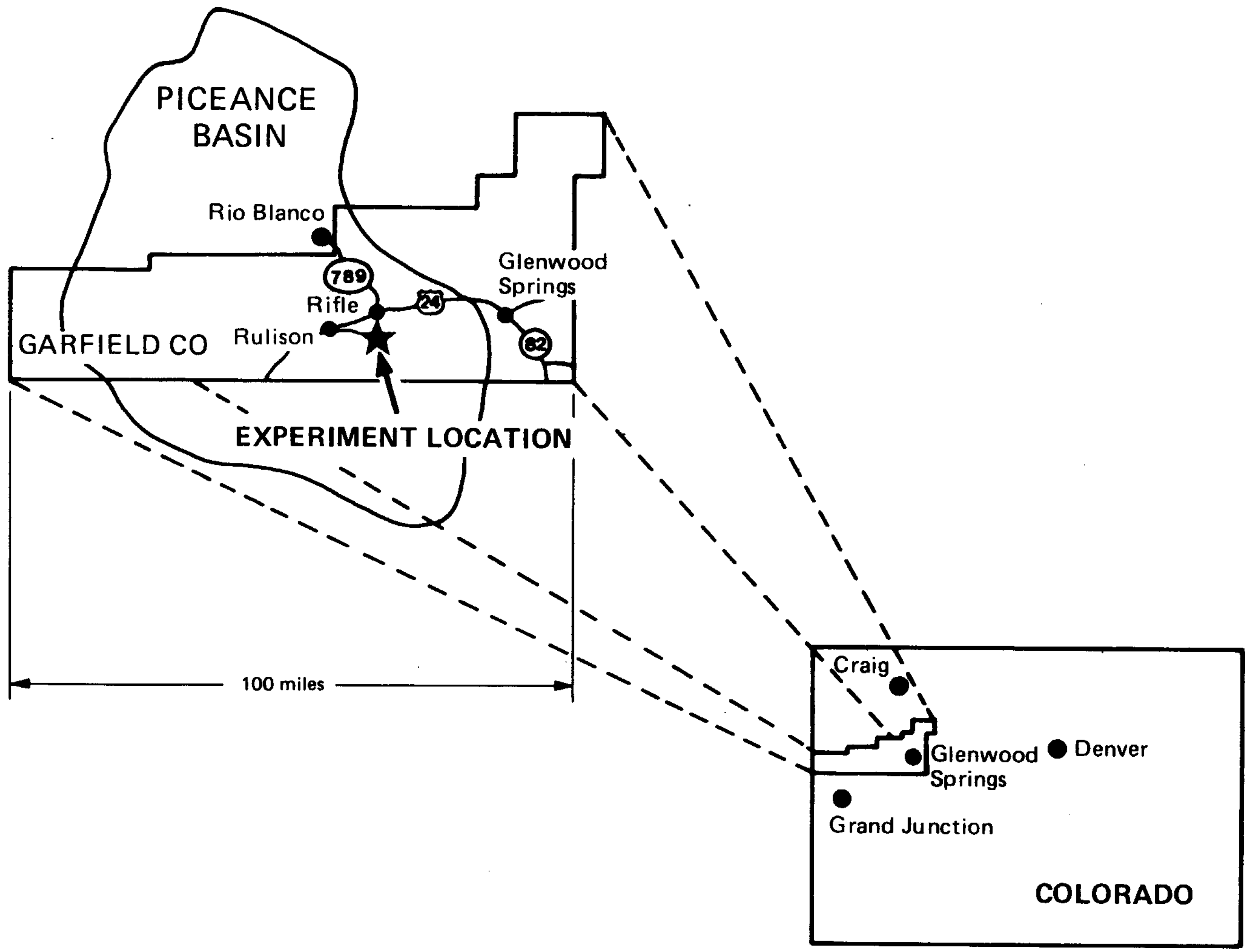

Fig. 2.1 Multiwell Experiment Location

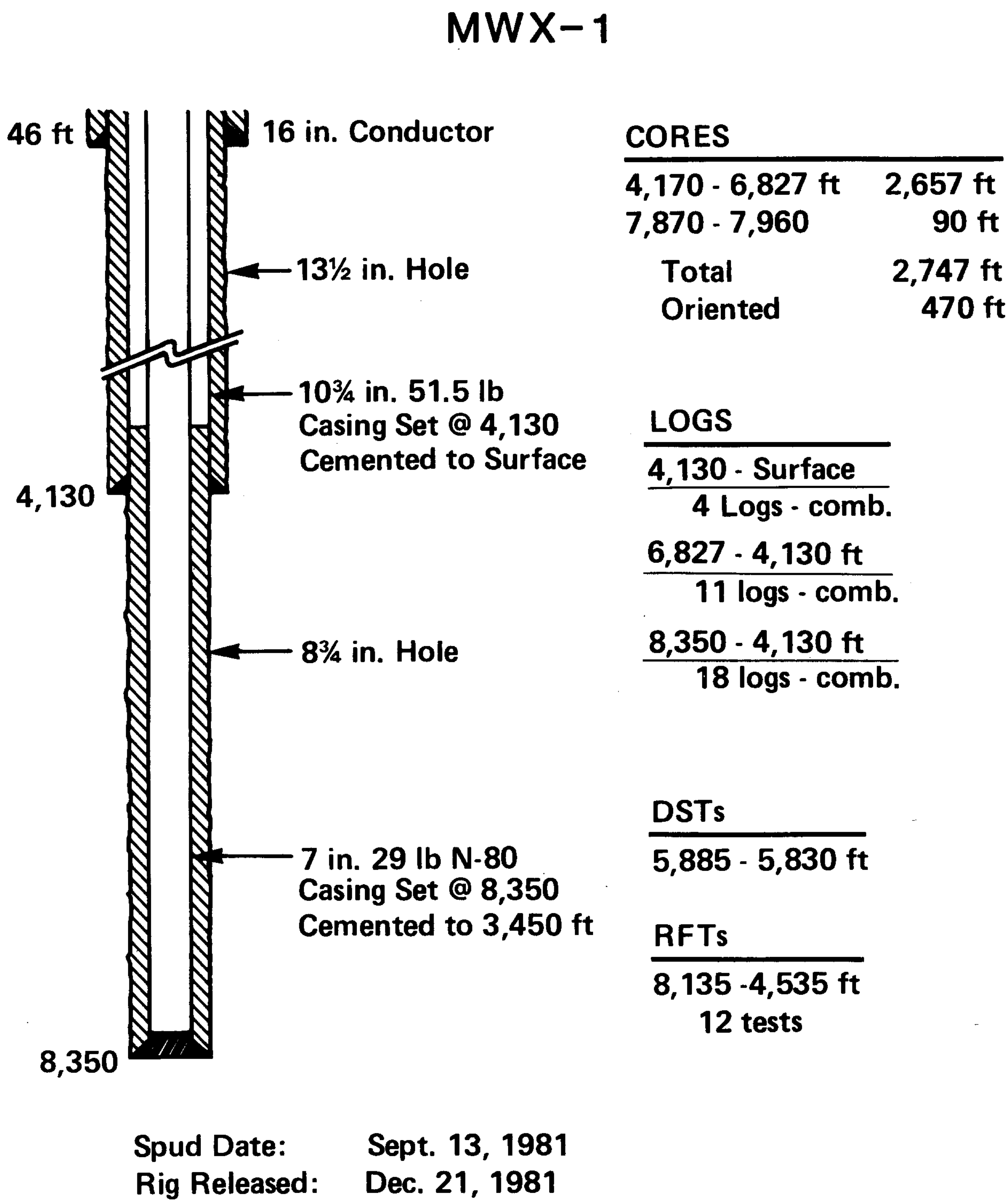

Fig. 2.2 MWX-1 Well Information

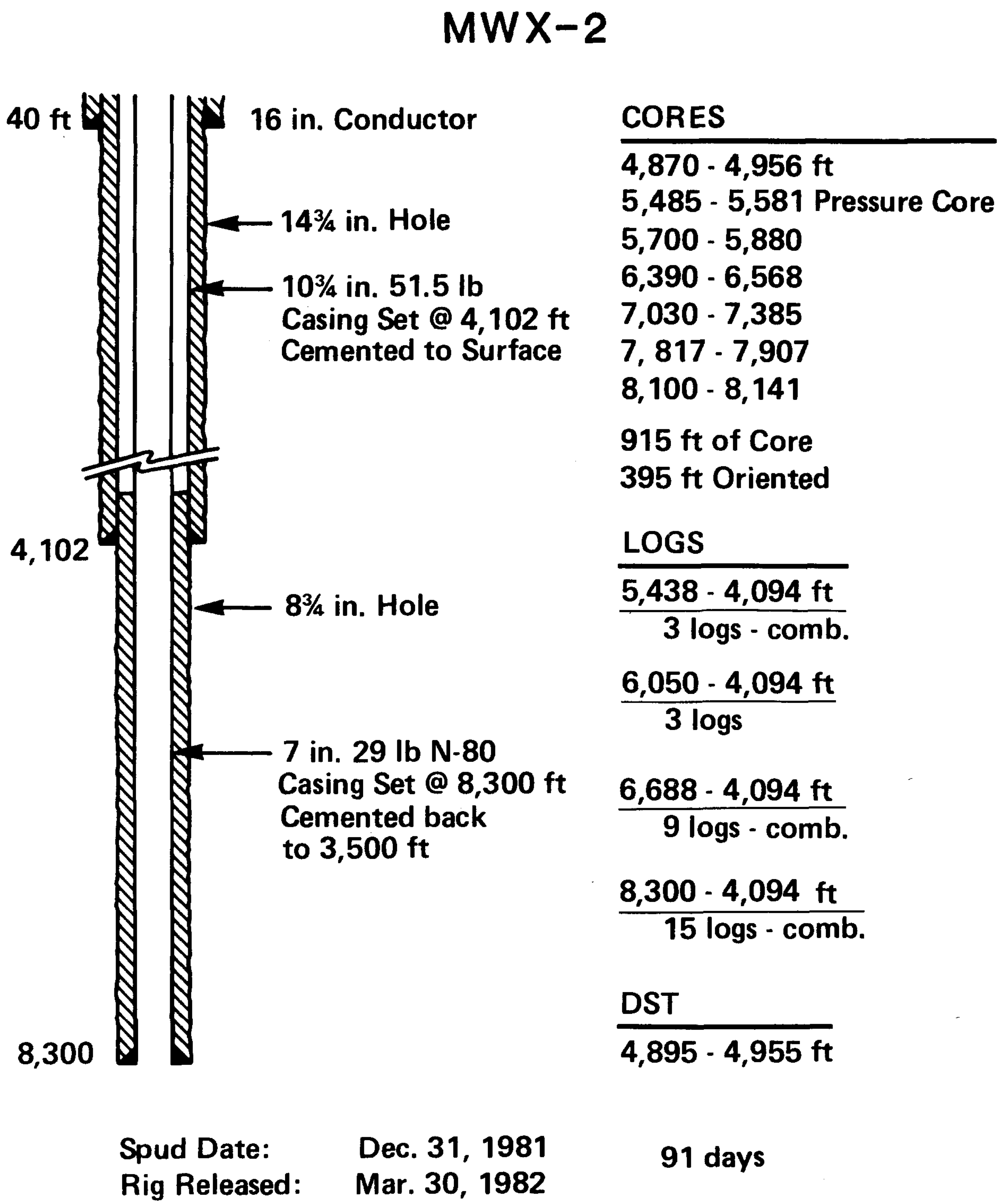

Fig. 2.3 MWX-2 Well Information

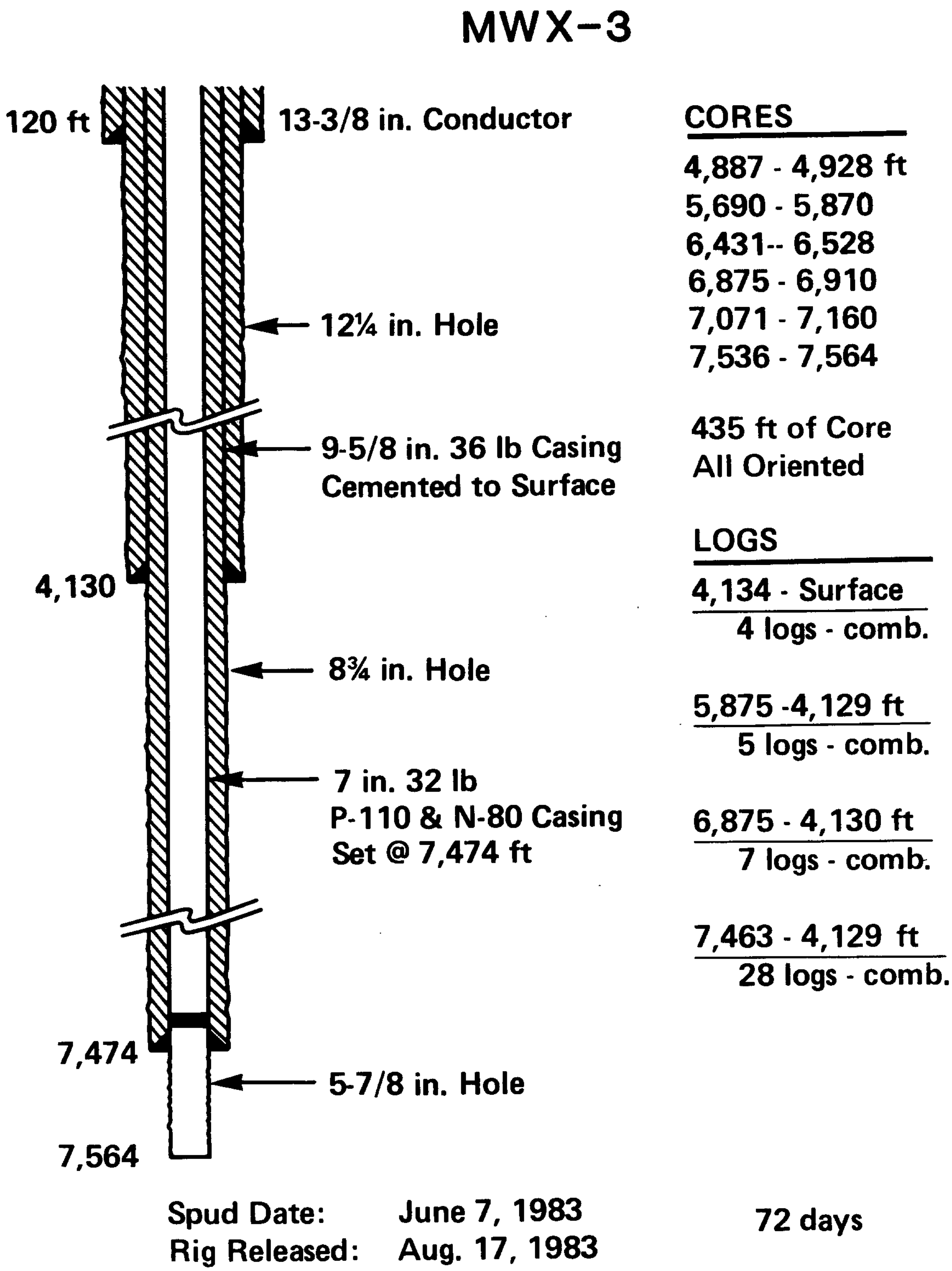

Fig. 2.4 MWX-3 Well Information

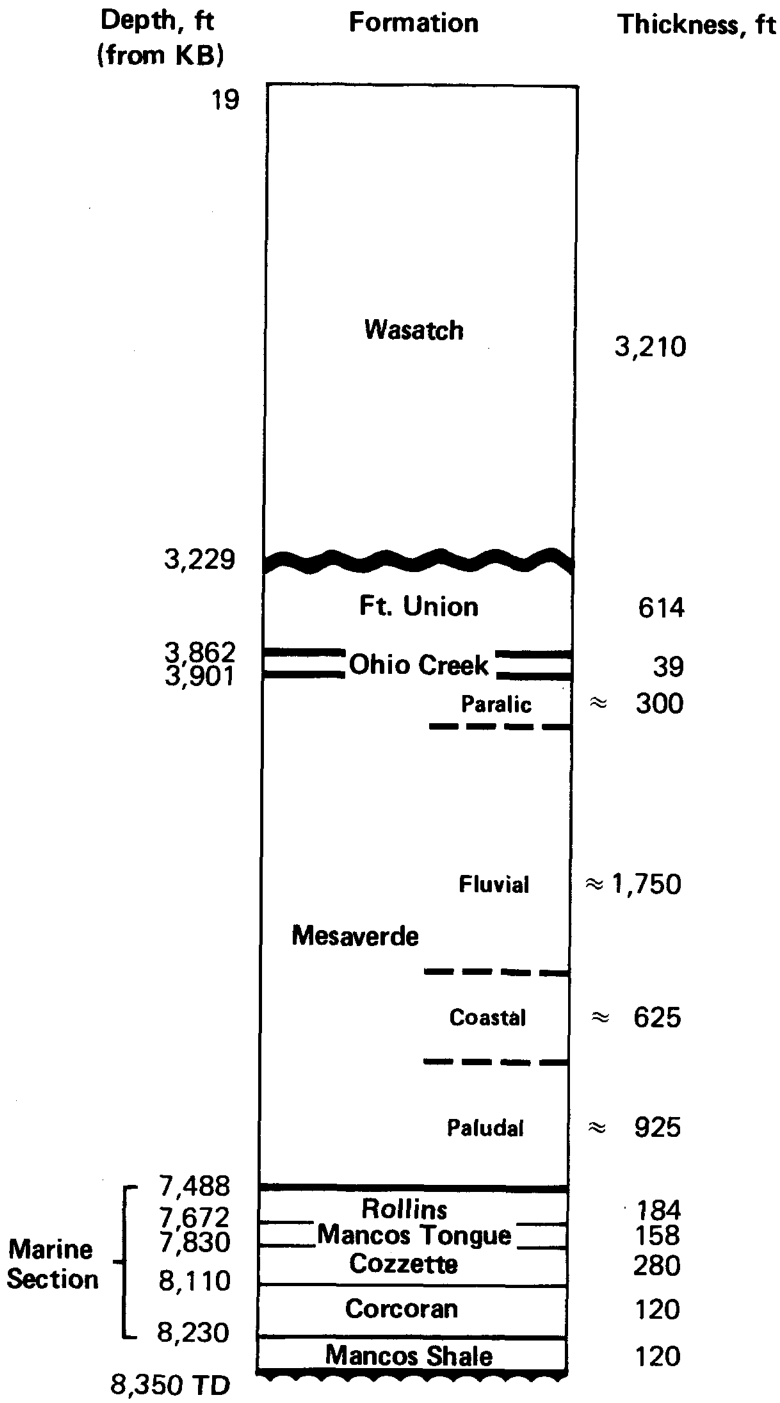

Fig. 2.5 Geologic Cross-section of MWX-1

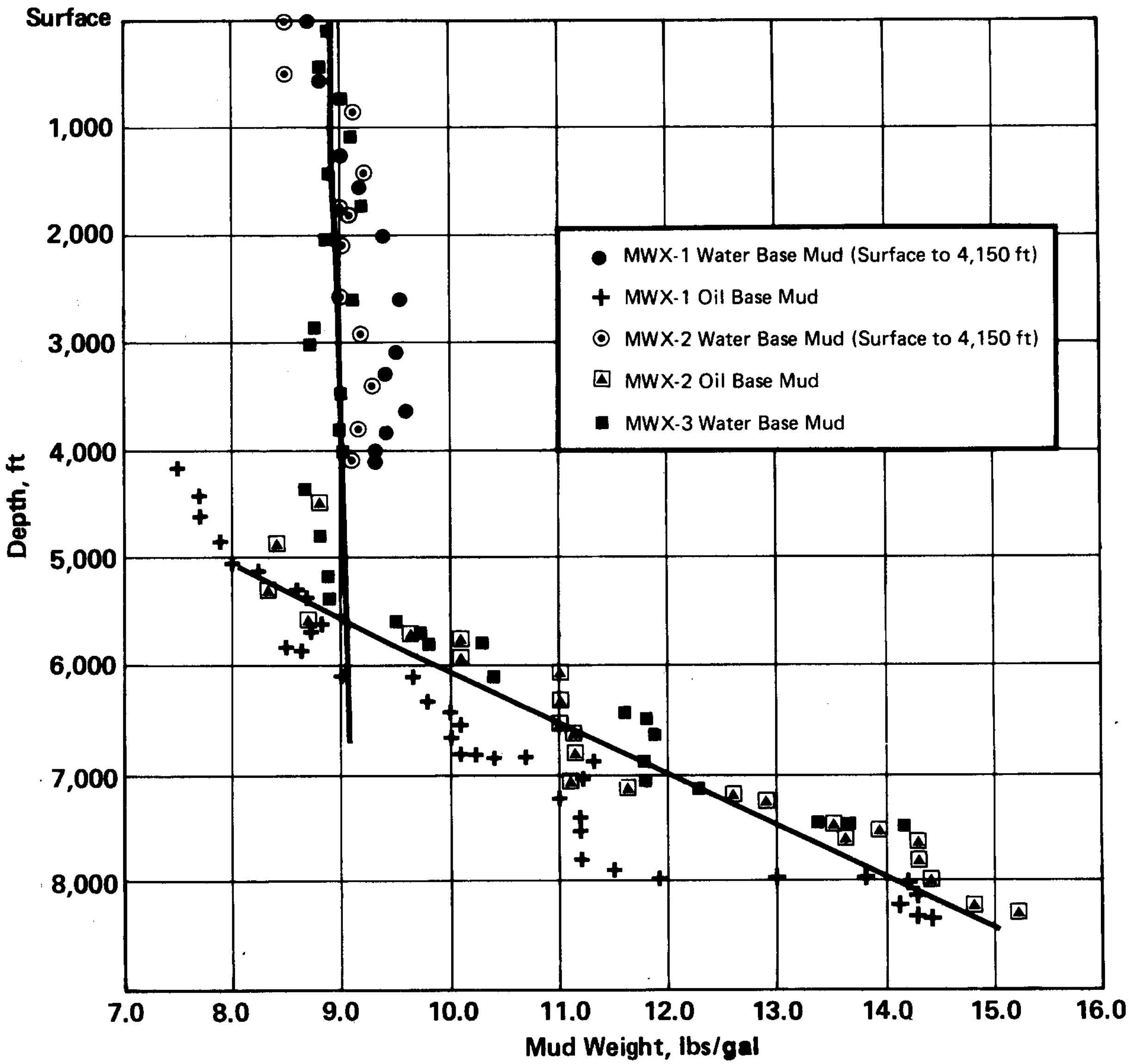

Fig. 2.6 Mud Weight Versus Depth

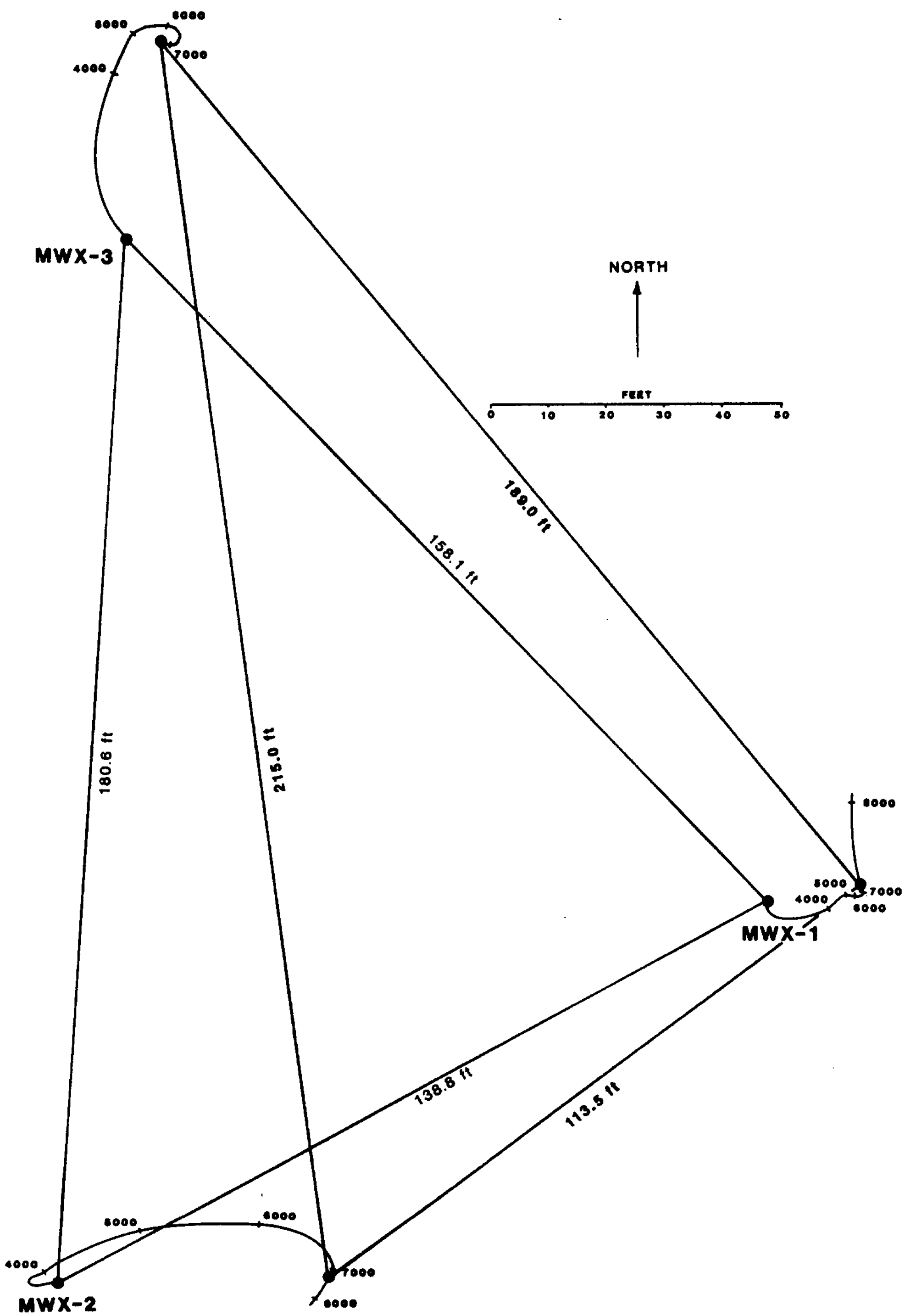

Figure 2.7 Relative Well Spacings at Surface and at 7300 ft (the deepest survey in all three wells).

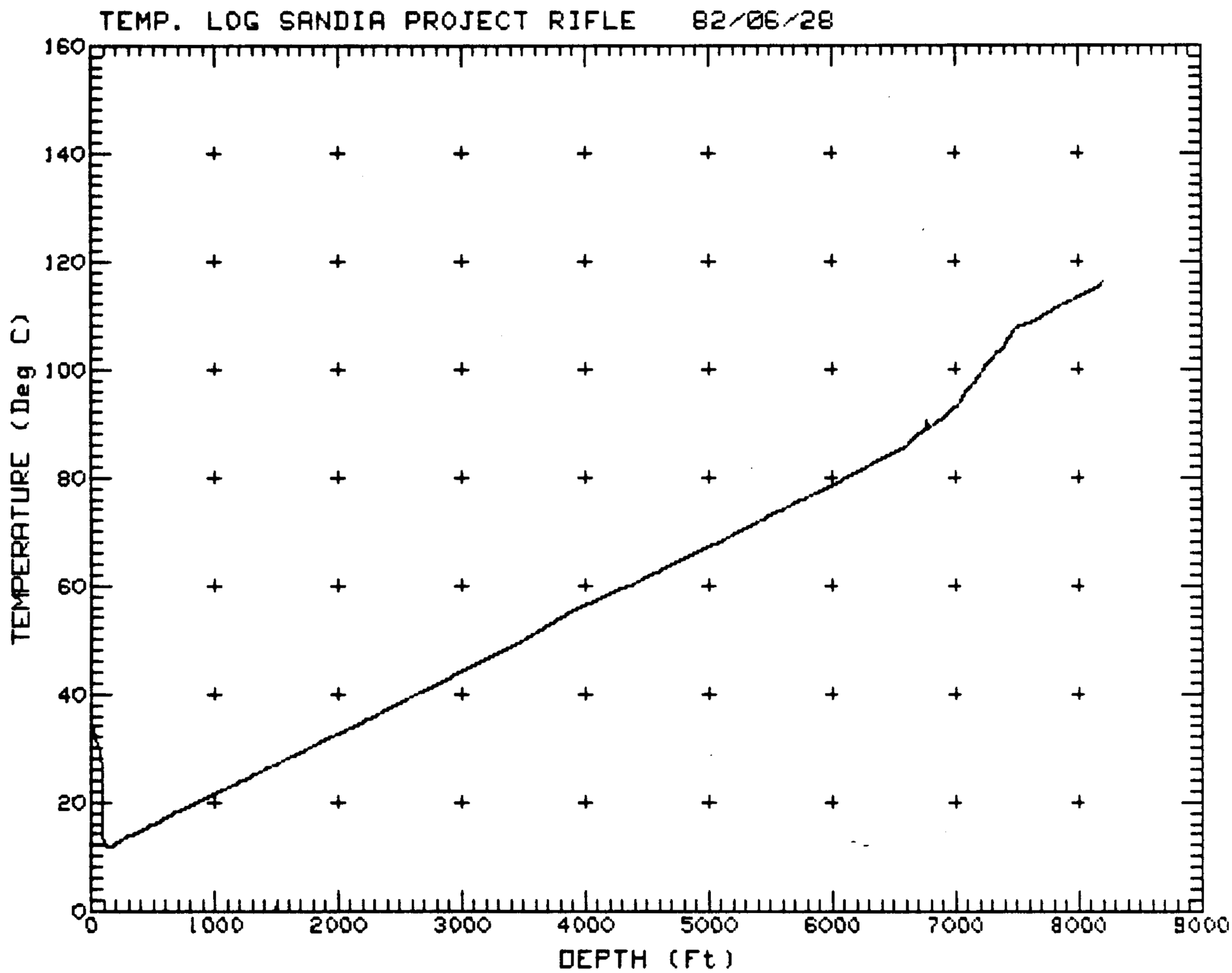

Figure 2.8 Temperature Log of MWX-1.

INTENTIONALLY LEFT BLANK

3.0 GEOLOGY

John C. Lorenz
Sandia National Laboratories

3.1 INTRODUCTION

The general structure of the Mesaverde Formation in the Piceance Creek basin (Figure 3.1) is that of gentle northeasterly dip toward the Grand Hogback. There the dip abruptly reverses to a steep southwesterly trend due to uplift of the adjacent White River Plateau. The blanket marine sandstones, which are the subject of this report, lie at the bottom of the Mesaverde Formation. There is no significant structural alteration of the gentle northeasterly dip at the top of the marine section in the vicinity of the MWX site (Figure 3.2, Johnson 1983).

The sandstone reservoirs between the depths of 7455 and 8350 feet subsurface at the Multiwell Experiment (MWX) site were deposited in environments which oscillated between shallow marine, shoreline and lower delta plains. The main sand bodies of the Corcoran, Cozzette and Rollins members of the Mesaverde Formation are shallow marine to wave-dominated shoreline deposits. The interbedded shales are predominantly deep marine shales, while the associated carbonaceous mudstones, coals, and lenticular sandstones are nonmarine, lower delta plain deposits. All of these environments are represented in both the MWX wells (Figure 3.3) and in the outcrops at Rifle Gap (Lorenz, 1982, 1983, Lorenz and Rutledge, 1985). This interval was penetrated by MWX-1 and MWX-2, while MWX-3 bottomed in the Rollins.

3.2 LITHOLOGY

3.2.1 Corcoran Member in MWX wells

The upper sandstone of the Corcoran Member was cored in MWX-2. It consists of a fine- to very-fine-grained sandstone with occasional carbonaceous laminae, over- and underlain by carbonaceous mudstones and shales (Figure 3.4).

Comparison of the MWX-1 and MWX-2 gamma ray and density logs of the Corcoran interval (separated by only 120 feet at this depth) shows an abrupt thinning from 30 to

15 feet of this upper sandstone, which combined with the carbonaceous nonmarine associated lithologies, suggests that it is a distributary channel. It is abruptly overlain by what appears to be a uniform tongue of the Mancos Shale.

The lower sandstone bed of the Corcoran interval (uncored) has a blocky gamma ray profile and seems to be underlain by the Mancos Shale. This suggests that it is an extensive shallow marine to shoreline sandstone, transitional between marine shale below and carbonaceous delta plain mudstones and distributary sandstones above.

3.2.2 Cozzette Member in MWX Wells

MWX-1 to MWX-2 correlations of the Cozzette Member show sandstones that are very continuous (Figure 3.5) with little variation between the wells. This, plus the virtual absence of coals, suggests that the depositional environments did not prograde sufficiently for nonmarine deposits to form in the MWX area (except for a ten-foot, coal-bearing zone at the top of the lower Cozzette sandstone) and that both sandstones are shallow marine to shoreline deposits.

This marine interpretation is supported by the core available for these intervals (the upper sandstone in MWX-2; the lower half of the upper sandstone, the upper few feet of the lower sandstone, and the intervening siltstones and shales in MWX-1). Fine-grained, well-sorted sandstones with well-defined, low-angle (and possibly hummocky) crossbedding and common marine-type trace fossils (Ophiomorpha) comprise these sandstones. The associated shales and siltstones are well laminated but abundantly burrowed, again suggestive of shallow marine conditions.

The upper 20 feet of the upper Cozzette sandstone is primarily a mixed zone of burrowed siltstone and sandstone with much of the pore space occupied by pyrobitumen. Sedimentologically, this may be a zone of reworked material produced by the subsequent major transgression, during which the 250-foot thick overlying tongue of the Mancos Shale was deposited. The pyrobitumen results from thermally altered oil (Pitman and Spencer, 1984).

3.2.3 Rollins Member in MWX Wells

The Rollins (or Trout Creek) Member in the MWX wells has little or no well-to-well variation. It displays a textbook coarsening-upward sequence (Figure 3.6) indicative of a prograding, wave-dominated shoreline. It grades up from the deep marine Mancos Shale into silt-shale laminations, thence into shale-silt-sand laminations, and finally into thick-bedded sandstone with marine burrows and sedimentary structures. An abrupt gamma ray kick near the top of the sandstone may record a placer deposit of radioactive minerals (zircon or monazite?) or a bentonite. Core from MWX-3 is fine-grained, well-sorted sandstone with well-defined sedimentary structures and good marine trace fossils.

3.2.4 Outcrops of the Corcoran, Cozzette, and Rollins Members at Rifle Gap

Outcrops at Rifle Gap have been correlated with the Rollins, Cozzette, Corcoran, and possibly underlying Sego Members (Warner, 1964; Lorenz and Rutledge, 1986). Figure 3.7 indicates the inferred correlation between Rifle Gap and the MWX wells. The major variation occurs in the Corcoran member, where the coal-bearing interval is associated with the lower sandstone at MWX, but is located over the upper sandstone at Rifle Gap. This suggests that these reservoirs are homogeneous and laterally continuous on a reservoir scale. However, there is considerable variation regionally, probably due to erratically advancing, and perhaps slightly embayed shoreline depositional environments.

Again the reservoir sandstones are fine grained and well sorted. The marine trace fossils and sedimentary structures are much better exposed in outcrop than in the limited four inch diameter MWX core, and fossils are common. This list includes <u>Inoceramus</u> fragments in the shoreline sandstones, ammonites in the marine shales, and oysters and other brackish water fossils (e.g., <u>Cerbula undifera meek</u>) in the associated nonmarine mudstones. Also found in the nonmarine interval of the Corcoran is at least one distributary channel and associated splay deposit.

3.2.5 Outcrops of the Corcoran, Cozzette, and Rollins Members along the Book Cliffs, and Regional Trends

Outcrops of these rocks in the Book Cliffs north of Grand Junction (50 miles distant from Rifle Gap, on the western edge of the basin) are lithologically similar, but the entire section is compressed. Although all of the members are present, the lower rate of subsidence on this edge of the basin allowed only thinner units to accumulate. This locality is approximately on depositional strike with Rifle Gap: the line between the two localities is parallel with the Corcoran and Cozzette shoreline trends as mapped by Warner (1964). Thus the thinner Book Cliffs deposits were deposited contemporaneously with the thicker units in the eastern part of the basin.

The excellent exposures of these rocks along the Book Cliffs indicate that, perpendicular to depositional strike, these rocks are traceable for miles with little or no variation. A similar character is inferred for the poorer exposures along the Grand Hogback on either side of Rifle Gap.

Balsley (1982) has mapped similar rocks in Utah and detailed their small-scale changes over distances on the order of miles. The major breaks in Balsley's rocks are subtle planes which cut diagonally through the sandstones, dipping seaward, and which record breaks in deposition. Such planes, sometimes associated with shale partings, probably provide the major permeability discontinuities within these blanket sandstones in the dip direction. In the strike direction, discrete large-scale (miles) depositional units have been documented by Flores et al (1984) in similar rocks of the Wasatch Plateau. These units probably correspond to different distributary discharge sites, and may be isolated from adjacent units by shale breaks and subtle, vertical, en echelon deposition. However, these units would appear to be continuous blanket-like deposits on the scale of most well control.

Regionally, the shorelines of the Sego, Corcoran, Cozzette and Rollins trended northeast-southwest and prograded to the southeast (Warner, 1964). First recognizable as marine units distinct within nonmarine sediments in the northwestern part of the basin, the blanket-like deposits extend southeastward as sandstone tongues into the marine Mancos Shale. The trend of the last associated coal-bearing sediments marks the southeastern limit of nonmarine deposits and delineates the shoreline trend, though the blanket sandstones extend farther southeastward as purely marine deposits.

Within the underlying marine shales, several sandstone turbidity current deposits occur. As studied on Mt. Garfield on the Book Cliffs, there are two kinds of these deposits, both of which may have reservoir potential. The first consists of shale and sandstone ripup clasts within a silty matrix in lenticular beds. The second is a silty to sandy deposit which occurs in thinner, more widely spread units. Where numerous, these deposits may coalesce into a wide target horizon such as the Mancos B in the northwestern part of the basin.

3.2.6 Reservoir Sandstone Petrology

Sandstone petrology (grain size, grain composition, and diagenetic history) is the primary control on reservoir porosity and permeability. Petrographic analyses of numerous samples were performed by Bendix Field Engineering (1982-84); the results are summarized in Table 3.1 and 3.2 and the individual analyses are given in Appendix 9.1.

Most of the sandstones for which core is available for this interval are well sorted. The Rollins is an exception to this, being predominantly moderately sorted but showing a range of sorting from well to poor. This parallels the generally larger grain size of the Rollins and may be a function of a more rapid rate of sediment influx and burial during Rollins time, related to the beginning of the Laramide orogeny.

In general, there is little compositional variation between the cored Cozzette of MWX-1 and MWX-2. Pitman and Spencer (1984) have classified the sandstones from the Corcoran and Cozzette as subarkoses (Figure 3.8). The variations shown in Table 3.1 can be attributed to small lateral changes in depositional environment and the fact that part of the upper and lower sandstones were cored in MWX-1, while only the upper sandstone was cored in MWX-2. The high percentages of quartz and low percentage of feldspars and lithic fragments are caused by a high energy depositional environment in which the softer feldspars and lithics are destroyed, leaving a higher percentage of resistant quartz.

The Corcoran core in MWX-2, as noted above, is probably from a distributary environment, rather than a shoreline deposit (although a shoreline deposit underlies it). This difference is reflected in the relatively lower percentage of resistant quartz and dolomite and the generally larger grain size. The higher percentage of void-space clays may also reflect the higher chance of preservation of lithic fragments in this lower energy environment and their subsequent alteration to clay during diagenesis.

The limited Rollins core in MWX-3 seems to reflect a change from the general pattern established by the Corcoran and Cozzette. Its overall larger grain size, higher percentage of lithics, and poorer sorting (probably caused by the initiation of the Laramide orogeny as noted above) combine to significantly decrease porosity. The higher percentage of lithics is also reflected in the higher percentage of clays outside voids, while the lower void-space clay and silica overgrowth content are a function of the lower initial porosity.

As interpreted by Bendix, the paragenetic sequence in all three intervals started with early calcite cementation (Table 3.3), but the Rollins was the only one to subsequently undergo significant compaction. Feldspars then underwent solution and alteration, while authigenic clay formed in all zones except the Corcoran. Quartz overgrowths were subsequently formed and a second episode of calcite cementation occurred in the Corcoran and upper Cozzette. Secondary porosity was then formed in the Rollins and upper Cozzette. Final episodes of authigenic clay formation and dolomitization of calcite completed the diagenetic sequence in most of the intervals.

Spencer and Pitman (1983) and Pitman and Spencer (1984), in overviewing the Bendix petrology reports of the marine blanket zones, noted the presence of an iron-rich chlorite which had previously been interpreted as kaolinite, and that some of the illite reported by Bendix may be sericite. They also noted that the thin section/point count value for porosity is higher than the values obtained by other porosity measurements for these rocks.

Spencer and Pitman (1984) also did SEM work and characterized the intergranular pores, especially the microporosity, as to types of associated clays and the sources of the porosity. According to them, dissolution of feldspars and rock fragments has provided the main source of permeability, the chemical dissolution products going to form authigenic illite and illite-smectite which significantly reduced the primary porosity and permeability. These clays also provide the large surface areas which allow the high water saturations in the reservoirs. Other authigenic mineral phases in the Corcoran and Cozzette include minor amounts of quartz, dolomite (iron-bearing?), and iron-rich chlorite.

3.3 ORGANIC CONTENT AND LEVEL OF MATURATION

3.3.1 Source of Organic Material

Organic material of two types is associated with the marine blanket sandstones. The associated deep-water marine Mancos Shale and its various tongues contain marine organic material that is capable of producing both oil and gas. The interbedded nonmarine coals and carbonaceous mudstones contain terrestrial organic material that produces primarily gas. Levels of maturation in this interval are sufficient that both types of organic material produced gas.

Rice (1983) has analyzed the composition of gases from this interval in MWX-1 and MWX-2 (Table 3.4) and concluded that the gas samples from the marine blanket interval originated primarily from marine source rocks. This agrees with Spencer and Pitman's (1983) observation of pyrobitumen ("cooked-out oil") in core from the upper 20 feet of the upper Cozzette sandstone, which also indicates a marine source rock. Higher CO_2 content and shorter hydrocarbon chains suggest to Rice that a few of the samples had coal or nonmarine organics for a primary source. This is compatible with the presence of coaly rocks within the Corcoran sequence.

3.3.2 Levels of Organic Maturation

The pyrobitumen in the Cozzette sandstone suggests a level of organic maturations equivalent to vitrinite reflectance levels (Ro) of greater than 1.35 (Spencer and Pitman, 1983). Data in Figure 3.9 show an average Ro of 2.11 for samples at 7950 ft in MWX-1 and an average Ro of 2.17 for MWX-2 at 8126 ft. Coal ranks below 7800 ft reach the semianthracite grade at MWX (Nuccio and Johnson, 1984), with Ro values between about 1.3 and 2.07 (Bostick and Freeman, 1984). Coals of this rank have a methane content on the order of 15-25 cm^3/g (Kim, 1977).

3.3.3 Organic Content

In this interval in MWX wells, there are four coals of significance (7, 5, 3 and 3 feet thick) all within the Corcoran interval. Core of a thin coal at 7949-7950 ft in MWX-1 (the only coal cored) was a semianthracite with a heating value of 15,602 Btu/lb (Table 3.5).

The coals are not the only source of organic material. The Total Organic Carbon content of the associated carbonaceous shales that have been analyzed is in the range of 0.12% to 1.42%, and the gas potential is low (Table 3.6). This contrasts with the high gas content present in the Corcoran and Cozzette reservoirs, but as noted above, the gas composition data in Table 3.4 indicate that much of the gas has a marine origin and probably was derived from the associated marine shales.

3.4 FRACTURES

Five vertical natural extension fractures are present in MWX core from the marine zone (Table 3.7). Three of these are oriented W-NW, but two others, in nonreservoir siltstones, are oriented N-NW, and may imply that a subsidiary orthogonal "connecting" set of fractures exists in the marine reservoirs. This would help to account for the high production capacity of these reservoirs. The extension fractures are mineralized with a combination of quartz (early phase) and calcite (later phase).

Numerous natural shear fractures also occur in this zone (Table 3.8). Their orientations appear to be more random than those of the extension fractures. This may be due in part to the low-angle dips and irregularity of the shear planes. Those shear fractures with dips of greater than 10° seem to cluster around an E-W orientation, although a secondary NW mode may also be present (Figure 3.10), possibly supporting the N-NW orientation of the two extension fractures.

Only three of these shear fractures show mineralization. These three contain isolated small pockets of quartz crystals. In other MWX fractures where both calcite and quartz occur, quartz is always the earlier phase. This, plus apparent syndepositional deformation along these shear planes, suggests that these shear fractures were formed early. The absence of later calcite suggests that they were not active or important during later phases of fracturing that affected the reservoir rock.

3.5 REFERENCES

1. Balsley, J. K., 1982, Cretaceous wave-dominated delta systems: East-central Utah: American Assoc. Petrol. Geol., Field Guide.

2. Bendix Field Engineering, 1982-1984, series of contractors' reports on the petrologic characteristics of sandstones in the MWX cores (unpublished).

3. Bostick, N. H., and Freeman, V. L., 1984, Tests of vitrinite reflectance and paleotemperature models at the Multiwell Experiment site, Piceance Creek basin, Colorado: USGS Open File Report 84-757, p 110-120.

4. Flores, R. M., Blanchard, L. F., Sanchez, J. D., Marley, W. E., and Muldoon, W. J., 1984, Paleogeographic controls of coal accumulation, Cretaceous Blackhawk Formation and Star Point Sandstone, Wasatch Plateau, Utah: Geol. Soc. America, Bull. v. 95, pp 599-609.

5. Heinze, D. M., 1984, Overview of Mineralogy/Petrology of the Corcoran, Cozzette and Rollins Sandstone, MWX-1, 2, 3 (2 memos to distribution, 12/6/84), unpublished.

6. Johnson, R. C., 1983, Structure contour map of the top of the Rollins Sandstone Member of the Mesaverde Formation and Trout Creek Sandstone Member of the Iles Formation, Piceance Creek Basin, Colorado: USGS Map MF1667.

7. Kim, A. G., 1977, Estimating methane content of bituminous coalbeds from adsorption data: U.S. Bureau of Mines, Report of Investigations 8245, 22 pp.

8. Lorenz, J. C., 1982, Sedimentology of the Mesaverde Formation at Rifle Gap, Colorado, and its implications for gas-bearing intervals in the subsurface: SAND82-0604, Sandia National Laboratories, 46 pp.

9. Lorenz, J. C., 1983, Reservoir sedimentology in Mesaverde rocks at the Multiwell Experiment site, SAND83-1078, Sandia National Laboratories, 38 pp.

10. Lorenz, J. C., and Rutledge, A. K., 1986 Description of Late Cretaceous Mesaverde Group outcrops at Rifle Gap, Piceance Creek basin, northwestern Colorado: Geol. Soc. America Centennial Field Guide (in press).

11. Madsen D., 1982, Computerized listing of natural fractures in wells MWX-1 and MWX-2: written communication, October 1, 1982.

12. Nuccio, V. F., and Johnson, R. C., 1984, Thermal maturation and burial history of the Upper Cretaceous Mesaverde Group, including the Multiwell Experiment (MWX), Piceance Creek basin, Colorado: USGS Open File Report 84-757, pp 102-109.

13. Pitman, J. K., and Spencer, C. W., 1984, Petrology of selected sandstones in the MWX wells (northwest Colorado) and its relationship to borehole geophysical-log analysis and reservoir quality: USGS Open File Report 84-757, pp 33-66.

14. Rice, D. D., 1983, written communication to A. R. Sattler, February 14, 1983. Spencer, C. W., and Pitman, J. K., 1983, USGS analysis of Corcoran and Cozzette reservoirs in CER #1 and #2 MWX (unpublished).

15. Verbeek, E. R., and Grout, M. A., 1984, Prediction of subsurface fracture patterns from surface studies of joints--an example from the Piceance Creek basin, Colorado, in Spencer, C. W., and Keighin, C. W. (eds.): USGS Open File Report 84-757, pp 75-86.

16. Warner, D. L., 1964, Mancos-Mesaverde (Upper Cretaceous) intertonguing relationships, southeast Piceance Creek basin, Colorado: American Assoc. Petrol. Geol. Bulletin, v. 48, pp 1091-1107.

Table 3.1

Petrologic Summary of Core from the
Corcoran, Cozzette and Rollins Sandstones*
(Summarized by Heinze (1984) from Bendix Reports 1982-84)

PROPERTY	WELL	ROLLINS	COZZETTE	CORCORAN
Mean Grain Size (mm)	1		0.08 (0.06-0.13)	
	2		0.08 (0.06-0.13)	0.11 (0.09-0.12)
	3	0.13 (0.10-0.16)		
Pore Space (%)	1		10.6 (6-18)	
	2		10.7 (2-18)	14.5 (9-18)
	3	4.7 (tr-12)		
Calcite (%)	1		0.2 (0-tr)	
	2		1.7 (0-21)	~0.2 (tr-1)
	3	3.1 (tr-10)		
Dolomite (%)	1		7.8 (0-15)	
	2		7.6 (3-23)	5.2 (1-7)
	3	7.9 (tr-16)		
Quartz (%)	1		59.2 (50-69)	
	2		59.7 (43-69)	49.5 (27-62)
	3	43 (17-53)		
K-feldspar (%)	1		1.1 (tr-3)	
	2		0.7 (tr-2)	~0.2 (0-tr)
	3	2.5 (1-5)		
Plagioclase (%)	1		4.7 (2-8)	
	2		7.6 (4-11)	5.4 (3-8)
	3	7.1 (4-10)		
Lithics (%)	1		2.8 (1-6)	
	2		4.0 (1-8)	5.4 (4-7)
	3	9.9 (7-17)		
Chert (%)	1		1.7 (tr-3)	
	2		1.2 (tr-5)	1.7 (tr-3)
	3	4.1 (3-6)		
Silica Overgrowths (%)	1		5.2 (3-10)	
	2		3.5 (1-5)	4.0 (2-7)
	3	0.7 (tr-2)		
Clay in Voids (%)	1		10.0 (5-18)	
	2		10.2 (2-17)	14.2 (9-18)
	3	4.7 (tr-12)		
Clay Outside Voids (%)	1		4.1 (tr-10)	
	2		1.9 (tr-8)	3.0 (tr-18)
	3	6.4 (tr-17)		

* Average and range of values measured in thin sections

Table 3.2

Further Petrologic Description of Core from the Rollins, Corcoran and Cozzette Sandstones (summarized by Heinze (1984) from Bendix Reports 1982-1984)

CHARACTER	ROLLINS	COZZETTE	CORCORAN
Clay Mineralogy by X-ray Diffraction	Dominant: illite-smectite, regularly interstratified Moderate to minor: illite-smectite, randomly interstratified Minor to trace: chlorite and kaolinite	Dominant: alternating zones of dominant illite-montmorillonite and chlorite	Dominant: illite-montmorillonite, except near bottom where chlorite is dominant
Porosity	Reduced intergranular from compaction, cementation, and authigenic clays Intergranular from partial dissolution of detrital grains	Microporosity in intergranular pore space	
Trace Minerals (inconsistent)	Biotite, muscovite, siderite, zircon, tourmaline, anatase, pyrite, glaucophane-celadonite, rutile, garnet, and carbonaceous material	Muscovite, biotite, zircon, tourmaline, garnet, epidote, detrital chalcedony, and carbonaceous material	

Table 3.3

General Paragenic Sequences Within the Corcoran, Cozzette and Rollins Sandstones in the MWX Wells (Compiled from the Bendix Reports 1982-1984)

TIMING	EVENT	ROLLINS	COZZETTE	CORCORAN
Late	Dolomitization of calcite		x	x
	Formation of authigenic clay	x	x	x
	Formation of secondary porosity	x	x	
	Precipitation of calcite cement		x	x
	Precipitation of quartz cement	x	x	x
	Formation of authigenic clay	x	x	
	Alteration of feldspar	x	x	x
	Compaction	x		
Early	Precipitation of calcite cement	x	x	x

Table 3.4

Chemical and Isotopic Composition of Gases from Core and Well Test Samples (Rice, 1984)

Sample		C_1	C_2	C_3	iC_4	nC_4	C_5	CO_2	N_2-air	^{13}C (per mil)
Core Gas Samples (Desorption)										
MWX-1:	5885'	84.25	5.08	1.19	0.32	0.21	-	0.01	8.93	-36.9
	6662'	72.19	3.77	0.22	0.08	0.06	0.10	4.6	18.97	-35.77
	6779'	51.99	2.27	0.35	0.08	0.03	0.01	2.3	62.98	-37.14
MWX-2:	4920'	90.74	1.58	0.11	0.05	tr	-	7.42	0.08	-36.74
	5788'	10.07	0.45	0.07	0.01	tr	-	0.02	89.38	-35.91
(coal)	7204'	50.93	0.64	-	-	-	-	2.01	46.41	-29.07
	7371'	24.2	0.4	0.01	-	-	-	1.96	73.44	-33.83
(coal)	7381'	67.93	0.66	-	-	-	-	2.77	28.63	-31.27
	7895'	41.73	0.14	-	-	-	-	1.02	57.11	-34.10*
	8132'	6.84	0.01	-	-	-	-	0.08	93.07	-35.81*
Well Test Gas Samples										
MWX-1:										
8110-8220	9/08/82	95.85	0.38	-	-	-	-	3.77	tr	-33.35*
7830-7890	9/09/82	96.87	0.25	0.30	0.04	tr	-	2.50	0.04	-33.34*
7830-7890	9/28/82	96.76	0.36	0.05	0.01	tr	-	2.77	0.04	-33.62*
7830-7890	10/12/82	96.02	0.27	0.02	0.02	tr	-	2.46	1.19	-33.29*

*Of interest to this report

Table 3.5

Coal Analysis Report for Cozzette
Coal Sample: 7949-7950 ft in MWX-1
(Memorandum: C. G. Tremain, Colorado Geologic Survey
to A. R. Sattler, Sandia, November 18, 1982)

	Coal (as recd)	Coal (moist. free)	Coal (moist./ash free)
Proximate Analysis (%)			
Moisture	3.72	n/a	n/a
Volatile Mater	11.76	11.84	14.39
Fixed Carbon	66.97	70.48	85.61
Ash	17.55	17.68	n/a
Ultimate Analysis (%)			
Hydrogen	3.51	3.45	4.19
Carbon	72.67	73.20	88.92
Nitrogen	1.24	1.24	1.51
Sulfur	3.98	4.01	4.87
Oxygen	1.05	0.41	0.50
Ash	17.55	17.69	n/a
Heating Value (btu/lb)	12,502	12,593	15,298

Table 3.6

Rock Eval. Pyrolysis Data from the Marine Interval
(Core Laboratories Reports: 3/6/84, 6/12/84 and 8/10/84)

Depth (ft)	Description	Total Organic Carbon (%)	Gas Evolved* (mg/gm rock)		
			S_1	S_2	S_3
	MWX-1				
7898.0	Laminated black siltstone and claystone (sealed)	0.93	0.09	-	0.21
7899.0	Black burrowed siltstone (sealed)	0.12	0.05	-	0.20
7923.5	Bioturbated sandstone-shale mixture	0.77	0.29	-	0.20
7938.0	Laminated mudstone with pyrite inclusions	1.42	0.15	-	0.19
7948.0	Grey-black laminated siltstone and mudstone	0.98	0.17	-	0.28
	MWX-2				
7825.0	Black carbonaceous mudstone	0.81	0.13	-	0.31
7830.0	Black carbonaceous mudstone (sealed)	0.73	0.02	-	0.22
7898.0	Grey-black laminated siltstone and mudstone	0.97	0.12	-	0.29
7900.0	Grey-black laminated siltstone and mudstone	0.58	0.20	-	0.38
7905.0	Laminated siltstone and mudstone	0.62	0.40	-	0.20

*S_1 free hydrocarbons present
S_2 hydrocarbons produced by thermal conversion of kerogen
S_3 organic carbon dioxide produced by pyrolysis of kerogen

Table 3.7

Marine Mineralized Extension Fractures

Core Depth of Frac	Frac Height (ft)	Max Width (mm)	Filling: Type	Filling: Amount	Strike: w/PSL	Strike: True	Dip	Rock Type	Terminations: Top	Terminations: Bottom	Comments
MWX-1											
7903.7-04.6	0.9	0.5	other + calcite	complete	040	N80W	90°	fine ss	out of core	at mudst. contact	These two fracs are connected in the core by what appear to be drilling-induced petalfracs
7903.7-04.6	0.9	0.25	other + calcite	partial	056	N64W	90°	fine ss	0.1' from mudst. contact	at mudst. contact	
MWX-2											
8112.6-15.3	2.5	2.0	calcite	complete	141	N84E	90°	ss	within ss, at or near carb. lamination	not avail. (sample out)	
8123.3-23.5	0.1-0.2	4.0	qtz + calcite	mostly complete	210	N32W	70-90°	muddy siltst	within siltst.	within siltst.	Mostly qtz-filled fracs intersect core in this general location
8124.2-24.7	0.5	8.0*	euhed. qtz + calcite	partial	045	N17W	80-90°	interlam. siltst. + organ.-rich mudst.	out of core or en echelon	within lith.	Lower part of this frac displays 5 mm offset

*Madsen (1983) data used for width; sample currently not in library.

Table 3.8 Marine Shear Fractures

Core Depth of Frac	Strike w/PSL	Strike True	Dip (degrees)	Rock Type	Comments
MWX-1					
7913.0	350	S53W	5	mudst.	Euhedral qtz in spots; plane is irreg.
7920.8	230	E-W	5	carb. mudst. lam. in ss	
7921.9	245	N75W	10	"	
7922.5	227	S87W	15	"	
7942.1	325	N48W	10	"	
7945.2	090	S77W	15	"	
7948.3	155	N37W	5	"	
7949.7	070	S58W	5	on contact between mudst. and coal	
MWX-2					
7817.0-17.1	005	S59W	40	siltst.)	From Madsen (1983);
7818.6-18.8	170	S44W	30	siltst.)	sample not in library
7836.2	303	S15W	5	carb. mudst. lam. in ss	now
7838.6	308	S20W	5	"	
7838.9	320	S32W	5	"	
7840.0	290	S3W	5	"	
7841.2	-	-	0-5	"	Euhedral qtz in patches, generally rough plane, polished in spots
7841.8	240	N52W	10	"	
7842.8	-	-	0	"	
7843.9-44.0	110	S2W	10-30	"	Slicks occur in patches, euhedral qtz occurs in spots
7845.1	280	N7W	10	"	
7850.7	245	N42W	5	"	
7852.4	233	N54W	10-15	"	
7896.2	090	N7W	10	"	
7896.4	020	N77W	10	"	
7897.9	170	-	5	"	
7898.1-98.2	303	-	15	"	
7903.2	020	S22W	10	"	
8118.6-18.7	340	N79W	20	"	
8121.6-21.7	345	N74W	15	"	

Table 3.8 Marine Shear Fractures (cont'd)

Core Depth of Frac	Strike w/PSL	Strike True	Dip (degrees)	Rock Type	Comments
MWX-2 (cont'd)					
8122.3	013	N46W	10	carb. mudst. lam. in ss	
8122.4-22.5	015	N47W	20	"	
8122.8-22.9	335	N87W	30	"	
8122.9	305	S63W	7	"	
8123.1-23.2	315	S73W	15	"	
8123.3	383	S41W	10	"	
8123.9-24.2	220	N22W	50	interlam. siltst. & mudst.	Very planar and polished cross-cut laminations. There are irreg. very small-scale faults associated with this shear plane
8124.9	343	S81W	12	carb. mudst. lam. in ss	
8126.7	345	S83W	15	carb. mudst.	

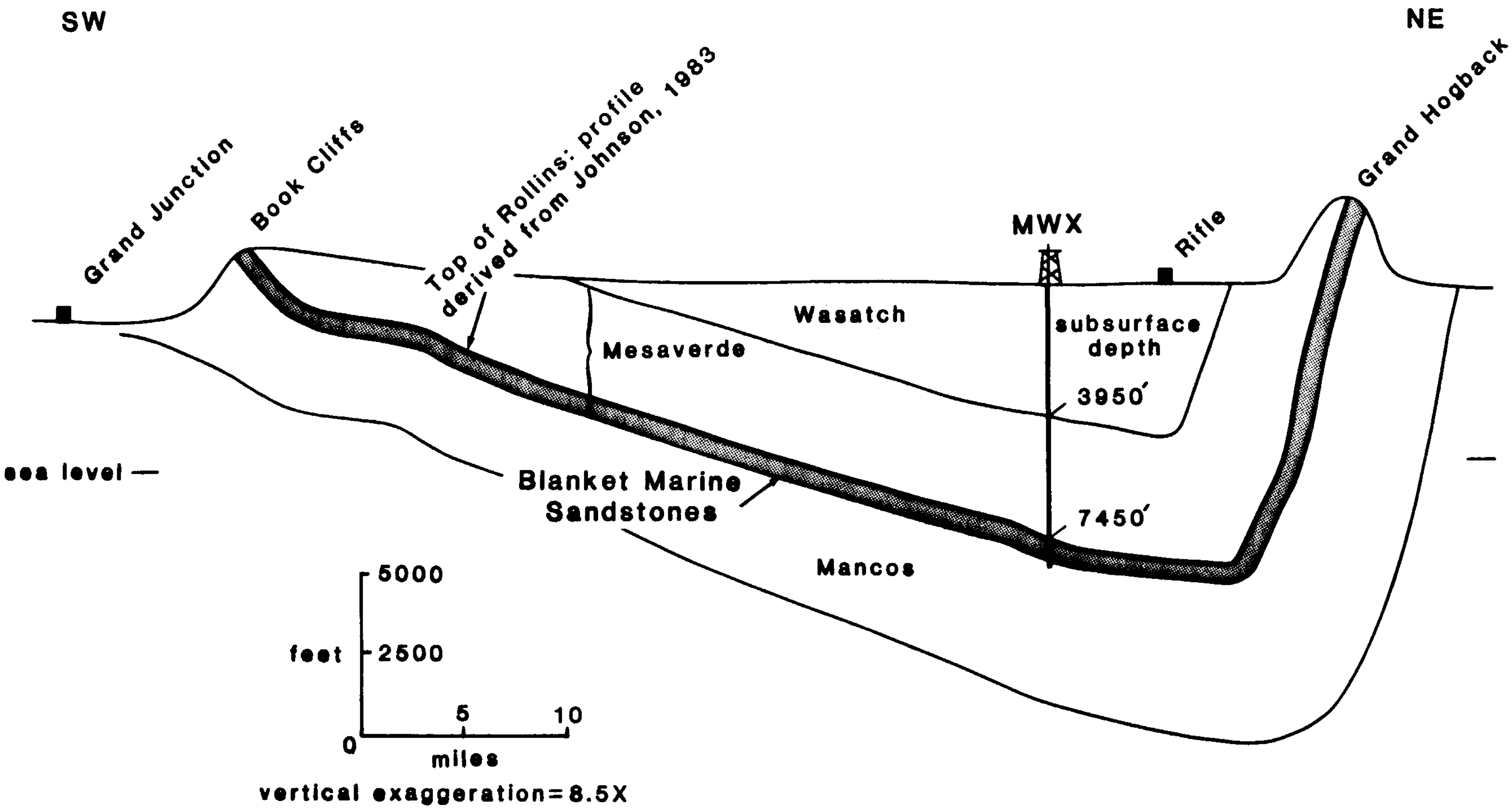

Fig. 3.1 General Structure of the Mesaverde Formation in the Piceance Creek Basin

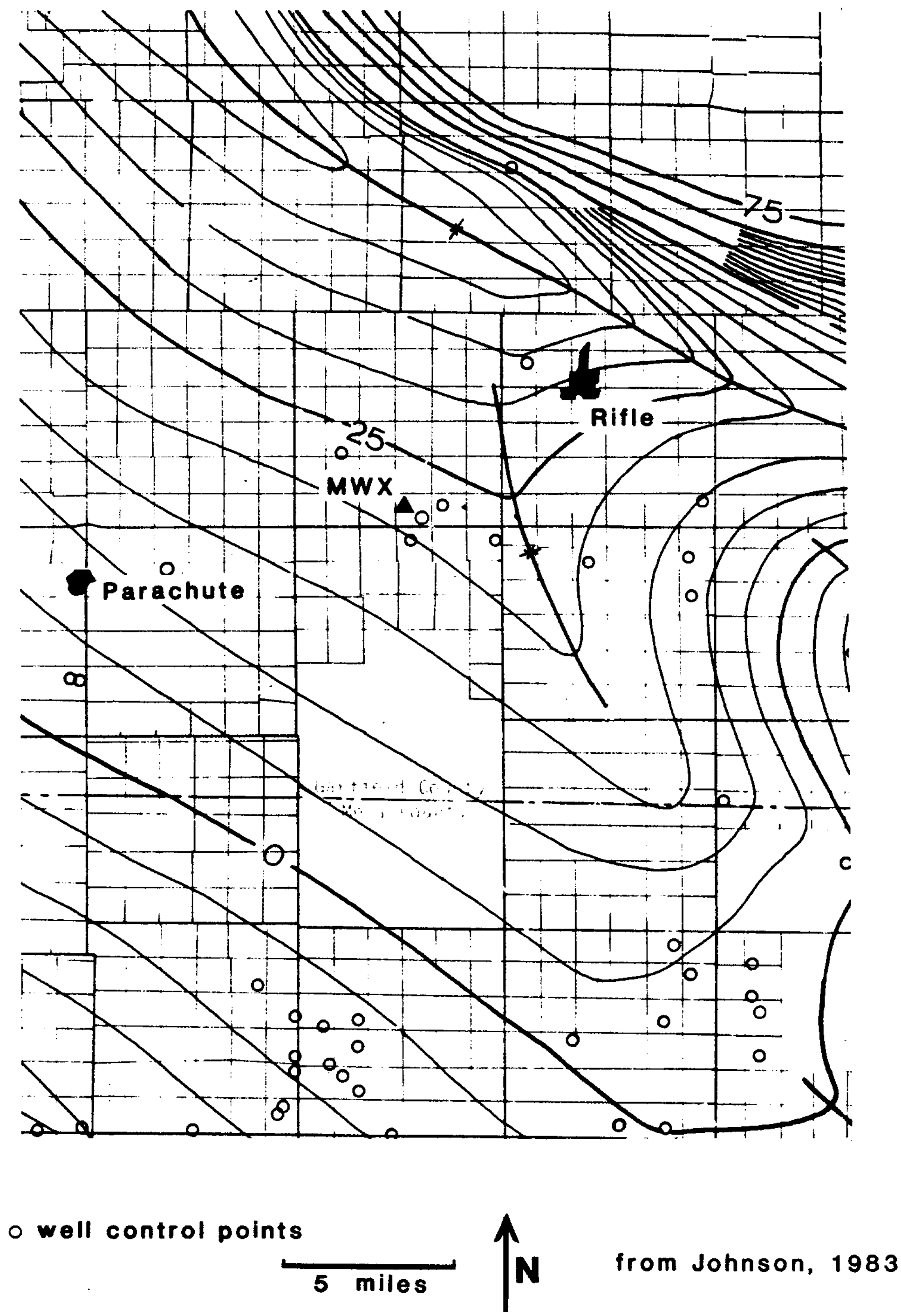

Fig. 3.2 Structure Contours on Top of the Rollins Sandstone Contours in Hundreds of Feet Above/Below Sea Level

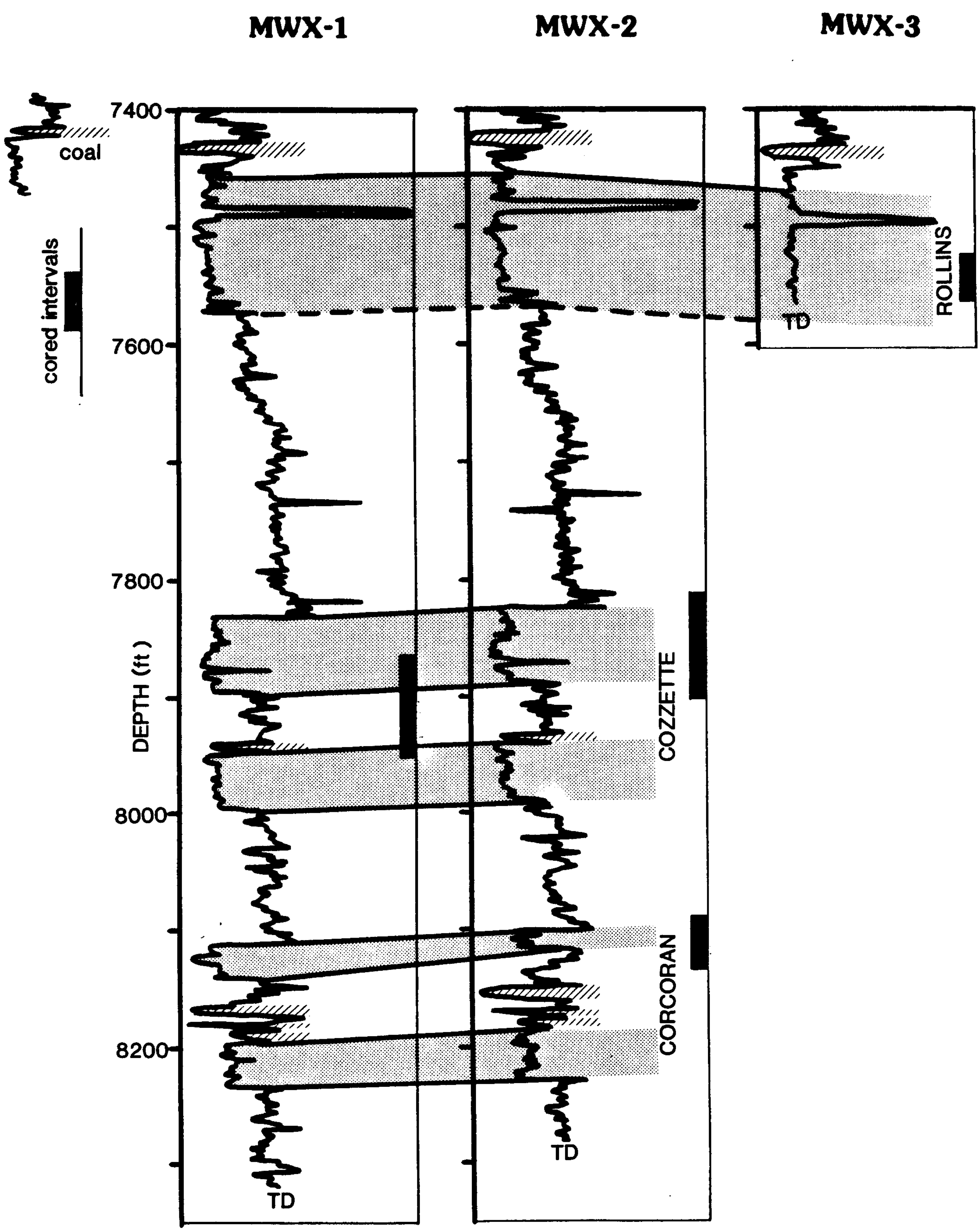

Fig. 3.3 Corcoran, Cozzette and Rollins Members of the Mesaverde Group in the MWX Wells: Gamma Ray Log

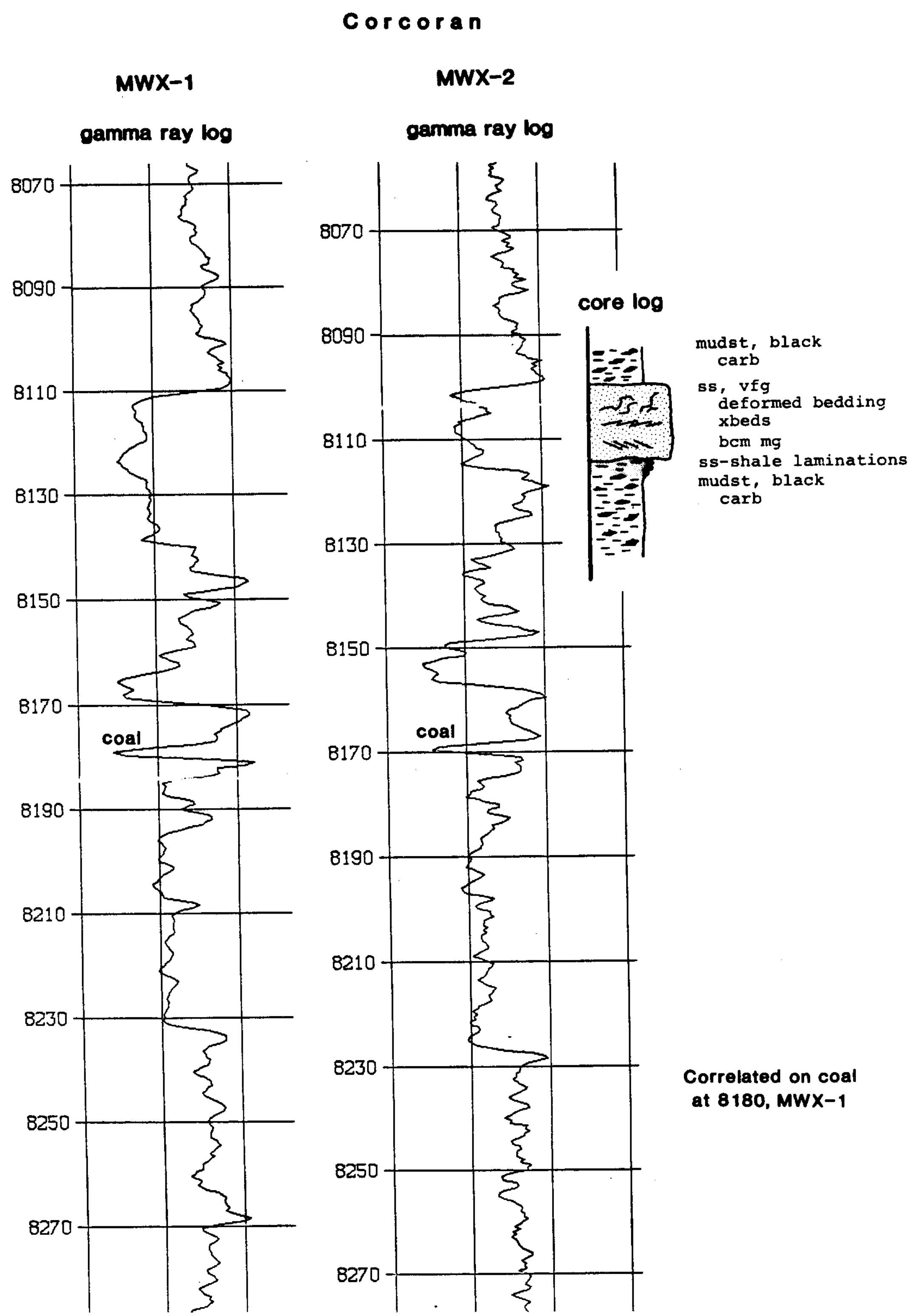

Fig. 3.4 Lithologic and Gamma Ray Logs of the Corcoran in MWX Wells

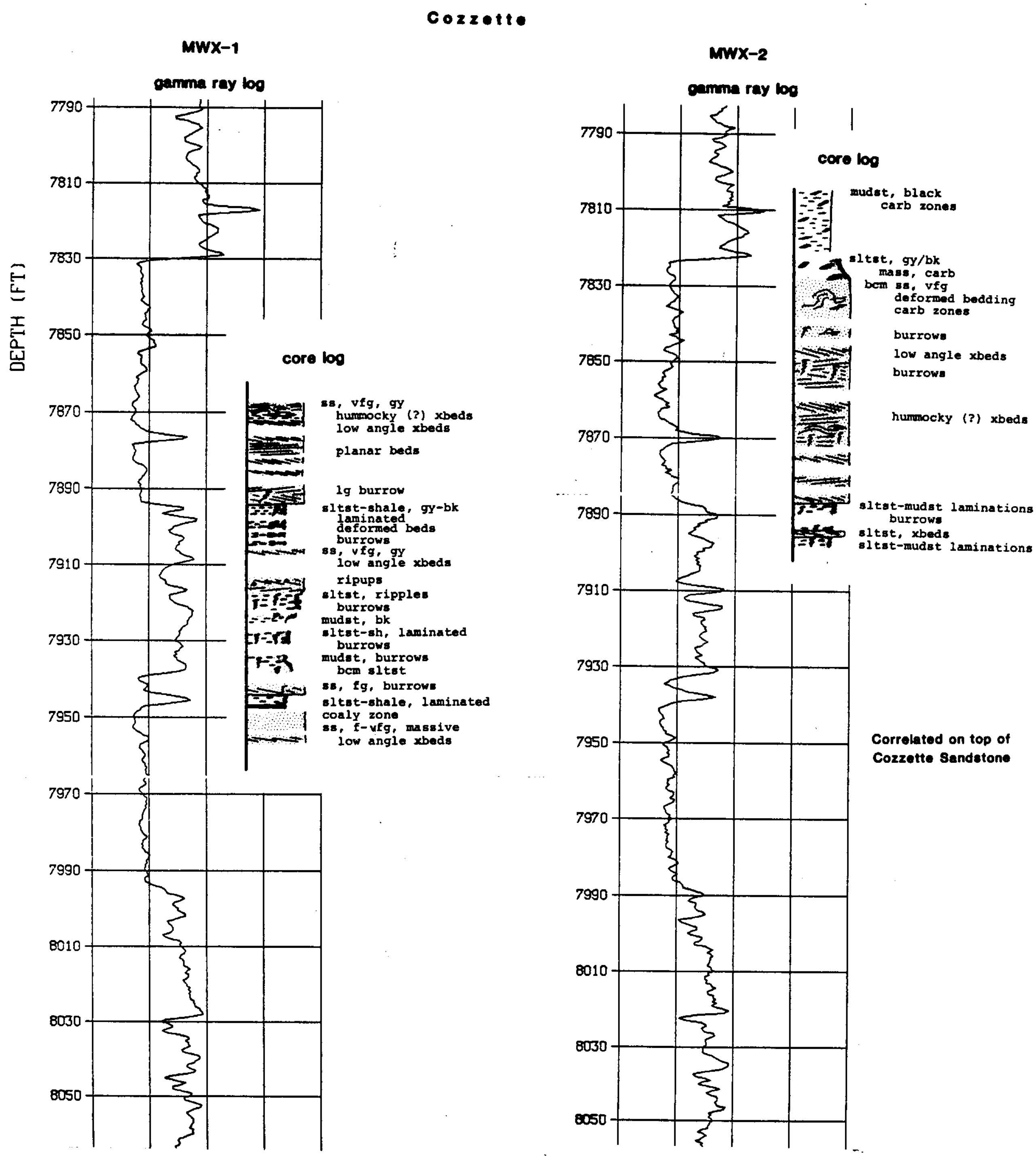

Fig. 3.5 Lithologic and Gamma Ray Logs of the Cozzette in MWX Wells

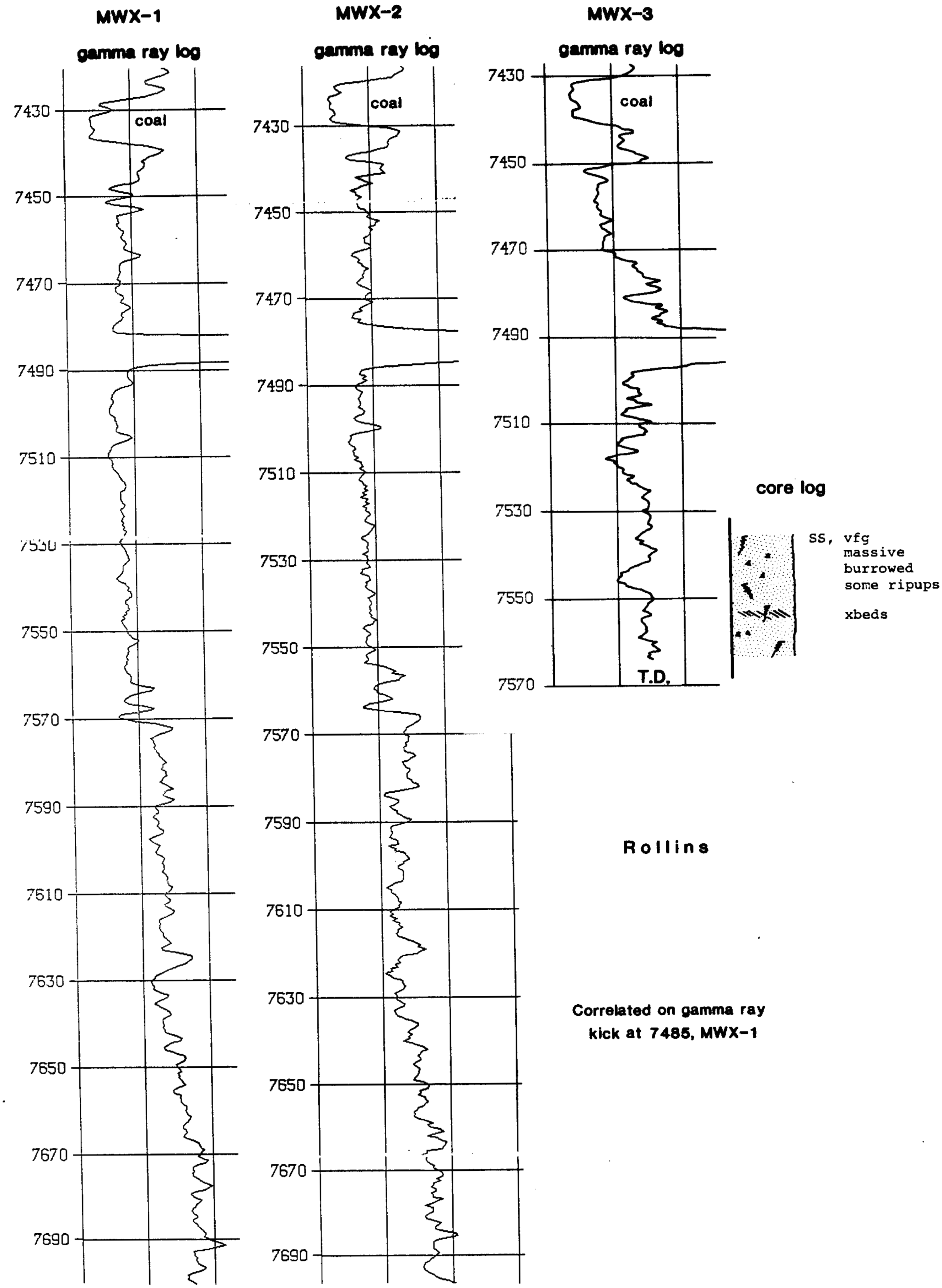

Fig. 3.6 Lithologic and Gamma Ray Logs of the Rollins in MWX Wells

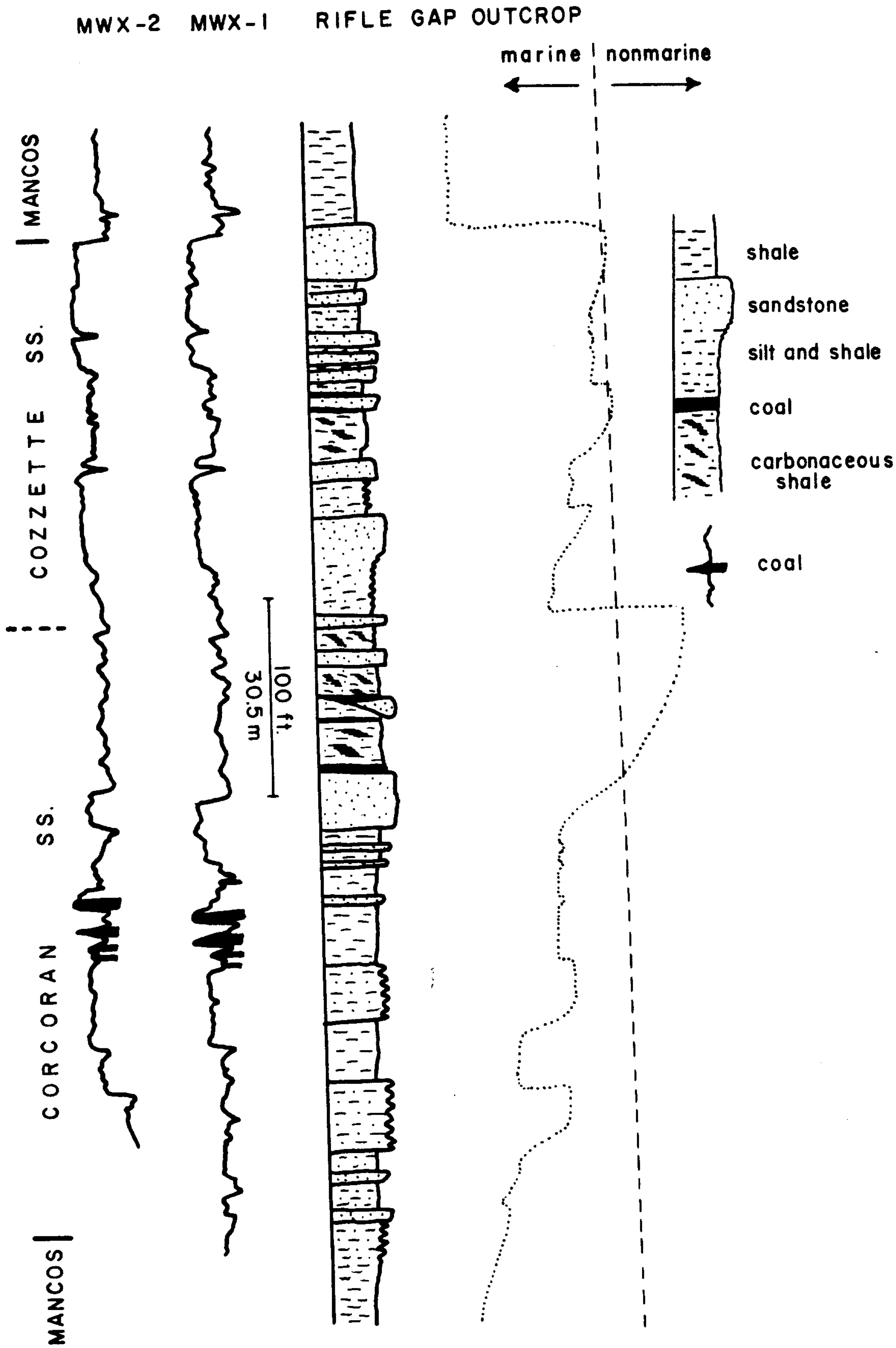

Fig. 3.7 Outcrop (Rifle Gap) to Subsurface (MWX Wells) Correlation of the Marine Section

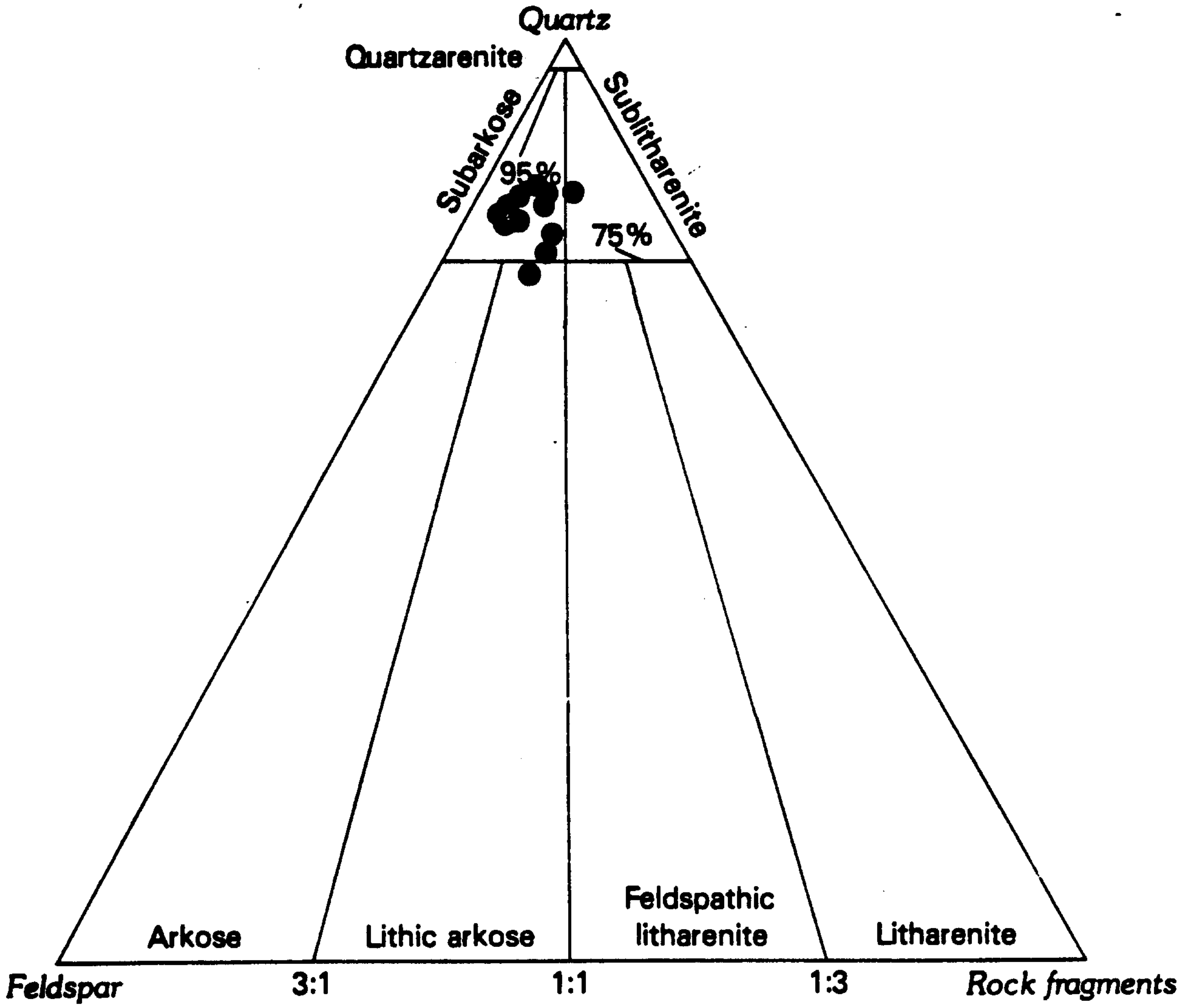

Fig. 3.8 Tertiary Diagram Showing Mineralogic Composition of Sandstones in the Corcoran and Cozzette Intervals (from Pitman and Spencer (1984), figure 22)

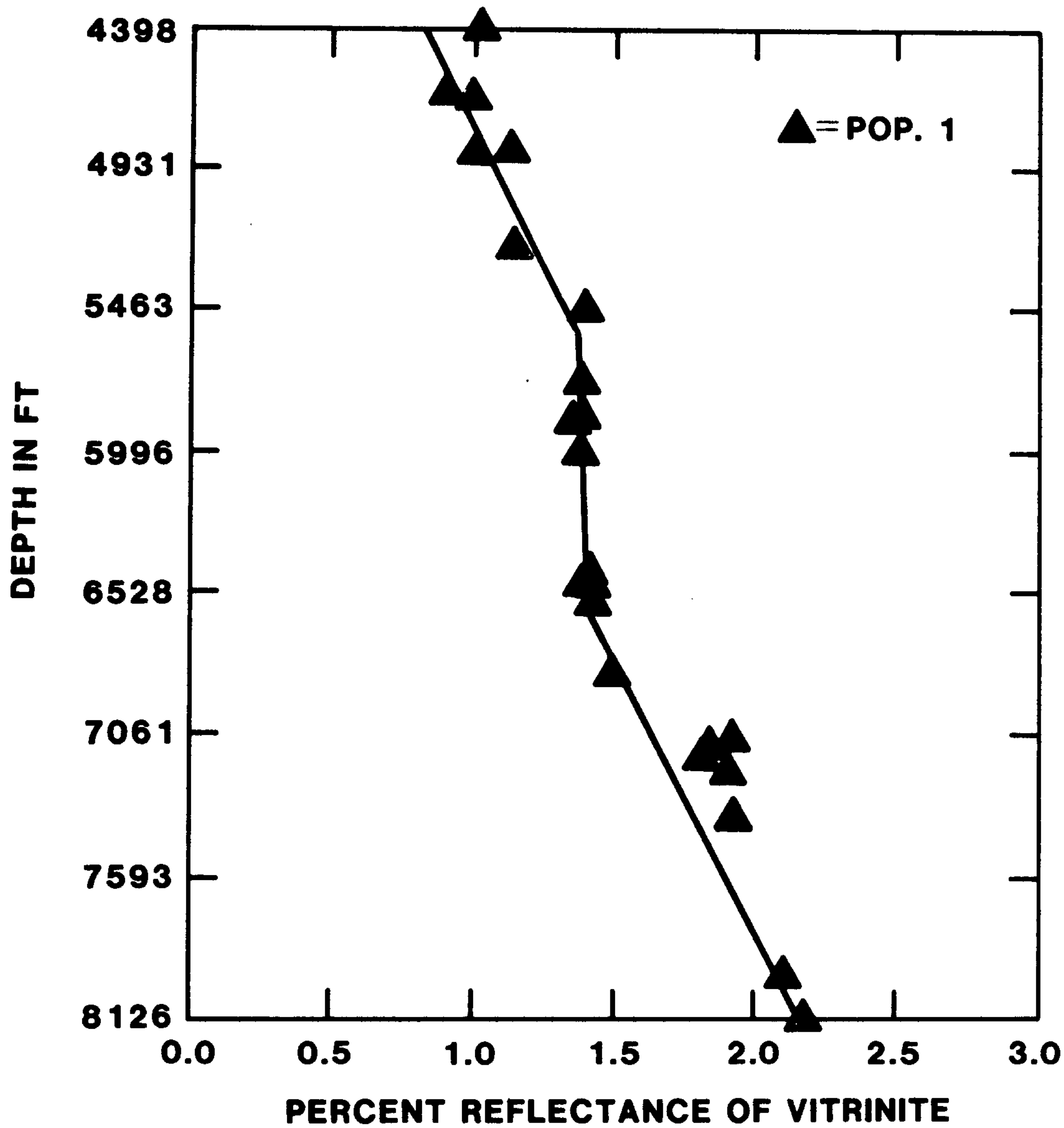

Fig. 3.9 Vitrinite Reflectance Data from MWX-1 and MWX-2 (written communication from Amoco, Denver, Colorado)

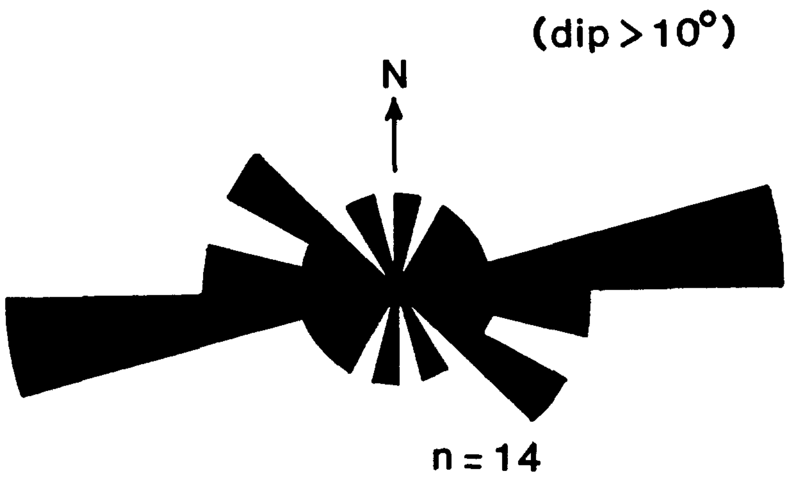

Fig. 3.10 MWX-1 and MWX-2 Shear Fractures

INTENTIONALLY LEFT BLANK

4.0 LOG ANALYSIS

G. C. Kukal
CER Corporation

4.1 LOG DATA

Extensive logging programs were conducted during the drilling of the Multiwell Experiment wells.[1,2] The Corcoran/Cozzette marine sand intervals in MWX-1 and MWX-2 were logged only once, as they were at the bottom of each well. The logging programs for these two wells were:

(1) MWX-1 (Reference 1)

Dual Induction/Gamma Ray/Spontaneous Potential
Lithodensity/Compensated Neutron/Gamma Ray/Caliper
Long Spaced Sonic
Epithermal Sidewall Neutron/Gamma Ray/Caliper
Electromagnetic Propagation/Gamma Ray/Caliper
Multiple Spaced Sonic
Dipmeter
Fracture Identification
Repeat Formation Test
Nuclear Magnetic
Natural Gamma Spectroscopy

(2) MWX-2 (Reference 2)

Dual Induction/Gamma Ray/Spontaneous Potential
Circumferential Microsonic/Gamma Ray
Lithodensity/Compensated Neutron/Gamma Ray/Caliper
Long Spaced Sonic
Multiple Spaced Sonic
Sidewall Neutron/Gamma Ray/Caliper
Dipmeter
Fracture Identification

The basic logs are given in Figures 4.1-4.10 according to the following format:

	MWX-1	MWX-2
Resistivity	Figure 4.1	Figure 4.6
Density-Neutron	4.2	4.7
Bulk Density	4.3	4.8
Spectral Gamma	4.4	4.9
Long-Spaced Sonic	4.5	4.10

4.2 LOG ANALYSIS

The analysis of the MWX-1 marine section incorporates data from the dual induction/gamma ray log (DIL/GR), the lithodensity/compensated neutron/gamma ray/caliper log (LDT-CNL), the long spaced sonic log (LSS), the cement bond log (CBL), and core measurements. The latter include core porosity (ϕ core), core permeability (k), grain density (ρgr), and water saturation (S_w core). Comparable data were used in MWX-2 analysis; an FDC bulk density was used, as no LDT was available.

The well logs have been analyzed with the tight gas sand log interpretation computer model TITEGAS, which was developed by CER to provide better determination of the physical and mechanical properties of tight gas sand formations.[3] The clay, volume, porosity, and water saturation (both of the flushed zone and the virgin formation) are computed in a model primarily based on the LDT/CNL and DIL/GR logs. The model also computes volume carbonate from the photoelectric effect recorded on the lithodensity log. The photoelectric response is corrected for clay content and is normalized for borehole effects. A volume carbonate is derived from the adjusted data.

The model corrects density porosity for variable grain density and, in conjunction with neutron porosity and a clay indicator such as the gamma ray, calculates the average flushed-zone saturation, S_{xo}. Neutron porosity is first corrected for volume carbonate and for mud, temperature, and pressure effects. Using the computed S_{xo}, porosity is obtained. R_w is computed in uninvaded sandstones by combining S_{xo}, porosity, and resistivity log data. Finally, the virgin formation water saturation is calculated by the total shale relationship. The two saturations, when compared, indicate the presence of invasion and allow the identification of permeable zones. In addition, calculated permeability based on porosity, clay content, and irreducible water saturation allows a quantitative estimation of in situ intrinsic permeability.

A useful byproduct of the analysis is the calculation of R_w. A value of R_w was determined in each tight, uninvaded zone through the well and these are plotted as an R_w profile in Figure 4.11. R_w does not maintain a constant rate of change with depth as is usually assumed, but is highly variable. The variability of the upper portion of the MWX-1 well is attributed to the influx of fresh meteoric waters; the zone at 4700 to 4900 ft appears to be in communication with the surface. Water in the central fluvial zone becomes less resistive with increasing depth and temperature. At 6500 ft in the paludal section, the water becomes unexpectedly fresh, probably due to dewatering of coals. At the top of the marine section, approximately 7500 ft, R_w drops to a value consistent with an extrapolation from the fluvial section and remains relatively constant.

The calculated water resistivity of the marine interval is approximately 0.11 ohm-m. A water sample from this interval in a nearby well, the Clough 21, located in Section 20, T6S, R94W, was obtained and analyzed. This well is approximately 2-1/2 miles to the northwest of the MWX site and the resistivity should remain relatively unchanged over the distance. The results of the analysis of the Clough 21 sample are shown in Table 4.1. The measured resistivity value of the water sample was 0.141 ohm-m, in agreement with the calculated MWX-1 value.

Additional details of the analysis, separated into discussions of saturation, porosity, lithology and permeability, can be found in Appendix 9.2 and Reference 3.

A separate analysis was performed on the long-spaced sonic log data to provide an estimate of formation mechanical properties. Calculated shear moduli, Young's moduli, and Poisson's Ratios are shown in Figure 4.12.

4.3 FORMATION EVALUATION

There are four major sands in the Corcoran/Cozzette interval that are candidates for stimulation and testing. The following description was derived using logs from MWX-1, the primary well. The upper two sandstones, separated by 44 ft of siltstone and shale, are called the Upper and Lower Cozzette sandstones. The two lower sand bodies, separated by 54 ft of siltstones, shales and coals are called the Upper and Lower Corcoran sandstones. The Cozzette is separated from the Corcoran by 115 ft of shale and siltstone. The sandstones are identified by the lithodensity/compensated neutron/gamma ray logs shown in Figure 4.13 for the Cozzette and in Figure 4.14 for the Corcoran interval.

The figures present two different density and neutron curves. The ϕd and ϕn curves are identical to the original logs. The "ϕn in situ" and "ϕd in situ" curves have been calculated by the TITEGAS model and represent the density and neutron response that would occur if the sands were totally uninvaded, i.e. if virgin conditions had been preserved.

Reservoir data for the marine sandstones in both wells are summarized in Table 4.2. Clay volume, porosity, water saturation, and core data are averaged for each sandstone. Figure 4.15 and 4.16 present the model results in log form for MWX-1. Figures 4.17 and 4.18 are the model results for MWX-2. The left-hand side is a bulk volume analysis of the rock. Amounts of clay, sand, and carbonate are calculated and plotted. Porosity is broken down into water-filled and hydrocarbon-filled pore space. The center track presents shallow and deep water saturation of the formation, with the difference accumulated on the left edge. This difference, ΔS_w x h, is a measure of invasion and inferred permeability. The right track contains porosity and permeability analysis. Calculated values are plotted with core data for comparison. Permeability is accumulated for each continuous section of sandstone.

Referring to Figures 4.15-4.18, the Cozzette sandstone appears to be more invaded than the Corcoran sandstone. This may indicate the true respective permeabilities of the units, or may indicate only that the upper sands were exposed longer to overbalanced drilling conditions at the time of the logging.

4.3.1 Cozzette Sandstone

The Cozzette sandstone is discussed using MWX-1 results. The unit appears nearly identical in MWX-2.

The Upper Cozzette sand extends from 7830 to 7895 ft, with a 3-ft shale break at 7875 to 7878 ft, and is a massive, uniform, fairly clean sand. This sand is invaded and has the highest core-measured permeability in the Corcoran/Cozzette cored interval. The lower two-thirds of the sand is relatively consistent in character, having moderate water saturation (51.0 percent) and low porosity (7.3 percent). The upper third of the unit has a high calculated water saturation and low core porosity (MWX-2 core data). The indicated occurrence of this wet zone over the lower gas zone is puzzling and a better interpretation has been sought.

C. W. Spencer of the USGS has noted the possible occurrence of pyrobitumen (i.e., solid hydrocarbon) in this same interval in MWX-2 core. This observation supports a different interpretation of the upper zone: that the pore space is filled with immobile water, pyrobitumen and probably gas. Log-derived porosity would represent the total porosity, regardless of pore fluids, and this would necessarily be larger than core-measured porosity, assuming the pyrobitumen would not be completely extracted from the core before measurement. Effective porosity is reduced because of the pyrobitumen, and since the pore throats are occupied by this solid material, effective permeability for all fluids is minimal. Accordingly, stimulation of this upper zone will result in little gas production but will not watercut gas being produced from the lower two-thirds of the sand.

The MWX-1 mud log (Figure 4.19) of the Cozzette recorded a gas show at 7854 to 7864 ft, directly below the possible pyrobitumen zone. Fractures were identified at 7862 ft and possibly at 7869 ft using the cement bond log.

The Lower Cozzette sandstone, extending from 7939 to 7995 ft, is a massive, relatively clean sand with a shale and coal break at 7944 ft, separating a thin upper sand from the lower main body. The upper sand exhibits low porosity and low water saturation, an unusual occurrence. A fracture was observed in the core at 7939 ft and was identifiable on the cement bond log. This sand is probably in natural fracture communication with the underlying potential gas-producing zone.

A major mud log gas show occurred at 7946 to 7957 ft, as shown in Figure 4.19. Fractures were noted in core at 7945 ft and 7946 ft and a fracture signature is present on the cement bond log at the same depth. The gas show on the mud log was not a sudden occurrence; there was a long buildup starting at 7897 ft immediately below the base of the Upper Cozzette sand. Gas shows increase through the siltstone and shale interval between the two sands and several fractures were noted on core from the same interval. Very probably, this fracture system was communicating gas upwards from the 7946 to 7957 ft zone and the gas was first detected while drilling at 7897 ft.

The zone at 7946 to 7957 ft appears to be one of the better reservoirs in the Corcoran/Cozzette interval; although the porosity is low, the likely presence of natural fracture permeability greatly enhances the production potential. Some matrix permeability is developed. S_w is about 50 percent.

The remainder of the Lower Cozzette sandstone is less attractive. No mud log gas shows or fractures were detected in this interval. Water saturation is generally on the high side; permeability is low except for a favorable section at 7976 to 7983 ft. Here water saturation is lower and a better porosity is developed.

Based on the foregoing, the Upper Cozzette sand is considered a good candidate for gas production. The sand is naturally fractured, is thick, has uniform reservoir properties, and contains gas. While the upper pyrobitumen zone is a poor reservoir, it should not adversely affect production from the lower zone should a hydraulic fracture extend upward. The best reservoir rock in this sand occurs between 7870 and 7893 ft.

The Lower Cozzette has two good permeable zones at 7948 to 7955 ft and 7976 to 7982 ft which should be tested separately. Because of the prolonged gas show obtained prior to penetrating this unit, it is inferred that the overlying shales have a conductive fracture network and will probably not act as an effective barrier to upward fracture propagation. However, the cementing is good in the Cozzette and adjacent rocks and effective fracture treatments of the overall unit should be possible.

4.3.2 Corcoran Sandstone

The Upper Corcoran sandstone in MWX-1 extends from 8110 to 8140 ft and consists of an upper 10 ft of clean sandstone overlying 7 ft of calcareous sandstone, with 12 ft of clean sandstone lying below. The uppermost zone has lower porosity and higher water saturation than the lowermost. Neither zone appears invaded, but this may be because of insufficient drilling time for flushing. The middle zone appears very clean, but has extremely low porosity. The photoelectric effect log in this interval detected a large amount of a heavy mineral not recorded by the gamma log; this mineral is postulated to be calcite, dolomite or a mixture of the two.

The mud log through this interval (Figure 4.20) recorded no gas shows. No fractures were identifiable on the cement bond log and the rock appears to be very tight. The net sand development in this interval correlates poorly between MWX-1 and MWX-2. In MWX-2, the Upper Corcoran sandstone is about half as thick (14 ft). It does not appear attractive.

Below the Upper Corcoran sand, in MWX-1, there is a 45-ft sequence of shales, siltstones, coals, and thin sands. The Lower Corcoran sand appears at 8194 ft and extends to 8232 ft. Generally, this sand exhibits low porosity except at 8202 to 8208 ft. A fracture was identified at 8209 ft. The unit appears invaded from 8194 to 8208 ft. The interval from 8217 to 8226 ft also appears to be somewhat invaded and a probable fracture was identified in the interval. In MWX-2, the unit appears tight throughout, except for a thin permeability development at 8221 to 8225 ft.

The MWX-1 mud log of the Lower Corcoran sand recorded two gas shows. The first, from 8193 to 8211 ft, includes the upper invaded zone and the high porosity zone. The second, from 8217 to 8237 ft, includes the lower invaded and fractured zone. Gas flow is obviously natural fracture related throughout the marine interval.

Although the Lower Corcoran was successfully cemented, there is no shale barrier above it and the cementing also deteriorates above the sand. Accordingly, it will be difficult to contain a fracture within this interval.

4.3.3 Evaluation Summary

The marine sandstones in MWX-1 are massive, relatively clean blanket units that have generally low porosity and permeability. Natural fractures are common and these control gas flow; each major gas show has been correlated to a natural fracture system. The lithology of these units is not as complex as the more arkosic fluvial intervals; however, clay, coal and carbonate material complicate porosity and saturation determinations.

The two Cozzette sands are candidates for testing and stimulation. The sands are thick, uniform in character, and are potential reservoirs. Individual fracture treatments of the two sands are possible, although it is likely that a fracture in the Lower Cozzette would extend into the Upper Cozzette.

The two Corcoran sands are less viable candidates for testing and stimulation, particularly the upper unit. The lower sand contains the best permeability and has a greater thickness, and this sand is a third candidate for testing.

4.4 REFERENCES

(1) CER Corporation, "Multi-Well Experiment: MWX-1 As-Built Report," Sandia National Laboratories Contractor Report, SAND82-7201, July 1982.

(2) CER Corporation, "Multi-Well Experiment: MWX-2 As-Built Report," Sandia National Laboratories Contractor Report, SAND82-7100, August 1982.

(3) Kukal, G. C., "A Systematic Approach for the Effective Log Analysis of Tight Gas Sands," SPE/DOE/GRI 12851, Proceedings of the 1984 SPE/DOE/GRI Unconventional Gas Recovery Symposium, Pittsburgh, PA, May 1984, pp 209-220.

Table 4.1

Chemical Analysis of Corcoran Cozzette Formation Water Taken from the Clough 21 Well, 2½ Miles Northwest of the Multi-Well Site

PARAMETER	RESULTS
Iron, mg/l:	8.2
Calcium, mg/l:	106.0
Magnesium, mg/l:	19.8
Potassium, mg/l:	351.0
Sodium, mg/l:	5,850.0
pH	7.1
Boron, mg/l:	0.29
Alkalinity:	
Carbonate, mg/l:	0
Bicarbonate, mg/l:	774.0
Hydroxide, mg/l:	0
Total Alkalinity, mg/l:	774.0
Chlorides, mg/l:	11,546.0
Sulfates, mg/l:	4.0
Total Solids, mg/l:	17,915.0
Electrical conductivity, μmhos/cm:	26,000.0
Electrical resistivity at 220°, ohm-m:	0.141

							CORE DATA		
DEPTH	SAND THICKNESS	Vcl	ϕ	Sw	ΔSw	Kh	ϕ	ρgd	Kmax
MWX-1									
1. Upper Cozzette 7831.0 - 7894.5 [1]	62.5	.093	.070	.588	.215	.42	.071	2.67	.024
(7854.0 - 7894.5) [2]	39.5	.079	.073	.511	.259	.37	.071	2.67	.024
2. Lower Cozzette 7939.5 - 7995.0	52.0	.110	.075	.647	.164	.29	.056	2.65	.018
3. Upper Corcoran 8111.5 - 8140.0	29.0	.094	.067	.575	.112	.20	-	-	-
4. Lower Corcoran 8195.0 - 8232.0	35.5	.183	.059	.449	.100	.30	-	-	-
MWX-2									
1. Upper Cozzette 7823.0 - 7887.0 [1]	61.0	.110	.067	.574	.235	.43	.055	2.65	.016
(7845.5 - 7887.0) [2]	39.5	.095	.069	.496	.281	.38	.062	2.65	.017
2. Lower Cozzette 7933.0 - 7987.0	51.0	.130	.072	.673	.144	.22	-	-	-
3. Upper Corcoran 8100.5 - 8114.5	11.0	.173	.067	.647	.172	.06	.053	2.65	.035
4. Lower Corcoran 8185.0 - 8226.0	29.5	.205	.056	.508	.035	.17	-	-	-

[1] Entire Upper Cozzette including pyrobitumen zone

[2] Upper Cozzette excluding pyrobitumen zone

TABLE 4.2 Reservoir characteristics of Corcoran/Cozzette Sandstones, MWX-1 and 2

FIGURE 4.1
MWX-1 RESISTIVITY LOG

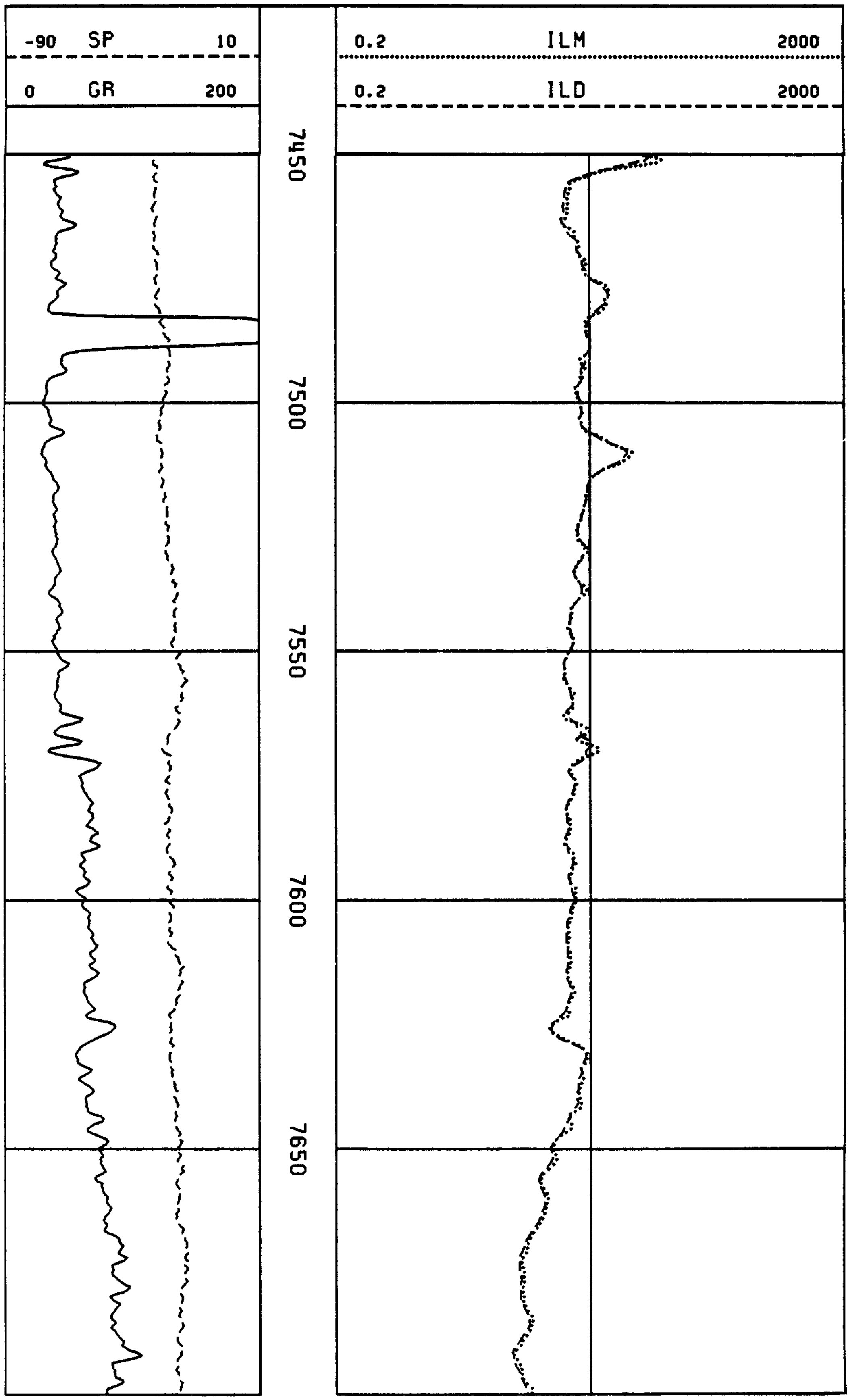

MWX-1

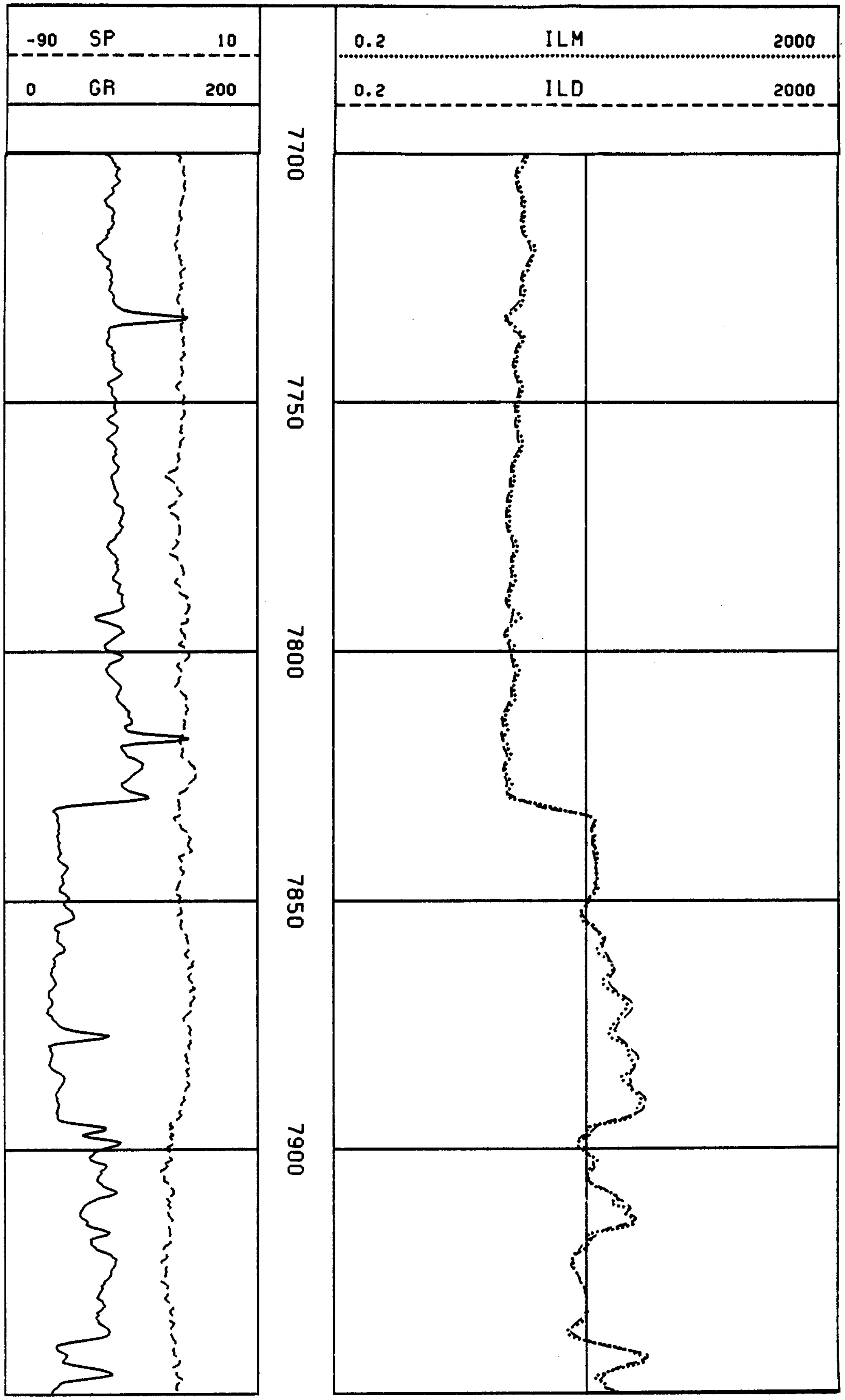
-90 SP 10
0 GR 200
0.2 ILM 2000
0.2 ILD 2000
7700
7750
7800
7850
7900

MWX-1

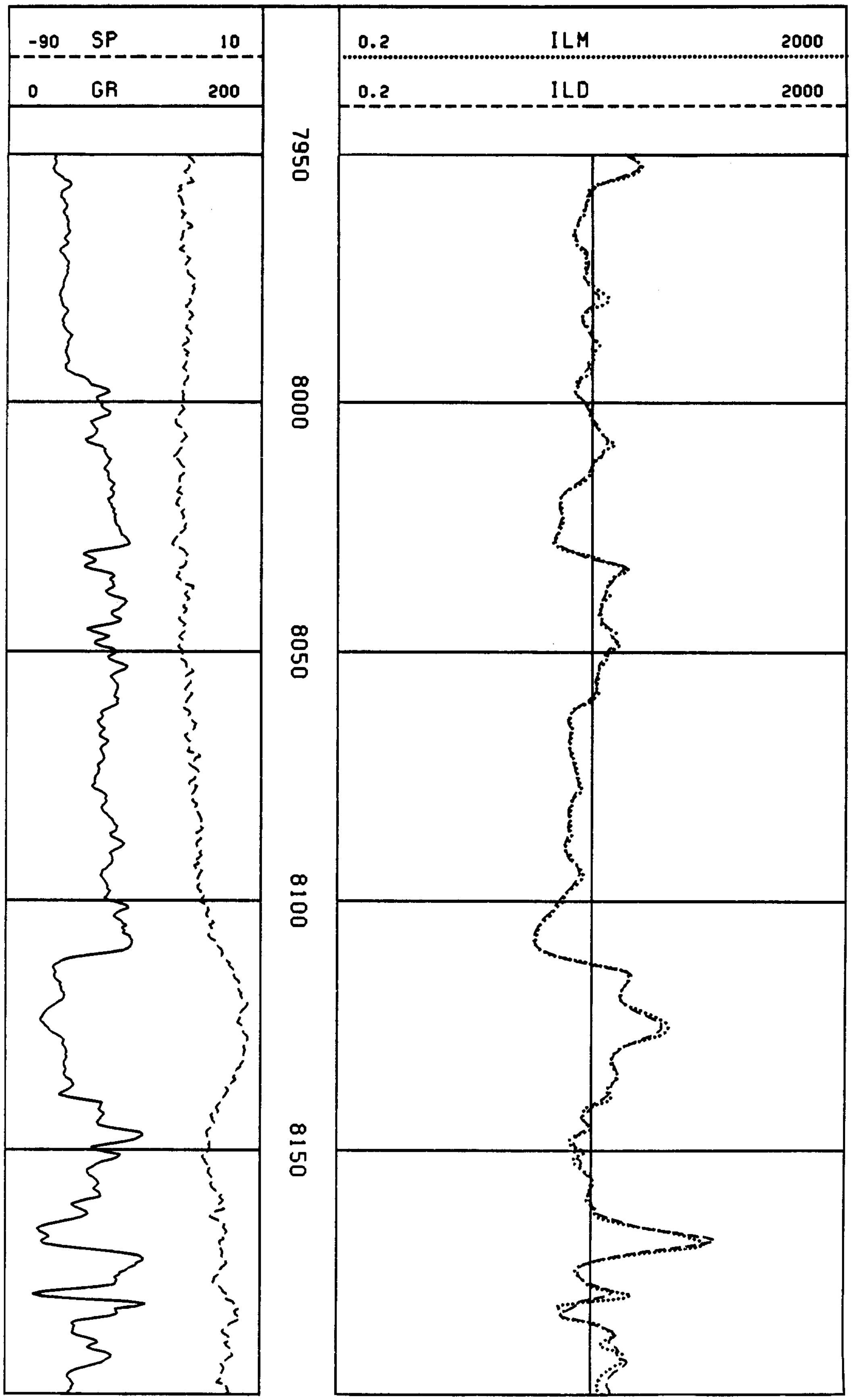

-90 SP 10
0 GR 200
0.2 ILM 2000
0.2 ILD 2000
7950
8000
8050
8100
8150

MWX-1

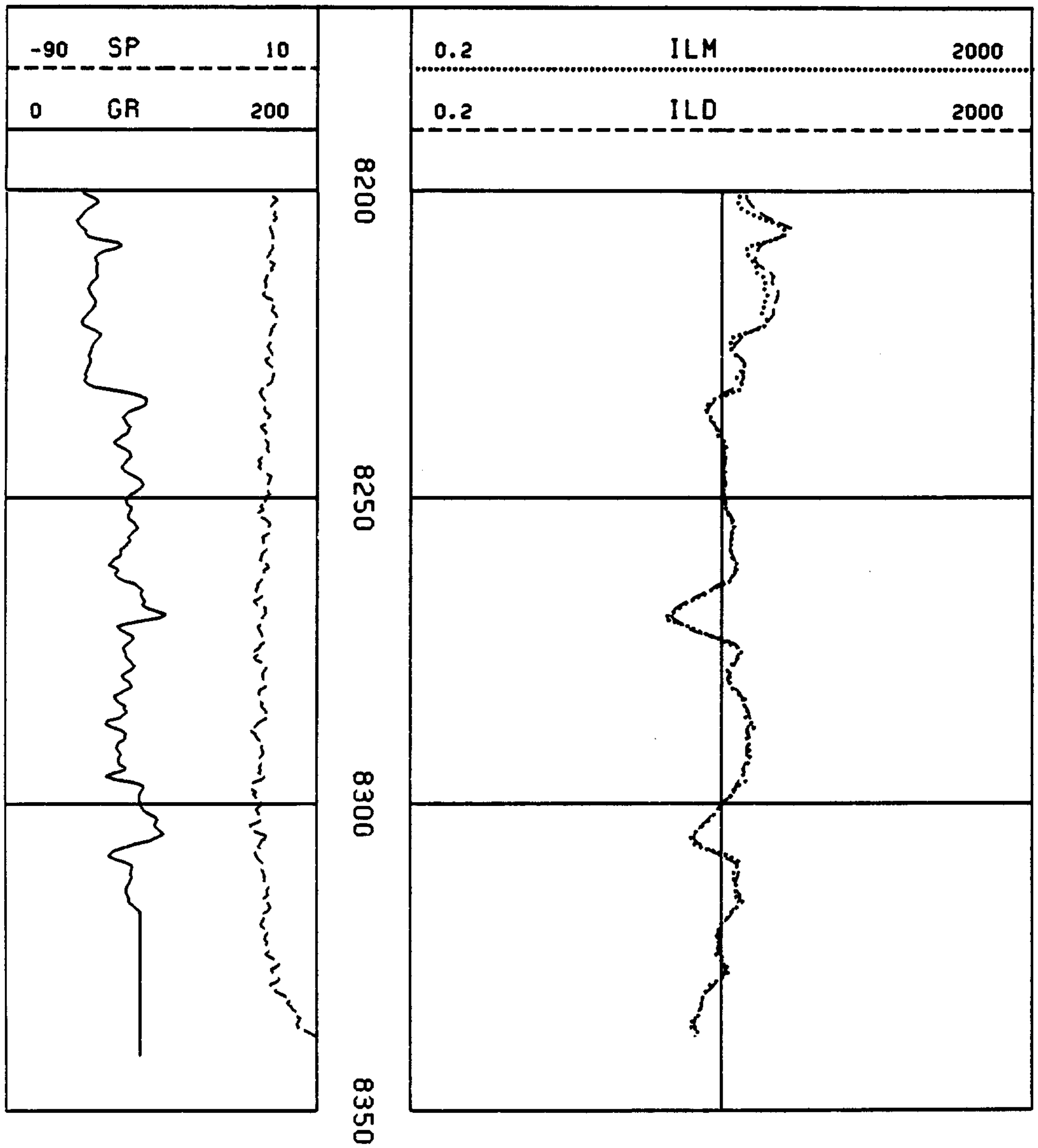

FIGURE 4.2
MWX-1 DENSITY-NEUTRON LOG

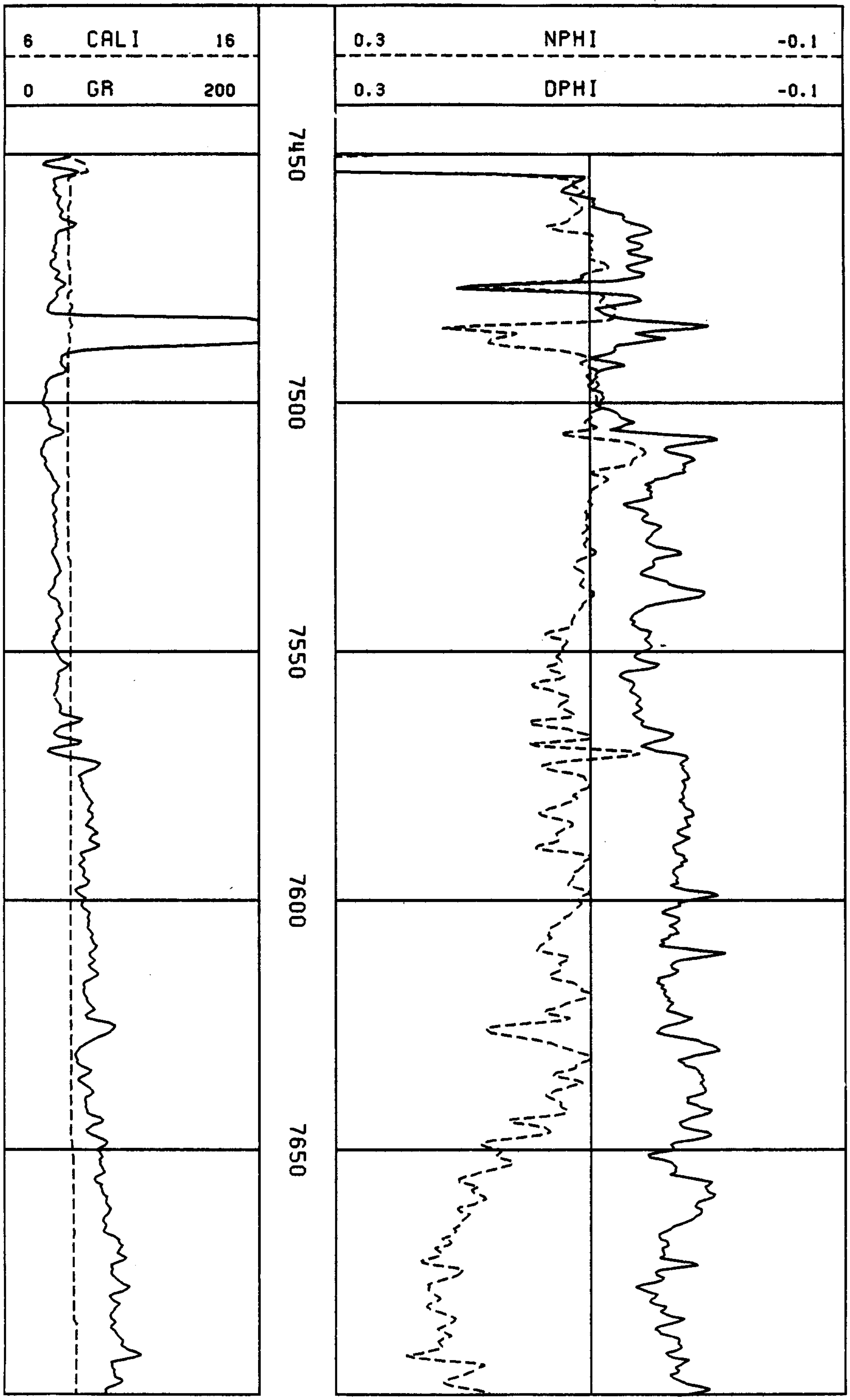

MWX-1

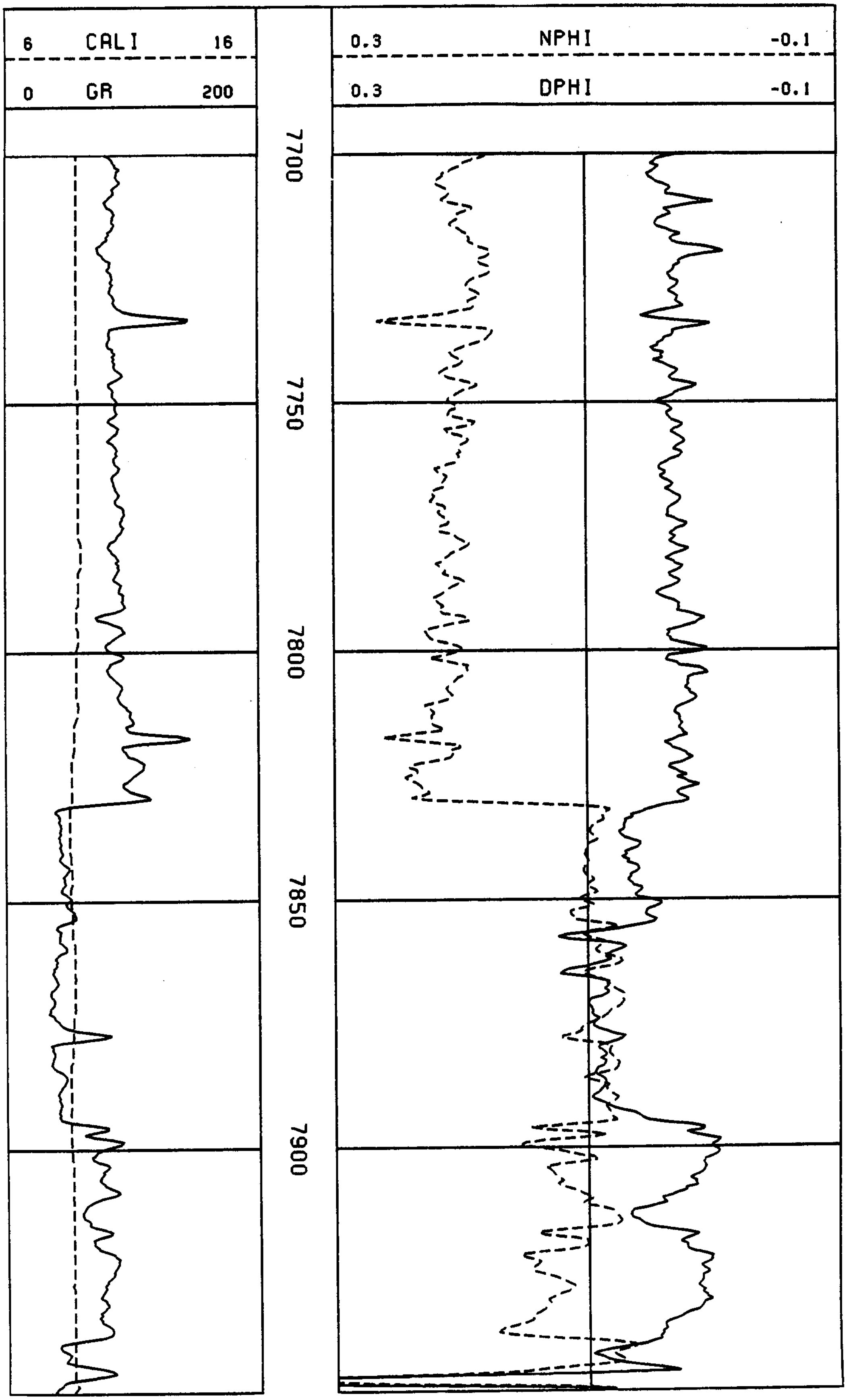

MWX-1

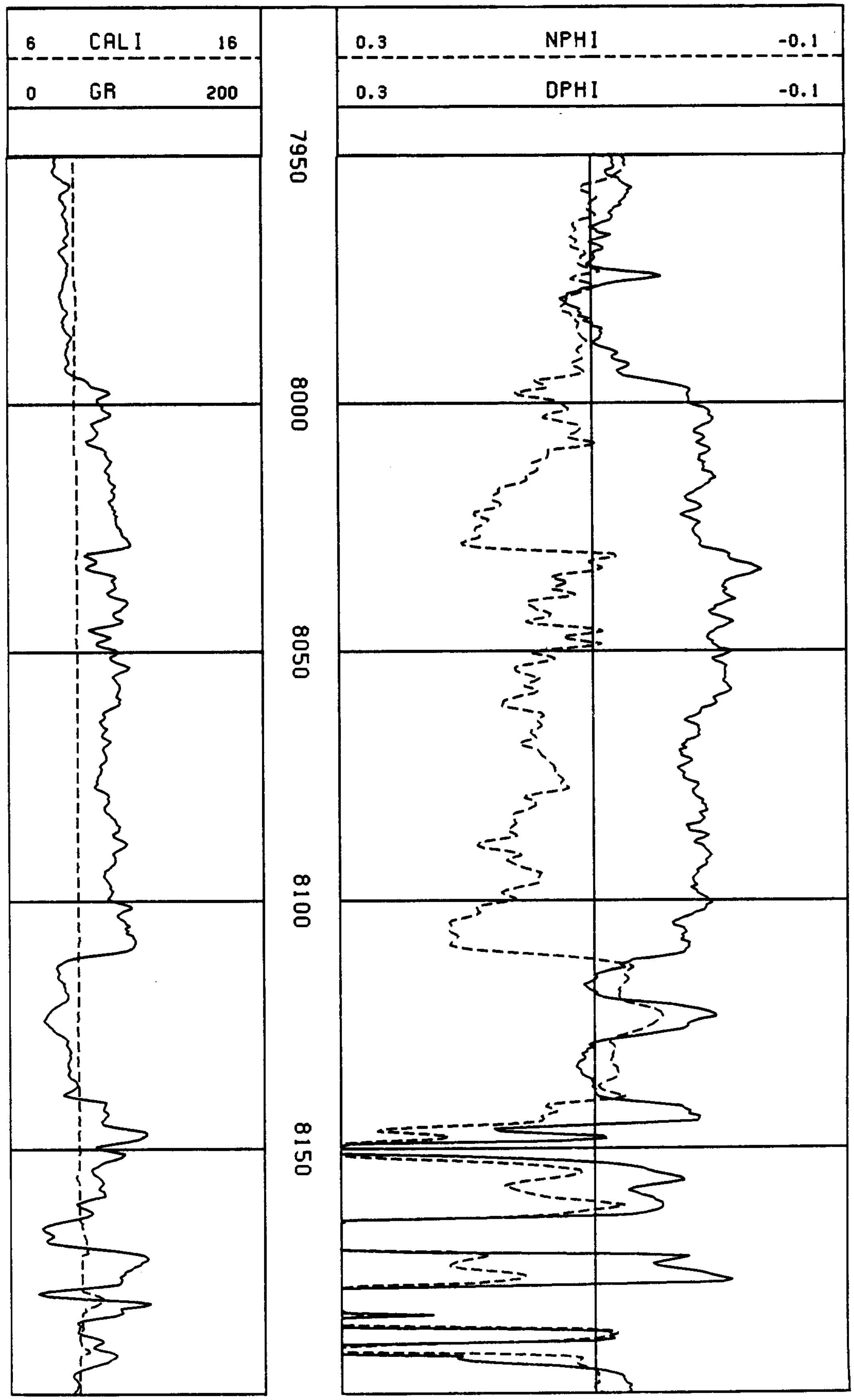

MWX-1

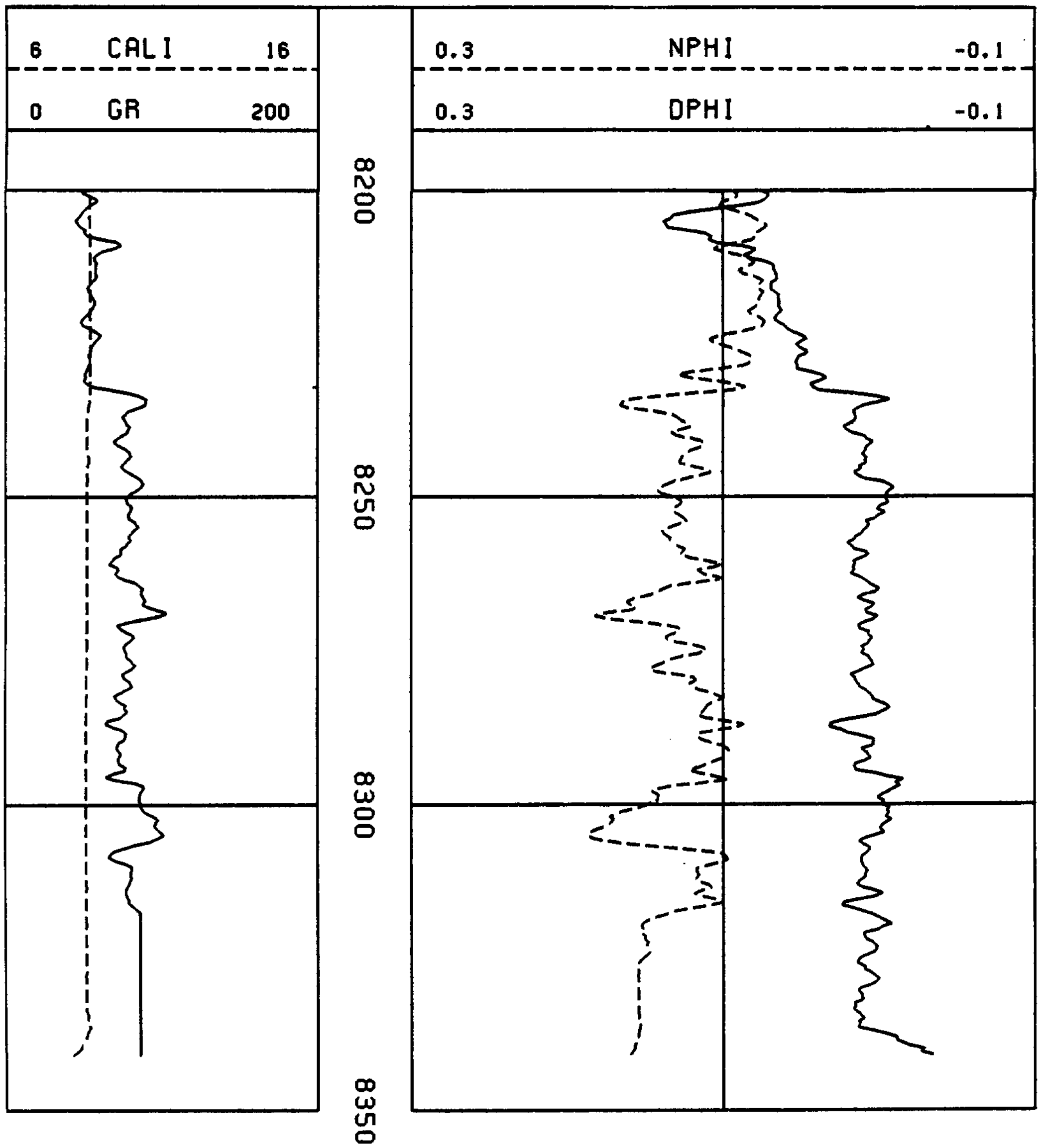

FIGURE 4.3

MWX-1 BULK DENSITY LOG

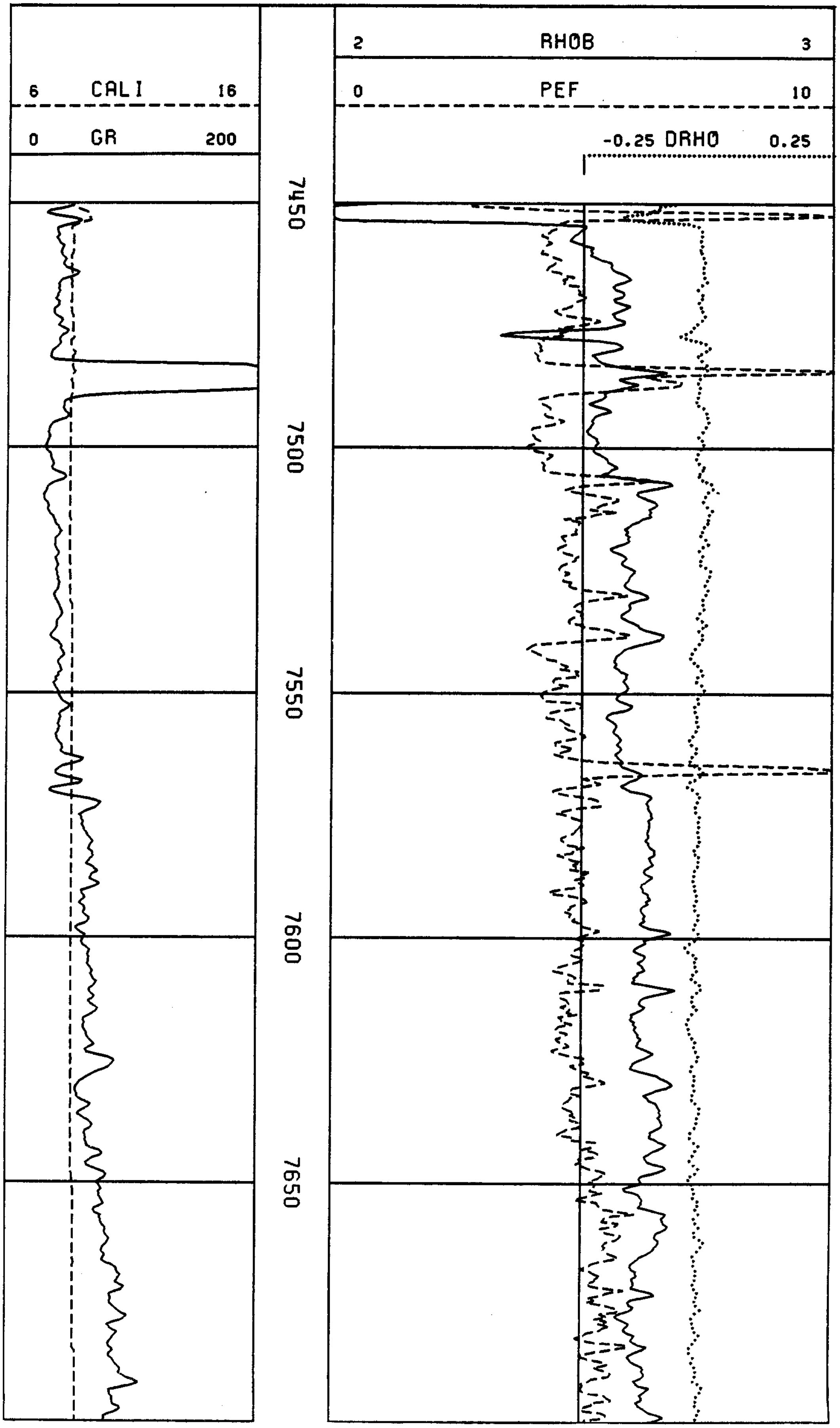

MWX-1

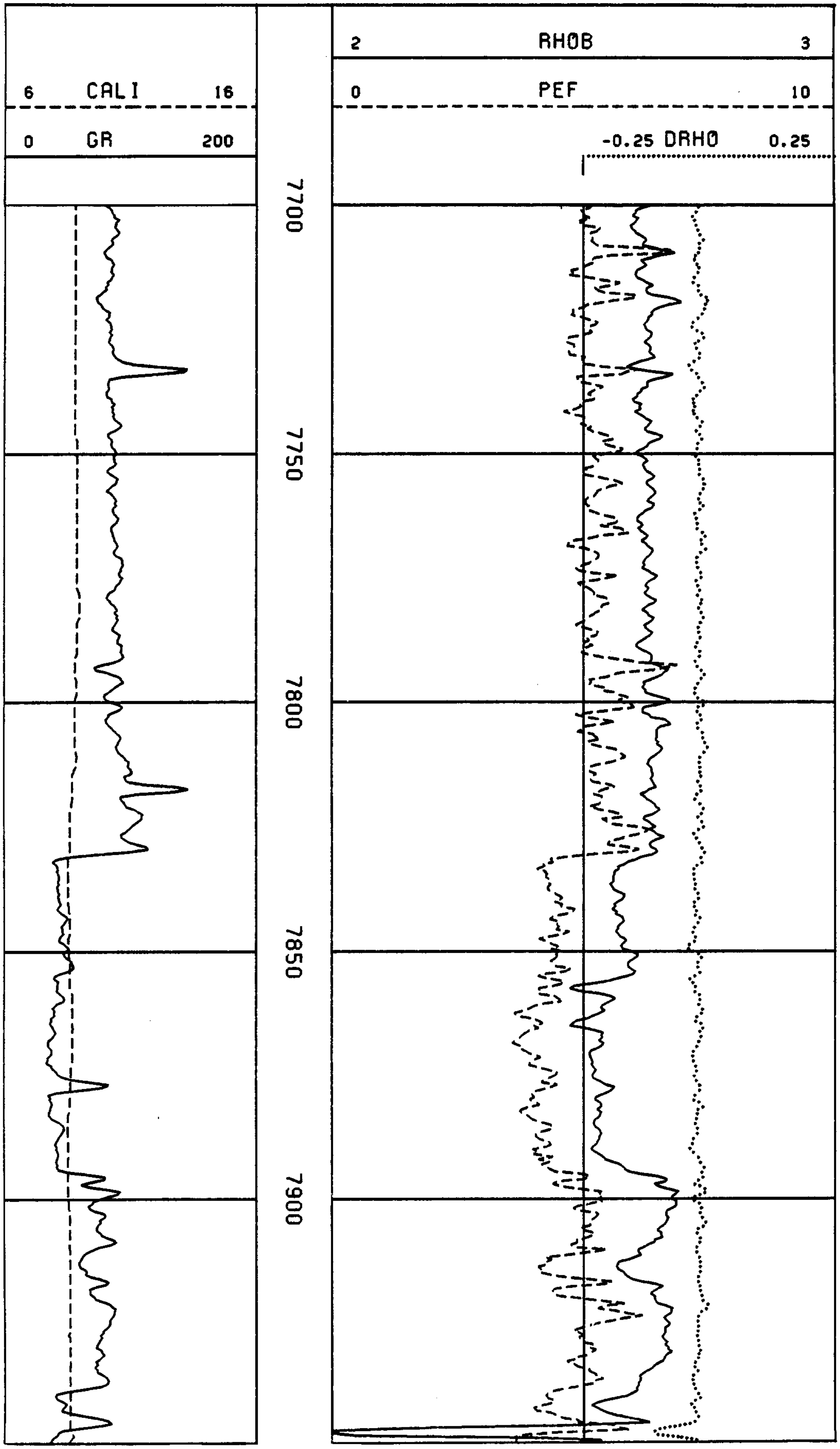
6 CALI 16
0 GR 200
2 RHOB 3
0 PEF 10
-0.25 DRHO 0.25
7700
7750
7800
7850
7900

MWX-1

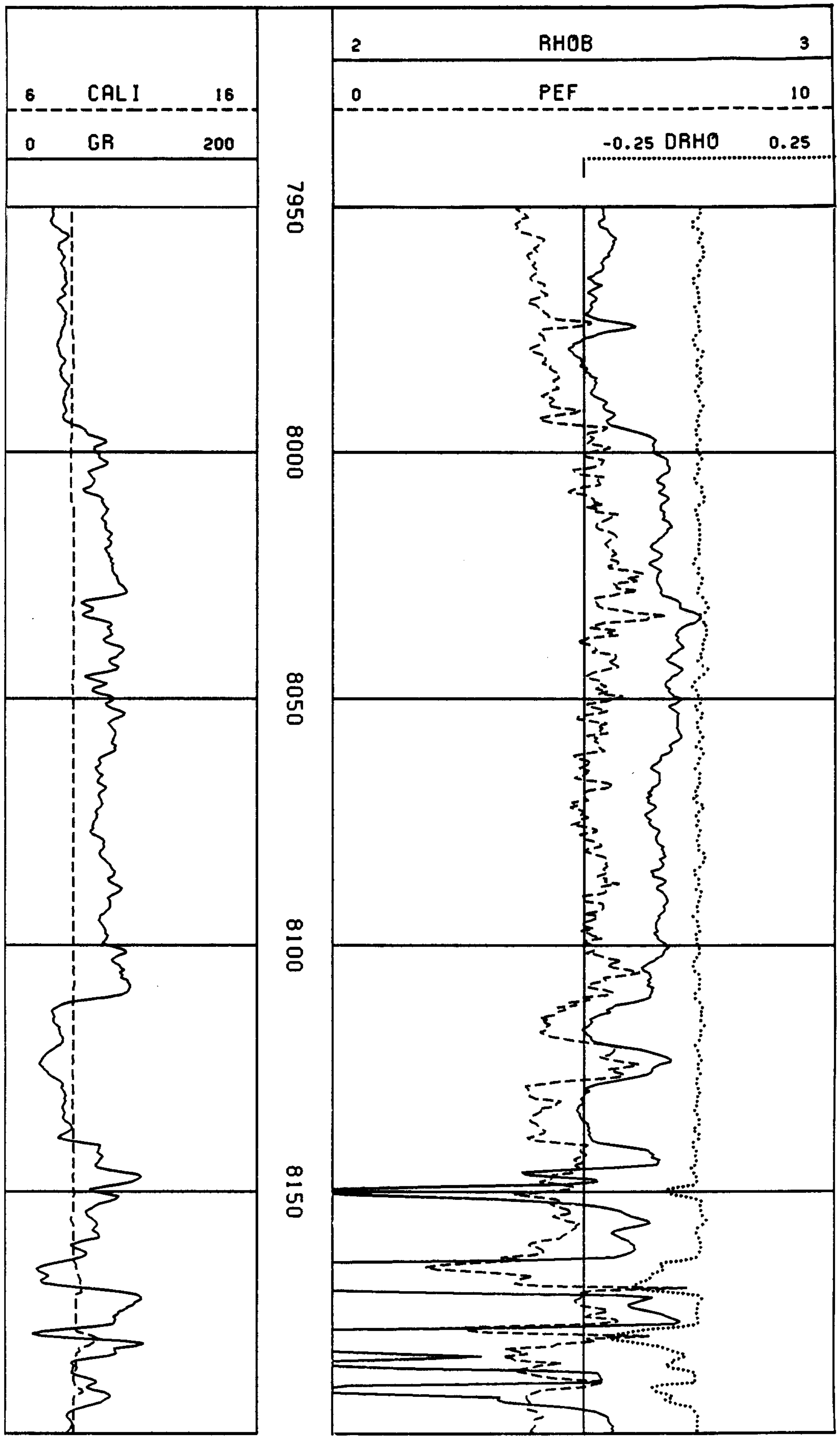
6 CALI 16
0 GR 200
2 RHOB 3
0 PEF 10
-0.25 DRHO 0.25
7950
8000
8050
8100
8150

MWX-1

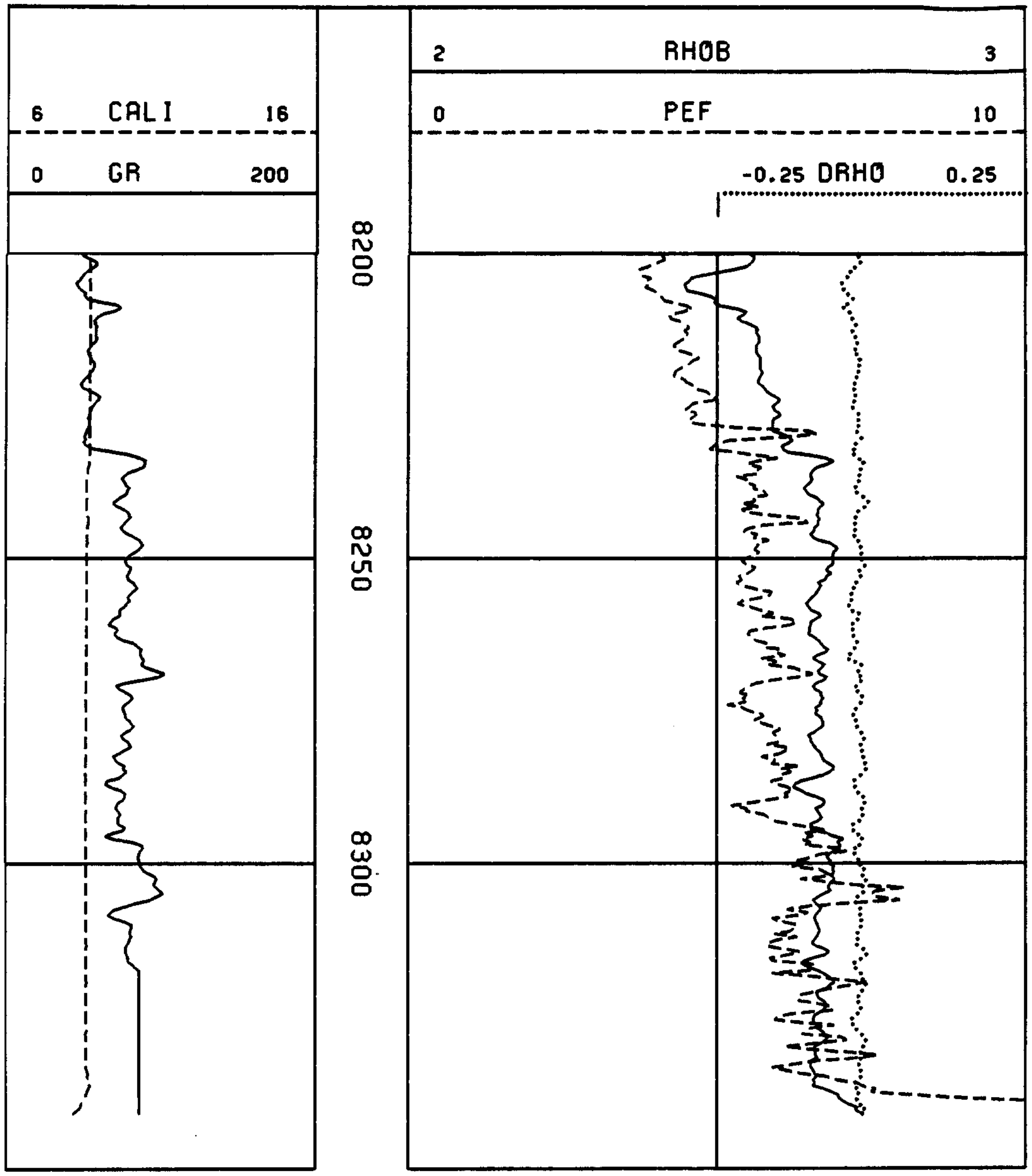

FIGURE 4.4

MWX-1 SPECTRAL GAMMA LOG

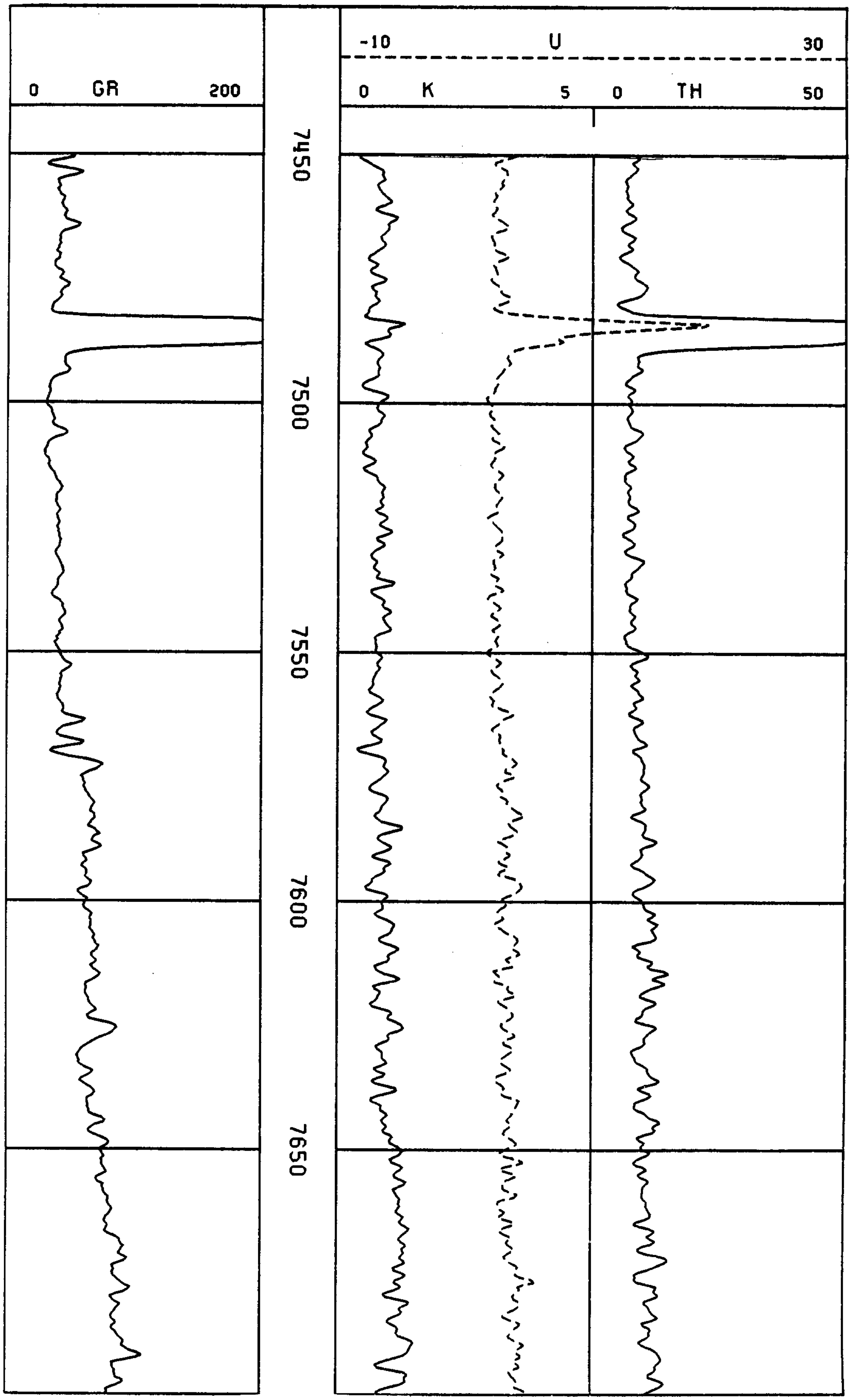

MWX-1

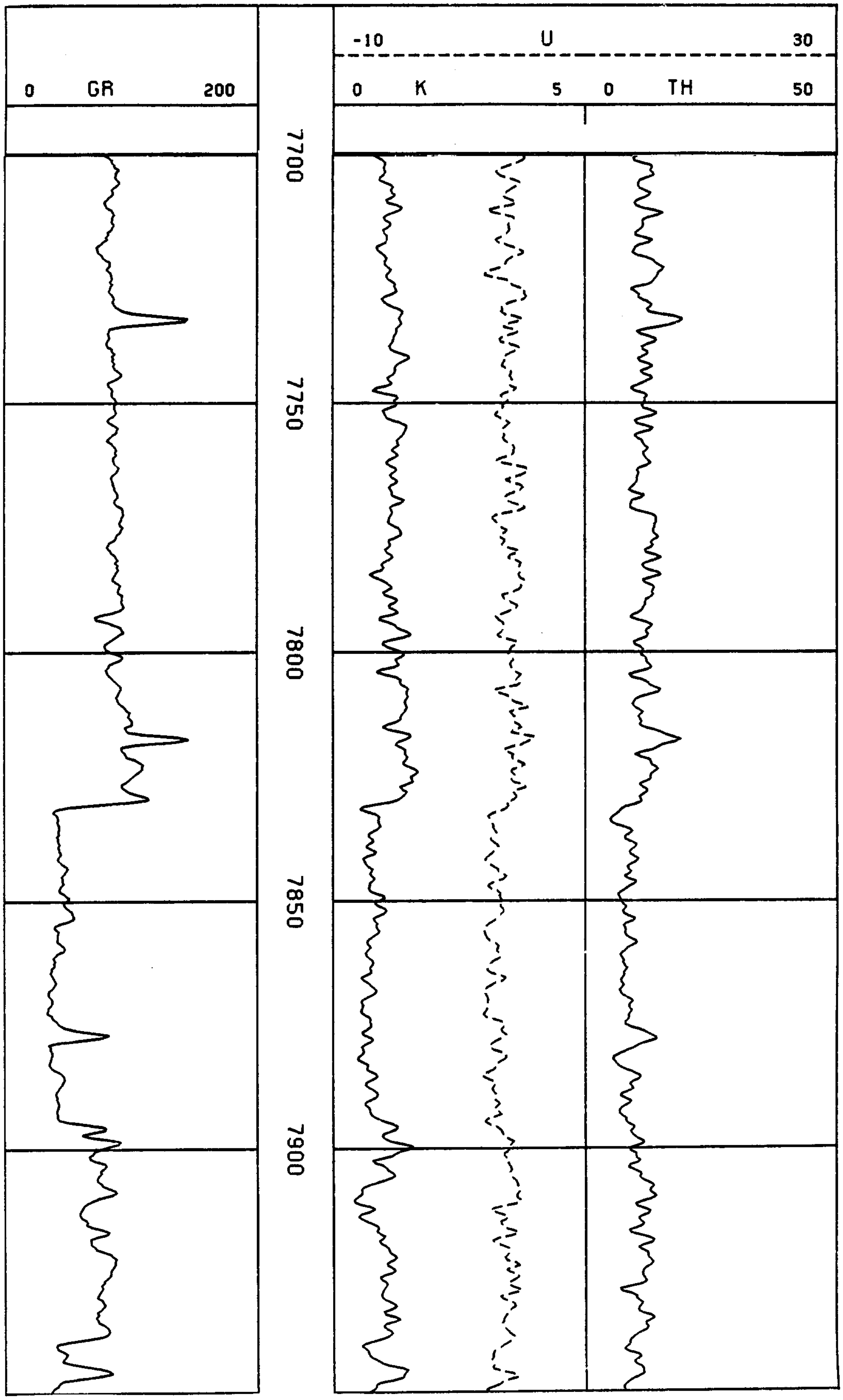

MWX-1

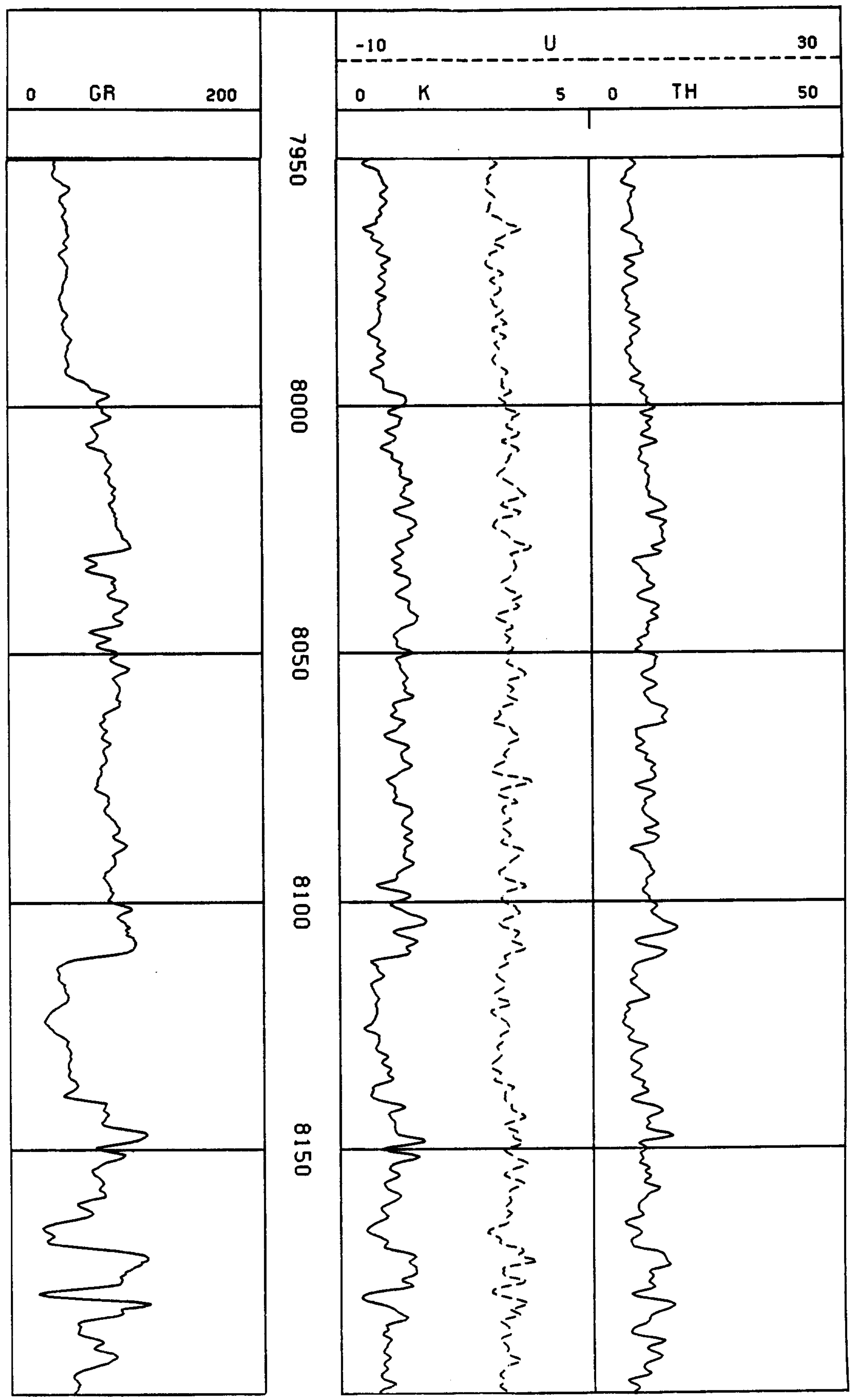

MWX-1

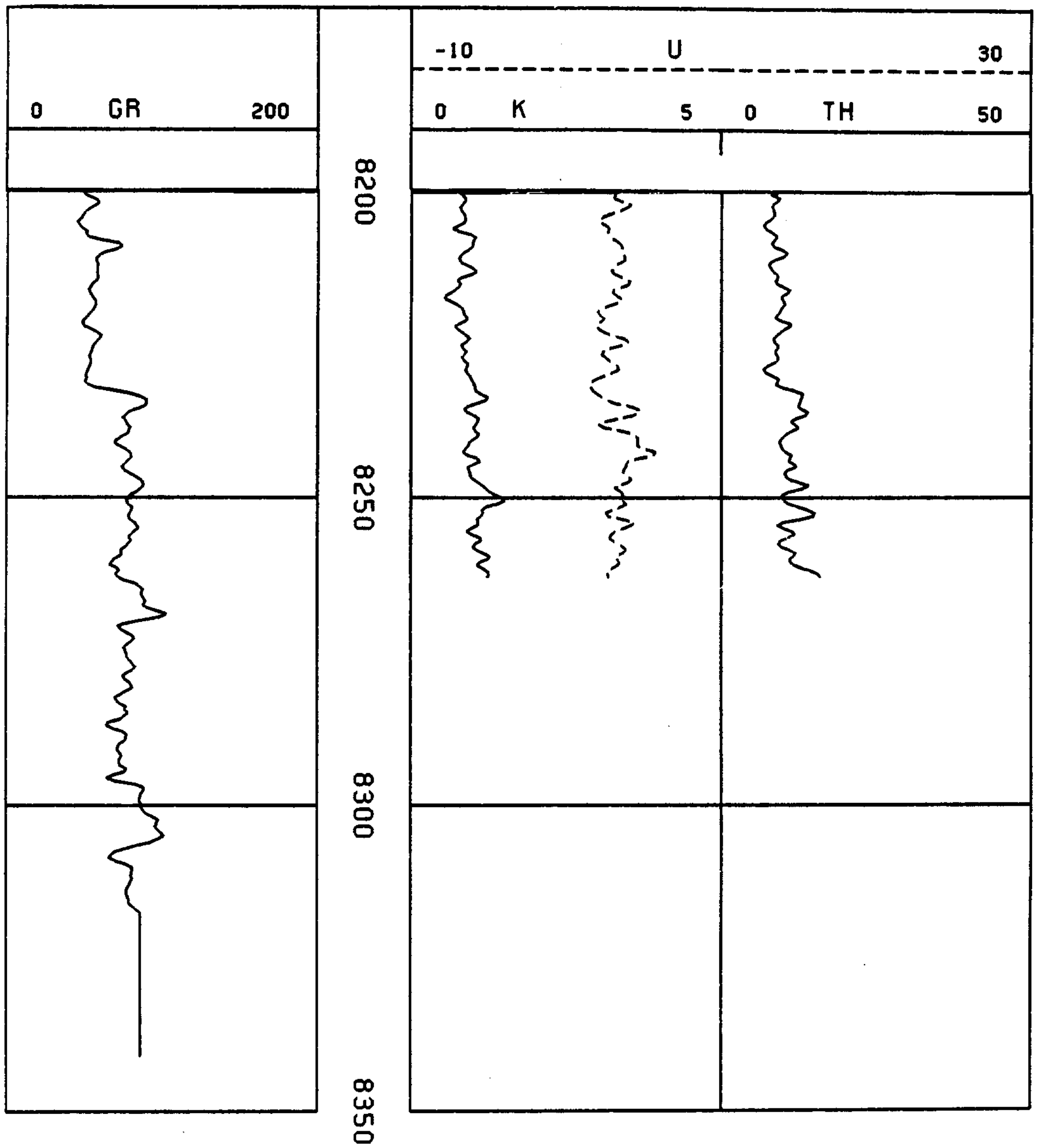

FIGURE 4.5

MWX-1 AMOCO LONG-SPACED SONIC LOG

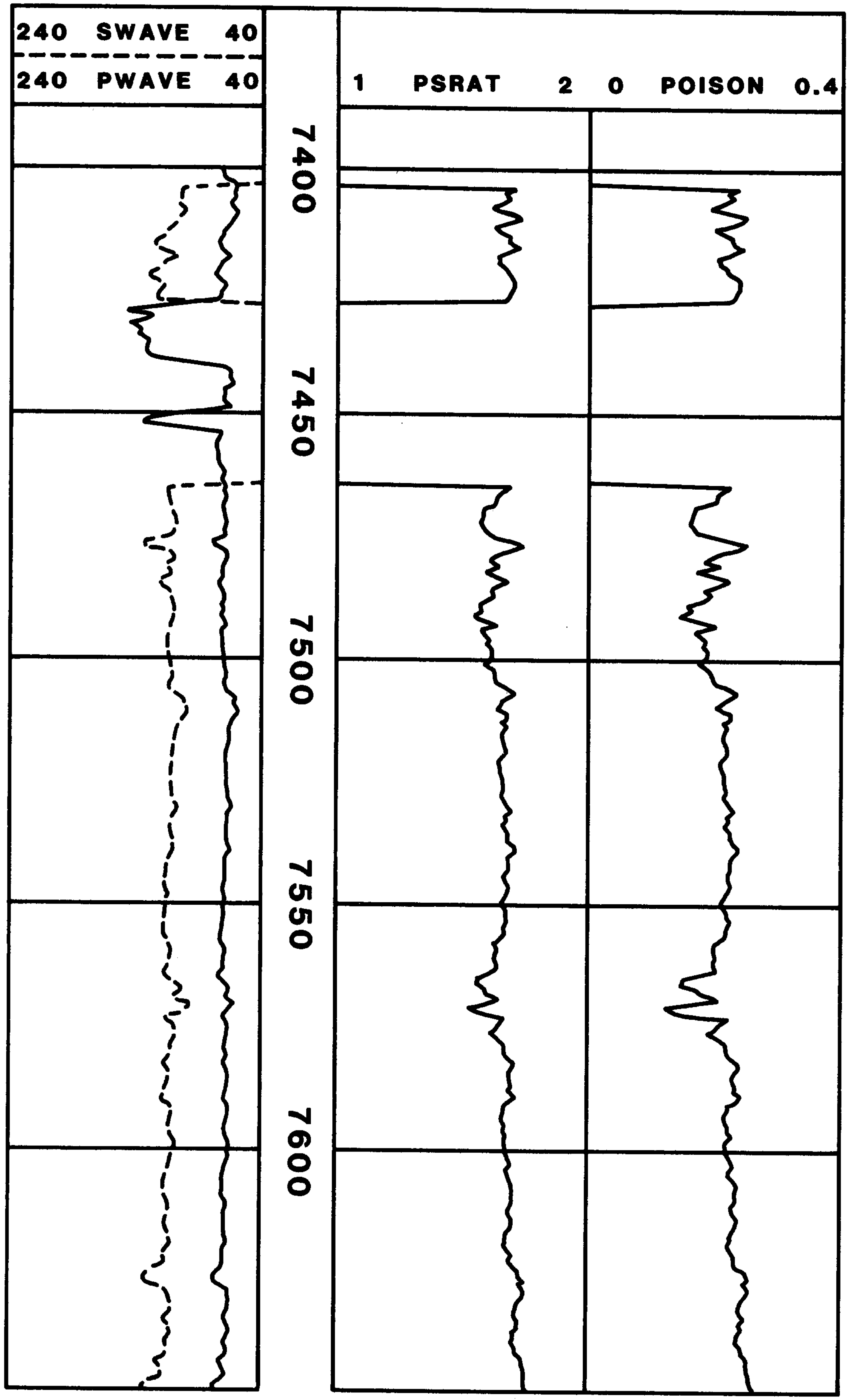

MWX-1

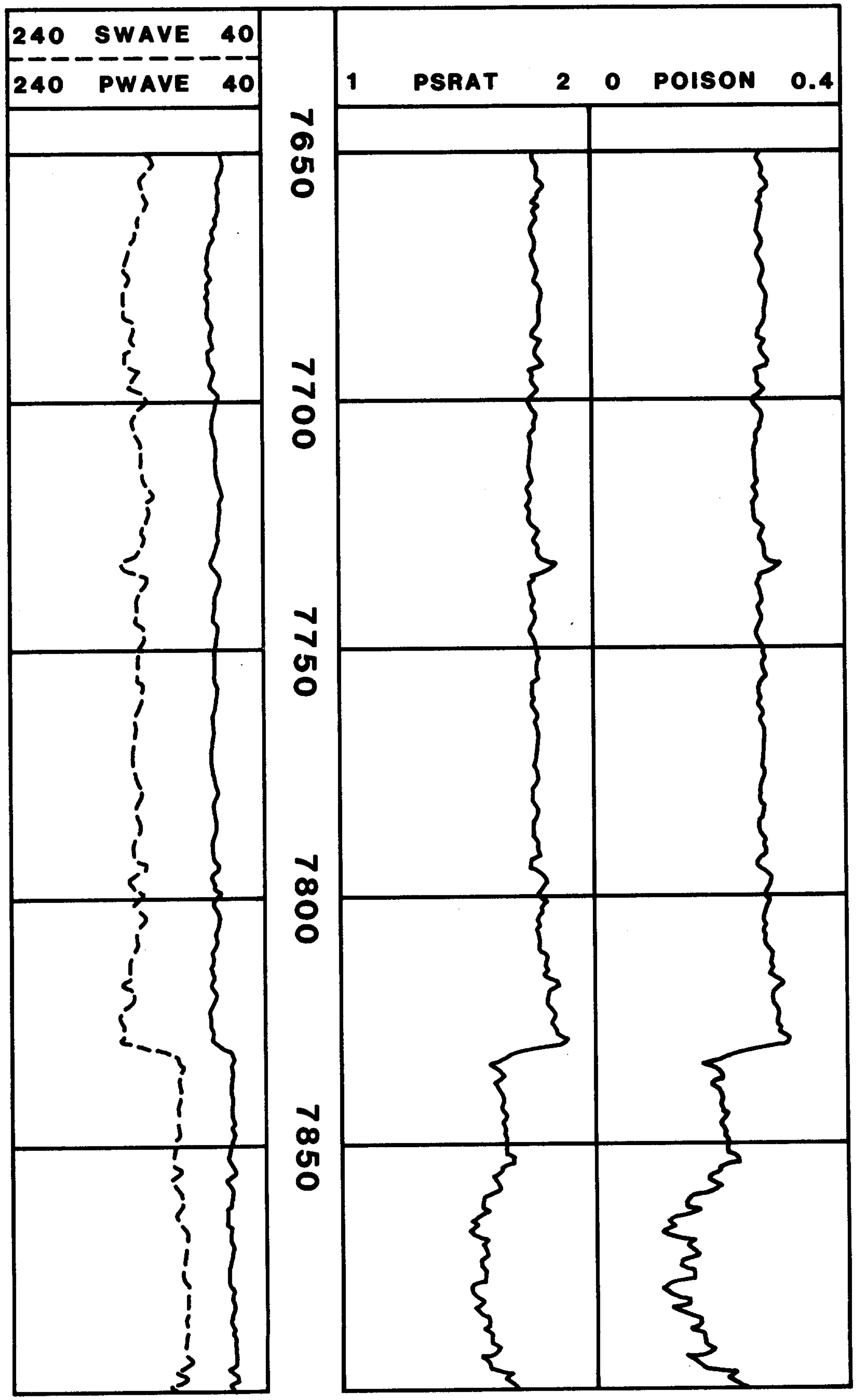
240 SWAVE 40
240 PWAVE 40
7650
7700
7750
7800
7850
1 PSRAT 2
0 POISON 0.4

MWX-1

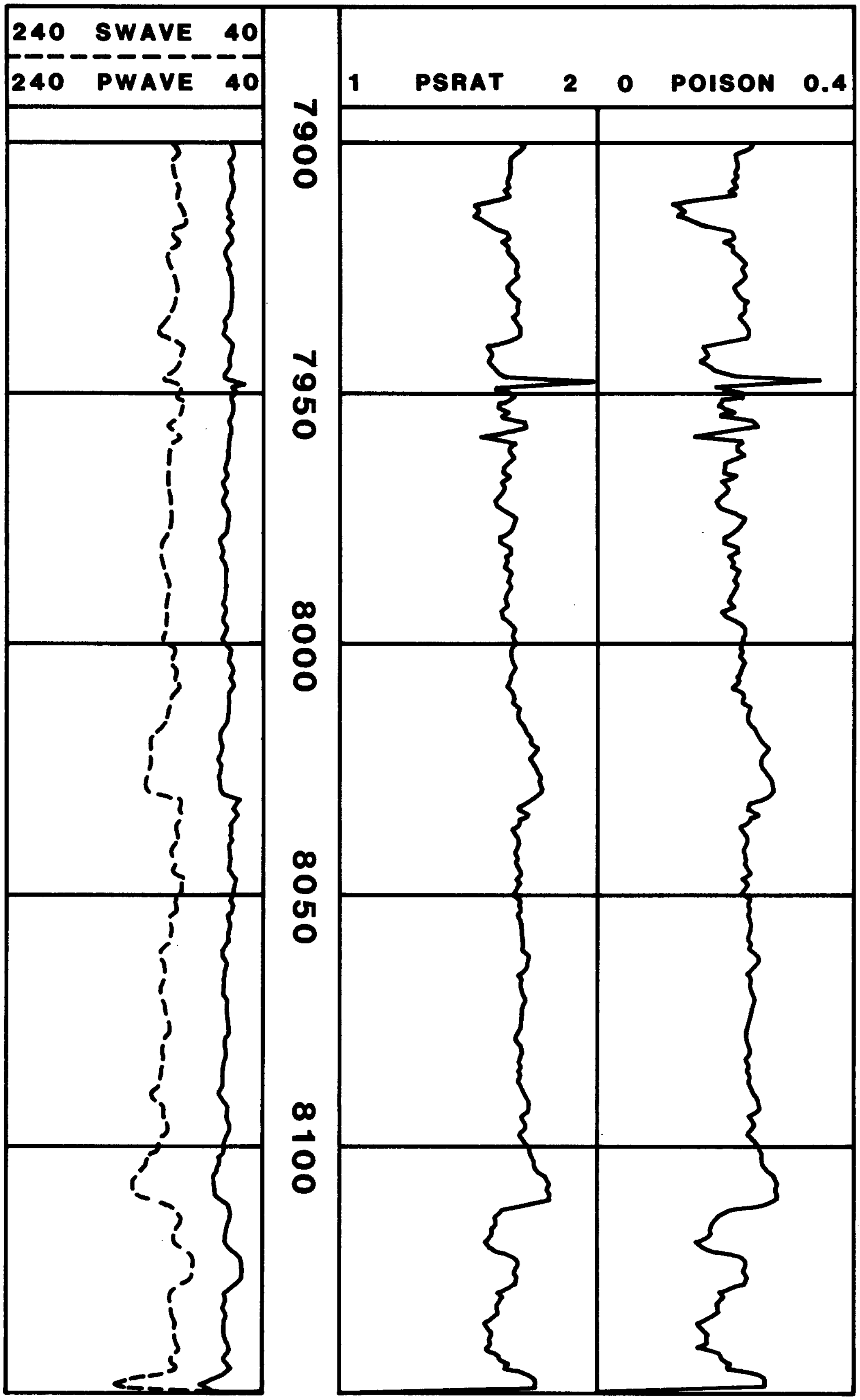

240 SWAVE 40
240 PWAVE 40
1 PSRAT 2
0 POISON 0.4
7900
7950
8000
8050
8100

MWX-1

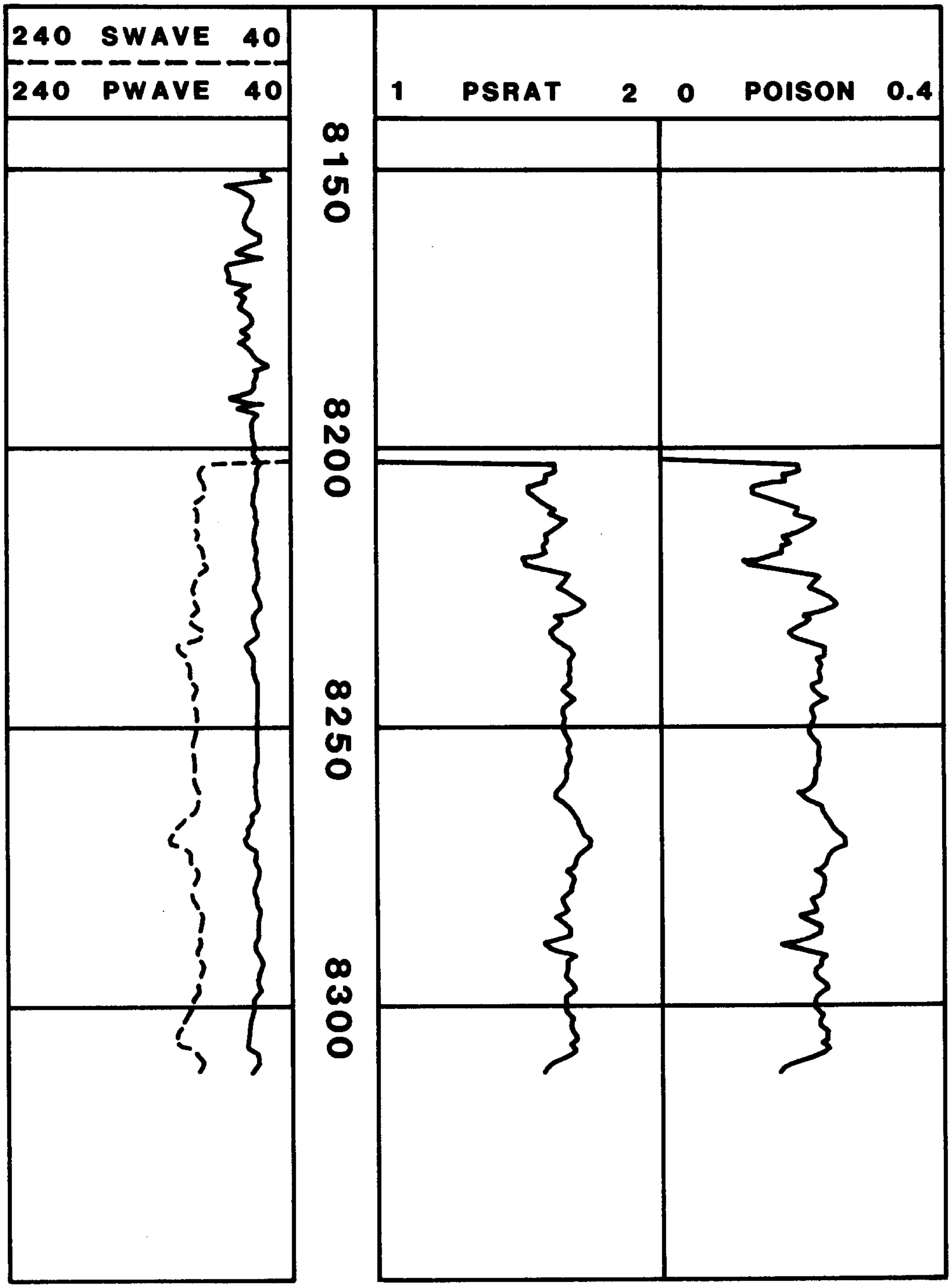

240 SWAVE 40
240 PWAVE 40
1 PSRAT 2
0 POISON 0.4
8150
8200
8250
8300

FIGURE 4.6

MWX-2 RESISTIVTY LOG

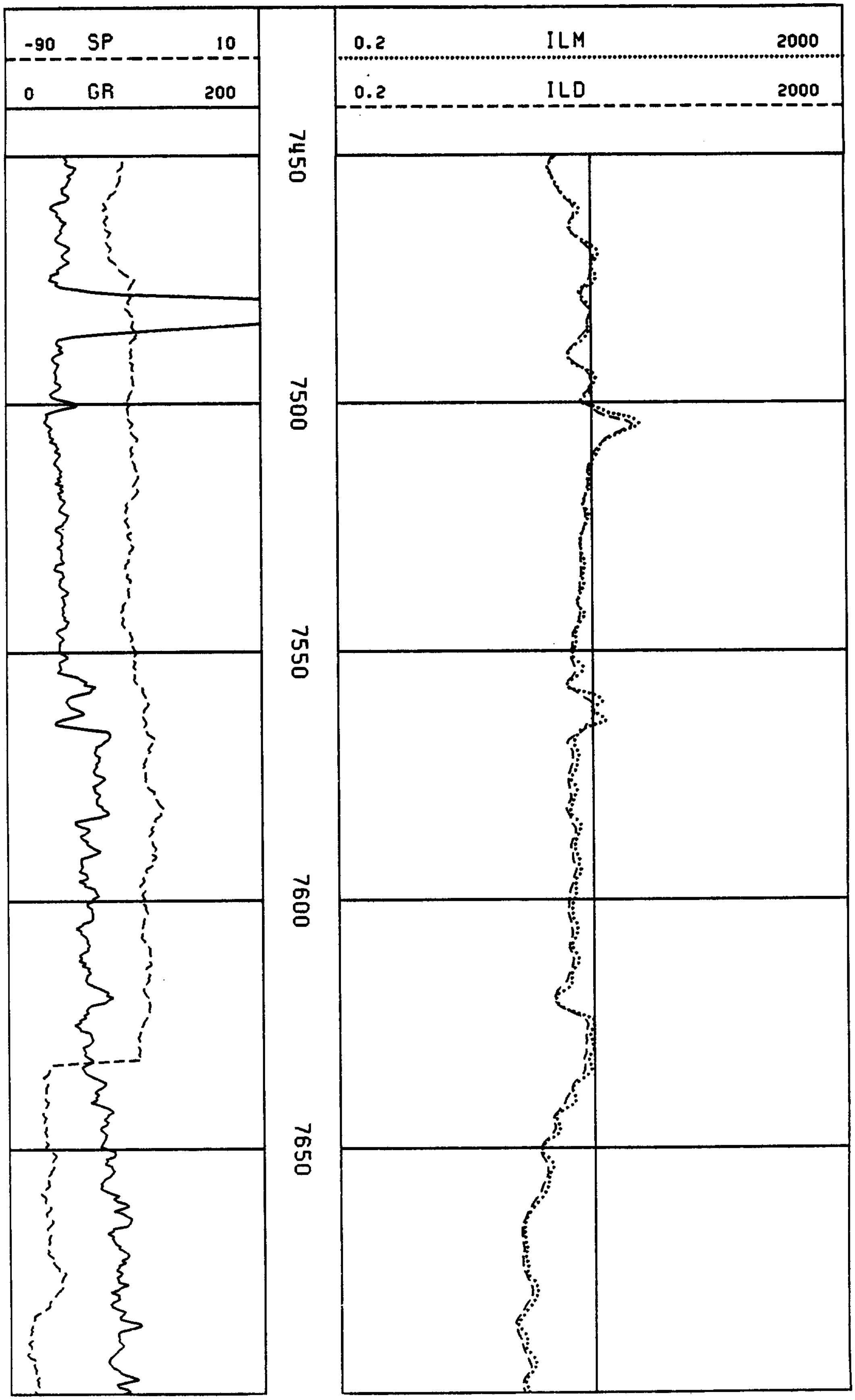

MWX-2

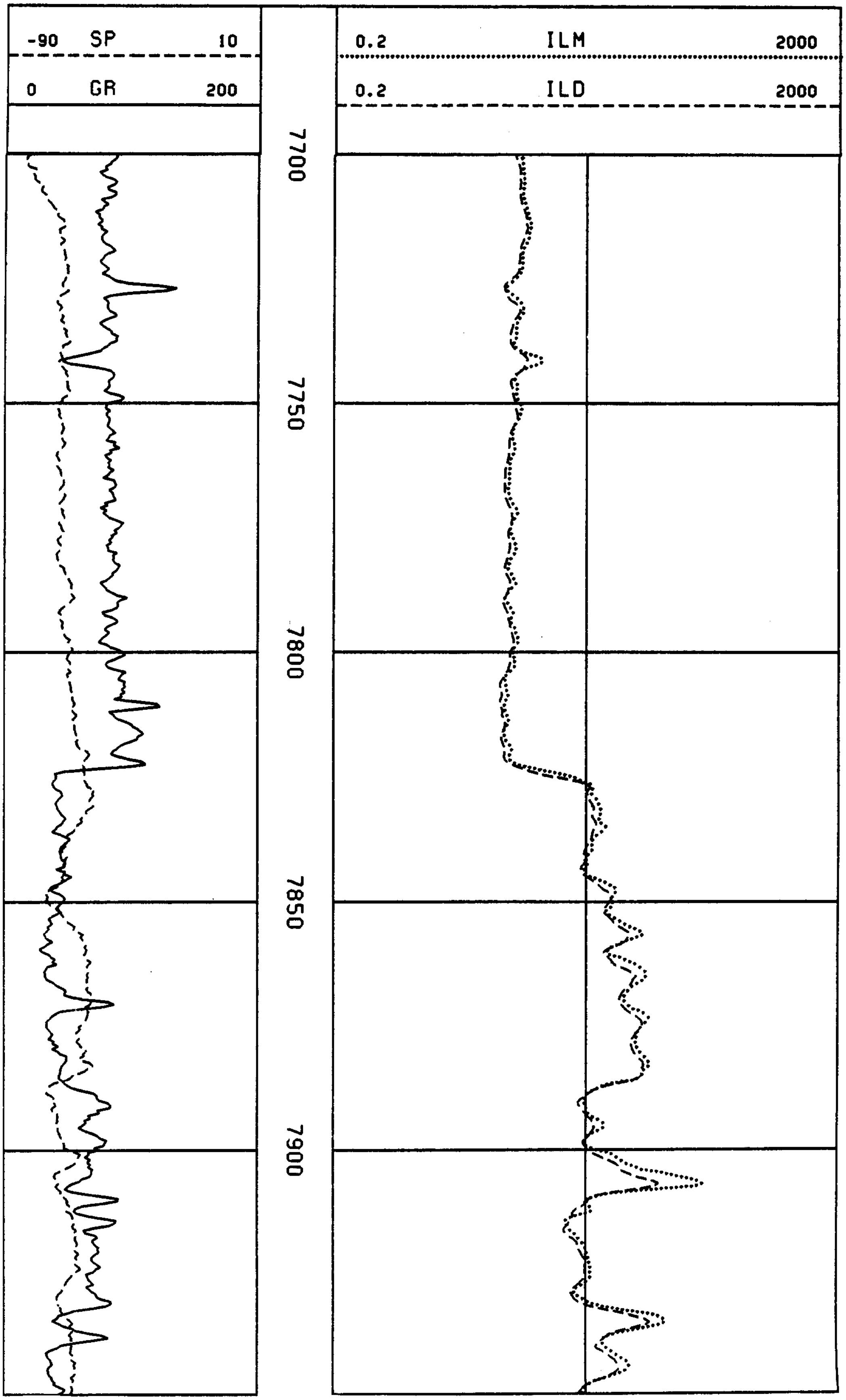

-90 SP 10
0 GR 200
0.2 ILM 2000
0.2 ILD 2000
7700
7750
7800
7850
7900

MWX-2

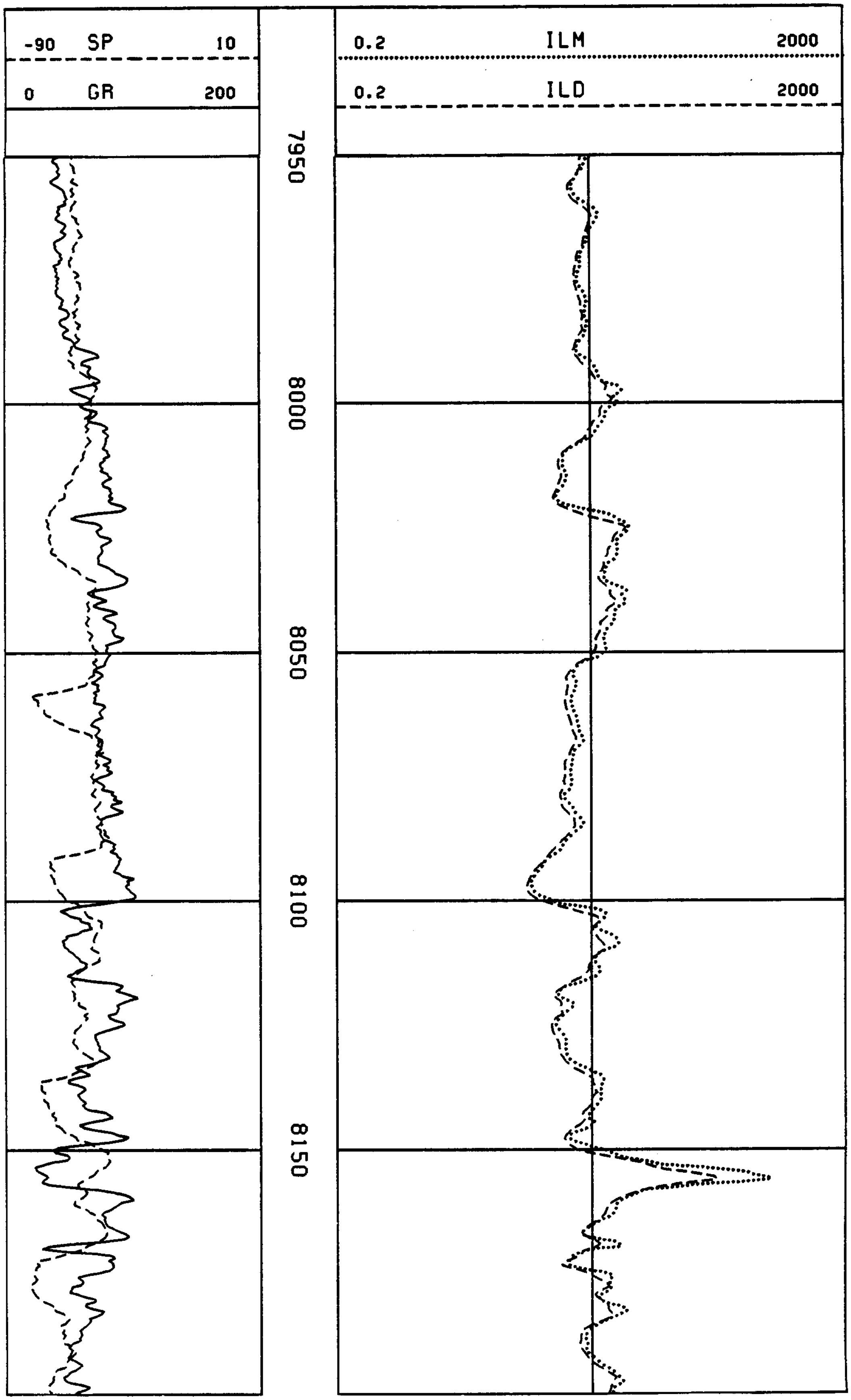

-90 SP 10
0 GR 200
0.2 ILM 2000
0.2 ILD 2000
7950
8000
8050
8100
8150

MWX-2

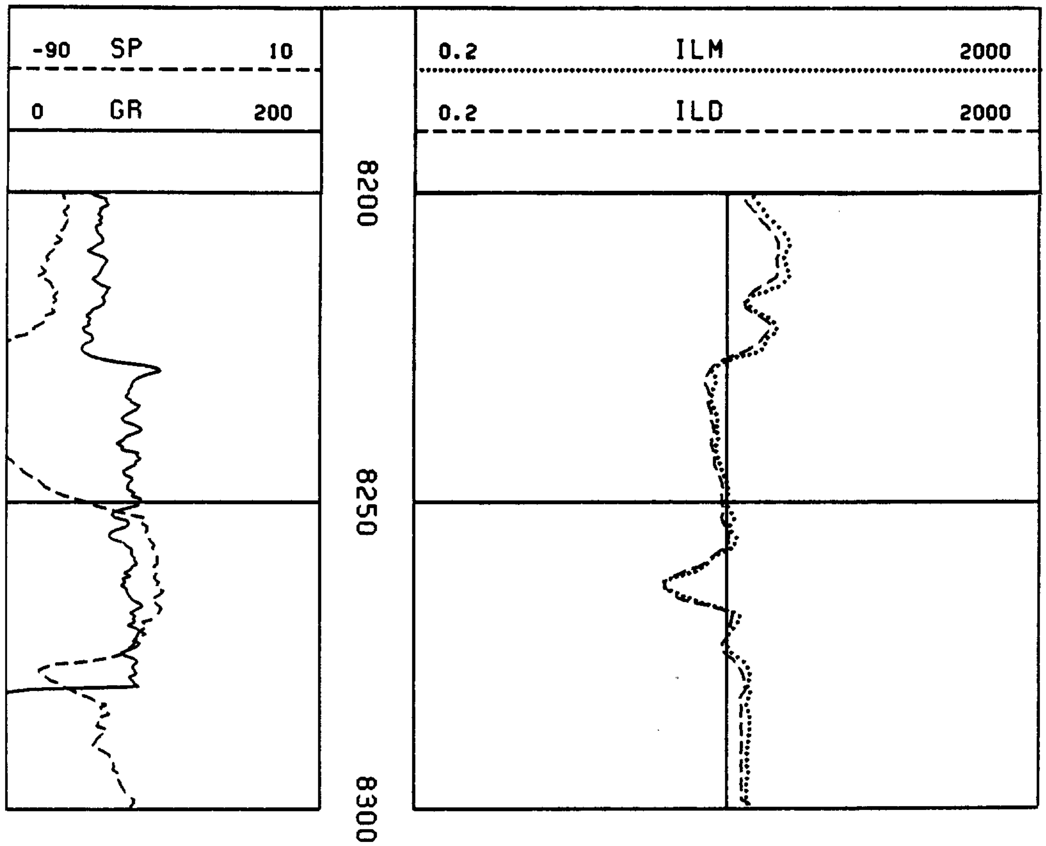

FIGURE 4.7

MWX-2 DENSITY-NEUTRON LOG

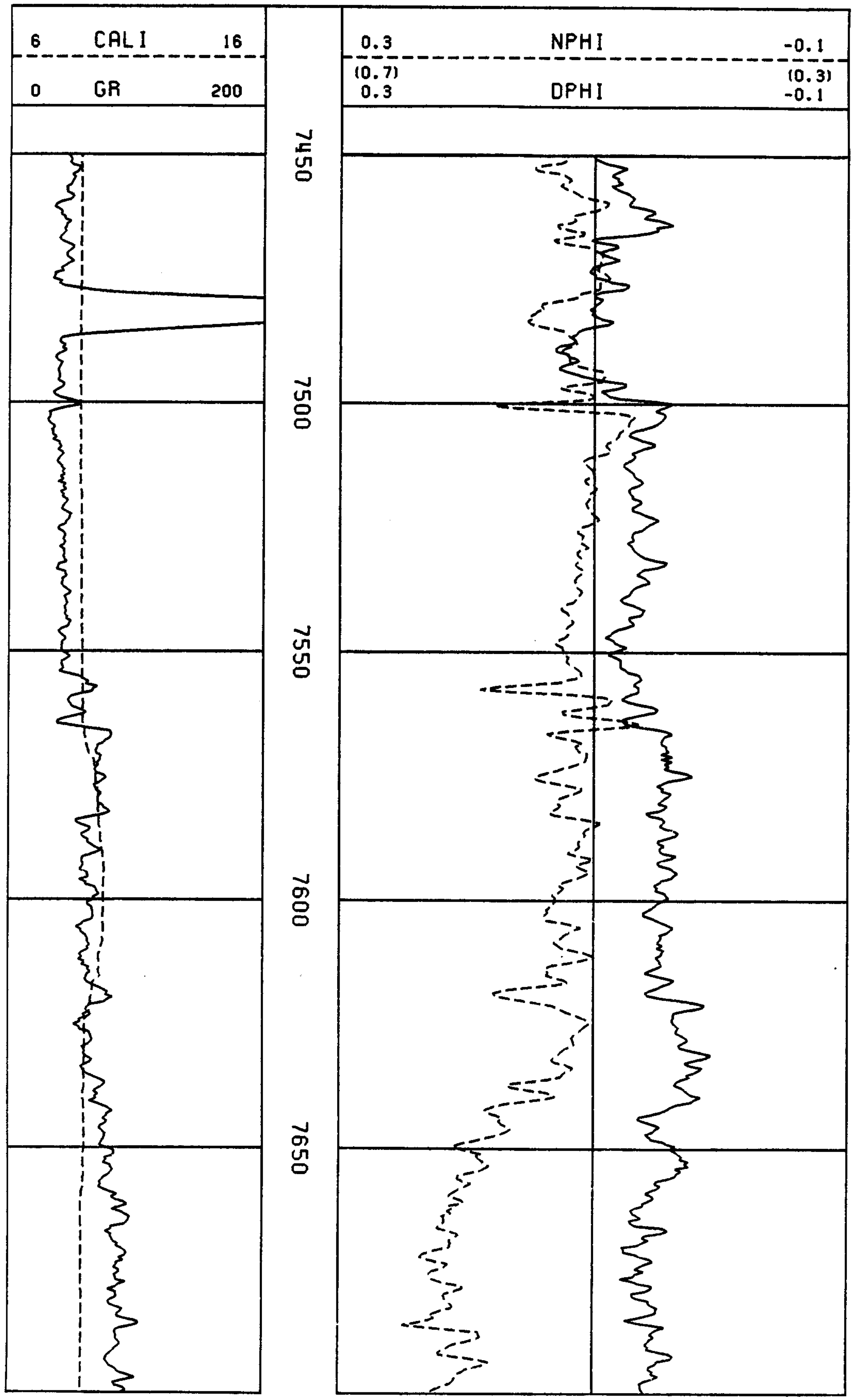

MWX-2

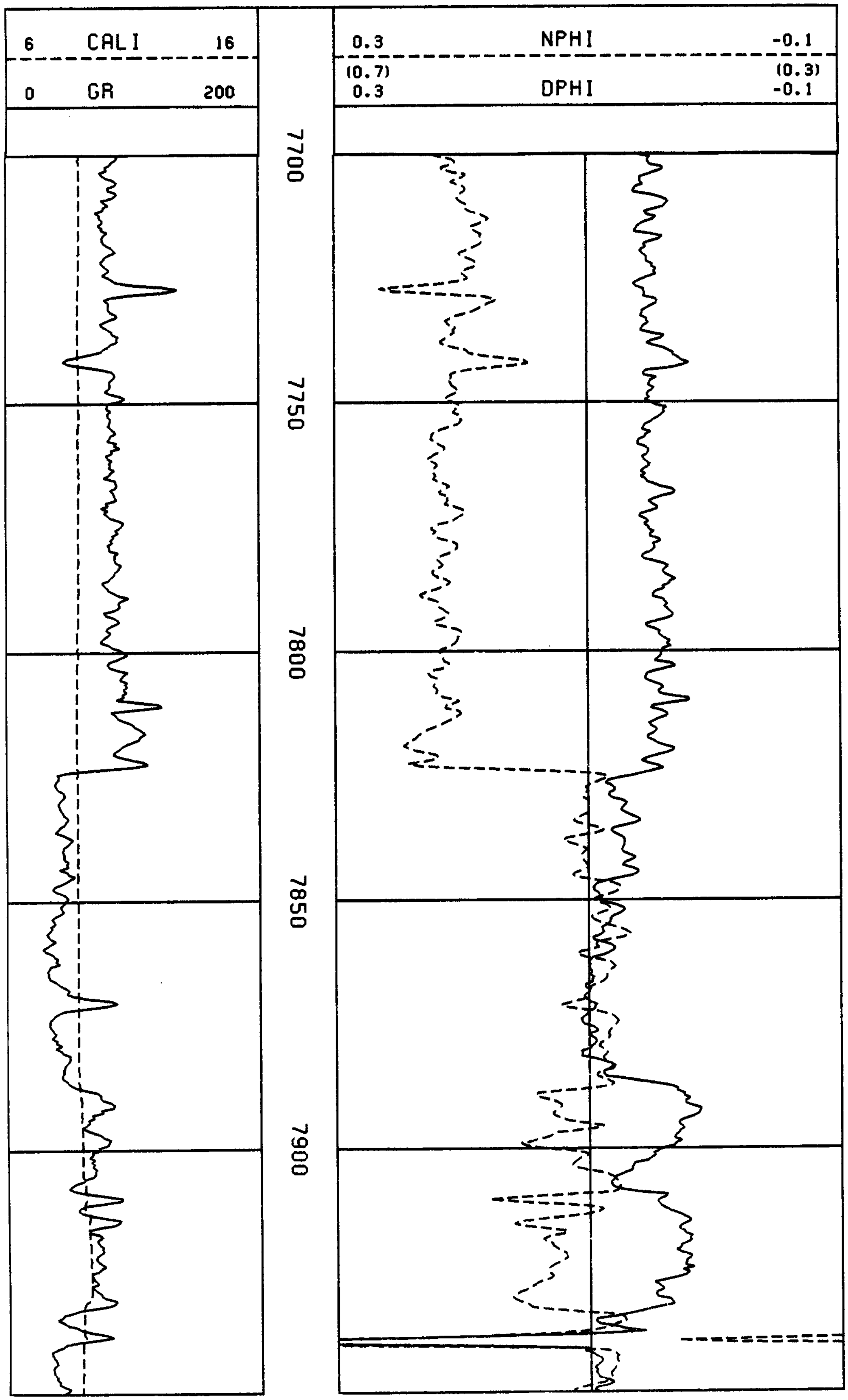
6 CALI 16
0 GR 200
0.3 NPHI -0.1
(0.7) (0.3)
0.3 DPHI -0.1
7700
7750
7800
7850
7900

MWX-2

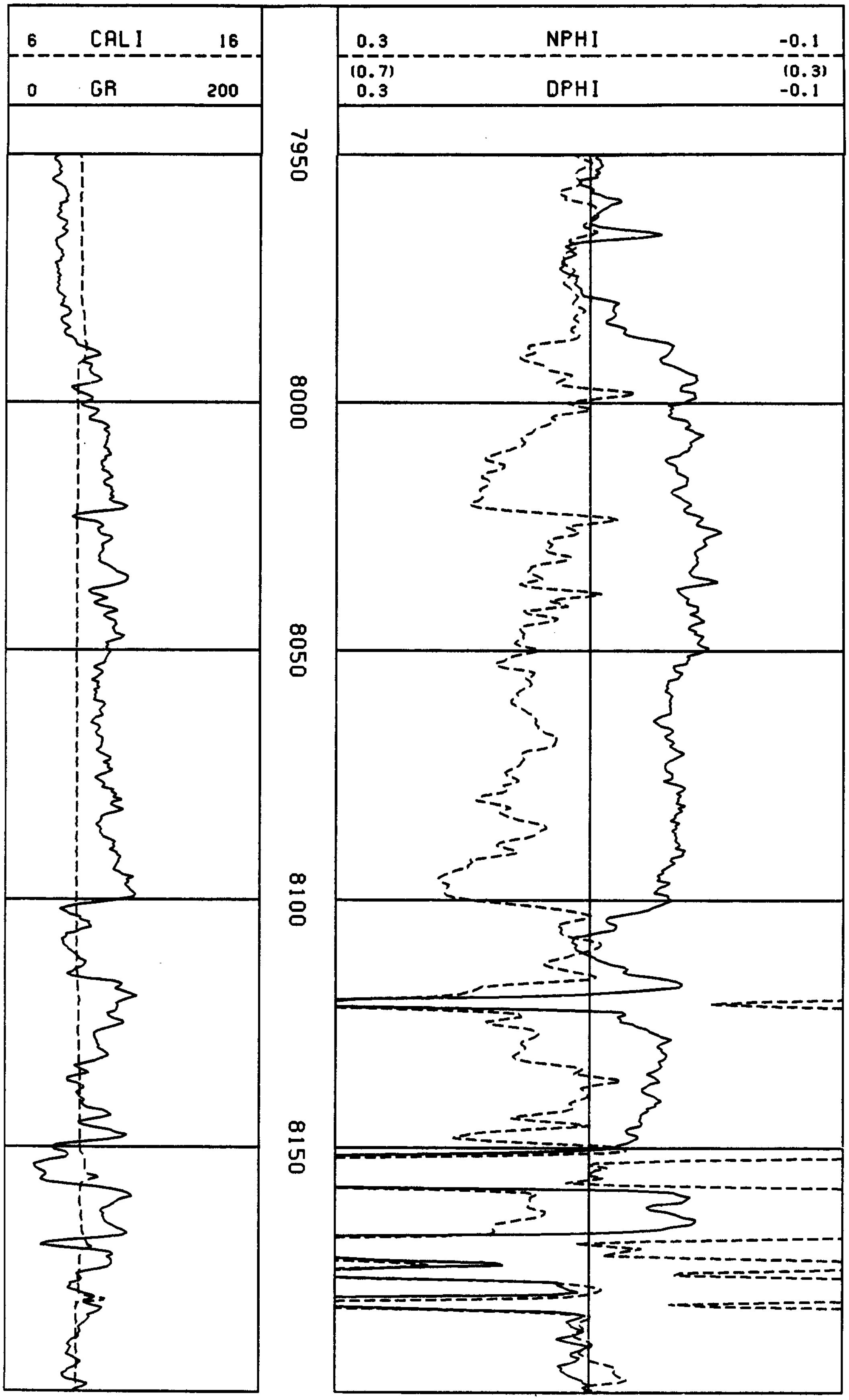

6 CALI 16
0 GR 200
0.3 NPHI -0.1
(0.7) (0.3)
0.3 DPHI -0.1
7950
8000
8050
8100
8150

MWX-2

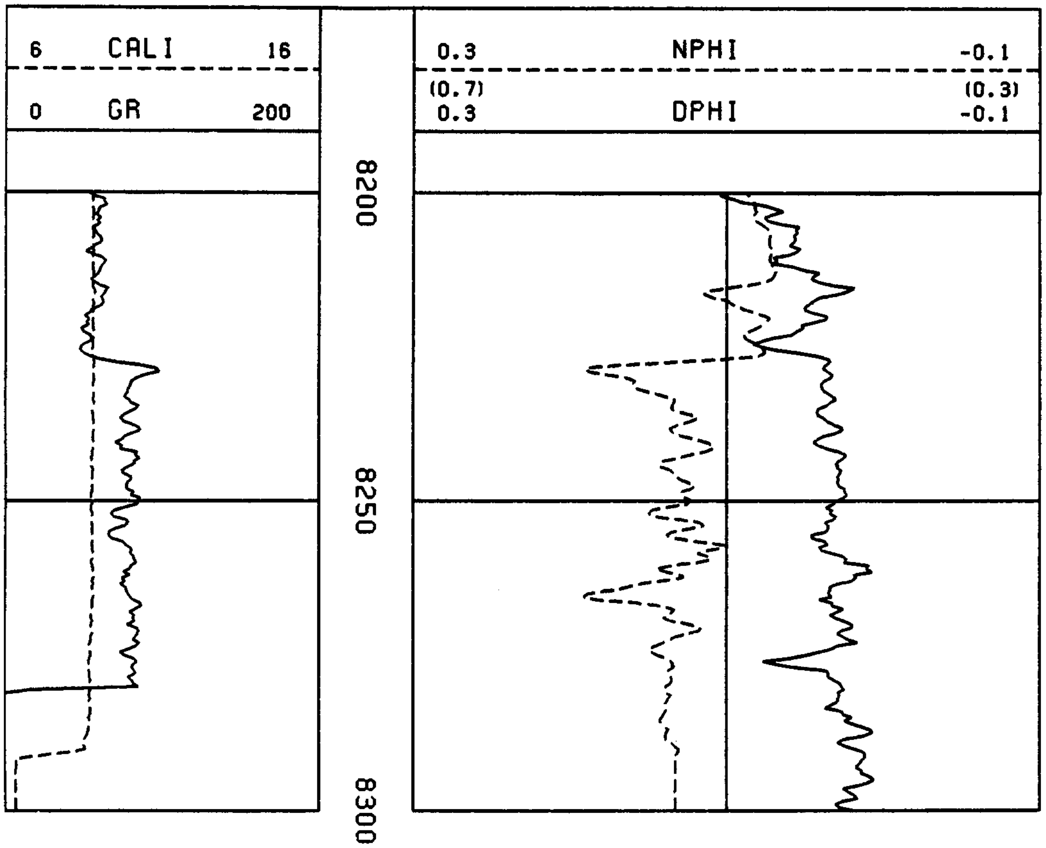

FIGURE 4.8
MWX-2 BULK DENSITY LOG

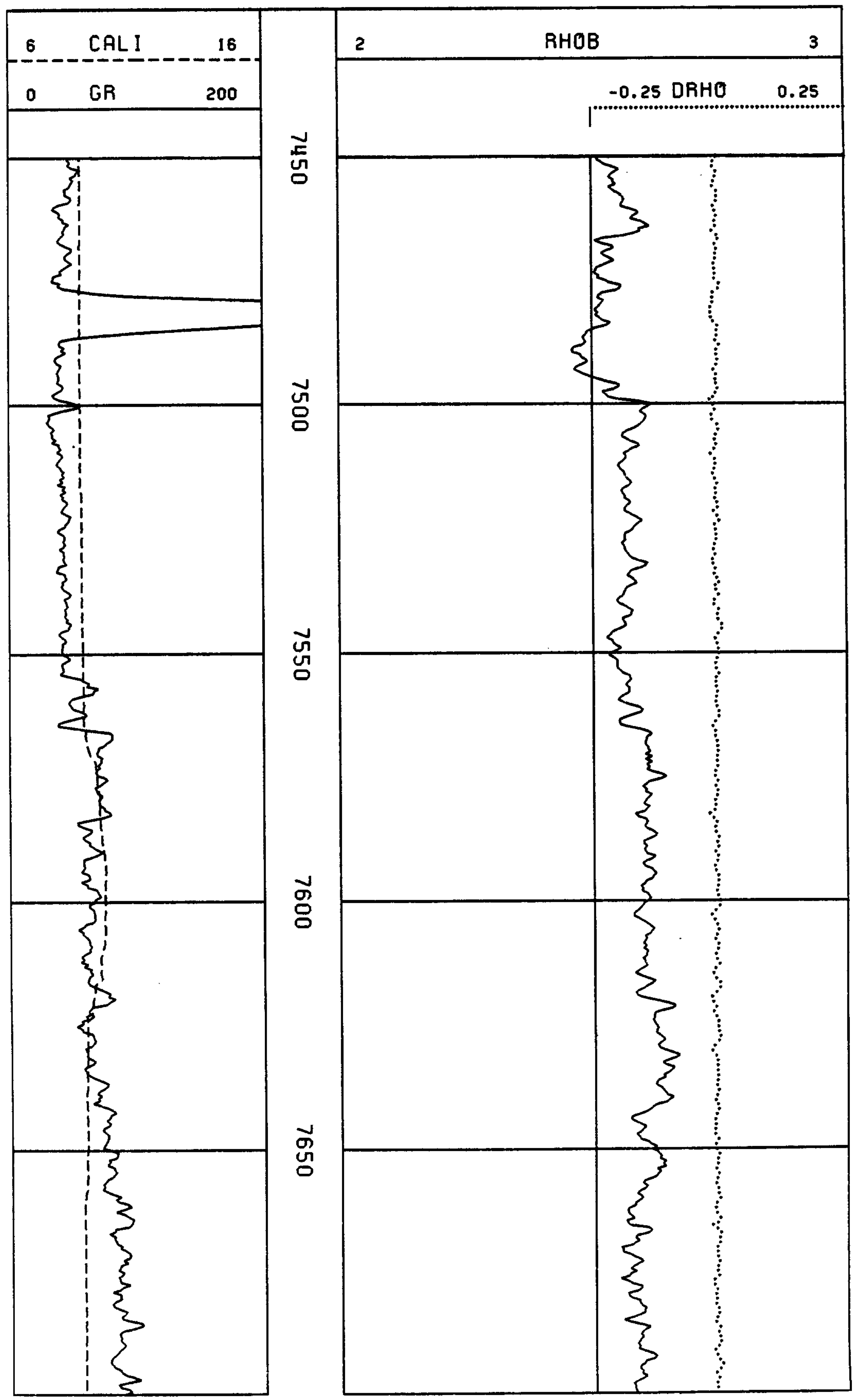

MWX-2

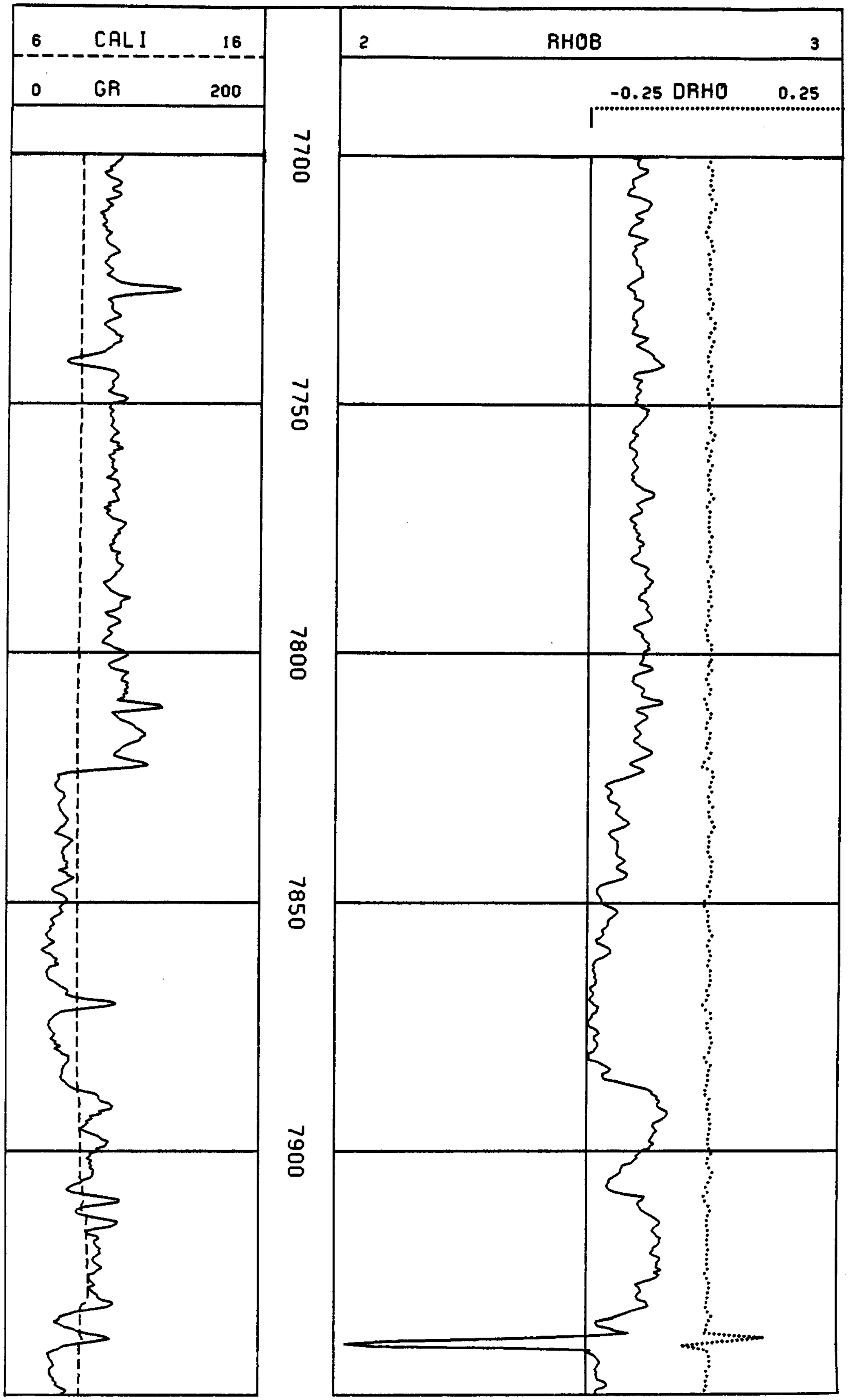

MWX-2

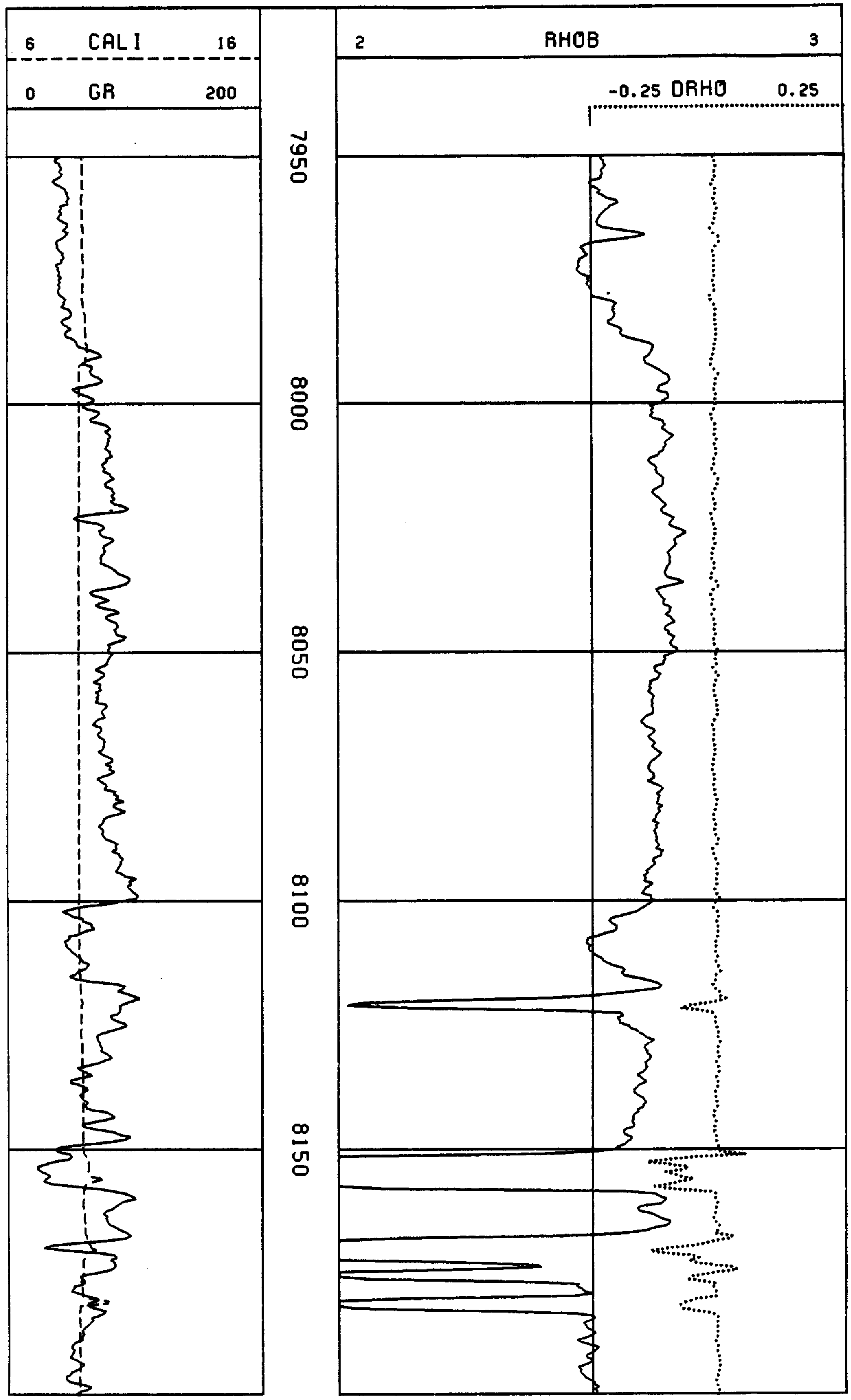

MWX-2

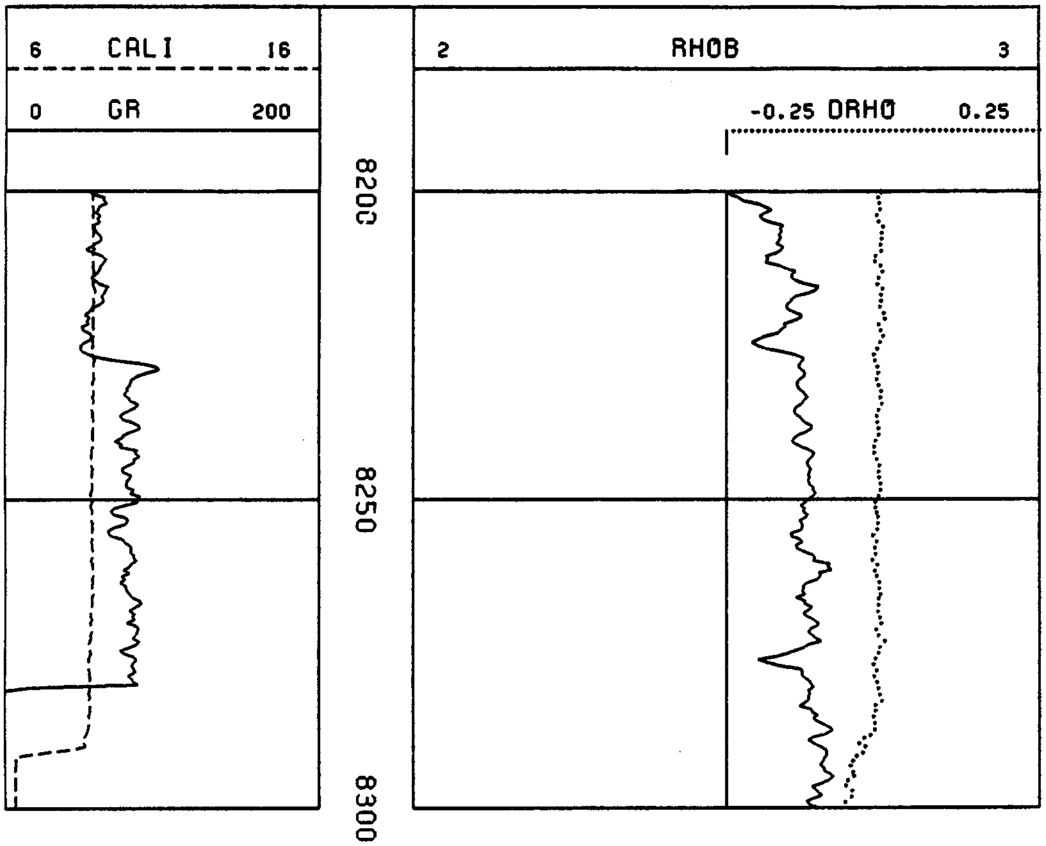

FIGURE 4.9

MWX-2 SPECTRAL GAMMA LOG

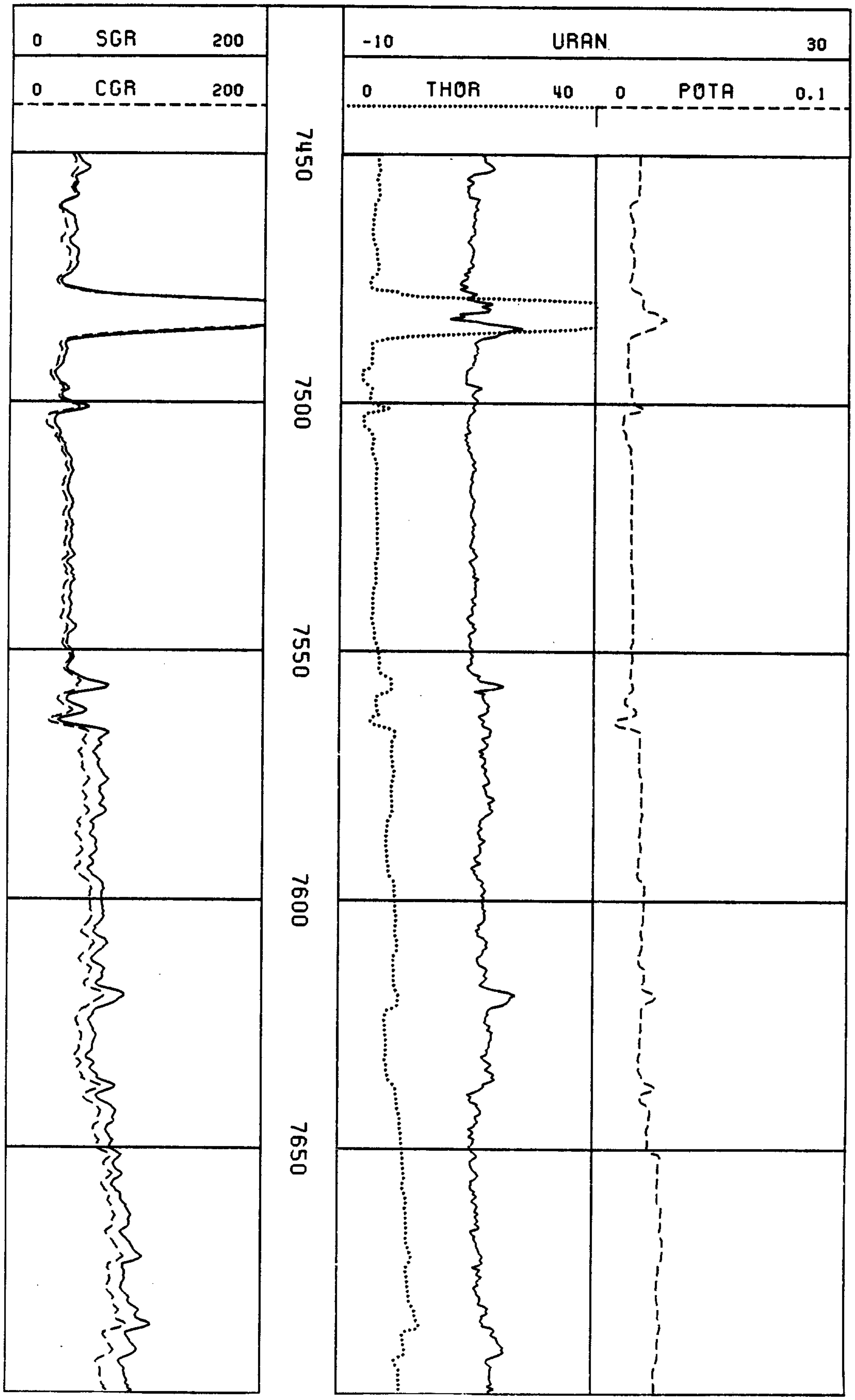

MWX-2

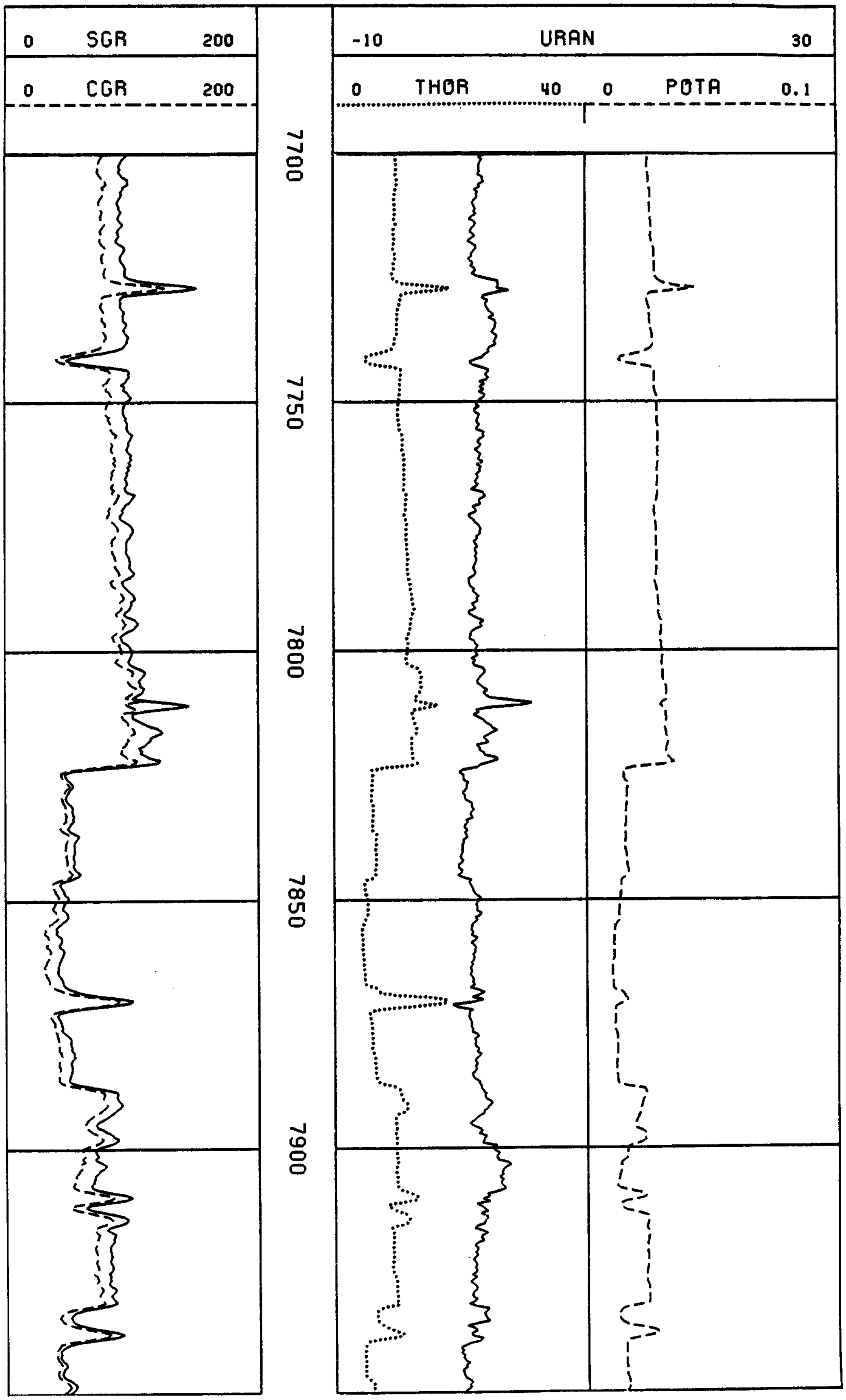

0 SGR 200
0 CGR 200
-10 URAN 30
0 THOR 40
0 POTA 0.1
7700
7750
7800
7850
7900

MWX-2

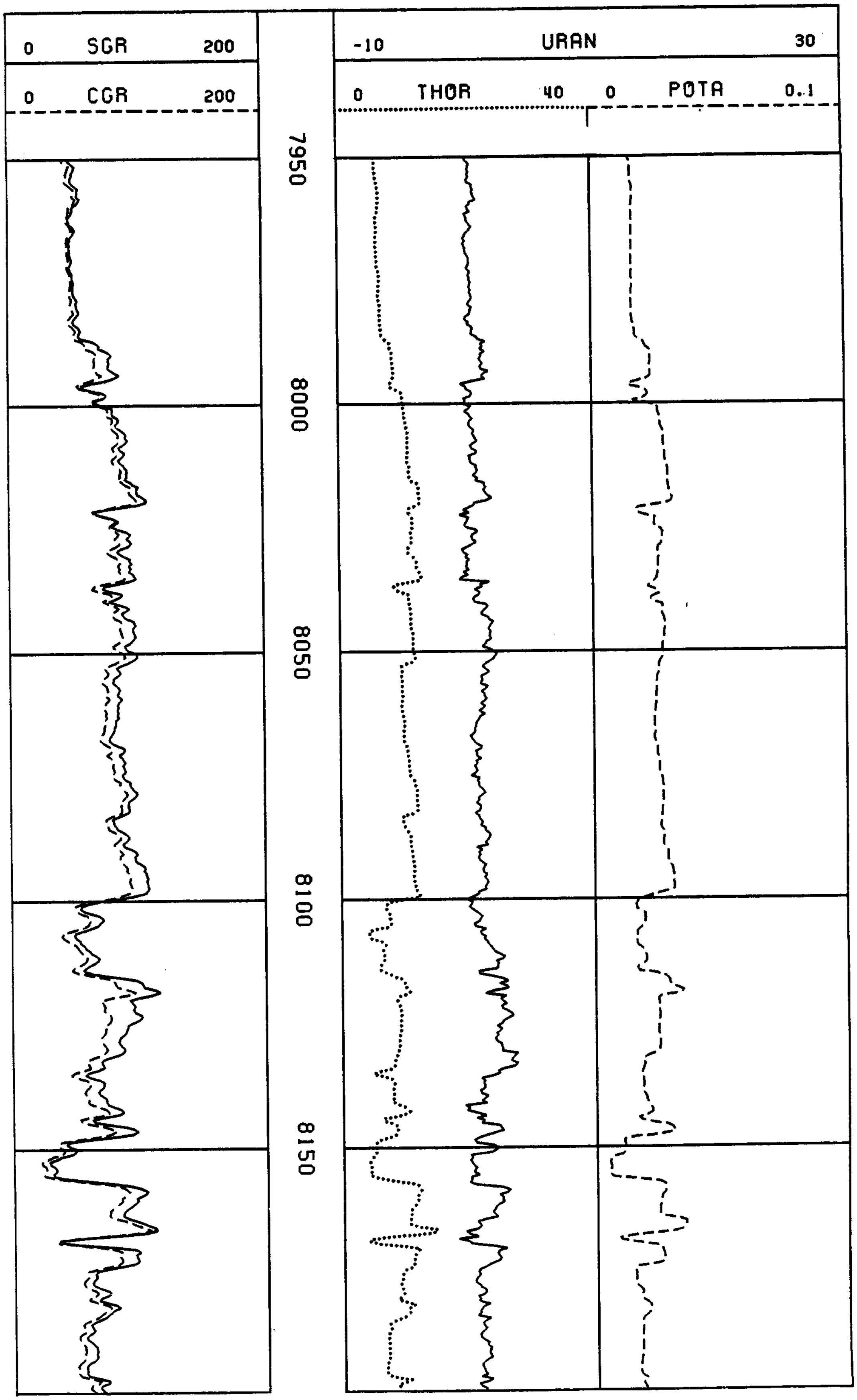

0 SGR 200
0 CGR 200
-10 URAN 30
0 THOR 40
0 POTA 0.1
7950
8000
8050
8100
8150

MWX-2

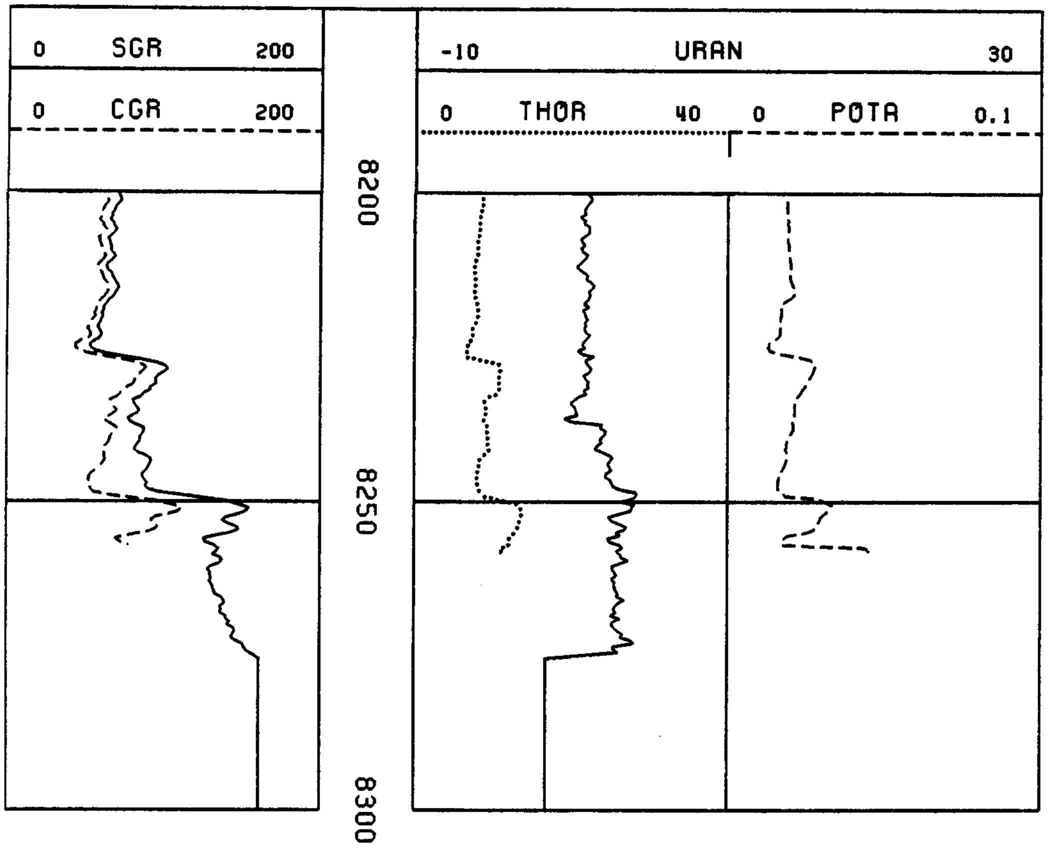

FIGURE 4.10
MWX-2, AMOCO LONG-SPACED SONIC LOG

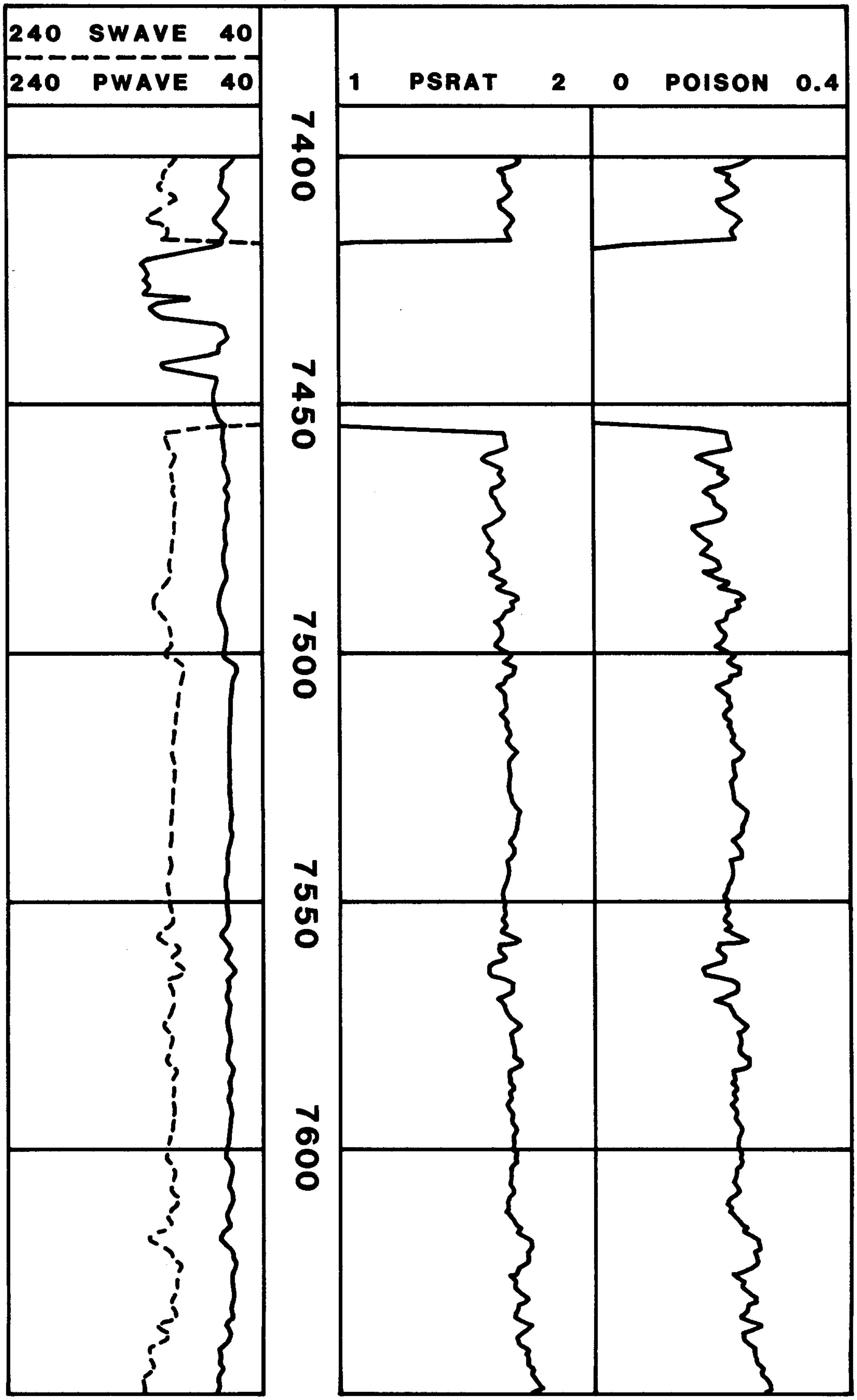

MWX-2

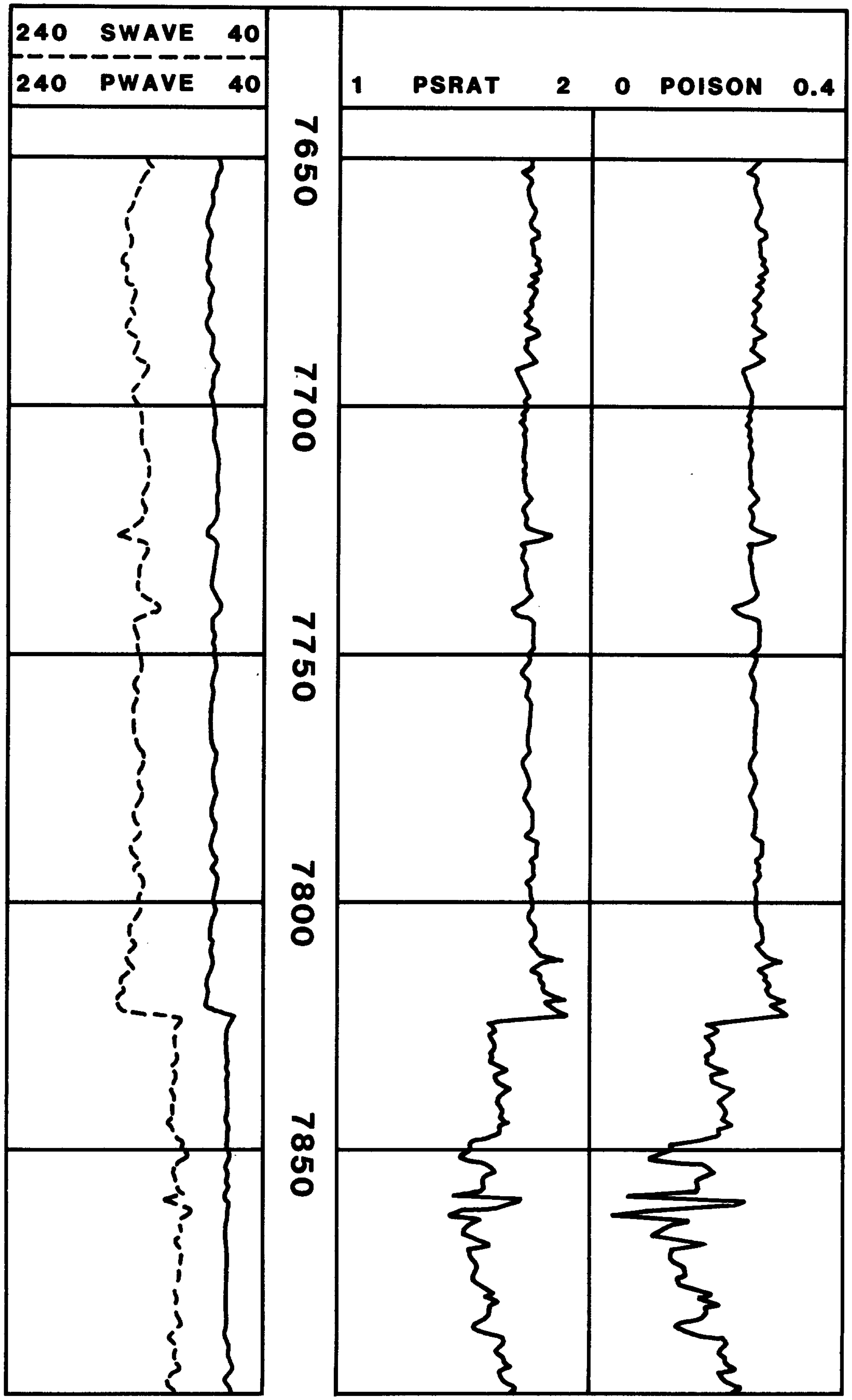
240 SWAVE 40
240 PWAVE 40
7650
7700
7750
7800
7850
1 PSRAT 2
0 POISON 0.4

MWX-2

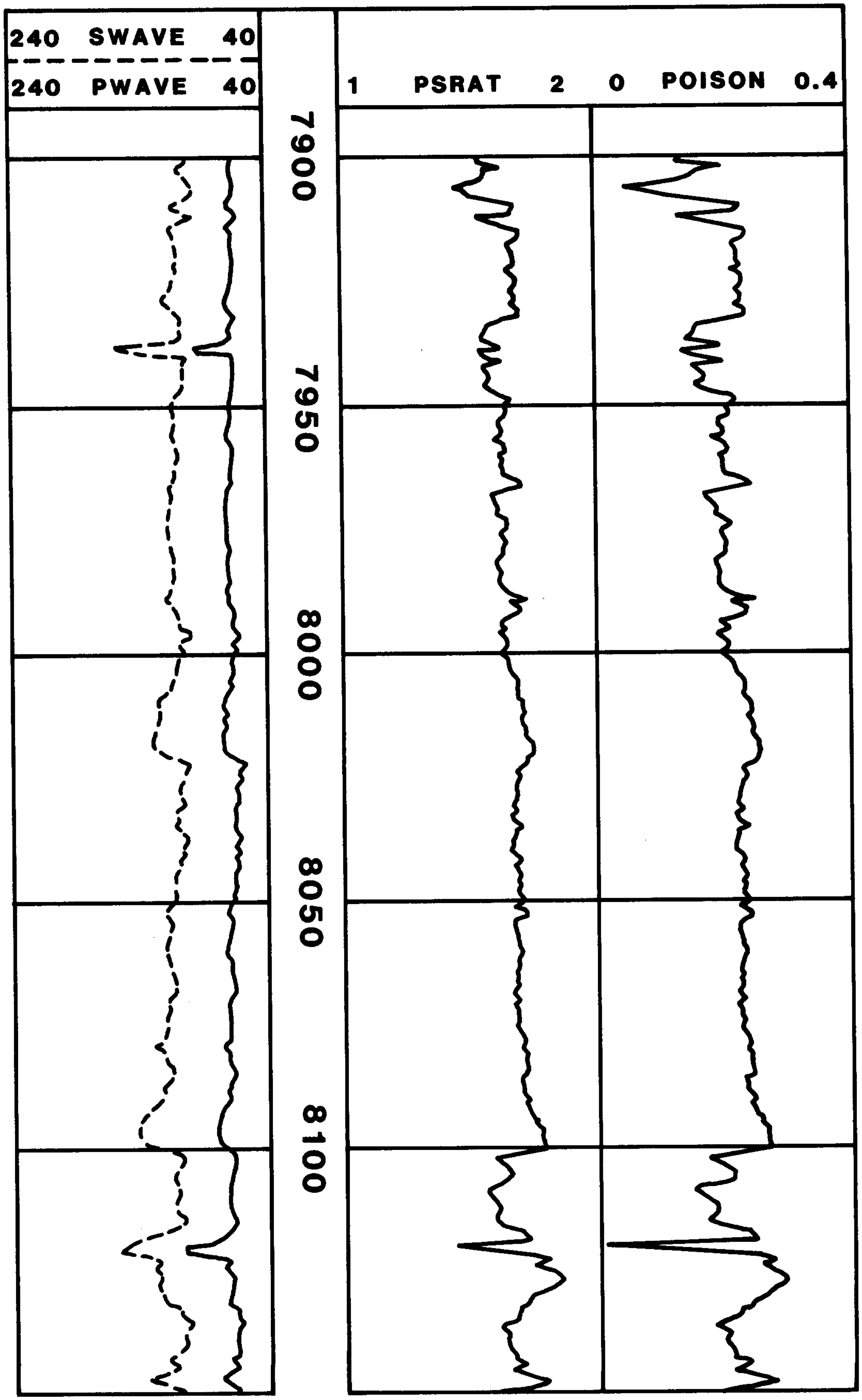

240 SWAVE 40
240 PWAVE 40
7900
7950
8000
8050
8100
1 PSRAT 2
0 POISON 0.4

MWX-2

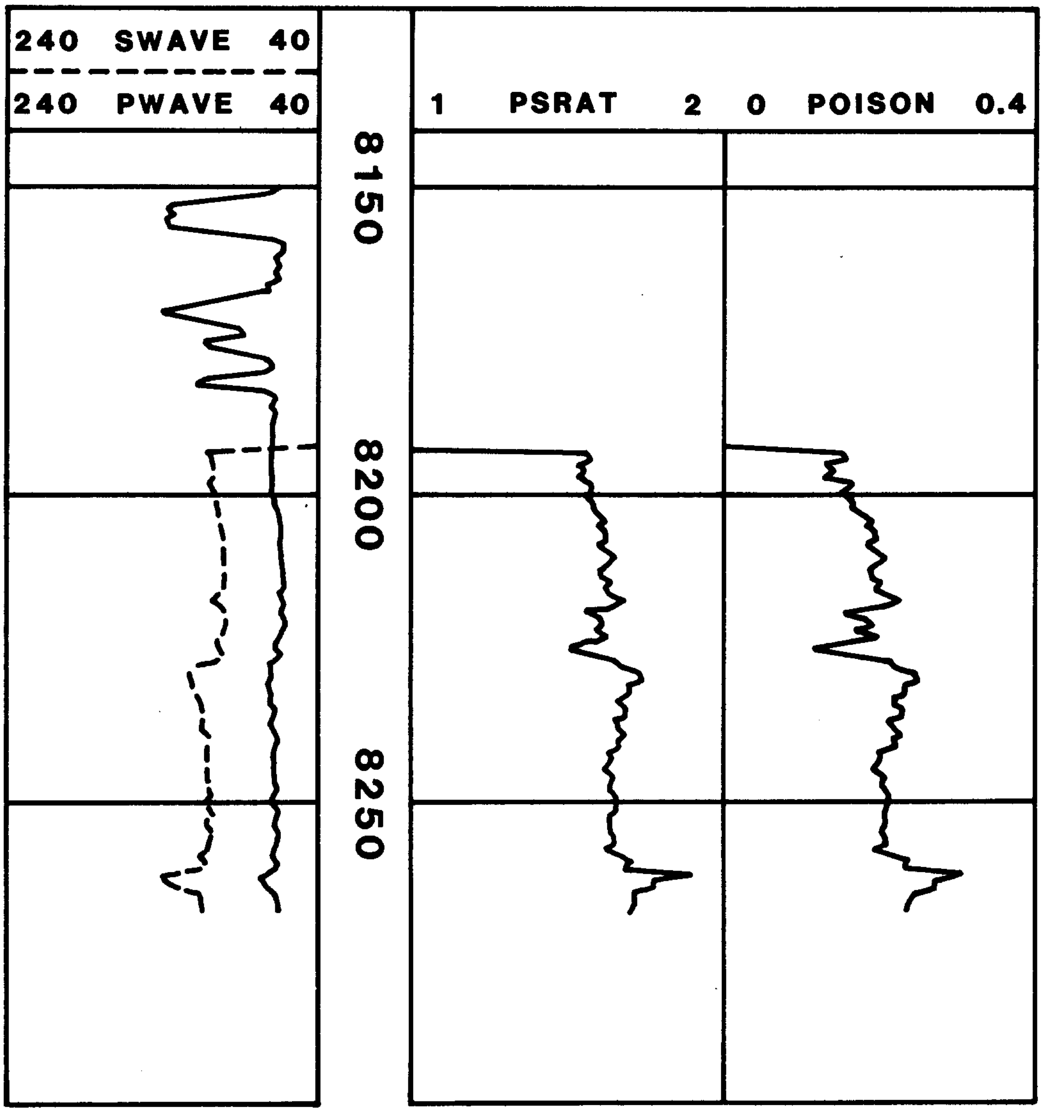

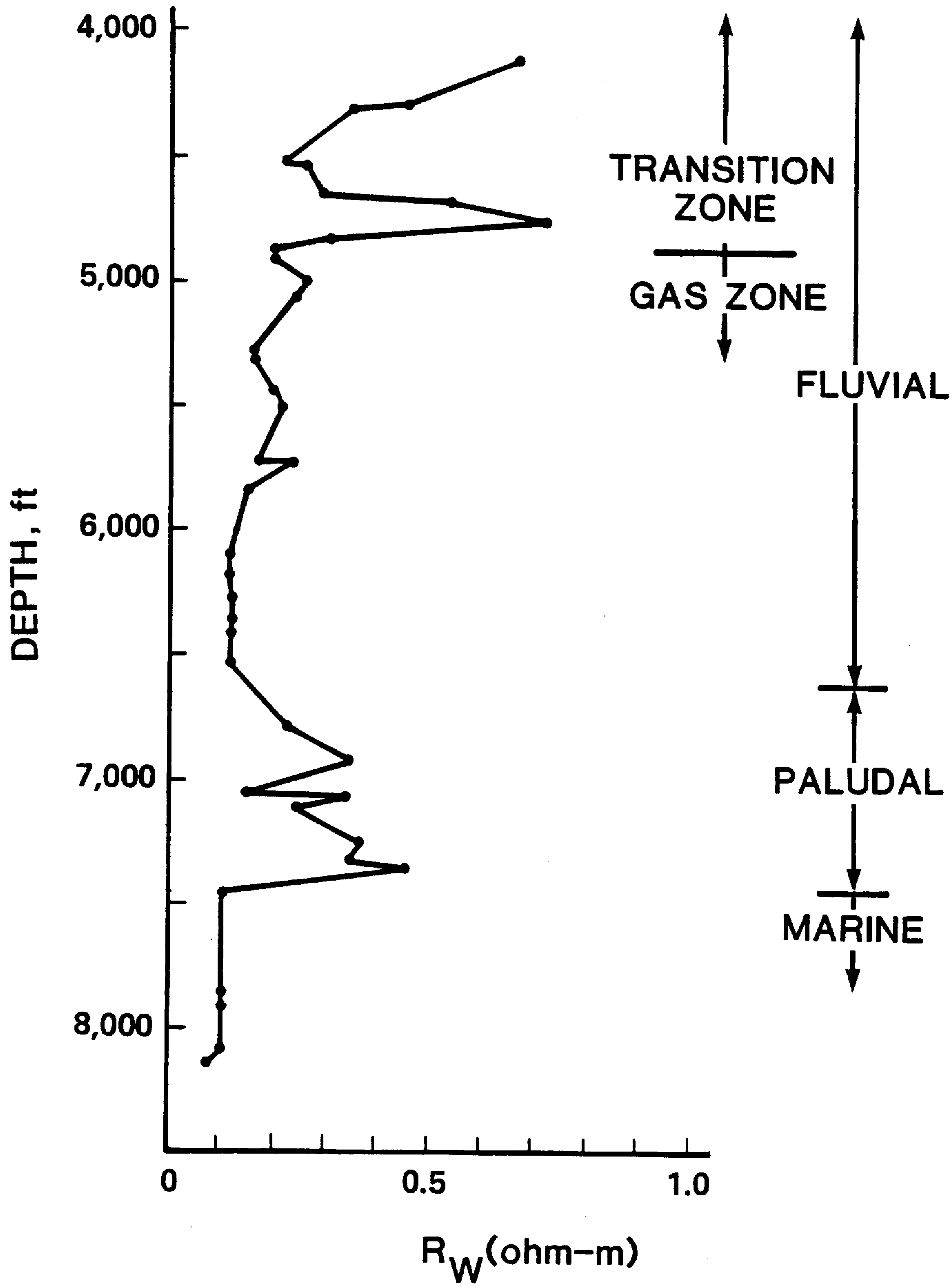

FIGURE 4.11 R_w Profile for MWX-1

FIGURE 4.12

MWX–2 SCHLUMBERGER LONG–SPACED SONIC LOG CALCULATIONS

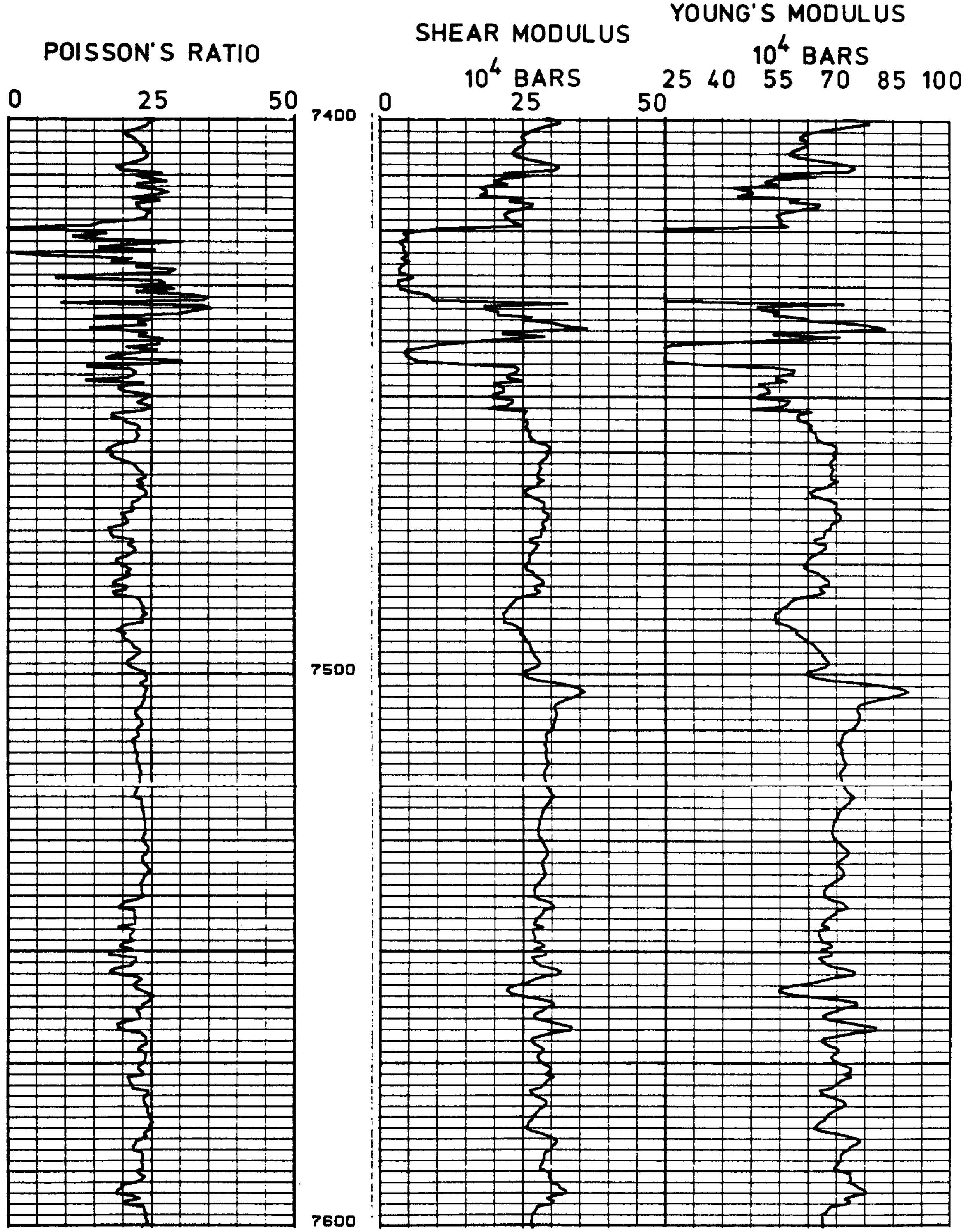

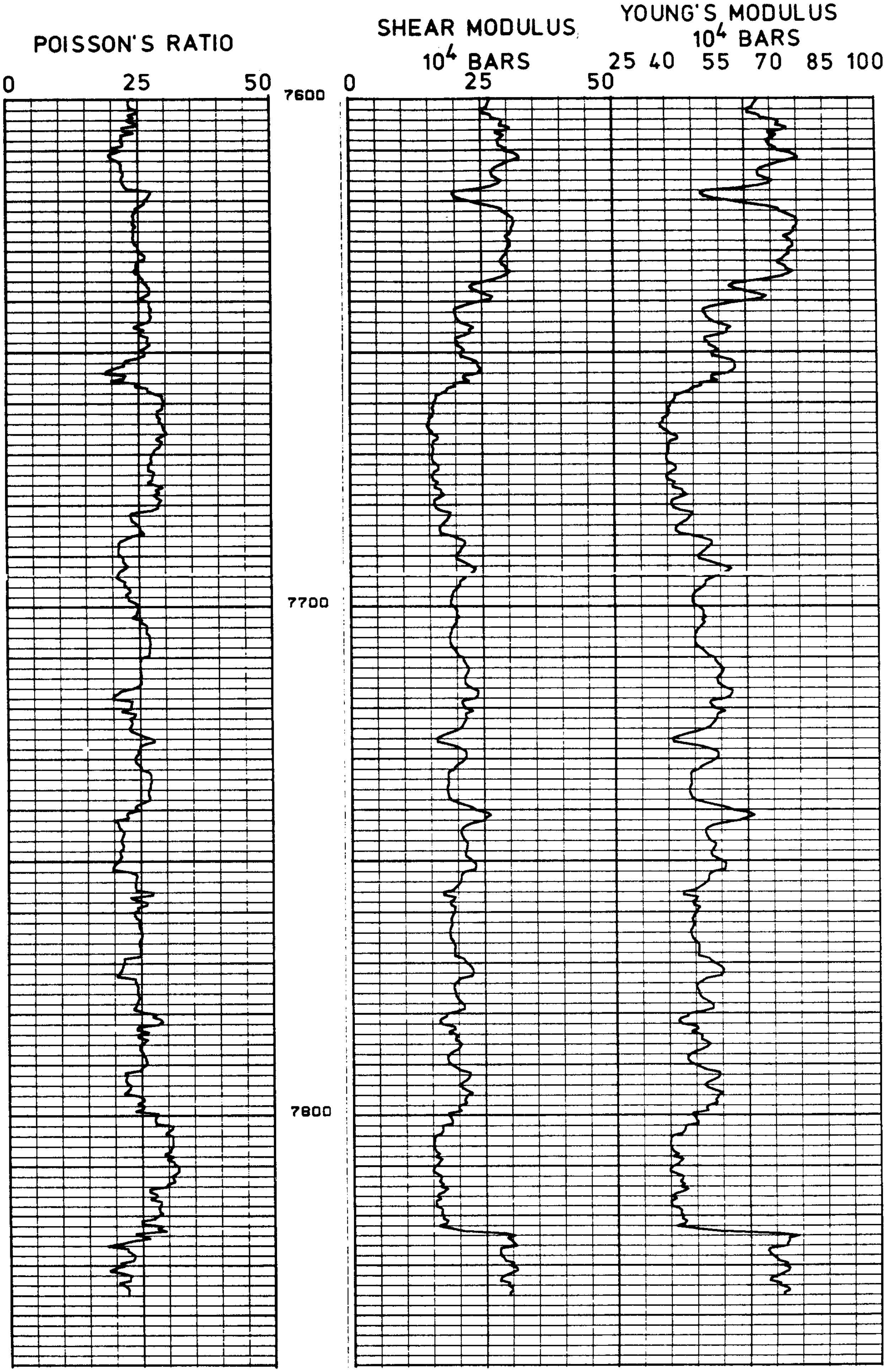
POISSON'S RATIO
0
25
50
SHEAR MODULUS
10^4 BARS
0
25
50
YOUNG'S MODULUS
10^4 BARS
25
40
55
70
85
100
7600
7700
7800

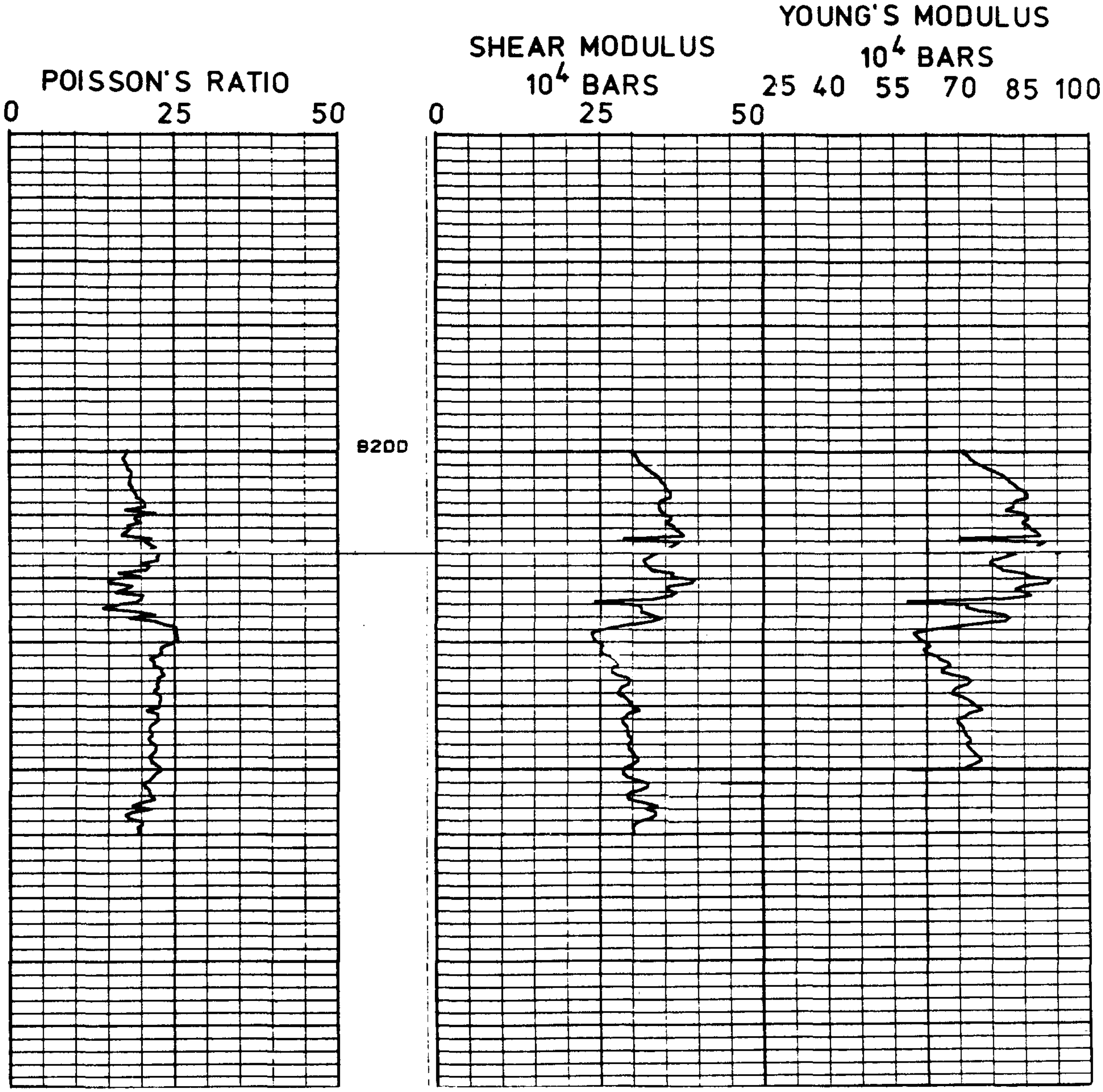
POISSON'S RATIO
0
25
50
SHEAR MODULUS
10⁴ BARS
0
25
50
YOUNG'S MODULUS
10⁴ BARS
25 40 55 70 85 100
8200

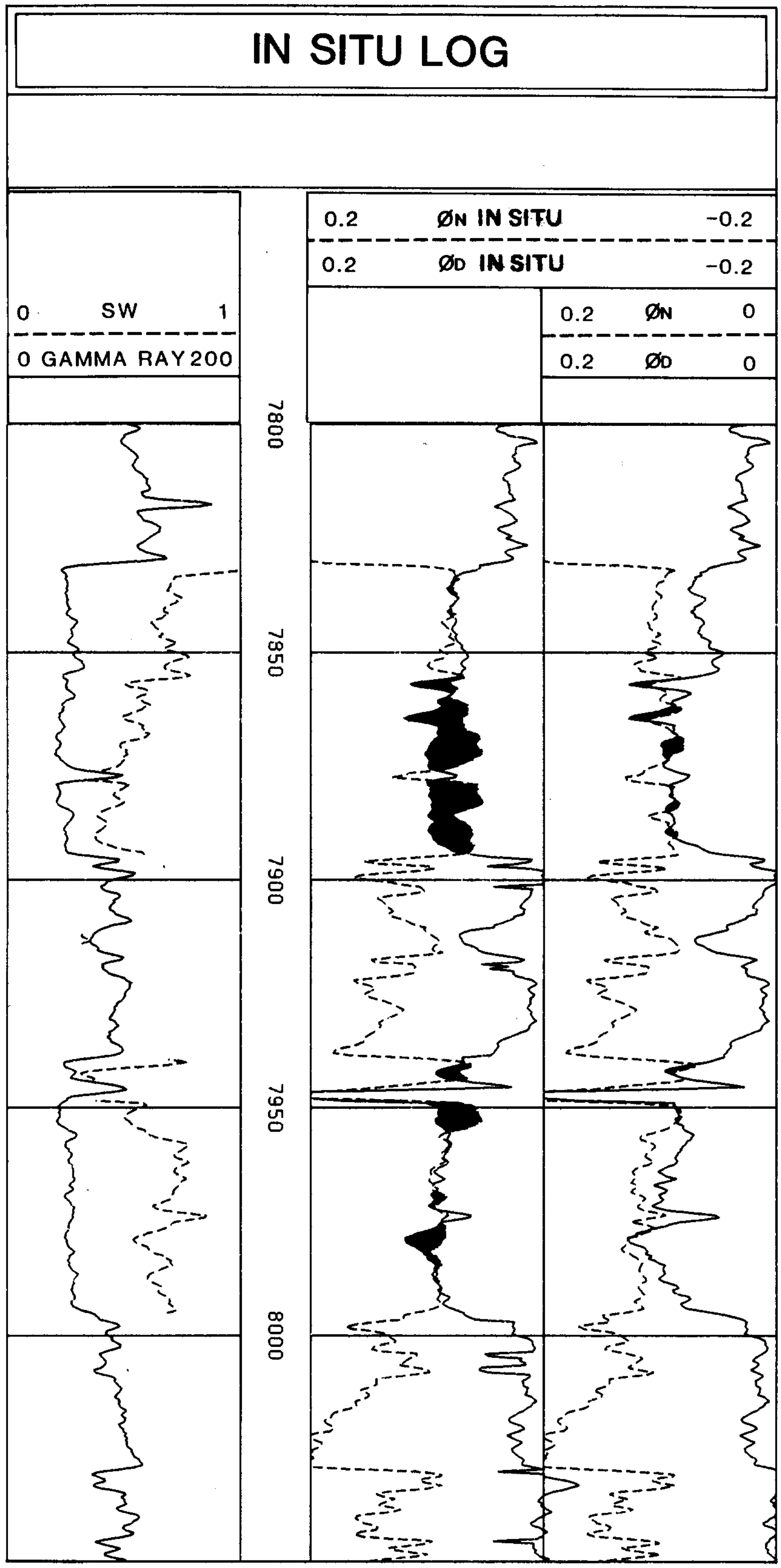

FIGURE 4.13 MWX—1 Cozzette Sandstone Density—Neutron/Gamma Ray Log, Uninvaded and Invaded Cases Presented

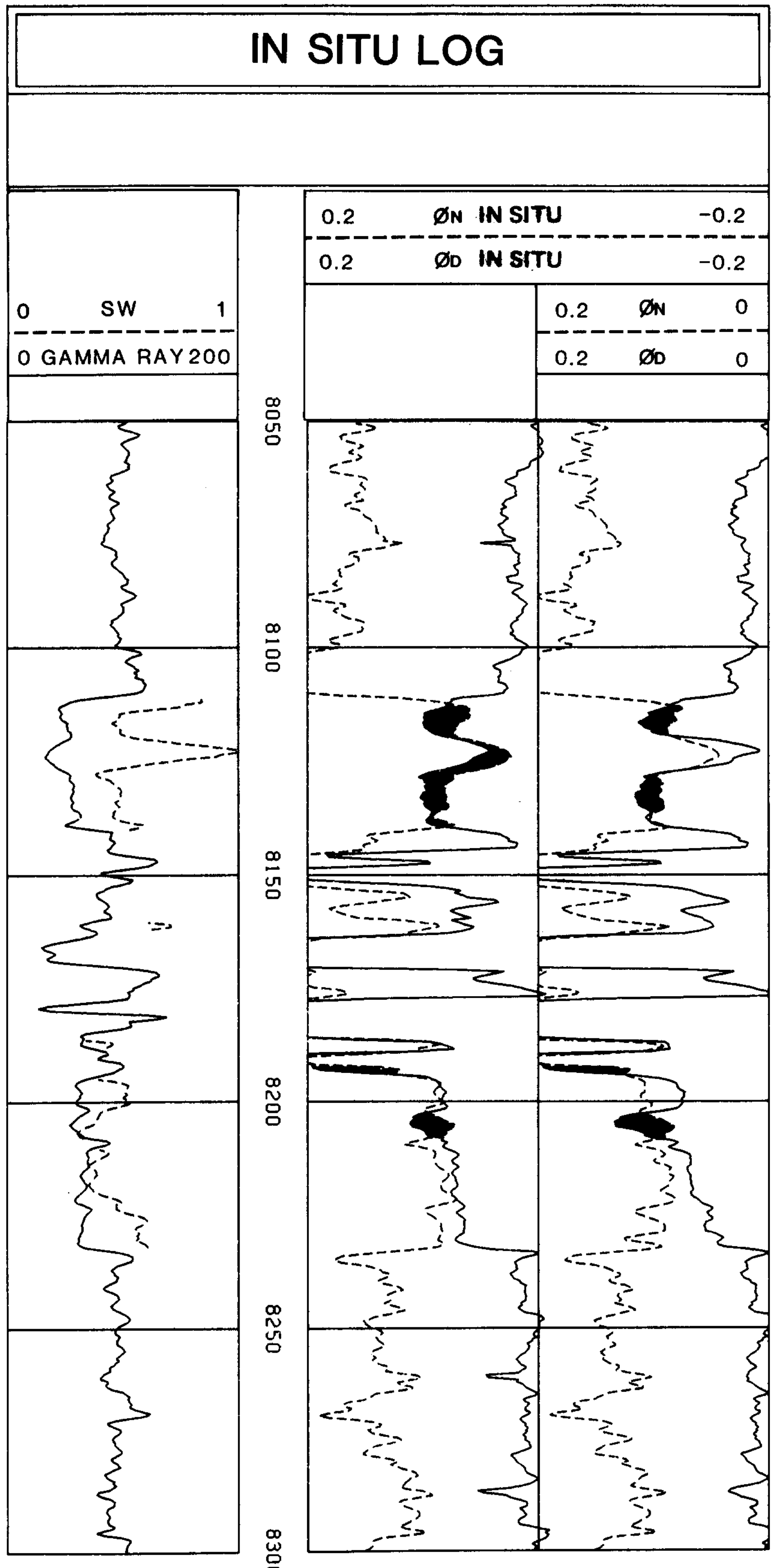

FIGURE 4.14 MWX—1 Corcoran Sandstone Density—Neutron/Gamma Ray Log, Uninvaded and Invaded Cases Presented

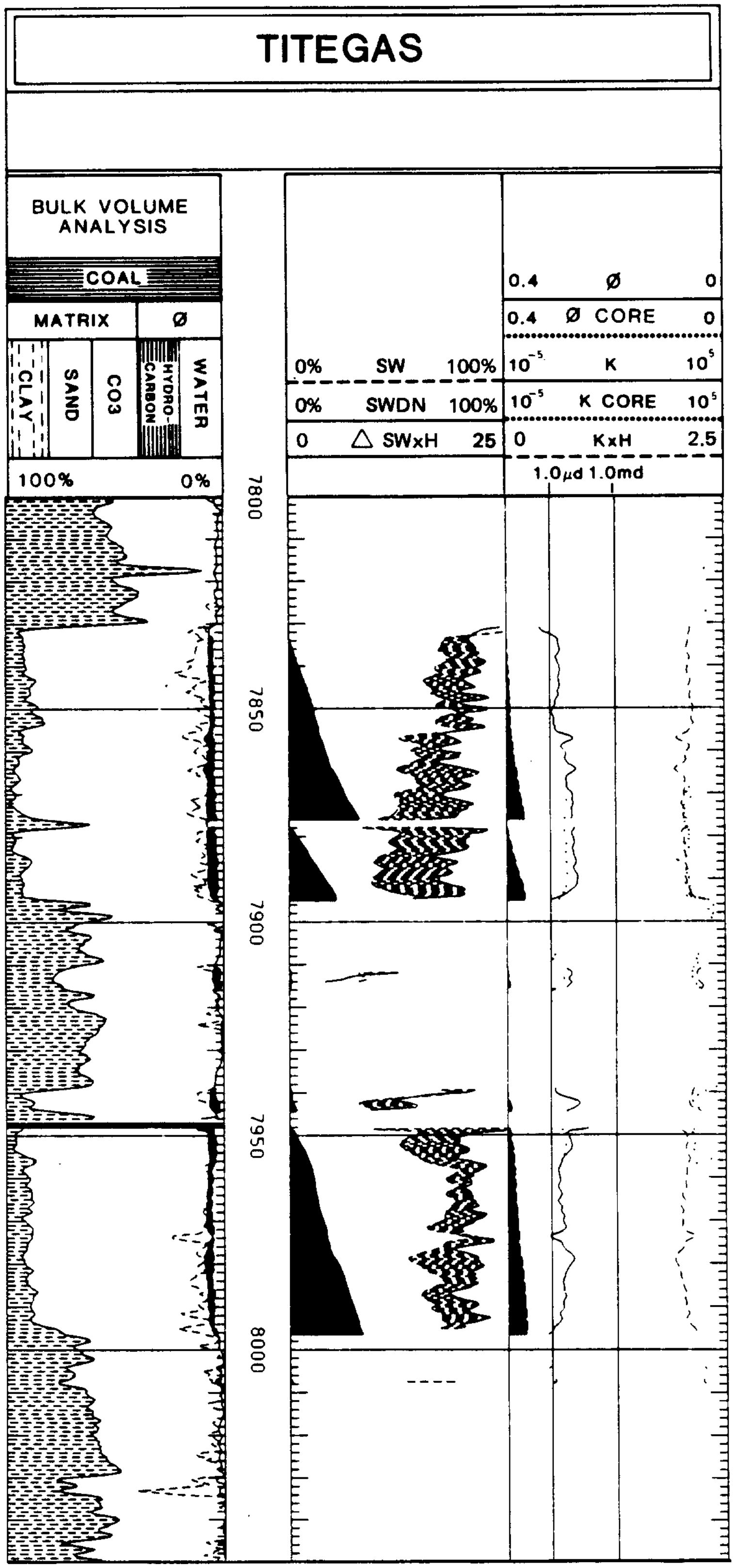

FIGURE 4.15 *MWX-1 TITEGAS model results for Cozzette Sandstone*

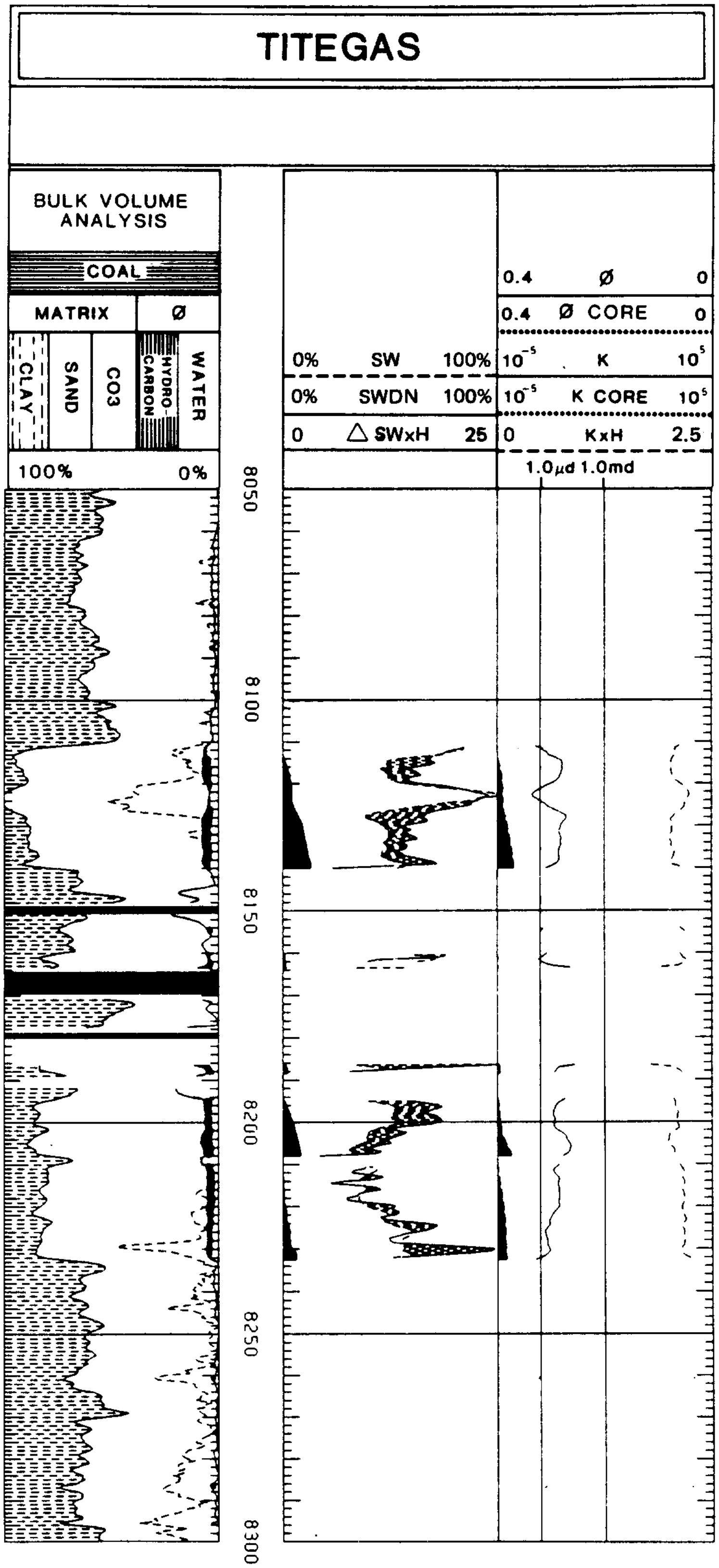

FIGURE 4.16 *MWX-1 TITEGAS model results for Corcoran Sandstone*

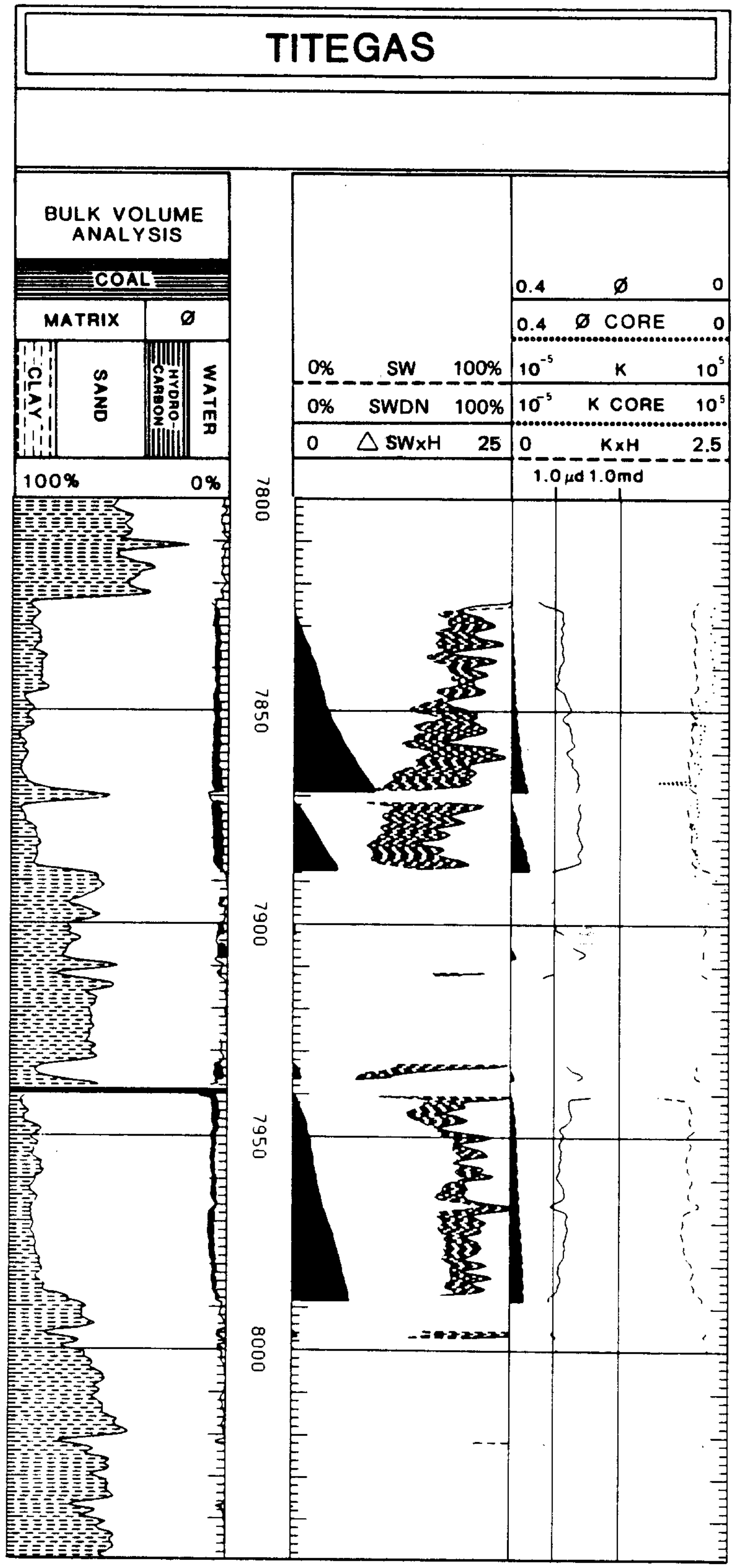

FIGURE 4.17 *MWX-2 TITEGAS model results for Cozzette Sandstone*

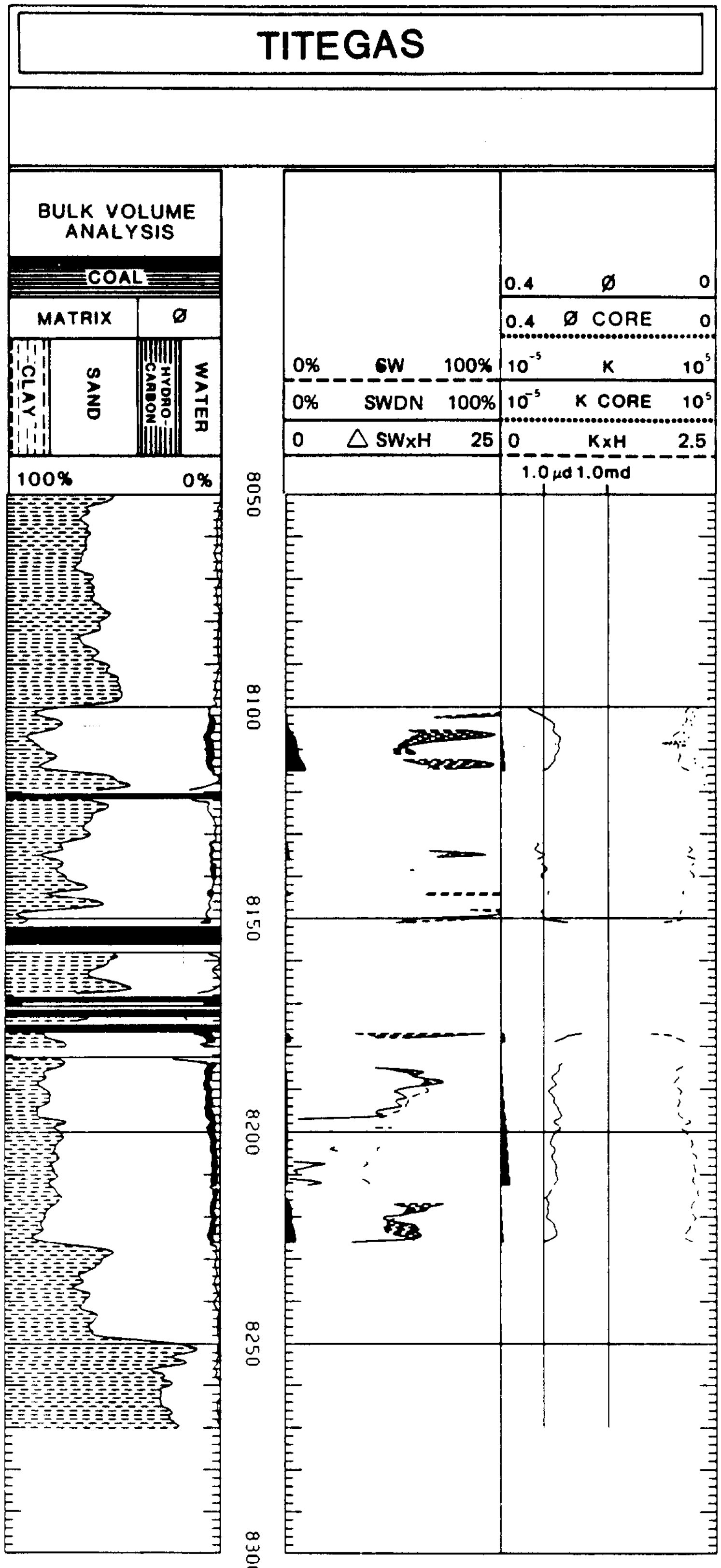

FIGURE 4.18 *MWX-2 TITEGAS model results for Corcoran Sandstone*

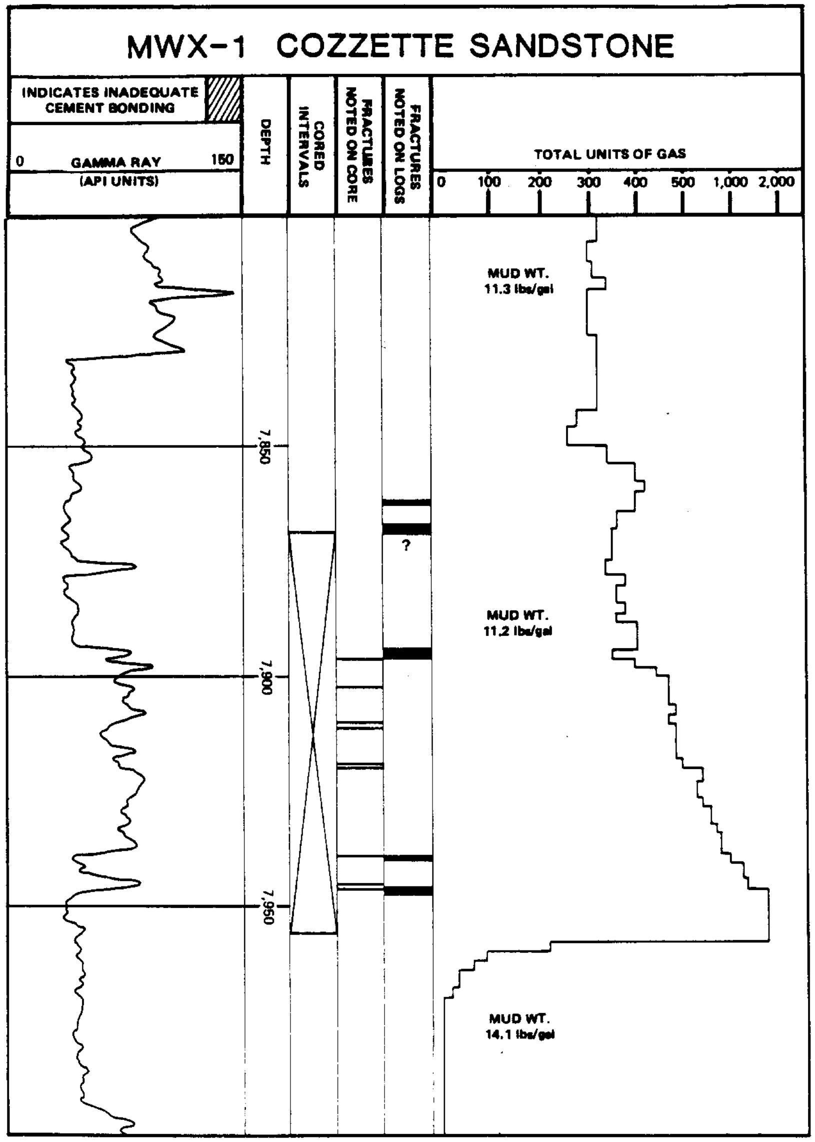

FIGURE 4.19 MWX—1 Cozzette Sandstone Mud Log

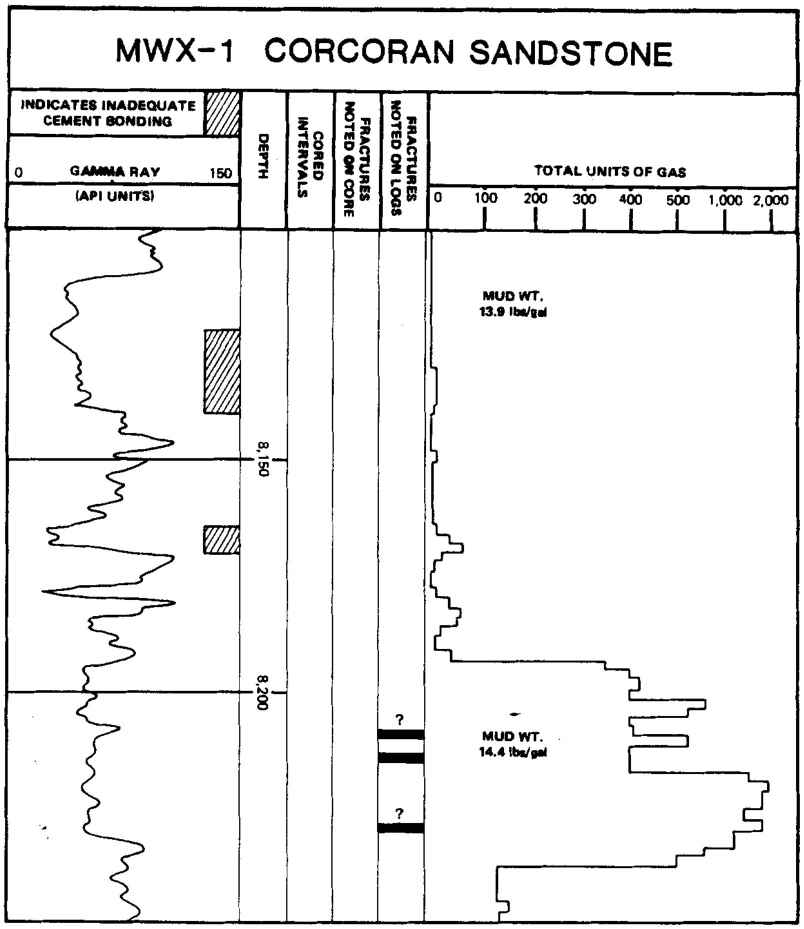

FIGURE 4.20 MWX—1 Corcoran Sandstone Mud Log

5.0 CORE ANALYSIS

Allan R. Sattler
Sandia National Laboratories

5.1 CORE PROGRAM

Limited core was taken from the Corcoran, Cozzette and Rollins blanket sandstones during the drilling of the Multiwell Experiment (MWX) wells. The Rollins, Cozzette and Corcoran sandstones occur at depths of about 7450-7600, 7800-8000 and 8100-8250 ft, respectively, as shown in Figure 5.1. The core data help describe the formations and the reservoir and provide input data for all MWX activities. In this section, these core data are presented and discussion is given to put the data into perspective. Specifically, these remarks indicate:

- what core was taken and what analyses were made;

- typical values of reservoir párameters, rock properties, and other measurements; and

- implications of the core data.

As described in section 3.0, the Corcoran, Cozzette and Rollins members of the Mesaverde Group are shoreline/marine blanket sandstones. They are abutted both by tongues of the marine Mancos shale and by associated carbonaceous mudstones, coals, and siltstones characteristic of a lower delta plain environment. In general, the Corcoran and Cozzette are productive (although tight) in the Piceance basin in the vicinity of the MWX site.

Four intervals were cored (Figure 5.1) as follows:

(1) MWX-1, 7870-7960 ft, 4 in. core: includes parts of the upper and lower Cozzette sands and the intervening material, including a thin coal stringer.

(2) MWX-2, 7817-7907 ft, 4 in. core: includes a few feet of the tongue of the Mancos shale, the upper Cozzette sand, and rock between the Cozzette sands.

(3) MWX-2, 8100-8141 ft, 4 in. core: includes the entire upper Corcoran sand and portions of the over- and underlying formations.

(4) MWX-3, 7536-7564 ft, 2 1/2-in core: entirely within the Rollins sandstone.

The MWX core analysis program is described in detail elsewhere.[1] The results of analyses presented in this section have been taken from various reports submitted by the various participants. These reports are specifically referenced where used in this section, and more comprehensive listings are found in Section 8.0 and Appendix 9.7. This section presents reservoir and mechanical properties obtained from core. Other core-derived properties are reported in other sections: lithology (3.2), minerology/petrology (3.2.6), organic content and maturation (3.3), natural fractures (3.4), and estimates of in situ stresses from core data (6.2.2).

5.2 RESULTS AND DISCUSSION

Reservoir parameter measurements were made at frequent intervals in the sands. Routine core analyses were made on plugs taken every foot. Restored pressure state permeabilities and cation exchange capacities (CEC) were performed every two or three feet. Other specialized measurements were made on selected samples; these include capillary pressure measurements and porosity versus confining pressure.

The water saturations were made with the Dean Stark distillation method.[2-4] Porosities were determined by Boyles law method with helium.[2-4] Core Laboratories used the nonsteady state, pulsed method to determine their Klinkenberg (gas slippage corrected) permeabilities.[5,6] The Institute of Gas Technology (IGT) used the steady state method to determine their Klinkenberg permeabilities.[7-9] Core Laboratories subjected each of the core plugs to toluene extraction to remove any residue from the oil-based drilling fluid and they leached any salts out of the pores using hot methyl alcohol. IGT made their permeability measurements without cleaning procedures. In some cases, the IGT data may appear a little lower than the Core Laboratories data, when both are corrected to the same confining pressures. Generally, the IGT data and Core Laboratories permeability data are in reasonable agreement.

In many core studies, analyses are confined to the reservoir rock only. In this case, however, the material abutting the sands was studied to determine the extent of the stratigraphic reservoir (through caprock analysis) and to obtain properties useful for hydraulic fracture design and analysis of stress test data. Mechanical property measurements were made on both sandstone and confining rock samples.[10-12]

Analyses from Core Laboratories, IGT, and ReSpec are given in Appendices 9.3-9.5, respectively. Summaries or portions of these data are presented in the following figures and tables:

(1) Reservoir Properties:

MWX-1 Cozzette Reservoir Properties	Table 5.1., Figure 5.2
MWX-2 Cozzette Reservoir Properties	Table 5.2., Figure 5.3
MWX-2 Corcoran Reservoir Properties	Table 5.3., Figure 5.4
MWX-3 Rollins Reservoir Properties	Table 5.4.

(2) Special Reservoir Properties:

Capillary Pressures		Figure 5.5.
Permeabilities Versus Net Stress and Water Saturation		Figure 5.6.
Marine Core Analyses	Table 5.5.	
Vertical Permeabilities	Table 5.6.	
Porosity Versus Pressure (Compressibility)	Table 5.7.	
Caprock Analyses	Table 5.8.	

(3) Rock Properties:

MWX-1 Mechanical Properties	Table 5.9.
MWX-2 Mechanical Properties	Table 5.10.
MWX-3 Mechanical Properties	Table 5.11.

The overall uniformity in reservoir properties extends vertically through the sandstones and also laterally for corresponding upper Cozzette core between MWX-1 and

MWX-2. In the upper Cozzette sandstone, water saturations are about 35%, porosities are 6%-7%, dry Klinkenberg permeabilities (at 1000 psi confining pressures) are 4-6 μd, CEC's are about 0.4 meq/100 g, and Young's modulus and Poisson's ratio are about 35 GPa and 0.22, respectively. As seen in Figure 5.3, the top third of the upper Cozzette sand has low porosity and permeability and high water saturation. This zone is characterized by pores filled with pyrobitumin ("cooked-out oil") and is clearly poor reservoir rock.[13]

The porosities, permeabilities and mechanical properties of the lower Cozzette and Corcoran sandstones are similar to the upper Cozzette. However, the water saturations in the Corcoran are somewhat higher (~50%) and the CEC values average about twice those of the Cozzette. The limited Rollins data (Table 5.4) show high water saturations; the Rollins is not gas productive at the MWX site.

The permeabilities of these tight sandstones are a strong function of the effective stress and water saturation.[14,15] On the other hand, the porosity appears almost independent of confining pressure, at least over the range of interest.[16] Well tests indicate that pore pressures in the Cozzette and Corcoran are 6500 and 6800 psi, respectively. Thus, the net confining stresses in situ are quite low (1000-1500 psi) as a consequence of these high pore pressures, but stresses can become greater during drawdown and production. Restored state permeability measurements were made routinely at 1000, 3000, and 4000 psi. In addition, two Cozzette samples were measured over a range of net stresses and at different water saturations (Figure 5.6). Significant decreases are seen for increasing stress and water saturation. At their expected values in the Corcoran and Cozzette sandstones, water saturation effects appear to reduce the effective permeability to gas by about an order of magnitude. Thus, the dry Klinkenberg permeabilities given in Tables 5.1-5.3 and Figures 5.2-5.4 should be reduced by at least a factor of 10 to obtain realistic estimates of reservoir matrix permeabilities.

Limited data were obtained on the vertical permeabilities (Table 5.6)[6] and compressibilities (Table 5.7)[16] of the Cozzette and Corcoran sandstones. The vertical permeabilities are about the same as the horizontal permeabilities (the direction for the other permeability data). The compressibilities are small and relatively constant over the limited range of pressures tested.

Some of the first capillary pressures of brine in tight sandstones were made in the Cozzette core (Figure 5.5).[17] Pressures above 500 psi were found at the prevailing water saturations of each sample. These high pressures clearly affect fluid imbibition and gas mobility in these rocks. Thus, stimulation treatments involving a minimum amount of water should be considered in treating these formations.

Formation permeabilities measured during well testing are much larger than the matrix permeabilities measured in core.[18] The formation permeabilities are in the range of hundreds and tens of microdarcies in the Cozzette and Corcoran, respectively. On the other hand, the realistic matrix permeabilities are in the range of tenths of microdarcies when net stress and water saturation effects are included. The formation-matrix difference is ascribed to the presence of natural fractures. Several such fractures were observed in core (Section 3.4). Three Corcoran permeability measurements were abnormally high; very thin, horizontal, carbonaceous stringers were observed in these core plugs and these, or possibly very small fractures, could be responsible for the higher permeability. (The presence of natural fractures is quite marked in MWX core, especially in other regions of the Mesaverde.)

CEC analyses were performed on a trimmed core plug end using the adsorbed water method.[5,6] CEC values are used as corrections to the formation factor determination in the Waxman Smits Thomas/Archies Law formalisms. These formalisms were used in log analysis along with other electrical properties of the formation for the determination of resistivity and water saturation. The CEC values can be used to obtain a relative estimate of clay concentration across a zone.

Caprock analyses (Table 5.8)[19,20] were made on selected samples from rock bounding the sandstones. These measurements included permeability to brine and the minimum gas threshold pressure necessary to displace water. A combination of very low permeability plus a large threshold displacement pressure would indicate good caprock. Permeability measurements were generally in the nanodarcy to subnanodarcy range, and displacement thresholds were in the hundreds of psi range. In MWX-1, these measurements were used to determine the limits of the pay zone. In MWX-2, measurements were made over the abutting material that had the highest core gamma ray signature, which was taken as an indication of the best caprock. The results indicated in both cases that there was good caprock, although this novel measurement is viewed as only a qualitative indicator.

Mechanical property data (Tables 5.9-5.11)[10-12] were obtained by ReSpec from core samples taken throughout each of the coring intervals. Estimates of tensile strength and fracture toughness were obtained from a limited number of samples. Triaxial tests were made at various confining pressures to obtain moduli and Poisson's ratios for the different lithologies. Results in Figure 5.7 show that low moduli typical of shales were found for the samples immediately overlying the Cozzette and Corcoran. However, the moduli of the sandstones and intervening and/or underlying lithologies are far less distinct. This lack of distinction may imply that stress contrasts between these strata are low. A definite correlation between these mechanical rock properties and the in situ stress state has not been established, but often contrasting rock properties and gamma ray signatures imply the presence of a stress barrier. These mechanical rock properties are used as inputs for stimulation design: moduli are used in frac height and width predictions, and fracture toughness is used in fracture height calculations.

5.3 REFERENCES

1. A. R. Sattler, "The Multiwell Experiment Core Program II," SPE 12854, Proceedings of the 1984 SPE/DOE/GRI Unconventional Gas Recovery Symposium, Pittsburgh, PA, May 1984.
2. Core Laboratories, Report RP-2-6714, November 1981.
3. Core Laboratories, Report RP-2-6806, March 1982.
4. Core Laboratories, Report 3806-7199, July 1983.
5. Core Laboratories, SCAL Report 203-820022, March 1982.
6. Core Laboratories, SCAL Report 203-820027, September 1982.
7. Institute of Gas Technology, Project 65056 Report, July 1982.
8. Institute of Gas Technology, Project 65056 Report, August 1982.
9. Institute of Gas Technology, Project 65056 Report, October 1982.
10. RE/SPEC Inc., Data Report RS1-0226, September 1983.
11. RE/SPEC Inc., Data Report RS1-0234, October 1983.
12. RE/SPEC Inc., Data Report RS1-0238, November 1983.
13. C. W. Spencer, USGS Letter Report to D. A. Northrop, Sandia National Laboratories, August 1982.

14. Institute of Gas Technology, Project 65056 Report, "Sandstone Permeability and Porosity Measurements: Relative Permeability Data," October 1982.
15. Institute of Gas Technology, Project 30568-03 Report, "Measurement and Analysis of Two Phase Flow through Low Permeability Media (Task 3)," Annual Report November 1983-November 1984.
16. Core Laboratories, SCAL Report 203-830019, June 1983.
17. Core Laboratories, SCAL Report 203-820023, July 1982.
18. P. T. Branagan et al., "Interference Testing of the Naturally Fractured Cozzette Sandstone: A Case Study at the DOE MWX Site," SPE 12869, Proceedings of the 1984 SPE/DOE/GRI Unconventional Gas Recovery Symposium, Pittsburgh, PA, May 1984.
19. Institute of Gas Technology, Project 65056 Report, "Caprock Analysis," June 1982.
20. Institute of Gas Technology, Project 65056 Report, "Caprock Analysis," September 1982.

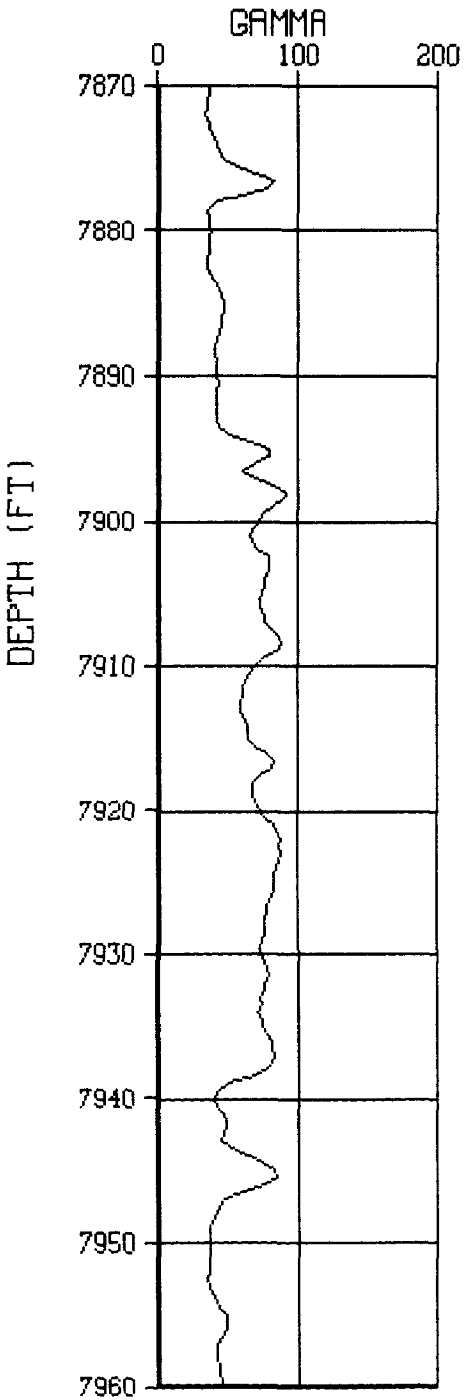

Table 5.1
Cozzette Reservoir Properties - MWX-1
(Core Laboratories)

Log Depth (ft)	Core Depth (ft)	Porosity (%)	Water Saturation (%)	Klinkenberg Permeability (μd) at Effective Confining Stress (psi) 1000	3000	4000
7871	7873	6.3	39.7	4.5	4.5	4.1
7872	7874	6.9	37.7	5.3	5.3	4.9
7876	7878	7.8	37.2	4.0	4.0	3.9
7879	7881	6.8	41.2	4.3	3.3	3.2
7881	7883	7.5	44.0	5.2	4.2	4.2
7884	7886	7.5	37.3	5.3	3.8	3.8
7885	7887	8.9	31.5	5.5	5.1	3.6
7889	7891	7.2	36.1	5.4	4.7	3.9
7892	7894	7.0	40.0	4.9	4.2	3.8
7893	7895	6.5	43.1	3.3	3.2	3.1
7895	7897	5.0	58.0	2.2	2.1	1.5
7908	7911	5.2	51.9	2.1	0.9	0.4
7909	7912	5.5	50.9	1.7	0.7	0.4
7913	7916	6.2	33.9	4.4	2.9	1.4
7916	7919	4.9	61.2	2.9	1.9	0.9
7949	7952	6.1	34.4	4.2	1.9	0.0
7950	7953	6.2	33.9	4.4	3.7	2.3
7952	7955	5.8	34.5	4.1	4.0	2.3
7954	7957	6.3	34.9	4.1	3.5	1.7
7956	7959	5.6	44.6	3.8	1.2	0.2

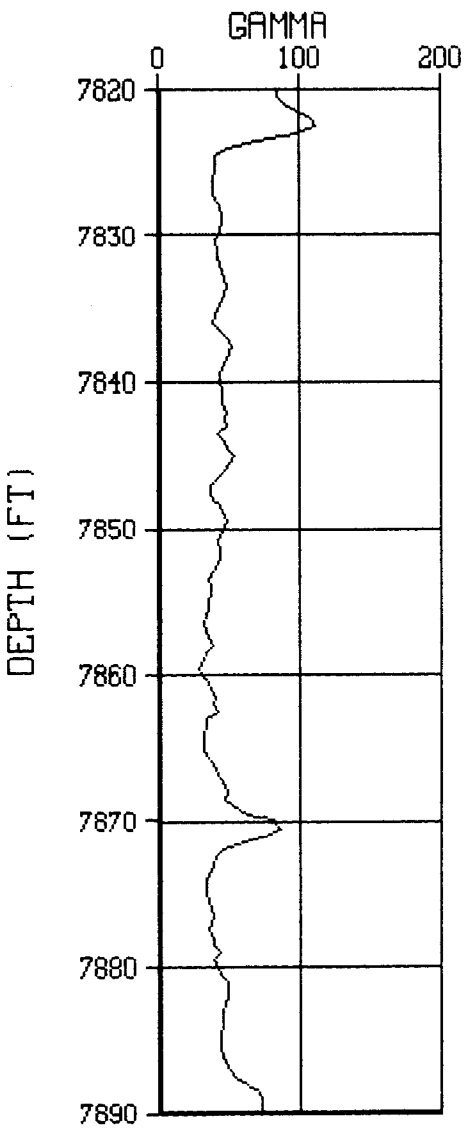

Table 5.2
Cozzette Reservoir Properties - MWX-2
(Core Laboratories)

Log Depth (ft)	Core Depth (ft)	Porosity (%)	Water Saturation (%)	Klinkenberg Permeability (μd) at Effective Confining Stress (psi) 1000	3000	4000
7825	7832	3.7	86.7	<0.1	<0.1	<0.1
7829	7836	3.7	73.5	<0.1	<0.1	<0.1
7833	7840	3.1	89.7	1.1	<0.1	<0.1
7837	7844	3.4	75.8	0.5	0.2	0.2
7843	7850	3.8	75.8	2.6	0.2	0.1
7845	7852	3.7	83.9	1.3	0.2	0.1
7847	7854	4.9	55.6	1.7	0.6	0.2
7848	7855	5.8	35.6	4.0	0.9	0.7
7851	7858	6.9	32.3	4.5	1.4	1.0
7855	7862	5.6	43.6	4.1	1.1	0.8
7857	7864	6.2	46.4	4.2	2.3	1.1
7861	7868	8.2	27.8	4.8	1.6	1.0
7864	7871	6.9	34.5	4.9	1.5	0.9
7867	7874	7.1	32.3	4.9	1.8	1.1
7870	7877	7.1	32.8	4.3	2.1	1.5
7873	7880	6.8	25.9	4.0	3.9	3.3
7875	7882	7.0	25.0	6.9	4.5	2.2
7878	7885	7.0	24.2	4.6	2.3	1.2
7882	7889	6.8	23.8	4.8	1.8	1.4
7885	7892	6.5	26.3	5.0	3.3	2.1
7886	7893	7.1	23.4	4.2	1.9	1.5
7889	7896	3.6	96.2	0.7	0.1	<0.1

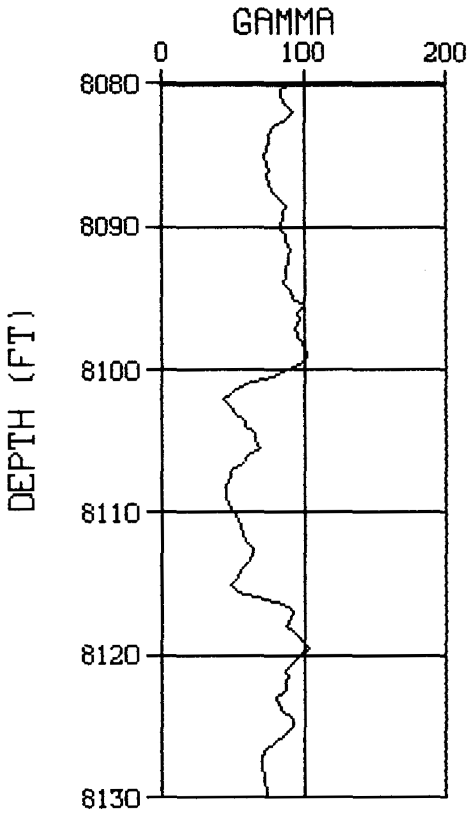

Table 5.3
Corcoran Reservoir Properties - MWX-2
(Core Laboratories)

Log Depth (ft)	Core Depth (ft)	Porosity (%)	Water Saturation (%)	Klinkenberg Permeability (μd) at Effective Confining Stress (psi) 1000	3000	4000
8098	8106	2.5	75.0	0.1	<0.1	<0.1
8100	8108	4.3	57.1	3.8	1.2	0.6
8101	8109	5.3	55.6	27.6	11.1	2.5
8104	8112	5.7	53.2	7.6	2.4	1.4
8105	8113	7.1	27.3	3.1	1.0	0.6
8106	8114	7.9	33.3	3.8	1.1	0.8
8107	8115	6.5	47.2	37.0	18.2	8.2
8108	8116	6.6	41.2	4.1	1.2	0.2
8109	8117	7.4	43.1	4.5	1.0	0.5
8113	8121	5.1	61.9	2.5	0.2	0.1
8113	8121	5.0	61.0	2.0	0.4	0.1
8114	8122	3.8	72.6	4.6	0.2	0.1
8116	8124	2.5	90.0	11.7	0.8	0.4
8120	8128	2.5	76.9	2.7	0.2	5.2

Table 5.4
Rollins Reservoir Properties - MWX-3
(Core Laboratories)

Core and Log Depth (ft)	Porosity (%)	Water Saturation (%)	Klinkenberg Permeability (µd) at Effective Confining Stress (psi) 1000	3000	4000
7536.5-36.8	5.4	78.3			
7538.4-38.7	5.7	75.0			
7540.4-40.7	5.6	73.7			
7542.3-42.6	3.9	65.3			
7544.3-44.7	4.1	75.6			
7546.2-46.5	3.9	74.0			
7548.4-48.7	5.8	72.5		NOT DETERMINED	
7550.3-50.6	6.6	76.1			
7552.4-52.7	7.3	64.7			
7554.4-54.7	7.5	76.6			
7556.5-56.8	8.0	77.2			
7558.5-58.7	7.7	71.6			
7559.6-59.9	7.1	73.4			
7563.2-63.4	13.3	59.1			

Table 5.5
Marine Core Analysis
(Institute of Gas Technology)

Core Depth (ft)	Log Depth (ft)	Well	Lab Net Confining Stress* (psi)	Porosity (%)	Water Saturation (%)**	Klinkenberg Permeability (μd)	Klinkenberg "B" (psi/μd)	Pore Volume*** Compressibility (10-6/psi)	Mercury Capillary Entry Pressure (psi)
7864.6	7858.0	MWX-2	4330	5.63	62	0.75	85.0	23.7	450
7868.0	7861.0	MWX-2	4330	5.82	92	1.50	80.0	22.9	390
7872.0	7870.0	MWX-1	4930	7.15	36	1.12	137.0	16.2	350
7886.0	7879.0	MWX-2	4340	7.30	48	1.40	106.0	7.9	500
7954.1	7951.0	MWX-1	4900	5.99	75	0.48	121.0	10.0	370
8117.5	8109.5	MWX-2	4430	6.41	61	0.63	43.1	8.9	610

* Calculated using (0.925)(core depth)-(0.5)(pore pressure estimated from mud weight)

** As received at IGT. Some values are so low that prior water loss is judged probable.

*** $\Delta V/V\Delta P$ determined by fractional changes in pore volume per psi of stepwise increase in confining pressure on first compression of rock from about 2000 psi net stress to the net stress used for testing. Low values would probably result from cycling of net stress to the maximum that would be experienced in reservoir depletion.

Table 5.6 Vertical Permeabilities in Cozzette and Corcoran Sandstones (Core Laboratories)

Log Depth (ft)	Core Depth (ft)	Porosity (%)	Water Saturation (%)	Klinkenberg Permeability (μd) at Effective Confining Stress (psi) 1000	3000	4000
MWX-1						
7885.3-86.7	7887.1-88.5	8.4	32	6.1	3.2	2.0
7953.4-54.2	7956.4-57.2	6.1	35	4.3	2.8	1.7
MWX-2						
7852.0-52.6	7859.1-59.7	7.1	32	4.3	1.5	1.1
8108.0-08.7	8116.0-16.7	10.0	41	3.8	1.1	0.7

Table 5.7
Porosity as a Function of Pressure, MWX-2 Core
(Core Laboratories)

Log Depth (ft)	Core Depth (ft)	Porosity (%) at Pressure (psi) 200	1000	2000	3000
7856.6	7863.8	7.2	7.0	7.0	6.8
7877.7	7884.8	8.2	8.0	8.0	7.9
8108.9	8116.9	9.8	9.6	9.5	9.4

Table 5.8
Caprock Analysis
(Institute of Gas Technology)

Well	Depth (ft)	Lithology	K_w* (nanodarcies)	Threshold (psig)	Effective** Porosity (%)
2	7852	Silty shale, siltstone	< 0.08	235	5.52
2	7893	Silty mudstone	2410	100	8.56
1	7899	Silty sandstone	< 0.05	375	2.55
1	7940	Silty mudstone	< 0.09	800	3.18
2	8103	Black shale	< 0.07	515	4.71
2	8123	Black shale	< 0.07	525	3.69
2	7822	Shale	0.3	775	–
2	7902	Shaley siltstone	2.6	575	–
1	7939	Silty shale	0.2	775	–
2	8101	Shale	2.3	750	–
2	8135	Silty shale	2.2	800	–

* Permeabilities to water measured in the vertical direction
** Determined under zero net stress and atmospheric pressure; in situ values will be less

Table 5.9
Rock Property Data for MWX-1 Core
(RE/SPEC)

Sample		Triaxial Tests					
Log Depth (ft)	Core Depth (ft)	Confining Pressure (MPa)	Compressive Strength** (MPa)	E*** (GPa)	ν***	Brazilian Tensile Strength (MPa)	Fracture Toughness ($MPa\cdot m^{-1/2}$)
Upper Cozzette Sandstone							
7879.7-80.5	7881.7-82.5*	0	152.9	31.6	0.24	-	
		10	226.9	34.9	0.22		
		20	275.1	34.8	0.23		
							1.52±0.09†
7883.8-84.8	7885.8-86.8*	30	342.8	40.5	0.21	-15.54±0.25	
Intervening Siltstone and Mudstone							
7898.3-98.9	7900.3-00.9	0	93.8	32.6	0.23	-	-
		10	113.5	31.5	0.11		
		20	143.4	31.7	0.22		
		30	153.5	29.8	0.23		
Intervening Mudstone							
7932.4-33.1	7935.4-36.1*	-	-	-	-	-	1.80±0.36
7933.1-33.9	7936.1-36.9*	0	83.6	31.4	0.21	-8.46±1.58	-
		10	143.8	29.3	0.21		
		20	146.1	27.6	0.18		
		30	165.7	28.9	0.20		
Lower Cozzette Sandstone							
7952.9-53.4	7955.9-56.4*	10	198.5	35.2	0.23		-
		20	247.1	35.4	0.22		
		30	281.5	36.7	0.25		
						-8.93±0.72†	
7954.2-55.0	7957.2-58.0	-	-	-	-		1.53±0.04

* Sealed at well
** Ultimate axial stress difference
*** Calculated for stresses between 20% and 60% of ultimate axial stress difference
† Data from both samples

Table 5.10 Rock Property Data for MWX-2 Core
(RE/SPEC)

Sample		Triaxial Tests					
Log Depth (ft)	Core Depth (ft)	Confining Pressure (MPa)	Compressive Strength** (MPa)	E*** (GPa)	ν***	Brazilian Tensile Strength (MPa)	Fracture Toughness ($MPa \cdot m^{-1/2}$)
Mudstone above Upper Cozzette							
7810.3-7811.2	7817.3-18.2*	-	-	-	-	-	1.45
7813.0-14.6	7820.1-21.7*	0	71.2	19.5	0.28	-6.86±1.44	-
		10	96.5	19.4	0.19		
		20	98.1	18.9	0.23		
		30	122.9	18.1	0.28		
		50	162.5	19.8	0.31		
Upper Cozzette Sandstone (Pyrobitumen)							
7830.0-31.0	7837.0-38.0*	-	-	-	-		1.77±0.38
						-8.05±1.96†	
7842.0-43.1	7849.0-50.1*	0	79.7	22.6	0.28		-
		10	178.2	35.1	0.16		
		20	231.7	38.8	0.15		
		30	253.5	38.0	0.20		
		50	308.2	37.3	0.19		
Upper Cozzette Sandstone							
7846.1-46.9	7853.1-53.9*	-	-	-	-	-10.38±3.35	1.48±0.12
7875.0-75.8	7882.2-83.0*	0	182.6	36.0	0.24	-	-
		10	263.3	39.8	0.22		
		30	362.0	40.2	0.20		
		50	486.4	46.0	0.26		
Intervening Silty Mudstone							
7893.5-94.3	7900.6-01.4*	0	114.0	45.8	0.18	-9.27±2.63	-
		10	153.7	35.3	0.09		
		20	172.5	35.7	0.15		
		30	180.5	33.3	0.18		
		50	327.9	45.8	0.22		

Table 5.10 (Cont'd)

Sample: Log Depth (ft)	Sample: Core Depth (ft)	Triaxial Tests: Confining Pressure (MPa)	Triaxial Tests: Compressive Strength** (MPa)	Triaxial Tests: E*** (GPa)	Triaxial Tests: ν***	Brazilian Tensile Strength (MPa)	Fracture Toughness ($MPa \cdot m^{-1/2}$)
Silty, Carbonaceous Mudstone from above Corcoran							
8092.0-93.1	8100.0-01.1*	0	88.6	21.1	0.24		–
		10	109.5	20.1	0.24		
		30	137.0	18.3	0.22		
		50	124.2	21.0	0.26		
						-7.46±0.65†	
8094.0-94.7	8102.0-02.7*	20	120.5	17.1	0.21		–
Upper Corcoran Sandstone							
8102.0-03.0	8110.0-11.0*	0	83.9	23.3	0.11	-8.66±3.22	0.69
8107.0-07.7	8115.3-16.0*	0	104.3	29.9	0.18	–	–
		10	150.1	27.7	0.17		
		20	219.5	32.5	0.18		
		30	254.6	33.2	0.18		
		50	287.6	32.8	0.19		
Intervening Mudstone and Siltstone							
8128.0-28.7	8136.0-36.7*	20	184.6	26.2	0.18	–	–
8132.0-33.0	8140.0-41.0*	10	129.8	30.2	0.12	-15.65±2.62	–
		30	305.3	41.8	0.20		
		50	243.0	39.9	0.19		

* Sealed at well
** Ultimate axial stress difference
*** Calculated for stress between 20% and 60% of ultimate axial stress difference
† Data from both samples

Table 5.11
Rock Property Data for MWX-3 Core
(RE/SPEC)

Sample		Triaxial Tests					
Log Depth (ft)	Core Depth (ft)	Confining Pressure (MPa)	Compressive Strength** (MPa)	E*** (GPa)	ν***	Brazilian Tensile Strength (MPa)	Fracture Toughness ($MPa \cdot m^{-1/2}$)
Rollins Sandstone							
7543.2-44.3	7543.2-44.3*	20	264.0	45.6	0.23	-15.3±1.5	1.75
		30	316.4	44.3	0.22		
Rollins Sandstone							
7556.8-57.9	7556.8-57.9*	20	185.3	26.5	0.19	-9.0±0.2	1.20
		30	205.4	26.5	0.22		

* Sealed at the well
** Ultimate axial stress difference
*** Calculated for stresses between 20% and 60% of ultimate axial stress difference

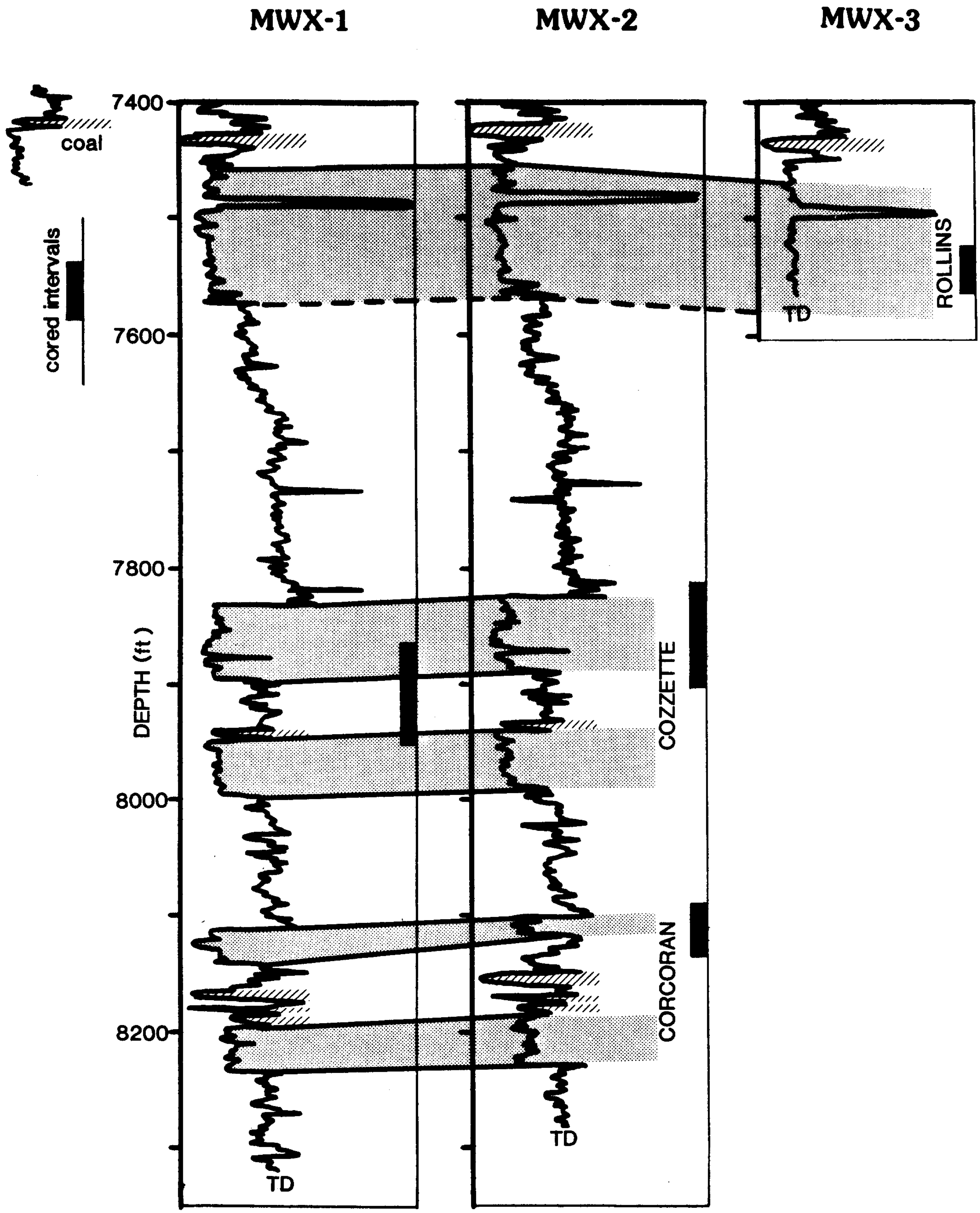

Figure 5.1 Intervals Cored in the Marine Section of the Mesaverde Group in New Mexico.

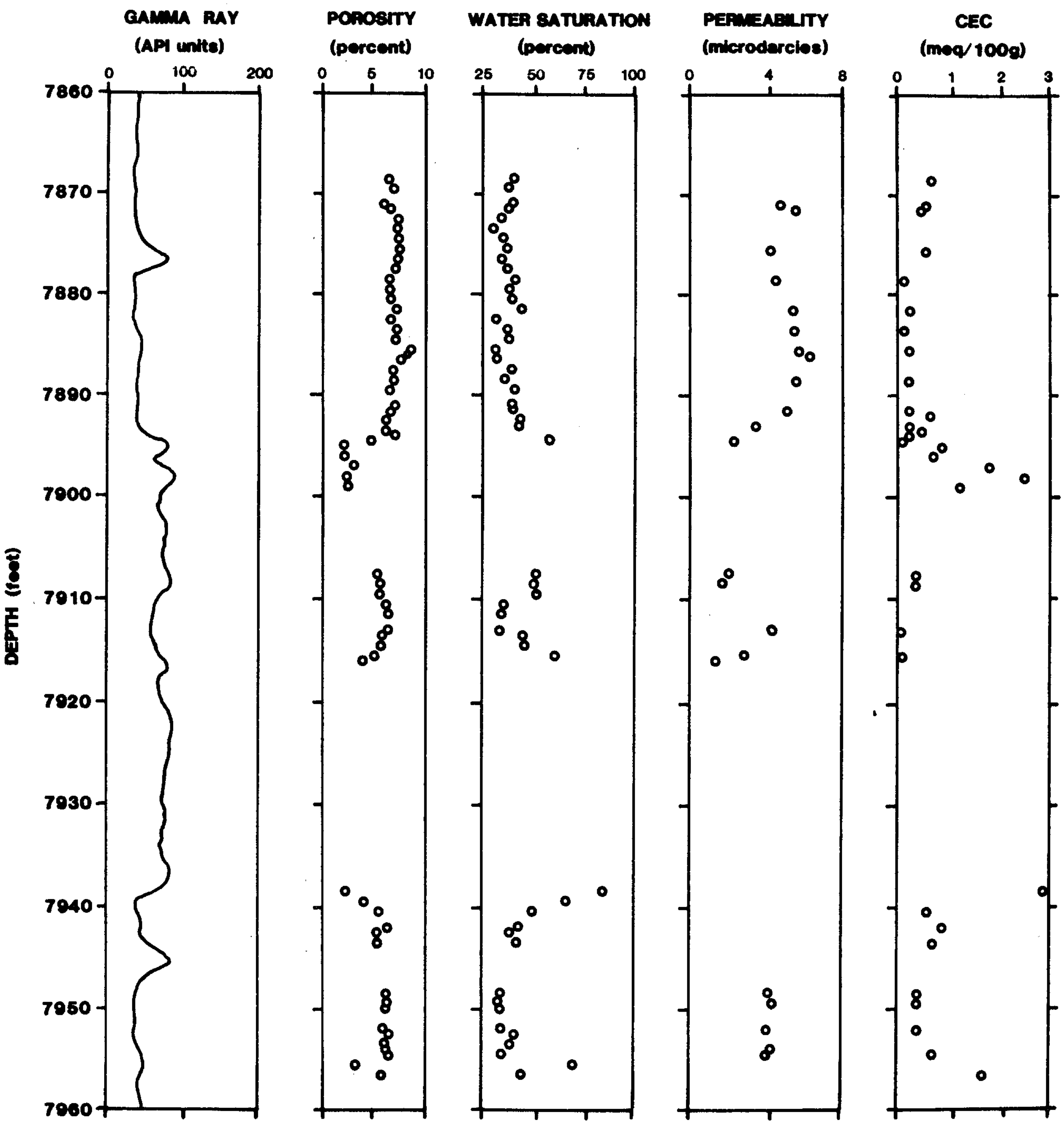

Figure 5.2 Reservoir Properties from Cozzette Core from MWX-1 (Core Laboratories).

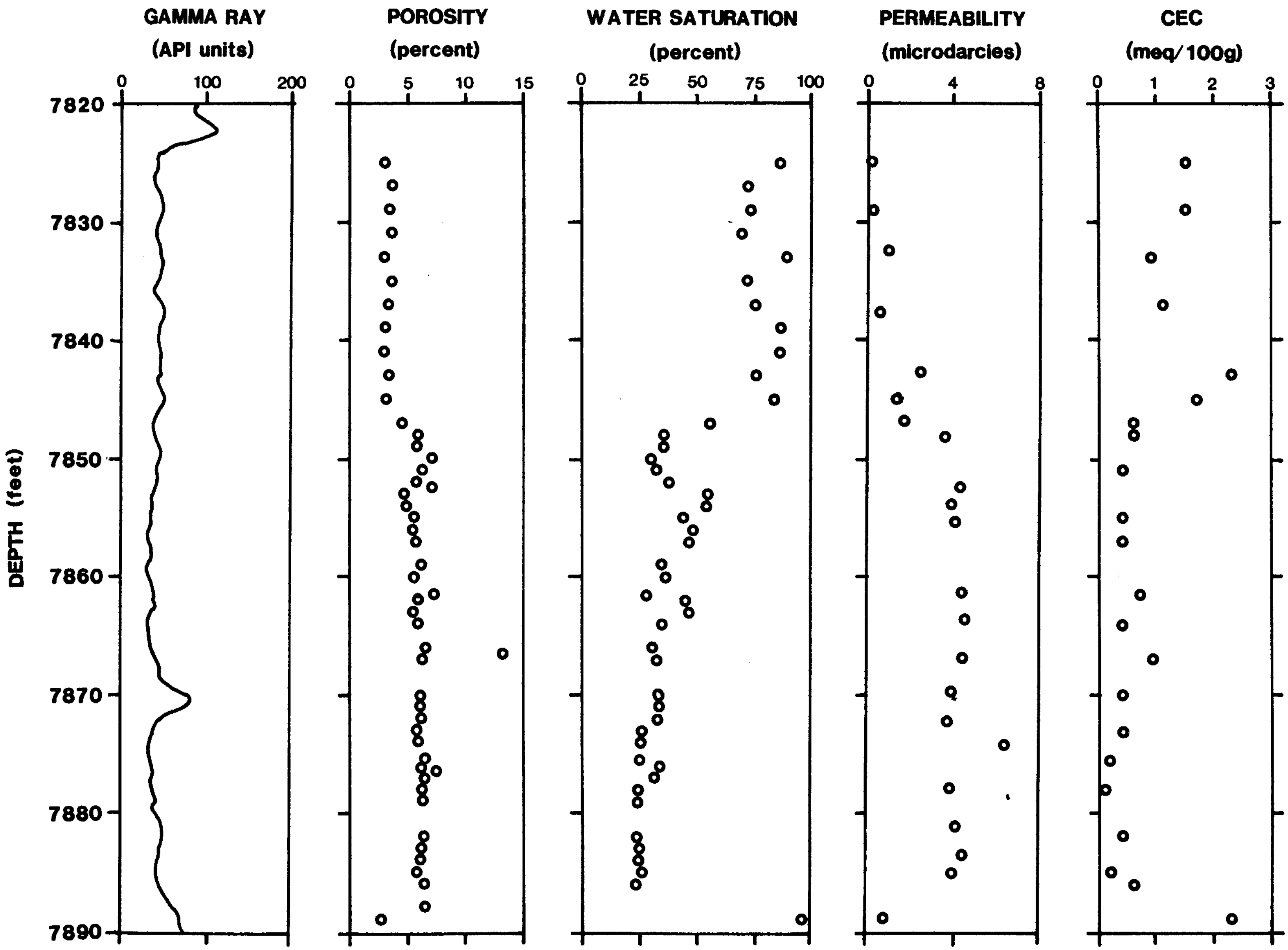

Figure 5.3 Reservoir Properties from Cozzette Core from MWX-2 (Core Laboratories)

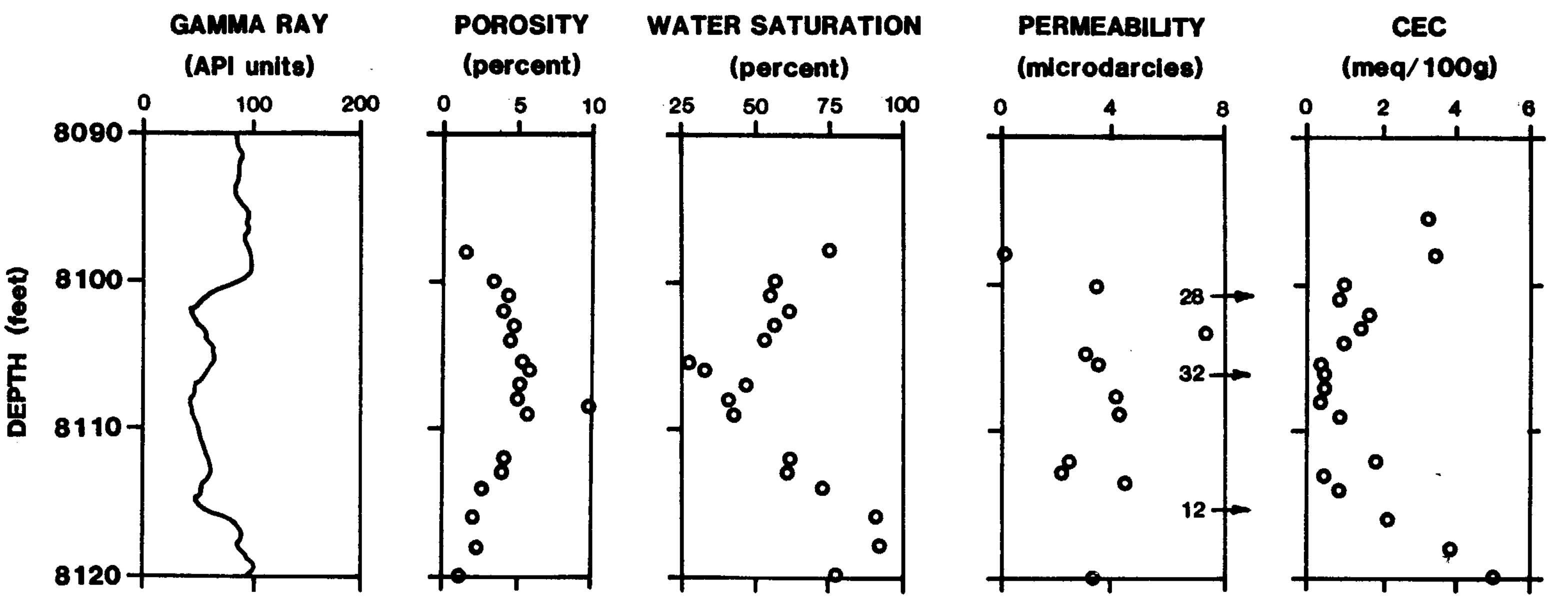

Figure 5.4 Reservoir Properties from Corcoran Core from MWX-2 (Core Laboratories)

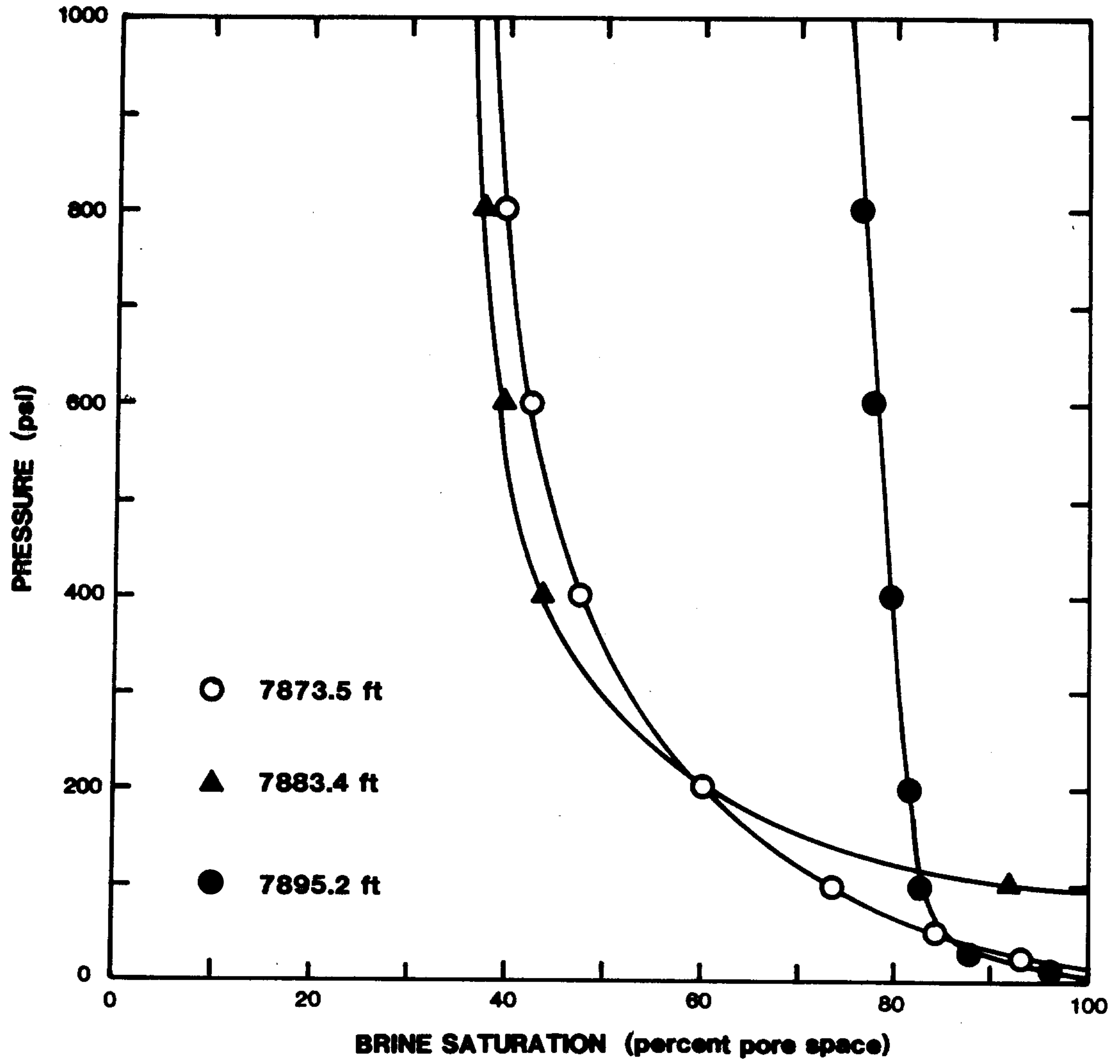

Figure 5.5 Capillary Pressure Data from Cozzette Core from MWX-1 (Core Laboratories).

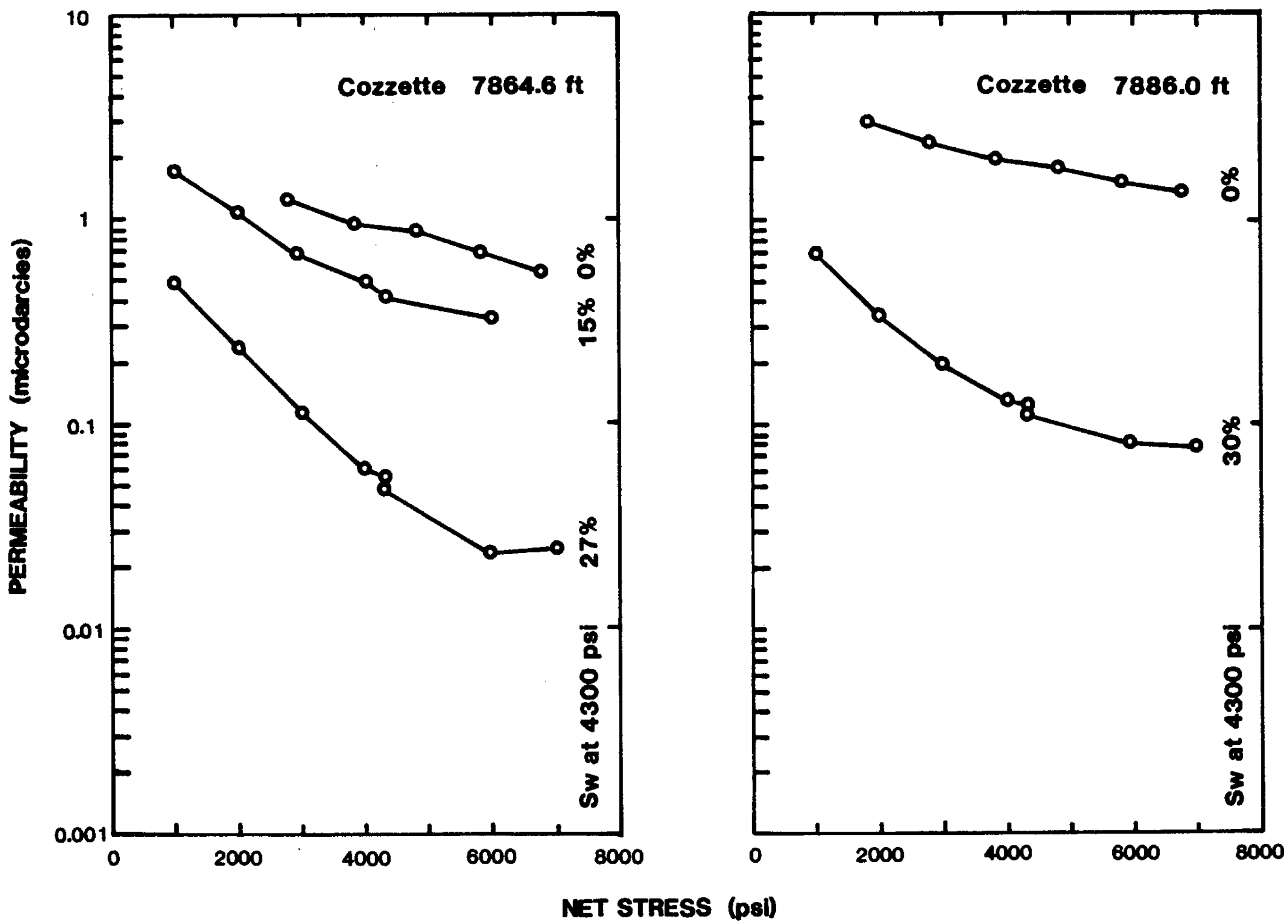

Figure 5.6 Permeability as a Function of Net Stress and Water Saturation (Institute of Gas Technology).

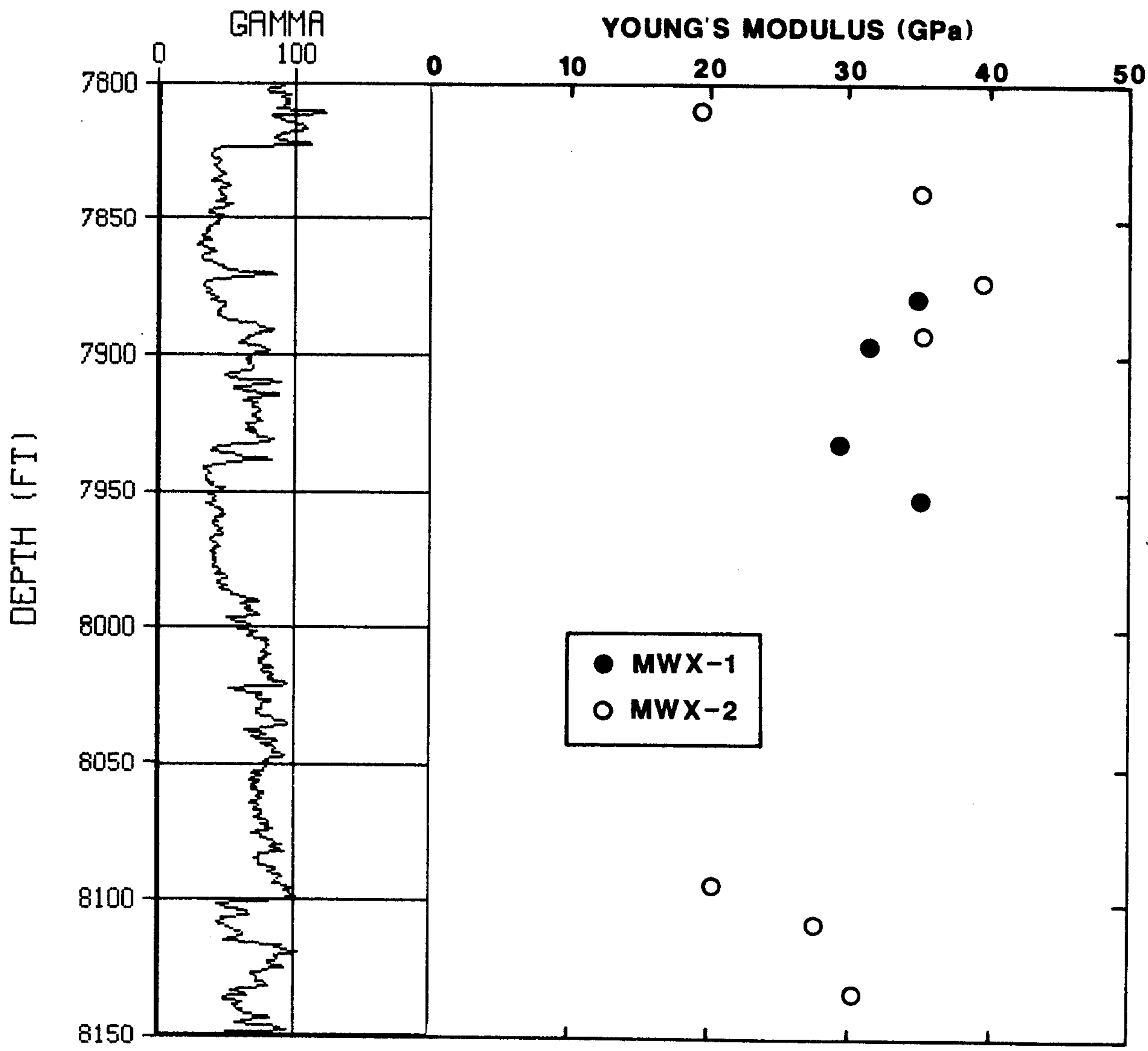

Figure 5.7 Young's Modulus as a Function of Lithology. (Data are at 10 MPa and are taken from Tables 5.9 and 5.10. MWX-2 Log Shown.)

INTENTIONALLY LEFT BLANK

6.0 IN SITU STRESS

Norman R. Warpinski
Sandia National Laboratories

6.1 INTRODUCTION

The in situ stress field at depth is now recognized to have an important effect on most in situ activities and processes, including those associated with drilling, completion and production of oil and gas wells. We are particularly interested in the in situ stress field because of its influence and control over hydraulic fractures and for the role it plays in the genesis and subsequent behavior of natural fractures--or joints--which are responsible for the productive capacity of many of these Mesaverde rocks.

The vertical distribution of the minimum principal horizontal in situ stress (hereafter referred to as the minimum in situ stress, σ_{Hmin}) has a significant influence on hydraulic fracture geometry. Perkins and Kern[1] noted its importance with respect to fracture height and Simonson et al[2] demonstrated how to calculate fracture height in a nonuniform, but symmetric, stress field. Laboratory[3,4,5] and mineback[6] experiments have proven the effect of minimum in situ stress differences on fracture height, but, as yet, field experiments have not yielded conclusive results. This is primarily due to the lack of detailed in situ stress data and viable fracture height measurement techniques.

The joint systems, which are the dominant flow paths through these tight rocks, are obviously the result of stress fields (and pore pressure) which existed in the geologic past. We would like to qualitatively recreate the stress history in the Piceance basin, but to do so in any meaningful sense requires some actual data points to compare with the analysis. These stress measurements provide important information on present day stresses in many different lithologies and at many different depths. Any realistic stress history must result in similar stresses at the present time.

In this section, we present the results of the initial series of in situ stress tests conducted for MWX[7]; these have been made at the base of the Mesaverde in marine sandstones and shales. Most of these tests have been conducted in cased holes through perforations; however, two open-hole stress tests were also performed and these provide additional valuable data. In addition, indirect data on the stresses and stress orientations using Anelastic Strain Recovery (ASR) and Differential Strain Curve Analysis (DSCA) are also given.

6.2 IN SITU STRESS MEASUREMENTS

6.2.1 Hydraulic Fracturing Measurements

At present the only reliable method of obtaining the minimum principal horizontal in situ stress distribution is by measurement with small volume hydraulic fractures. Two techniques are currently in use. One is the step-rate/flowback procedure pioneered by Nolte[8,9] and Smith[10]; this yields a reliable, reproducible estimate of the minimum in situ stress and is typically conducted in an interval soon to be stimulated. These have been called minifracs because they typically use small volumes of fluid, 500-10,000 gal, compared to conventional fracture treatments. The other technique, which we used in this study, is also called a minifrac, but very small volumes are pumped, typically 1-250 gal. These are usually conducted by injecting a small volume into the formation, shutting-in, and measuring the instantaneous shut-in pressure (ISIP). For open-hole tests, several authors[11-14] have discussed the details of the technique. It is clear that when the test is adequately conducted it yields an accurate, reproducible estimate of the minimum principal in situ stress and a somewhat less reliable estimate of the maximum horizontal in situ stress. Two open-hole stress tests were performed in these marine rocks.

For most oil and gas applications, however, it is usually impossible or impractical to conduct these tests in an open-hole environment. Problems with hole stability, gas pressure, cementing and cost factors usually require that the tests be conducted in cased holes through perforations. This causes additional complications because of the effects of the casing, cement annulus, explosive perforation damage, and random perforation orientation. However, Warpinski[15] has shown that with a carefully designed perforation schedule, accurate in situ stress measurements can be made through perforations. In general, a reasonable number (8) of medium size perforations (5-15 gm) with 90° or 120° phasing is sufficient. Also, it was found that the pressure record provides a good diagnostic on the quality of the data obtained from the minifrac. When the injection pressure is much greater (500 psi) than the apparent ISIP, these stress test results may not be accurate. Small pressure drops at shut-in indicate good tests.

Some data have previously been obtained in cased holes through perforations. Results by Kry and Gronseth[16] and Greenfield et al[17] provide examples of the stress distributions found in sand/ shale sequences at depth. In addition, the step-rate/flowback tests of Nolte[8,9] and Smith[10] are often conducted through perforations.

For both open-hole and cased-hole tests, the horizontal principal in situ stresses are determined by analysis of the pressure-time records obtained from the minifracs. It is generally accepted that the minimum in situ stress is approximately given by

$$\sigma_{Hmin} = \text{ISIP} , \tag{1}$$

and it is obvious that a good test is dependent upon a clear ISIP. For minifracs, this is usually obtained by pumping small volumes of low viscosity fluids at low flow rates; obviously, good perforations are also required. Often, several repeat pumps are necessary to obtain a clear indication of the ISIP. This is probably due to size effects or to damage around the perforations (for cased-hole tests) which cleans up with each additional pump and repeated exercising of the fracture.

For open-hole tests, the maximum horizontal in situ stress is usually calculated two ways. The first uses the breakdown pressure[11-13] (if one is obtained) of the first pump according to

$$\sigma_{Hmax} = 3\sigma_{Hmin} - P_c + T - P_i , \tag{2}$$

where

P_c is the breakdown pressure,
T is the rock tensile strength, and
P_i is the pore pressure.

This assumes that the breakdown pressure is the pressure required to overcome the stress concentrations around the borehole induced by drilling of the hole plus any tensile strength of the rock. In general, this technique is inherently inaccurate because the tensile strength is seldom known very accurately at downhole conditions and the breakdown pressure might be much lower than anticipated due to flaws, washouts or other wellbore problems. This would lead one to believe that the maximum stress will often be overestimated using Equation 2.

The second calculation uses the reopening pressure (P_{op}) of the second pump, which is assumed to reflect only the stress concentration around the borehole since the crack is already there (T = 0). This works best when the breakdown pump is very short. It is given by

$$\sigma_{Hmax} = 3\sigma_{Hmin} - P_{op} - P_i \tag{3}$$

Both of the calculations assume that poroelastic effects are negligible; that is, the rock is tight and the fluid is nonpenetrating. Haimson and Fairhurst[18] and Rice and Cleary[19] discuss how to include poroelasticity into the analysis.

For tests in cased holes through perforations, it is usually impossible to obtain reliable estimates of the maximum horizontal principal in situ stress from these stress tests because of problems induced by the casing, cement annulus, stress concentrations around the perforation hole, and damage due to the perforation hole. In addition, only a small portion of the borehole is pressurized by the fluid, namely the perforation area, unless an annular fracture develops around the rock/cement interface. At best, a gross estimate of σ_{Hmax} is possible.

The vertical or overburden stress is assumed to be due only to the weight of the overburden rocks. It is given by

$$\sigma_v = \int \rho g dz \tag{4}$$

and the accuracy of this assumption is not known, although it is generally believed to be adequate.

6.2.2 Strain Recovery Measurements

Two types of indirect stress measurements using strain recovery techniques have been made on MWX cores. These include Anelastic Strain Recovery (ASR) and Differential Strain Curve Analysis (DSCA).

The determination of the in situ stress state in deep formations from ASR measurements[20,21] of oriented core is, in part, an extension of the stress relief method used to determine in situ stresses near underground openings. The stress relief method is generally accomplished by an overcoring process which allows the physical detachment of a body of rock from the rock mass, thus permitting the body to undergo differential relaxation in relief of in situ stored strain energy. The recovered strain is measured with strain or displacement gauges and generally involves both an instantaneous, elastic component and an anelastic component. Usually gauges are installed at the bottom of a borehole prior to overcoring and stress relief, and the measured strain recovery can be related to the total stress components which acted prior to relief.[22] A measure of the total strain relief (both elastic and anelastic) and the calculated stress state is restricted to shallow depths. However, if gauges are installed subsequent to stress relief, a partial component of the anelastic strain recovery can still be determined. Voight[23] first suggested that if the assumption is made that the partial recoverable strain is proportional to the total recoverable strain, then an approximate estimate of the in situ stress state at depth can be made by instrumenting oriented cores immediately upon removal from the borehole. Voight noted that there is empirical justification to consider that the recovered anelastic strains will be proportional to the total recoverable strain, and hence, will be related to the in situ stress state. If the rock is isotropic and homogeneous at depth and the recovery behavior is linearly viscoelastic, then the strain relief along principal strain directions will be uniform with time, and the directions of principal strain relief determined over a given time interval will correspond to the initial in situ strain conditions. Thus, principal strain directions determined from ASR measurements will be homothetic with the principal in situ stress directions. Teufel[24] found good agreement between stress directions inferred from elastic and ASR measurements and hydraulic fractures exposed by a mineback operation in volcanic tuff at the Nevada Test Site.

In situ principal stress magnitudes can also be calculated from ASR measurements of oriented core. Using modern viscoelastic theory, Blanton[25] considered two cases of practical interest: (1) recovery of isotropic core and (2) recovery of transversely isotropic core. In the first case the following assumptions are made: (1) the rock is homogeneous and linearly viscoelastic, (2) the viscoelasticity of the rock can be characterized by one viscoelastic parameter (either creep compliance D(t), or relaxation modulus, E(t)), (3) Poisson's ratio is not time-dependent, and (4) the in situ stresses are removed instantaneously. If these assumptions are valid, the principal stress magnitudes can be calculated if (1) all three principal recovery strains are known, (2) Poisson's ratio is known, and (3) one of the principal stresses is equal to the overburden. The transversely isotropic case is intended to represent a rock whose mechanical properties perpendicular to bedding are different from those parallel to bedding. In this case at least one viscoelastic parameter, in addition to the requirements of the first case, is needed for calculation of the stress magnitudes. Blanton and Teufel[26] included the effect of pore pressure in the viscoelastic recovery model.

Warpinski and Teufel[27] developed a more complete viscoelastic model for ASR which does not require the severe assumptions of the Blanton model. In particular, the model allows for a variable Poisson's ratio, accommodates different material behavior in dilatation compared to distortion, and, while also assuming instantaneous relief of the effective stresses, accommodates time-dependent relief of the pore pressure. Four material constants are necessary and these are obtained through a least-squares curve fit of the strain recovery data. The major problem with this approach is that all of the desired stress and material property data cannot be obtained without some additional information. The analysis also needs an input overburden stress (as does the Blanton model) and either a minimum stress value from minifrac data or a distortional creep compliance from either lab or previous data from the same rock type.

Differential Strain Curve Analysis (DSCA)[28,29,30] is somewhat different from ASR in that core samples are brought back to the lab, instrumented, subjected to various levels of hydrostatic confining stress, and monitored for strain behavior. A clear transition from closure of microcracks (due to stress relief) to hydrostatic compression of the rock matrix is usually seen on most rocks and the level of pressure at which this transition occurs for each direction is indicative of the original in situ stress in that direction. Assuming an overburden stress, the values of the horizontal stresses can then be estimated.

6.3 INTERVAL TESTED

The interval tested in this study was 600 ft of Marine rocks in the lower Mesaverde group, including the Cozzette sandstone member, Mancos tongue shales, and Rollins sandstone member of the Iles Formation. This section is shown in Figure 6.1 and occurs at a depth of 7450-8060 ft at the MWX site.

6.4 STRESS TEST EQUIPMENT AND PROCEDURE

The stress test equipment, particularly the pump system and electronics, was specifically designed for conducting these low volume, low flow rate stress tests. The pump system consists of a high pressure, low flow rate triplex pump powered by a hydraulic drive system. As seen in Figure 6.2, a 100 hp electric motor drives a hydraulic pump which feeds the hydraulic motor that powers the pump. This elaborate design, which had been used before in pump systems at DOE's Nevada Test Site for hydraulic fracture mineback experiments, provides for tight control of the flow rate.

Bottomhole pressure, which is the critical measurement in these tests, is obtained from a quartz crystal oscillator gauge and data acquisition system which was modified to sample at a rate of 10 per second. This is necessary in order to have sufficient data in the shut-in portion of the curve to determine the ISIP accurately. These data are then sent to a minicomputer for storage and initial processing. Bottomhole pressure, surface tubing pressure, surface casing pressure, and flow rate are the primary measured and stored parameters.

Accurate bottomhole pressures at shut-in are obtained by using a downhole closure tool. It consists of a beveled seating nipple sub and a matching seating mandrel with o-ring. The seating mandrel has a single conductor wireline feed-through so that the pressure transducer can be positioned in the isolated zone beneath the seating location. As shown in Figure 6.3, this assembly is located above the packer that isolates the frac interval from the annulus. The bottom of the hole is isolated by a retrievable bridge plug or a straddle packer configuration.

6.4.1 Cased Hole Tests

The procedure is typically as follows. Several intended minifrac intervals are first perforated with a casing gun. Zones are perforated 1000-3000 psi underbalanced to optimize the perforating and no washing or other cleaning of the perforations is attempted. Starting with the lowest interval, the perforations are then isolated with a bridge plug and a packer or the straddle packers. The pressure transducer and seating mandrel are lowered downhole and situated a few feet above the seating nipple. The first minifrac is conducted and the wireline is lowered to shut-in downhole; simultaneously the pump is left running at a reduced flow rate to keep a positive pressure differential on the closure tool. After sufficient pressure decay in the frac interval, the tubing pressure is equalized, the wireline is raised a few feet, and the second minifrac is conducted. After several of these injections, the packers are moved to the next higher interval and the process is repeated. Flow rates in these tests are usually 10-15 gpm using KCl water as the frac fluid. Total volume injected is generally on the order of 5-100 gal. These rates and volumes were chosen based on previous work.[15]

All of the cased-hole stress tests were conducted in MWX-2. With the exception of the upper Cozzette sand, all intervals were perforated with eight 14 gm shots over a two-foot interval. The upper Cozzette sand had an interference test conducted in it before stress testing and three ten-foot intervals were perforated for maximum communication. Although it was originally planned to stress test each 10 ft (3 m) interval separately, hardware stuck in the hole made it necessary for all three zones to be tested together.

6.4.2 Open-Hole Tests

The open-hole tests were conducted in an open-hole section at the bottom of MWX-3. To minimize the risks, the approach chosen for conducting these tests was to drill and case MWX-3 as originally planned and then drill out another 90 ft with a 5 7/8" bit and leave this section open hole. This 90 ft section is in the Rollins member which is a marine sandstone at the top of the marine section. This blanket sandstone was a desirable location because it should be at least fairly well-behaved both vertically and laterally with respect to stress variations (unlike the lenticular zones above). This gives us the assurance that the two tests conducted in this sand should have the same stresses and that the stress tests conducted through perforations in MWX-2 (180 ft away) should also exhibit the same stress magnitudes (within reason).

The first zone, shown in Figure 6.4, was at a depth of 7535-7551 ft and was isolated with a backfill of sand on the bottom and an inflatable packer above. Oriented core was obtained throughout this section (7535-7564 ft) and from the logs and core it was clear that this was a fine-grained sandstone with no observable natural fractures and no obvious shale breaks. In addition, a pre-frac impression packer showed no observable natural fractures. Strain relaxation tests were conducted on the core, some samples were sent to Core Labs for reservoir property testing (Table 6.1) and others to RE/SPEC for rock property measurements.

The stress tests were conducted using a Dowell pump truck with 2% KCl water at about 1 bpm. As usual we had our bottomhole shut-off tool and HP pressure gauge downhole to obtain pressure measurements. A post-frac impression packer was run to attempt to obtain fracture orientation but the results were equivocal. Many linear features, which were not present on the pre-test packer, were observed but they were extremely narrow, an echelon, unconnected and only on one side of the wellbore. Their orientation varied from N50°W to N70°W, but this could have been due to a twisting of the impression packer as it inflated. Although these features appeared to be fractures, no unrefutable conclusion as such could be made.

The second zone was at 7502-7519 ft, as shown in Figure 6.5, and the zone was isolated by backfilling with sand to 7519 ft and positioning an inflatable packer at 7502 ft. In this interval, no core was obtained (it couldn't be oriented) and the logs indicate the probable existence of shale stringers in the frac interval (the pre-frac impression packers had some blowouts which may have been washouts). It is also fairly close to the large gamma anomaly six feet above. The stress tests in this zone were conducted at 0.5-1 bpm with 2% KCl water.

6.4.3 Strain Recovery Procedures

ASR measurements were made on Cozzette sandstone core in MWX-2 and Rollins sandstone core in MWX-3. An attempt to obtain data in MWX-1 in the Cozzette failed because the time for core retrieval was excessively long due to pressure problems.

Immediately upon retrieval from the wellbore the core was sealed with polyurethane wrapping to avoid the effects of moisture evaporation. Measurements were made in a temperature controlled environment (±1°C) to minimize thermal effects. Following Teufel,[20] the displacements associated with anelastic strain recovery were determined with spring-loaded, clip-on gauges, which incorporate precision gauge heads. Since the cores used in this study were from a vertical wellbore, only three independent displacement measurements were required to determine the directions and magnitudes of the two principal horizontal strains. Three gauges were mounted at 45° to each other in the horizontal plane of each core. The vertical strain was determined by mounting a gauge parallel to the center axis of the core. Displacement data for each gauge, the room temperature, and the temperature of the core was recorded manually every hour. All displacements were normalized to strain from the initial gauge length settings. For MWX-2 data the accuracy of the strain measurements were ±5-20 $\mu\varepsilon$ whereas the MWX-3 data were ±5 $\mu\varepsilon$.

In order to correct the recovery data for any temperature variations, the superposed thermal strains were subtracted from the recovery strains by determining the coefficient of thermal expansion in the four different strain directions. A series of tests were run in the laboratory on the totally relaxed cores in order to characterize the strain/temperature response of each core. The magnitudes and orientations of the principal horizontal strains and the vertical strain magnitude were calculated from the temperature corrected strain data following Frocht.[31]

A description of the DSCA procedure is given in references 29 and 30.

6.5 STRESS TEST RESULTS

Figure 6.6 shows the results of all of the initial stress tests conducted in MWX-2. The most striking feature of Figure 6.6 is the much higher stresses in the shales compared to the surrounding sandstones and siltstones. Frac gradients in the marine Mancos tongue shales vary from 1.02 psi/ft to 1.10 psi/ft. On the other hand, the sandstones and siltstones of the Cozzette member have a significantly lower stress at a frac gradient of about 0.86 psi/ft. There are also somewhat lower stresses in the Rollins member, but they vary considerably with lithology. The maximum horizontal stress is also found to be only 400 psi greater than the minimum horizontal stress; this can have significant effects on hydraulic fracturing.

All of the cased hole stress results comprising the data in Figure 6.6 are given in more detail in Figures 6.7-6.9. Each of these pressure records is the best result for the respective zone and indicates the degree of accuracy to which the ISIP can be determined and also the variation in pressure response with lithology and depth. In most cases it is possible to determine the ISIP to an accuracy of ±30 psi by visual inspection; only a few tests, such as the shale at 7665 ft in Figure 6.7c have ambiguous pressure declines at shut-in. This good definition of the ISIP is due to a combination of a well-designed perforation schedule, small volumes of low viscosity frac fluid, a downhole closure system and the ability to monitor pressure downhole with high sample rate instrumentation. The open-hole stress data are given in Figures 6.10 and 6.11. The entire pressure record for all pumps is shown in these figures. The analysis of these data will be discussed in a later subsection.

6.5.1 Shale Behavior

The minifracs conducted in the marine shales all had very similar pressure responses. In general, on the first pump they exhibit a breakdown pressure which is not much greater than the injection pressure (20-100 psi). An example of a breakdown pump is shown in Figure 6.7a. Successive pumps then result in a constant injection pressure during repumping, as seen in Figure 6.7b and 6.7d. With the exception of the zones at 7665 ft the ISIP's of the shale tests are well defined. The zone at 7766 ft is anomalous because the pump time was not long enough to allow the pressure to stabilize; its behavior will be discussed later.

6.5.2 Sandstone Behavior

The sandstones generally show larger breakdown and reopening pressures, 50-300 psi over the injection pressure, than the shales. This is shown in Figure 6.8. The ISIP is also usually fairly clear. If the reopening pressure of the second pump is used to determine a maximum horizontal principal stress, σ_{Hmax} is typically 500-3000 psi greater than σ_{Hmin}. The accuracy of this estimate is probably not good. The test of the upper Cozzette sand in Figure 6.8b is different from the other tests. Three sets of 10 ft perforated intervals were fractured together because of downhole problems. Flow rates of about 70 gpm were required to fracture the zone. In addition this interval was produced for several months and the drawdown may have lowered the stress.

6.5.3 Siltstone Behavior and Dual-Closure Stresses

Siltstones exhibit behavior that may be similar to either sands or shales or may be a combination of both. For example, the test at 7895 ft in Figure 6.9b has the pressure characteristics of a shale, but the stress is low like the sands. The test at 7924 ft in Figure 6.9a shows a dual closure stress of 0.98 psi/ft and 0.86 psi/ft. Six repeat injections were conducted in this zone and all showed this dual closure behavior except for the initial injection. The first pump showed a low fracturing pressure and a low frac gradient of 0.86 psi/ft. These data suggest that there may be a thin (1-2 ft) siltstone or sand surrounded by shale/carbonaceous material with much higher stress. Such severe bounding of the fracture above and below would result in extreme fracturing pressures which would propagate the frac into the bounding materials. At shut-in, the higher stress shales would close first, followed by closure in the sand. Because of the "routine" first pump, where the fracture appeared to propagate normally, it does not seem likely that alternate explanations such as natural fractures or cement bond problems can explain this behavior.

Such a dual-closure stress mechanism would probably be observable only for small volume, low viscosity treatments where conditions in the crack can reach equilibrium rapidly. In larger treatments with thicker intervals, the effect would be both attenuated due to crack size and masked due to other competing effects, e.g., leakoff and continued crack extension and fluid movement.

6.5.4 Multiple Injection Behavior

As seen in Figure 6.7a, the breakdown pump will sometimes result in a very clear ISIP. More often than not however, several pumps are required to obtain an accurate measurement of the stress. Figure 6.12 shows an example of three pumps conducted in a sandstone at 7531 ft. The breakdown pump is not very useful for determining the stress because of the gradual decay after shut-in. Sometimes, even the second pump does not provide an accurate estimate of the ISIP. Generally, after the 3rd or 4th run the ISIP is quite clear. The fifth run, shown in Figure 6.12, illustrates how well-defined the ISIP becomes with additional pumping. This behavior is probably because of perforation-induced damage around the wellbore. This damage cleans up with additional pumping as the fracture is repeatedly opened and closed and fluid is forced through the perforations.

6.5.5 Damage Examples

In some cases the damage apparently never cleans up. The shale in Figure 6.7d may illustrate this. When open-hole tests in low permeability rocks are conducted correctly, there is usually a clear, easily defined shut-in. The fact that this is not always the case through perforations indicates that the perforations themselves can have a significant effect on the tests. Shales and coals seem to be the rocks that are most vulnerable to damage.

In addition, the test shown in Figure 6.7c is probably affected by the perforations--the manifestation in this case is the large pressure drop at shut-in. Warpinski[15] has shown that such large pressure drops at shut-in are indicative of perforation problems and the ISIP value may not be very accurate--in this case probably $\pm$100 psi. This interval also required a much larger volume of fluid to be injected in order for the injection pressure to stabilize. No other tests showed this type of behavior and the reason for it is not known.

6.5.6 Open-hole Stress Test Results

The pressure record from the first open-hole minifrac (at 7535-7551 ft) is shown in Figure 6.10. On the breakdown pump, the glitch in the pressure-up side is due to changing gears on the pumper. The breakdown occurs at 8295 psi and the well is shut in immediately. This is probably the reason why there is no definable instantaneous shut-in pressure (ISIP)--the fracture may be too small. On the second pump a clear reopening pressure (7115 psi) is observed and the ISIP is about 6800 psi. On the final two pumps the reopening pressure decreases (as expected) and the ISIP is very clear at about 6750 psi. A fifth pump was also conducted with about three times the volume and is not shown; its ISIP was about 6725 psi.

The pressure records from the second open-hole stress test (7502-7519 ft) are shown in Figure 6.11. Obviously, the fracturing is much more complex than it was in the previous zone. The first two tests were conducted at about 0.5 bpm while the last two were at 1 bpm. The breakdown pump shows an increase of pressure up to breakdown at about 7575 psi. The pressure then dropped rapidly to about 7200 psi and started back up. The zone was shut in and no ISIP was evident. The second pump started with a clear reopening pressure at 7225 psi and then started back up again. The ISIP was again difficult to obtain. Finally, the third pump showed a better ISIP at about 6835 psi. The reopening pressure was 7230 psi--consistent with pump #2. Soon after the 4th pump was started, we began to fracture around the packer and the casing pressure increased. The well was shut in with an ISIP of 6785 psi. Because of the high pressure, the amount of gas and the high temperature, no post-frac impression packer was run.

The results of these data are given in Table 6.2. The tensile strength is an average of Cozzette and lower-paludal tensile strengths for sands (both about the same) since rock property tests on the Rollins core have not yet been conducted. The minimum stress is about 6800 psi with an accuracy of about ± 30 psi. For the lower zone, the maximum stress is calculated to be 7600 psi using both techniques. This gives us good confidence in these data. On the other hand, the upper zone is inconsistent. The breakdown pressure approach yields too high a stress, as should be apparent from looking at the data in Figure 6.12. The reopening pressure calculation, on the other hand, gives a σ_{Hmax} which is consistent with the lower zone. This increases our confidence that the initial maximum in pressure for pump #2 actually is the reopening pressure and not just an anomaly. There are many reasons why the pressure could begin to rise again afterwards.

Thus the maximum stress at this location is about 7600 psi, while the minimum stress is about 6800 psi. With such a contrast in stresses, large frac treatments where the pressure becomes large (> 1000 psi over the minimum in situ stress) can produce unusual results such as secondary fractures, opening of natural fractures, etc. This should be carefully considered in any frac design.

6.5.7 ASR Results

Example ASR data from the Rollins sandstone in MWX-3 are shown in Fig. 6.13. The top curves show the measured strain recoveries in the horizontal directions and the middle curve shows the calculated principal strains in the horizontal directions along with the vertical strain (assumed to be a principal strain). The lower curve shows the calculated stress orientation for each time that data were obtained. The best estimate of the maximum stress direction (hydraulic fracture direction) is thus N55°W with a standard deviation of 4°.

A summary of the data from MWX-2 is shown in Table 6.3. Measurements were attempted in eleven zones, but tests in three shales were not successful. The upper four tests were in the Cozzette sandstone for which the average azimuth is 117° or N63°W. The lower four tests were in the Corcoran sandstone for which the average azimuth is 96° or N84°W. Based on the accuracy and the limited number of data, it is not clear whether there is a true stress rotation from the Corcoran to the Cozzette or whether instrument error is responsible for the apparent change.

A summary of the data from MWX-3 in the Rollins sandstone is shown in Table 6.4. The Rollins data are more accurate than the previous MWX-2 results because of a new design for the clip-on displacement gauges. In this zone the average azimuth is 117° or N63°W, the same as the Cozzette.

Calculations of stresses were also attempted for these data. Tables 6.5 and 6.6 show the elastic properties used for the calculations. Blanton's model gives the results shown in Table 6.7 and 6.8 for MWX-2 and MWX-3, respectively. Compared to the minifracs, the minimum stresses are much too large, but the maximum stresses may not be too far from the true value, particularly for the Rollins sandstone.

The new method of Warpinski and Teufel[27] was used on the data at 7564 ft in the Rollins. No attempt was made to measure the distortional creep compliance in the lab, so the minimum stress from the minifracs in the Rollins (6800 psi) was input and a maximum stress of 7625 psi was calculated along with a distortional creep compliance of 0.067x 10^{-6} psi^{-1}. The results also showed that Blanton's model would not fit well because Poisson's ratio was not constant throughout the process (12% change) and the distortional creep compliance was about 15% different from the dilatational creep compliance.

6.5.8 DSCA Results

Only two DSCA samples were tested in the marine rocks. The results are shown in Table 6.9 and they agree well with the ASR data. The orientation of the stresses is N76°W. Minimum stresses, assuming a 1.05 psi/ft overburden would be 6400-6930 psi, which is somewhat higher than the measured value of 6300 psi.

6.6 DISCUSSION

6.6.1 In Situ Stresses

The results of the stress tests show that the minimum in situ stress at depth is dependent on lithology and large stress differences are observed between sandstones and the surrounding shales. Also indicative of the effect of lithology is the stress behavior above the Cozzette member. From 7800 ft up to 7500 ft the measured in situ stress decreases with decreasing shaliness as measured with the gamma log.

Table 6.10 shows the stress data, the estimated accuracy of each measurement, the measured or estimated (from mud weight) reservoir pressure, Poisson's ratio as determined from the long-space sonic log (Figure 4.10), Young's modulus determined from laboratory measurements, the estimated overburden stress (1.05 psi/ft), a calculated minimum stress, and the frac gradient. The calculated minimum in situ stress is based on elastic behavior in uniaxial strain as given by

$$\sigma_{Hmin} = \frac{\nu}{1 - \nu} (\sigma_V - P_i) + P_i \quad . \tag{5}$$

Poisson's ratio, ν, is obtained from the long-space sonic log averaged over a 10 ft (3 m) interval about the perforated zone, but these values were also consistent with available laboratory measurements. It should also be noted that if the rock state deviates from uniaxial strain, then Young's modulus will also have an effect on the stress magnitudes. Equation 5 is, of course, a gross approximation because it neglects tectonic and thermal components and ignores viscoelastic effects.

In Equation 5, the pore pressure, P_i, has a significant influence on the calculated in situ stress value, but the pore pressure is often not accurately known. Pore pressures in the sandstones are often estimated from the mud weights during drilling or short build-up tests which are not always accurate indicators of that pressure. Pore pressures in marine shales are extremely difficult to measure and must be assumed. Thus, calculated stress values, particularly in shales, may be in serious error.

The comparison of the calculated and measured values, which is shown in Figure 6.14, indicates that stresses cannot reliably be determined from the uniaxial strain assumption. Shale measurements, in particular, deviate widely from the model. Only the Cozzette member seems to show a good correlation, but this may be because of the high pore pressure which dominates the elastic component. A correlation would also require that either (1) the tectonic and thermal stress components of the minimum in situ stress are small or (2) they roughly balance each other (this requires an extensional tectonic environment). Regardless, the high minimum horizontal stress value in the Cozzette (0.86 psi/ft) is probably due to the high pore pressure. The high pore pressure also results in Equation 5 yielding an acceptably accurate calculation for any value of Poisson's ratio between 0.15 and 0.3, so the good correlation is incidental and is not a validation of Eq. 5.

The shales surrounding the Cozzette member are all near the lithostatic stress (Figure 6.6 or Table 6.10), but comparisons with the calculated stress value are questionable here because of a lack of useful data on pore pressures in shales and whether the usual effective stress concept is even applicable for the pore structure of shale rocks. Assuming the pore pressure in the surrounding shales is similar to the sand pore pressure as in Table 6.2, one would deduce that the shales do not behave elastically. This is quite acceptable since shales are known to creep readily. However, the pore pressure in the shale may be much greater, even as high as lithostatic, in which case the calculation of Eq. 5 would provide the obvious result that $\sigma_{Hmin} = \sigma_V$. Again, this is not a validation of Eq. 5, because any Poisson's ratio would provide correct results. Additional work on pore pressure and in situ stresses in shales is certainly needed.

Since the measured minimum stresses in the marine shales are near the lithostatic pressure, the possibility exists that horizontal fractures are created in the minifracs in the shales and the ISIP is a reflection of the overburden stress. In this case, the minimum horizontal in situ stress might even be greater than measured here. These shale measurements should be considered minimum values for σ_{Hmin}.

6.6.2 Stress Orientations

The orientation of the stress field has been determined using ASR, DSCA and an impression packer after an open-hole minifrac. For the Corcoran sandstone, four ASR tests gave an average orientation of the maximum horizontal in situ stress (hydraulic fracture direction) of N83°W with a standard division of 4° (using a method of weighted variances). In the Cozzette sandstone, four ASR tests yielded an azimuth of N63°W with a standard deviation of 5° while two DSCA tests gave N76°W. Four ASR tests in the Rollins yielded an azimuth of N61°W with a standard deviation of 2°. An impression packer gave a possible fracture orientation of N50°-70°W in the Rollins. These results show that the hydraulic fracture orientation is closely aligned with the natural fracture orientation.

6.6.3 Comparison of Open-Hole and Cased-Hole Results

Figure 6.15 shows a comparison of the open-hole stress tests with the data through perforations in MWX-2. The difference in the tests is well within the experimental error, particularly when one takes into account the lateral variability in stress which should be expected over the distance that the two wells are separated (180 ft). Our stress tests through perforations clearly give good estimates of the minimum in situ stress.

6.6.4 Containment of Hydraulic Fractures

The stress distribution found around the Cozzette sandstone is ideal for hydraulic fracture containment. The stress difference between the upper sand and the overlying Mancos tongue is on the order of 2000 psi while the stress difference between the lower sand and the underlying Mancos tongue is about 1300 psi. Calculations of the expected fracture height as a function of treatment pressure were performed using the measured stress state. The calculations are similar to those of Simonson et al[2] except they can be used for multiple, nonsymmetric (with respect to thickness and stress) layers. Material property variations are not considered. The only problem is how to incorporate the varied stress state in the siltstone between the Cozzette sands (the dual closure stress). For the purposes of these calculations, it is modeled as a single layer of high stress even though it is probably several thin layers of high stress. The calculations, however, will only depend on the thickness of this single high stress region.

Figure 6.16 shows the predicted fracture height as a function of treatment pressure for the given stress distribution with a 20 ft thick high stress layer between the two sands. The layer labeled "frac interval" is the upper Cozzette sandstone which is the most favorable zone. Treatment pressures of less than 600 psi over the minimum in situ stress would be required to keep the fracture in only the upper sand. This is unrealistic for a large treatment and the fracture is expected to propagate through both sands to some degree. Treatment pressures should be kept below 1000 psi over the minimum in situ stress to avoid extensive fracturing through the marine shales. For pressures above 1200 psi over the minimum in situ stress, the fracture can be expected to break down into the Corcoran sand.

A more efficient treatment procedure would be to fracture the entire Cozzette since it will be impossible to avoid breaking into the lower sand with any reasonable size treatment. This should keep the pressures lower and enhance containment.

6.6.5 Perforations

The most important design consideration for in situ stress measurements using minifracs through perforations is the perforation schedule. In low permeability formations such as shales, tight sands and siltstones, open-hole minifracs generally result in small pressure drops at shut-in (100-400 psi) and well-defined ISIP values. If the perforations are good and have little or no damage, then the ISIP values obtained in minifracs through perforations should be the same since the rock mass is no different. Any deviations from this, such as large pressure drops at shut-in or poorly defined ISIP values, are often indications of perforation problems. These problems are due to the response of the rock and/or cement to the perforation size (charge) or design. Unfortunately, the problems may be different from one formation to another as rock properties vary and also from one location to another within a formation as hole conditions vary. The ultimate result is that it becomes almost impossible to always obtain good results. For example, of the eleven stress tests shown in Figures 6.7-6.9, eight were good, one was abnormal (dual closure) because of what is believed to be formation variability, and two tests showed obvious perforation effects.

6.6.6 Comparison with Other Data

Bredehoeft et al[32] have previously conducted open-hole minifracs in the Piceance basin, mostly at shallow depths. These tests were conducted farther to the northwest in the Green River Formation but they also show high frac gradients. At depths from 500-1100 ft, where fractures were definitely vertical, fracture gradients of 0.5-1.1 psi/ft were measured with an average of about 0.73 psi/ft. However, no correlation with lithology was attempted.

6.6.7 Estimate of Tectonic Strain

For our stress history/natural fracture modeling, these data provide valuable insight into the tectonic conditions. For example, if we assume that the difference measured in the open-hole stress tests is due entirely to tectonic strain in the maximum direction and also assume no strain in the minimum direction (x), we can obtain a simple estimate of the tectonic stresses as

$$\Delta\sigma_y = \frac{E\varepsilon_y}{1-\nu^2} \tag{6}$$

and

$$\Delta\sigma_x = \frac{\nu E\varepsilon_y}{1-\nu^2}, \tag{7}$$

where

- E is Young's modulus,
- ν is Poisson's ratio,
- ε_y is the tectonic strain in the maximum stress direction,
- $\Delta\sigma$ is the tectonic stress <u>above</u> the base stress (the base stress is assumed to be equal in the x and y directions since it depends on material properties, temperature and other factors which should not show large changes with horizontal directions.

Clearly,

$$\Delta\sigma_y = \Delta\sigma_x + 800 \text{ psi}, \tag{8}$$

so we can solve the three equations for $\Delta\sigma_y$, $\Delta\sigma_x$ and ε_y. Assuming $E = 5.5 \times 10^6$ psi and $\nu = 0.2$, we obtain:

$$\Delta\sigma_y = 1000 \text{ psi},$$
$$\Delta\sigma_x = 200 \text{ psi},$$
$$\varepsilon_y = 175\ \mu\varepsilon .$$

The fact that $\Delta\sigma_x$ is low is good because our Cozzette minimum stress data indicates that it cannot be large. We hope to check ε_y from calcite twinning and see if it matches our understanding of the structural history of this area of the basin. (Note that this analysis can be reversed to give the same magnitude of <u>extensional</u> strain in the x-direction and no strain in the y-direction.)

6.7 CONCLUSIONS

Accurate, reproducible measurements of the minimum principal in situ stress can be made by using small volume hydraulic fractures (minifracs). For minifracs in cased holes, a good test requires a considerable amount of care and preparation. Important factors include: 1) perforation schedule, particularly the charge, 2) small volumes (5-100 gal) of a low viscosity fluid, 3) a downhole closure tool, and 4) bottomhole pressure measurements at rapid sampling rates.

Good estimates of stress orientations can be made using ASR and DSCA techniques; these range between N61°W and N83°W. Less reliable estimates of stress magnitudes can also be calculated.

Marine shales at the base of the Mesaverde group were found to have stresses near the lithostatic value. Creep may be an important process whereby the horizontal stresses become so large.

The stress in the Cozzette sandstone approaches the value calculated from elastic behavior in uniaxial strain. The stress in the Rollins sandstone is somewhat higher than predicted.

The stress distribution around the Cozzette sandstone shows a 1300-2000 psi stress difference between the sand and the shale. This is ideal for fracture containment if the treatment is properly designed.

The difference between the two horizontal in situ stresses is only about 800 psi. This can have important implications for hydraulic fracturing.

The open-hole stress tests confirmed the accuracy of the minifracs conducted through perforations.

The orientation of the hydraulic fracture in the Rollins sandstone open-hole section appeared to be N50-70°E, but this measurement is questionable and should not be relied upon. However, it is consistent with the strain recovery data.

6.8 REFERENCES

1. Perkins, T. K. and Kern, L. R.: "Widths of Hydraulic Fractures," Journal of Petroleum Technology, Vol. 13, Sept. 1961, p. 937.

2. Simonson, E. R., Abou-Sayed, A. S. and Clifton, R. J.: "Containment of Massive Hydraulic Fractures," Society of Petroleum Engineers Journal, Vol. 18, Feb. 1978, p. 27.

3. Warpinski, N. R., Clark, J. A., Schmidt, R. A. and Huddle, C. W.: "Laboratory Investigation on the Effect of In Situ Stresses on Hydraulic Fracture Containment," Society of Petroleum Engineers Journal, Vol. 22, No. 3, June 1982, p. 333.

4. Teufel, L. W. and Clark, J. A.: "Hydraulic Fracture Propagation in Layered Rock: Experimental Studies of Fracture Containment," SPE/DOE 9878, Proceedings, 1981 SPE/DOE Symposium on Low Permeability Gas Reservoirs, May 1981, Denver, Colorado, p. 449.

5. Hanson, M. E., Anderson, G. D., Shaffer, R. J. and Thorson, L. D.: "Some Effects of Stress Friction, and Fluid Flow on Hydraulic Fracturing," Society of Petroleum Engineers Journal, Vol. 22, No. 3, June 1982, p. 321.

6. Warpinski, N. R., Schmidt, R. A., and Northrop, D. A.: "In Situ Stresses: The Predominant Influence on Hydraulic Fracture Containment," Journal of Petroleum Technology, Vol. 34, March 1982, pp. 653-664.

7. Northrop, D. A., Sattler, A. R. and Westhusing, J. K.: "Multi-Well Experiment: A Field Laboratory for Tight Gas Sands," SPE 11646, presented at SPE/DOE Symposium on Low Permeability Reservoirs, Denver, Colorado, March 14-16, 1983.

8. Nolte, K. G.: "Determination of Fracture Parameters From Fracturing Pressure Decline," SPE 8341, presented at 54th Annual SPE Meeting, Las Vegas, Nevada, Sept. 23-26, 1979.

9. Nolte, K. G.: "Fracture Design Considerations Based on Pressure Analysis," SPE 10911, presented at 1982 SPE Cotton Valley Symposium, Tyler, Texas, May 20, 1982.

10. Smith, M. B.: "Stimulation Design for Short Precise Hydraulic Fractures--MHF," SPE 10313, presented at 56th Annual SPE Meeting, San Antonio, Texas, Oct. 5-7, 1981.

11. Hubbert, M. K. and Willis, D. G.: "Mechanics of Hydraulic Fracturing," Petroleum Transaction, AIME, Vol. 210, 1957, p. 153.

12. Scheidegger, A. E.: "Stresses in Earth's Crust as Determined from Hydraulic Fracturing Data," Geologic und Bauwesen, Vol. 27, 1962, p. 45.

13. Kehle, R. O.: "Determination of Tectonic Stresses Through Analysis of Hydraulic Well Fracturing," Journal of Geophysical Research, Vol. 69, 1964, p. 259.

14. Fairhurst, C.: "Measurement of In Situ Rock Stresses, with Particular Reference to Hydraulic Fracturing," Rock Mechanics and Engineering Geology, Vol. 2, 1964, p. 129.

15. Warpinski, N. R.: "Investigation on the Accuracy and Reliability of In Situ Stress Measurements Using Hydraulic Fracturing in Perforated, Cased Holes," Proceedings, 24th U. S. Symposium on Rock Mechanics, June 1983, Texas A & M University, College Station, Texas.

16. Kry, R. and Gronseth, M.: "In Situ Stresses and Hydraulic Fracturing in the Deep Basin," presented at 33rd Annual Meeting of CIM, #82-33-21, June 6-9, 1982.

17. Greenfield, H., Ahmed, U., Holland, M. T. and Schatz, J. F.: "Resource Evaluation and Production Research on Tight Sands in the Pindale Unit, Sublette County, Wyoming, Final Report," Gas Research Institute Report, GRI-81/0049, Dec. 1981.

18. Haimson, B and Fairhurst, C., "Hydraulic Fracturing in Porous-Permeable Materials," J. Pet Tech, Vol. 21, July 1969, p. 811.

19. Rice, J. R. and Cleary, M. P., "Some Basic Stress Diffusion Solutions for Fluid-Saturated Elastic Porous Media with Compressible Constituents," Rev of Geophysics and Space Physics, Vol. 14, No. 2, May 1976, p. 227.

20. Teufel, L. W., "Determination of In Situ Stress from Anelastic Strain Recovery Measurements of Oriented Core," SPE 11649, presented at 1983 SPE/DOE Symposium on Low Permeability Reservoirs Denver, CO, March 14-16, 1983.

21. Teufel, L. W. and Warpinski N. R., "Determination of In Situ Stress from Anelastic Strain Recovery Measurements of Oriented Core: Comparison to Hydraulic Fracture Stress Measurements in the Rollins Sandstone, Piceance Basin, Colorado," Proceedings of the 25th U.S. Symposium on Rock Mechanics Northwestern University, Evanston, IL June 25-27, 1984.

22. Obert, L. and Duval, W. E., "Rock Mechanics and the Design of Structures in Rock," Wiley, New York, 558 pp. (1967).

23. Voight, B, "Determination of the Virgin State of Stress in the Vicinity of a Borehole from Measurements of Partial Anelastic Strain Tensor in Drill Cores," Felsmechanik V. Ingenieureol 6, pp. 201-215 (1968).

24. Teufel, L. W., "Prediction of Hydraulic Fracture Azimuth from Anelastic Strain Recovery Measurements of Oriented Core," in 23rd US National Rock Mechanics Symposium, Berkeley, CA, ed. R. Goodman and F. Hueze, 238-246 (1982).

25. Blanton, T. L., "The Relation between Recovery Deformation and In Situ Stress Magnitudes," SPE 11624, presented at 1983 SPE/DOE Symposium on Low Permeability Gas Reservoirs, Denver CO, March 14-16, 1983.

26. Blanton, T. L. and Teufel, L. W., "A Field Test of the Strain Recovery Method of Stress Determination in Devonian Shales," SPE 12304, presented at the Eastern Regional SPE Meeting, presented at the Eastern Regional SPE Meeting, Champion, PA, November 9-11, 1983.

27. Warpinski, N. R. and Teufel, L. W. "A Viscoelastic Constitutive Model for Determining In Situ Stress Magnitudes from Anelastic Strain Recovery of Core," SPE 15368, SPE Annual Meeting, New Orleans, LA, September, 1986.

28. Strickland, F. and Ren, N., "Predicting the In Situ Stress for Deep Wells Using the Differential Strain Curve Analysis, Using the Strain Curve Analysis," SPE 8954, Proc. of the Unconventional Gas Recovery Symposium, Pittsburgh, PA, May 1980.

29. Strickland, F. G. and Ren, N-K., "Predicting the In Situ Stress State for Deep Wells Using Differential Strain Curve Analysis," presented at the 31st Ann. Tech. Meeting of the Pet. Soc. of CIM, Calgary, paper no. 80-31-33, May 1980.

30. Ren, N. K. and Roegiers, J. C., "Differential Strain Curve Analysis--A New Method for Determining the Preexisting In Situ Stress State from Rock Core Measurements," presented at the 5th ISRM Congress, Melbourne, April 1983.

31. Frocht, M. M., "Photoelasticity," John Wiley and Sons, New York, v 1, 441 pp., 1948.

32. Bredehoeft, J. D., Wolff, R. G., Keys, W. S. and Shuter, E., "Hydraulic Fracturing to Determine the Regional In Situ Stress Field, Piceance Basin, Colorado," Geological Society of America Bulletin, v 87, Feb, 1976, pp. 250-258.

Table 6.1 Rollins Core Data for Open Hole Tests

Sample Number	Core = Log Depth (ft)	Permeability (md, max.)	Helium Porosity (%)	Saturations Oil (%)	Saturations Water (%)	Grain Density (g/cm^3)
1	7536.5-36.8	<0.01	5.4	0.0	78.3	2.68
2	7538.4-38.7	<0.01	5.7	0.0	75.0	2.67
3	7540.4-40.7	<0.01	5.6	0.0	73.7	2.68
4	7542.3-42.6	<0.01	3.9	0.0	65.3	2.70
5	7544.3-44.7	<0.01	4.1	0.0	75.6	2.74
6	7546.2-46.5	<0.01	3.9	0.0	74.0	2.73
7	7548.4-48.7	<0.01	5.8	0.0	72.5	2.67
8	7550.3-50.6	<0.01	6.6	0.0	76.1	2.69
9	7552.4-52.7	0.02	7.3	0.0	64.7	2.68
10	7554.4-54.7	0.01	7.5	0.0	76.6	2.69
11	7556.5-56.8	0.02	8.0	0.0	77.2	2.68
12	7558.5-58.7	0.02	7.7	0.0	71.6	2.69
13	7559.6-59.9	0.02	7.1	0.0	73.4	2.69
14	7563.2-63.4	0.07	13.3	0.0	59.1	2.87

Table 6.2 Open Hole Stress Data in Rollins Sandstone

Depth (ft)	P_c (psi)	P_{op} (psi)	P_i (psi)	σ_{min} (psi)	σ_{max} (psi)
7535-51	8295	7115	5600	6765	7600* 7580**
7502-19	7575	7225	5600	6810	8455* 7605**

*Calculated from $\sigma_{max} = 3\ \sigma_{min} - P_c + T - P_i$ T = 1200 psi

**Calculated from $\sigma_{max} = 3\ \sigma_{min} - P_{op} - P_i$

Orientation: Possibly N50°-N70°W

Table 6.3 Summary of Anelastic Strain Recovery Measurements of MWX-2 Oriented Core (Cozzette and Corcoran Sandstones)

Depth (ft)	Lithology	Final Principal Strain Magnitudes* ε_v	ε_{Hmax}	ε_{Hmin}	Average Ratio of Principal Strains* $\varepsilon_{Hmax}/\varepsilon_v$	$\varepsilon_{Hmin}/\varepsilon_v$	Average Azimuth of ε_{Hmax}
7884	sandstone	N	178	110	N	N	N49°W±10
7888	sandstone	152	166	105	1.06±0.25	0.63±0.21	N60°W±8
7894	sandstone	N	238	144	N	N	N74°W±9
7895	sandstone	238	251	155	1.14±0.18	0.74±0.24	N69°W±11
7903	shale	-	-	-	-	-	-
7904	shale	-	-	-	-	-	-
7905	shale	-	-	-	-	-	-
8118	sandstone	N	283	162	N	N	N92°W±9
8119	sandstone	180	228	148	1.20±0.20	0.77±0.18	N82°W±11
8120	sandstone	N	198	135	N	N	N83°W±7
8121	sandstone	194	266	165	1.28±0.16	0.85±0.14	N78°W±8

*N means not measured on this core

Table 6.4 Table of Anelastic Strain Recovery Measurements of MWX-3 Oriented Core (Rollins Sandstone)

Depth (ft)	Lithology	Final Principal Strain Magnitudes ε_v	ε_{Hmax}	ε_{Hmin}	Average Ratio of Principal Strains $\varepsilon_{Hmax}/\varepsilon_v$	$\varepsilon_{Hmin}/\varepsilon_v$	Average Azimuth of ε_{Hmax}
7560	sandstone	146	110	72	0.76±0.04	0.54±0.05	N66°W±4
7561	sandstone	168	124	80	0.73±0.05	0.48±0.04	N59°W±3
7562	sandstone	182	146	102	0.80±0.05	0.56±0.04	N72°W±6
7564	sandstone	204	172	88	0.84±0.05	0.39±0.06	N55°W±4

Table 6.5 Elastic Properties of Oriented Core Used in Stress Calculations

Depth (ft)	Lithology	Elastic Modulus* (10^6 psi)	Poisson's Ratio*
7888	sandstone	5.7	0.23
7895	sandstone	5.9	0.22
8119	sandstone	5.2	0.18
8121	sandstone	4.9	0.17

*Elastic properties were measured in triaxial compression tests at 60 MPa (8700 psi) confining pressure. Specimens were perpendicular to bedding.

Table 6.6 Elastic Properties of Rollins Sandstone*

P_c	Parallel to ε_v		Parallel to ε_{Hmax}		Parallel to ε_{Hmin}	
(psi)	E (10^6 psi)	ν	E (10^6 psi)	ν	E (10^6 psi)	ν
0	3.8	0.25	4.1	0.23	4.6	0.22
10	4.5	0.22	4.6	0.21	4.8	0.20
20	4.7	0.21	4.8	0.19	4.9	0.20
40	4.9	0.21	4.9	0.20	5.0	0.20
60	5.1	0.20	5.1	0.20	5.1	0.19

*determined at room temperature in triaxial compression tests at 10^{-5} sec^{-1} strain rate.

Table 6.7 Summary of In Situ Stress Magnitudes from ASR in Cozzette and Corcoran Using Blanton's Model

Depth (ft)	σ_V(calc) (psi)	P_O (psi)	σ_{Hmax} (psi)	σ_{Hmin} (psi)	$\Delta\sigma_H$ (psi)	σ_{Hmax}/σ_V	σ_{Hmin}/σ_V
7888	8280	6300	8365	8000	365	1.01	0.97
7895	8290	6300	8340	7955	385	1.01	0.96
8119	8525	6600	8800	8340	460	1.03	0.98
8121	8525	6600	8915	8370	545	1.05	0.98

Table 6.8 Summary of In Situ Stress Magnitudes from ASR in the Rollins Using Blanton's Model

Depth (ft)	σ_V(calc) (psi)	P_O (psi)	σ_{Hmax} (psi)	σ_{Hmin} (psi)	$\Delta\sigma_H$ (psi)	σ_{Hmax}/σ_V	σ_{Hmin}/σ_V
7560	7940	5600	7610	7260	350	0.96	0.91
7561	7940	5600	7590	7235	355	0.96	0.91
7562	7940	5600	7680	7365	315	0.97	0.93
7564	7940	5600	7731	7183	548	0.97	0.90

Table 6.9 Summary of DSCA Results for Cozzette Sandstone, MWX-2 by Dowell Schlumberger

Depth (ft)	Lithology	Three-Dimensional Analysis: Orientation σ_{max}	σ_{int}	σ_{min}	Magnitude $\sigma_{max}:\sigma_{int}:\sigma_{min}$
7914	Sandstone	N76°W	v*	N10°E	1.4(±0.2):1.2(±0.2):1.0
7942	Sandstone	N76°W	v*	N20°E	1.4(±0.2):1.3(±0.1):1.0

* vertical, ±10°

Table 6.10 In Situ Stress Data

Depth (ft)	Lithology	σ_{Hmin} (psi)	Estimated Error (± psi)	P_i (psi)	ν	E (psi)	σ_v (psi)	σ_{Hmin} Calculated (psi)	Frac Grad (psi/ft)
				Cased Hole Stress Data					
8061	Shale	8230	20	6600*	0.229	$2.9x10^6$	8465	7160	1.02
8015	Shale	8150	30	6375*	0.245	$2.9x10^6$	8415	7040	1.02
7971	Sandstone	6885	30	6300	0.194	$5.0x10^6$	8370	6800	0.86
7924	Siltstone/ Shale†	6850 7800	50 50	6300	0.226	$4.2x10^6$	8320	6890	0.86 0.98
7895	Siltstone	6830	30	6300	0.220	$5.0x10^6$	8290	6860	0.86
7850	Sandstone	6645	50	6150**	0.162	$5.4x10^6$	8245	6555	0.85
7766	Shale	8590	100	6065*	0.260	$2.8x10^6$	8155	6800	1.11
7665	Shale	8150	100	5890*	0.265	NA	8050	6670	1.06
7601	Siltstone	7610	20	5775*	0.224	NA	7890	6410	1.00
7531	Sandstone	6590	20	5600	0.225	NA	7910	6270	0.875
7467	Sandstone	6800	30	5600	0.195	NA	7840	6140	0.91
				Open Hole Stress Data					
7535-51	Sandstone	6765	30	5600	0.2	$4.8x10^6$	7920	6180	0.90
7502-19	Sandstone	6810	30	5600	0.2	$4.8x10^6$	7885	6170	0.91

* Estimated from linear interpolation of pressures measured in adjacent zones.
** Measured after three months of production.
† Dual closure stress.

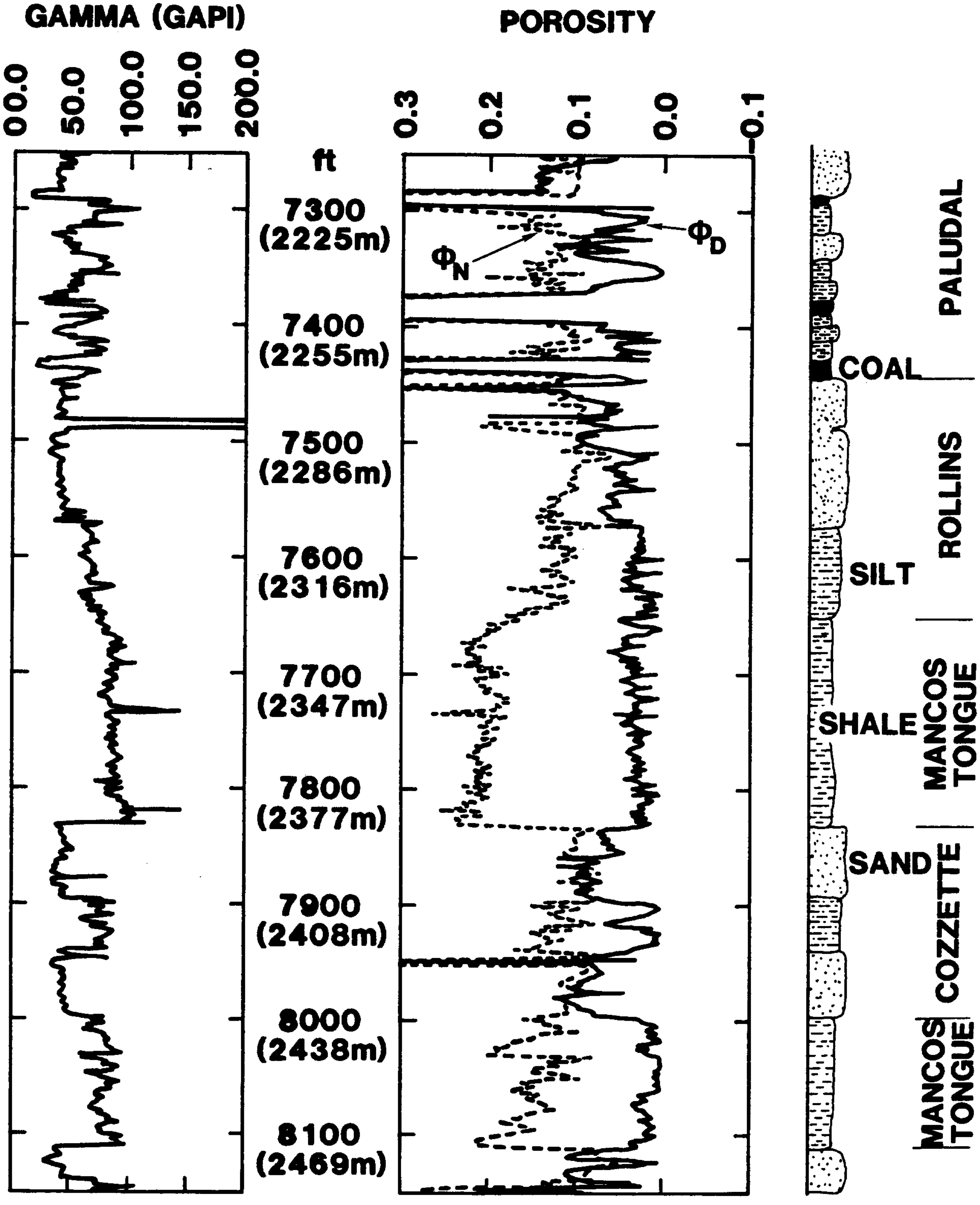

Figure 6.1 Section for Stress Measurements

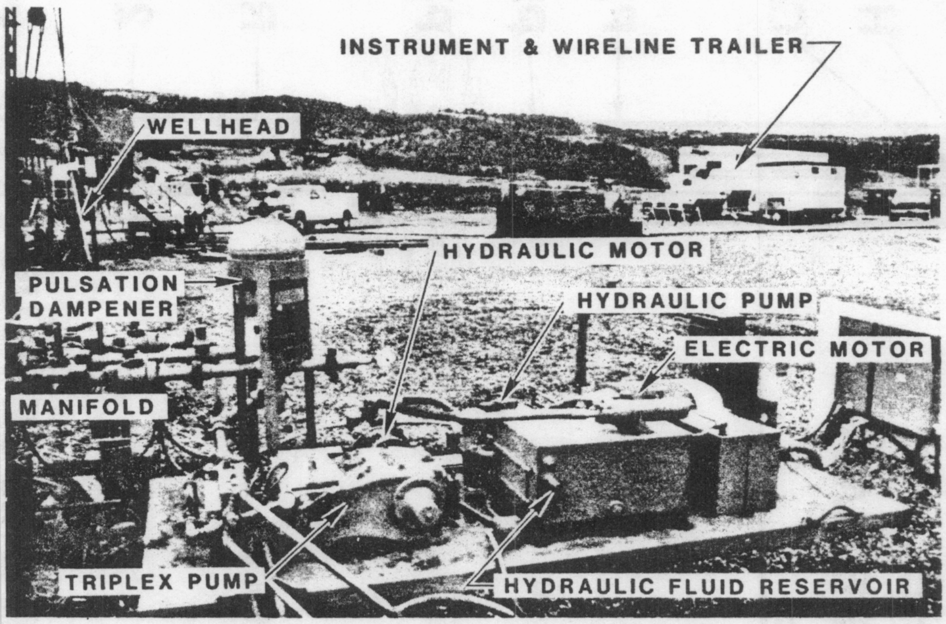

Figure 6.2 Stress Test Pump System

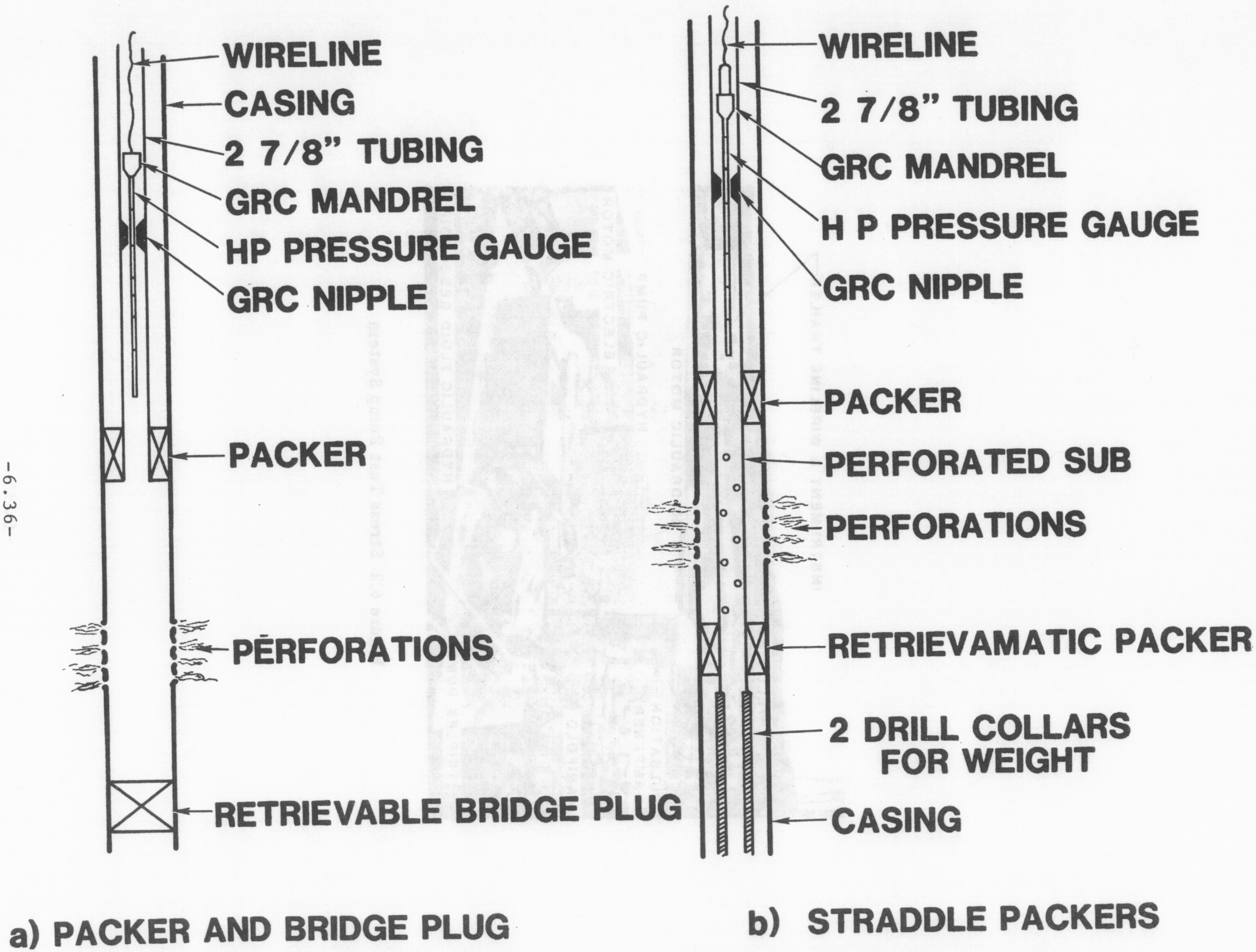

Figure 6.3 Instrument and Packer Configurations for Cased Hole Stress Tests

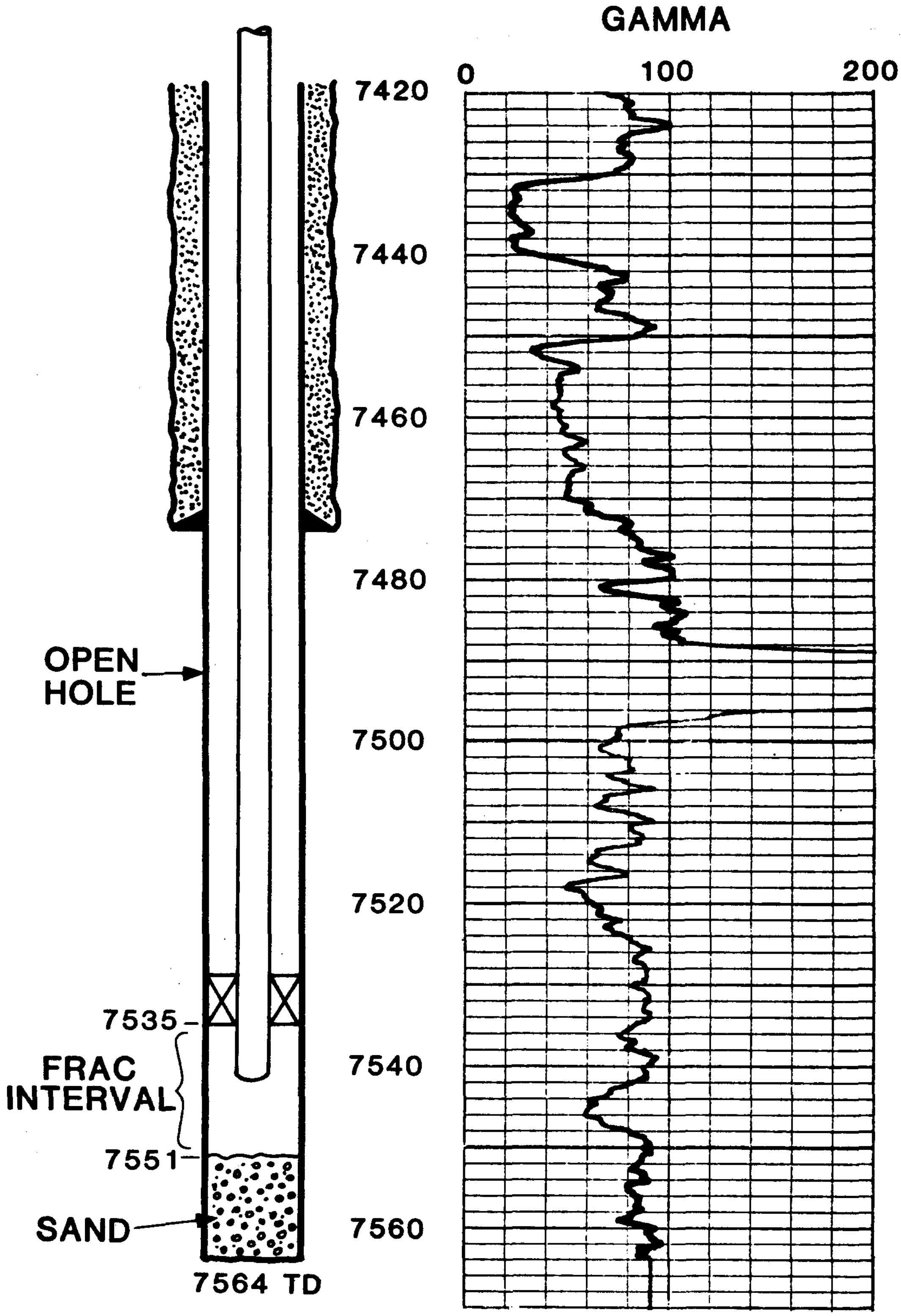

Figure 6.4 Open Hole Stress Test at 7535-7551 ft

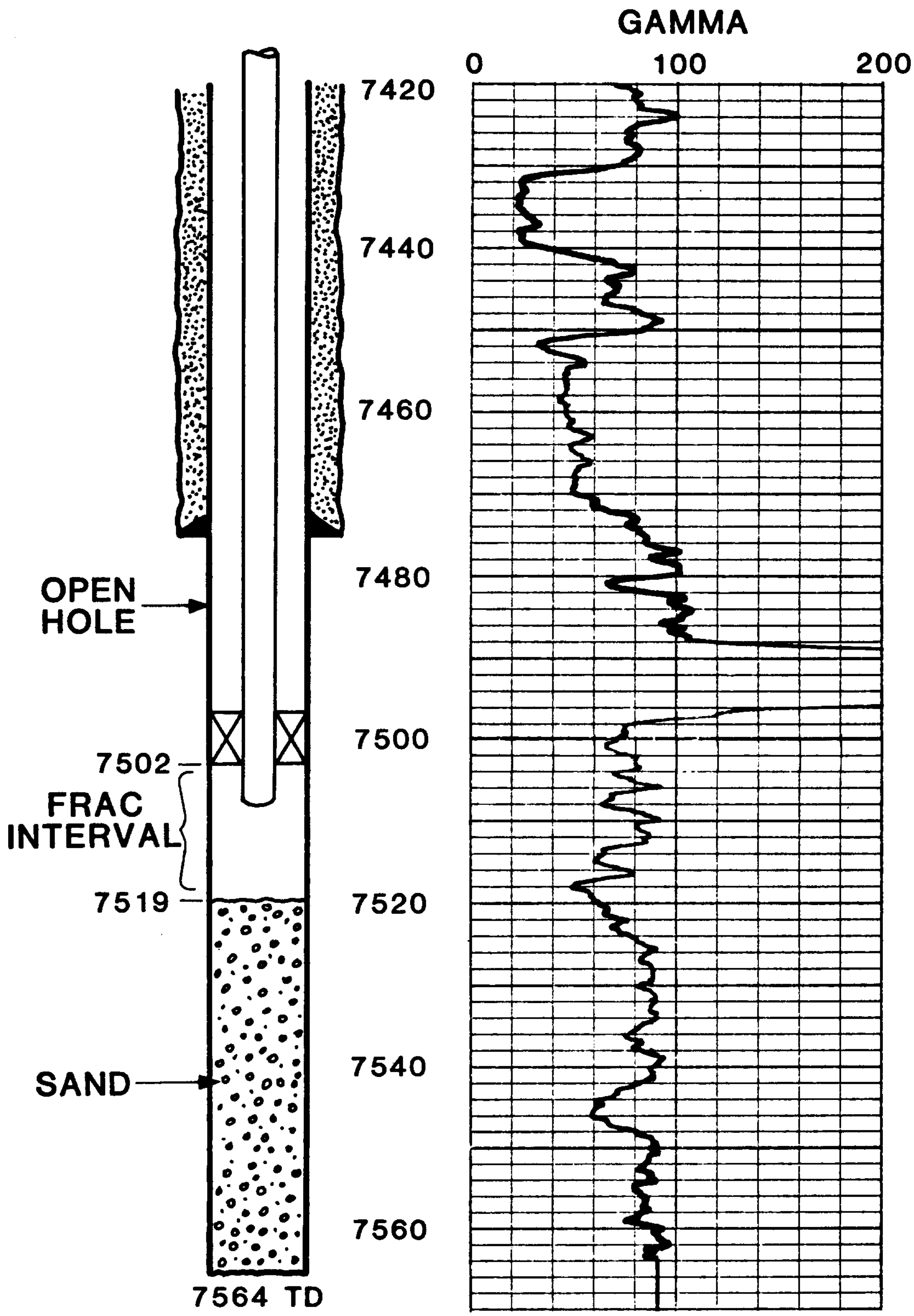

Figure 6.5 Open Hole Stress Test at 7502-7519 ft

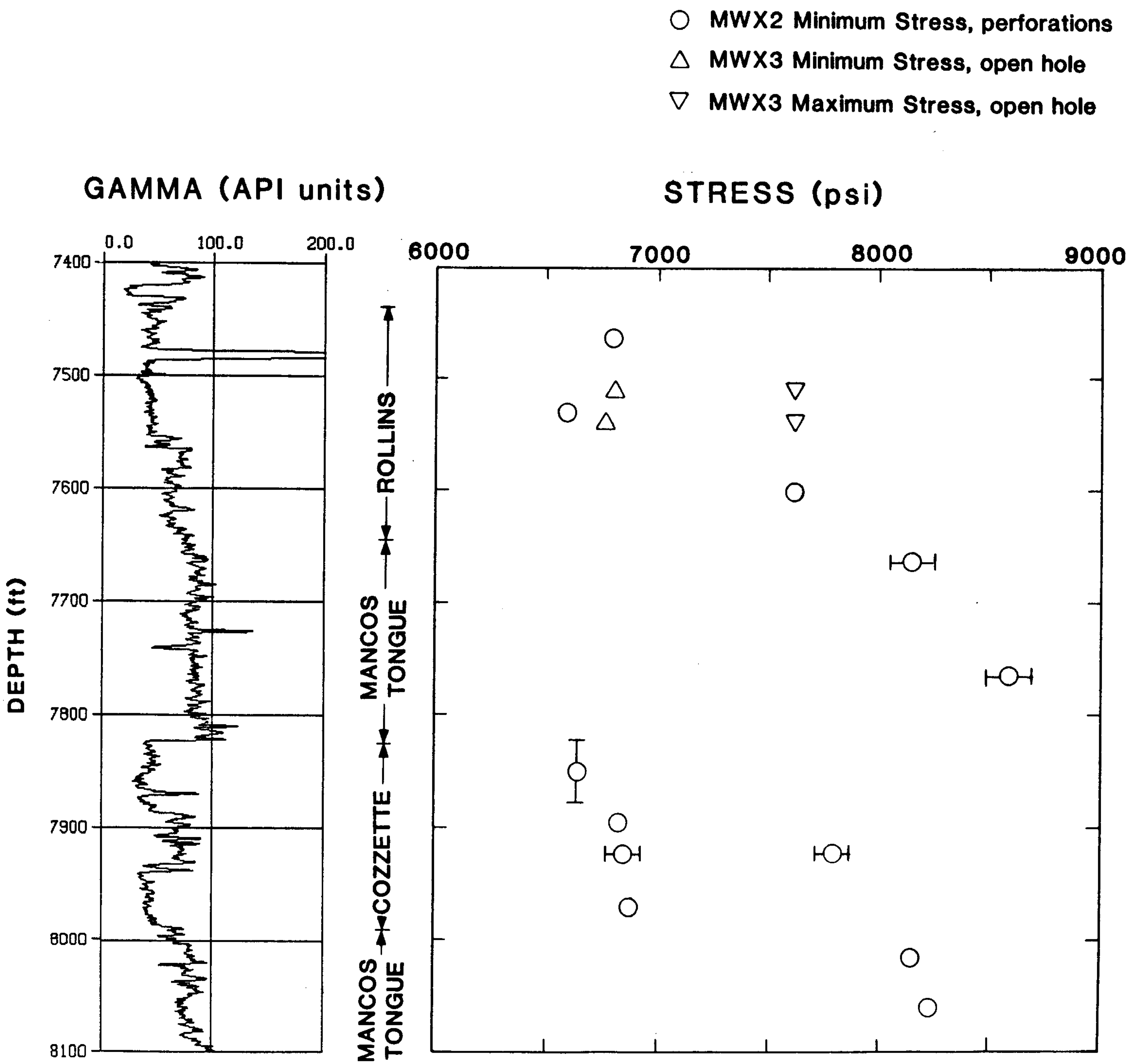

Figure 6.6 MWX Hydraulic Fracture Stress Measurements

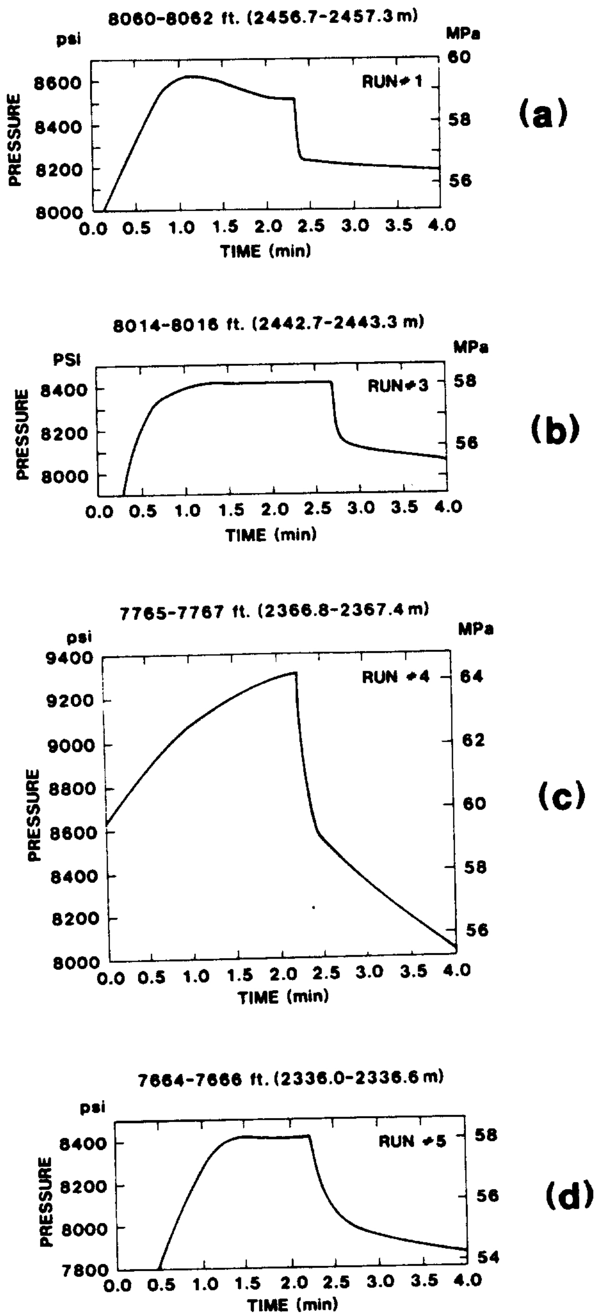

Figure 6.7 Shale Stress Results

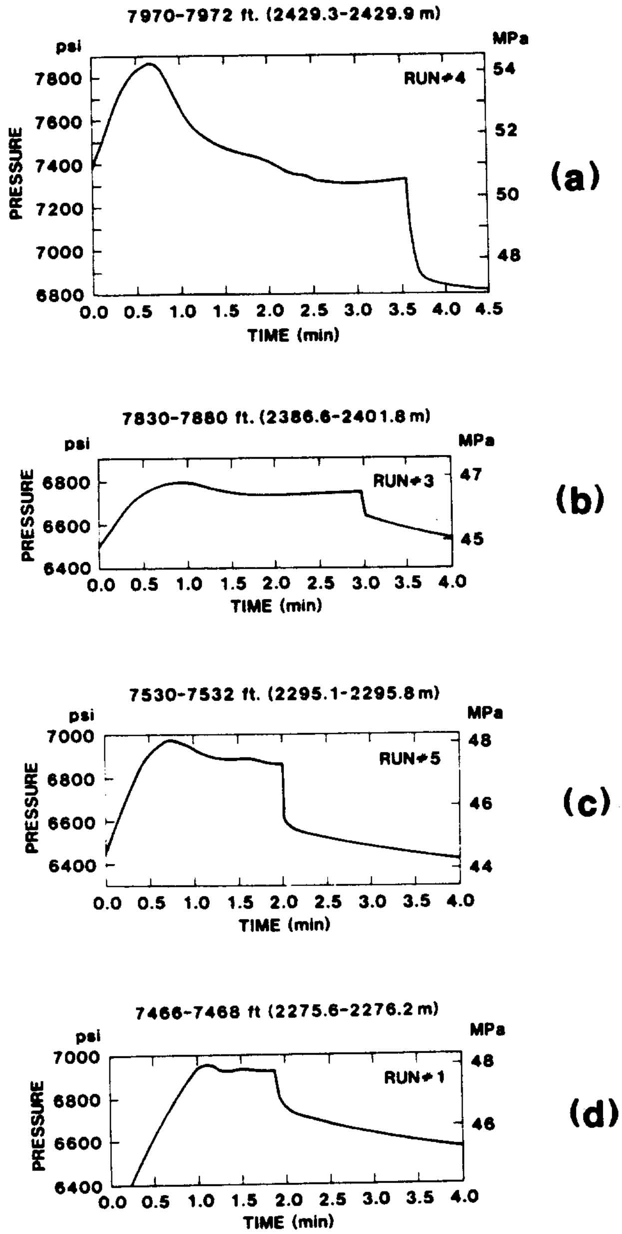

Figure 6.8 Sandstone Stress Results

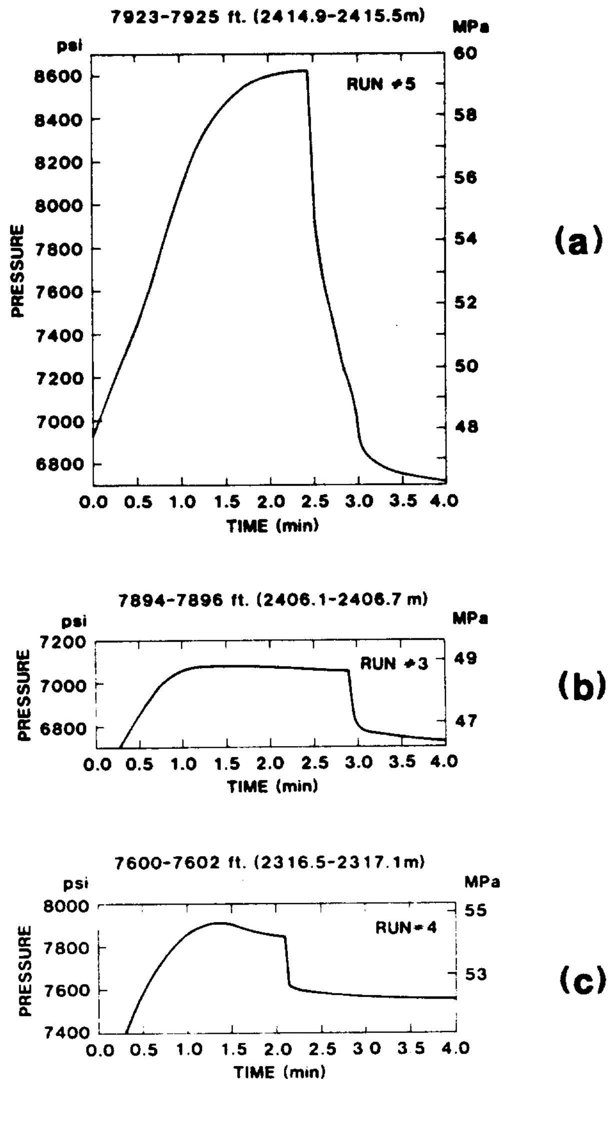

Figure 6.9 Siltstone Stress Results

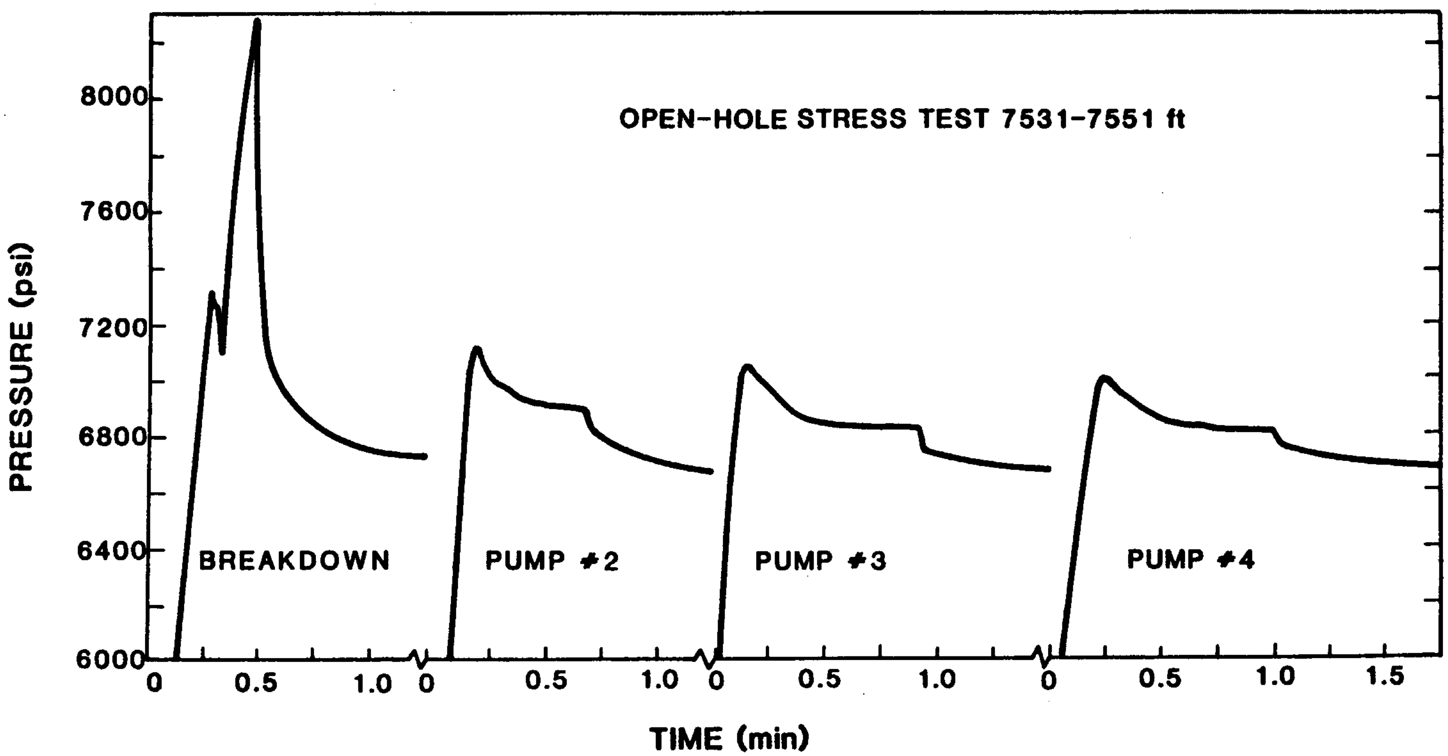

Figure 6.10 Open Hole Stress Test Results, 7531-51 ft

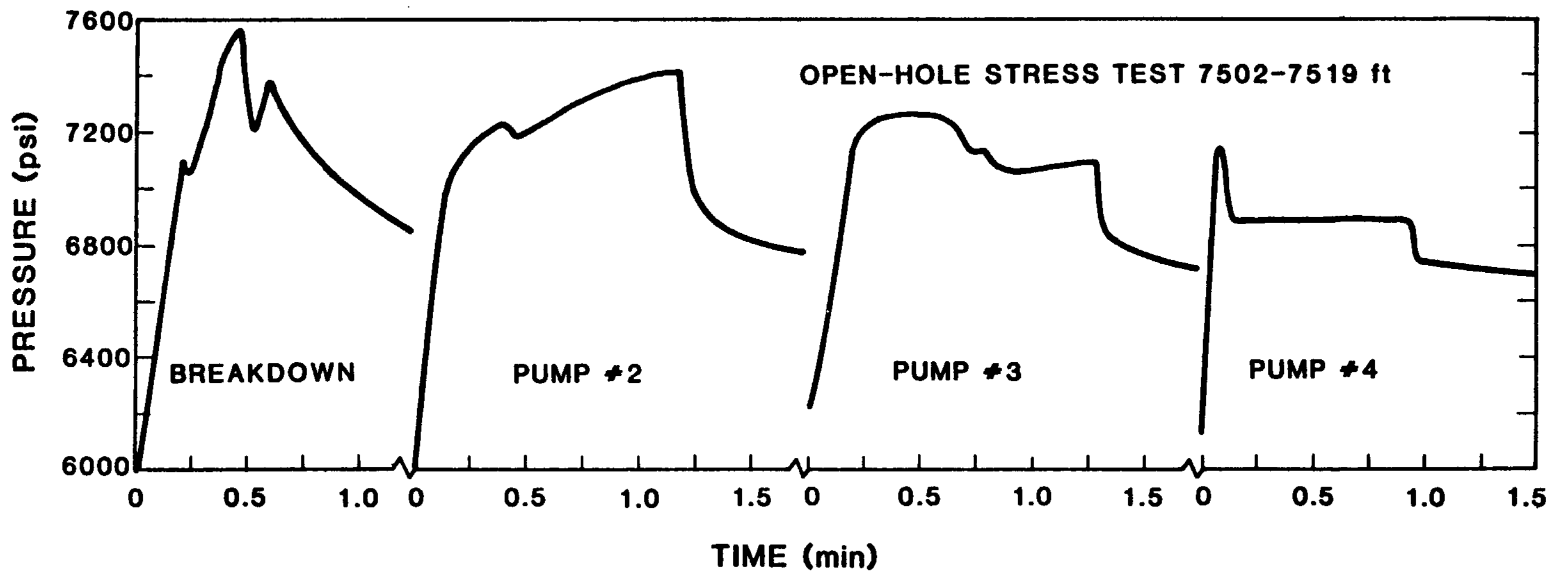

Figure 6.11 Open Hole Stress Test Results, 7502-19 ft

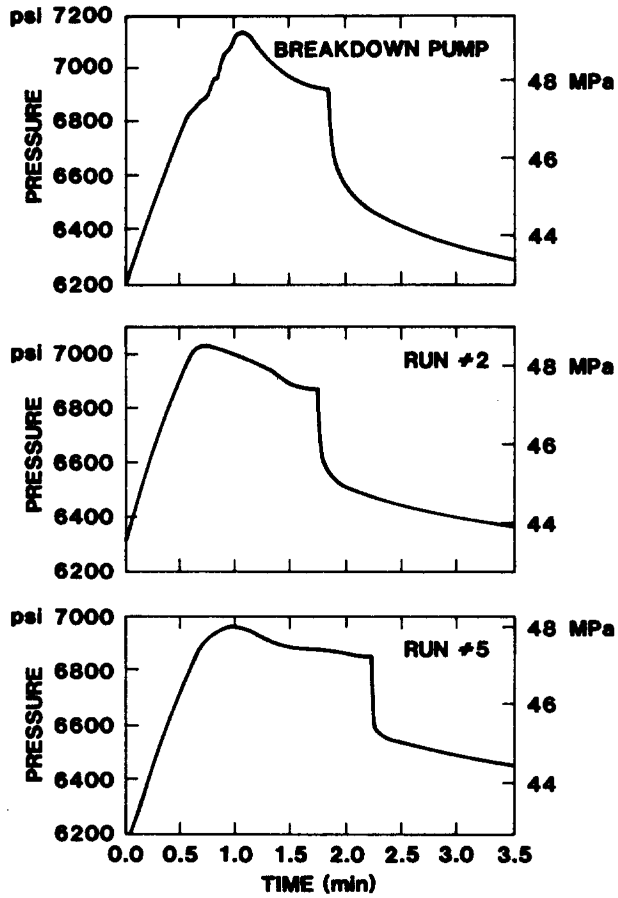

Figure 6.12 Repeat Pumps at 7531 ft

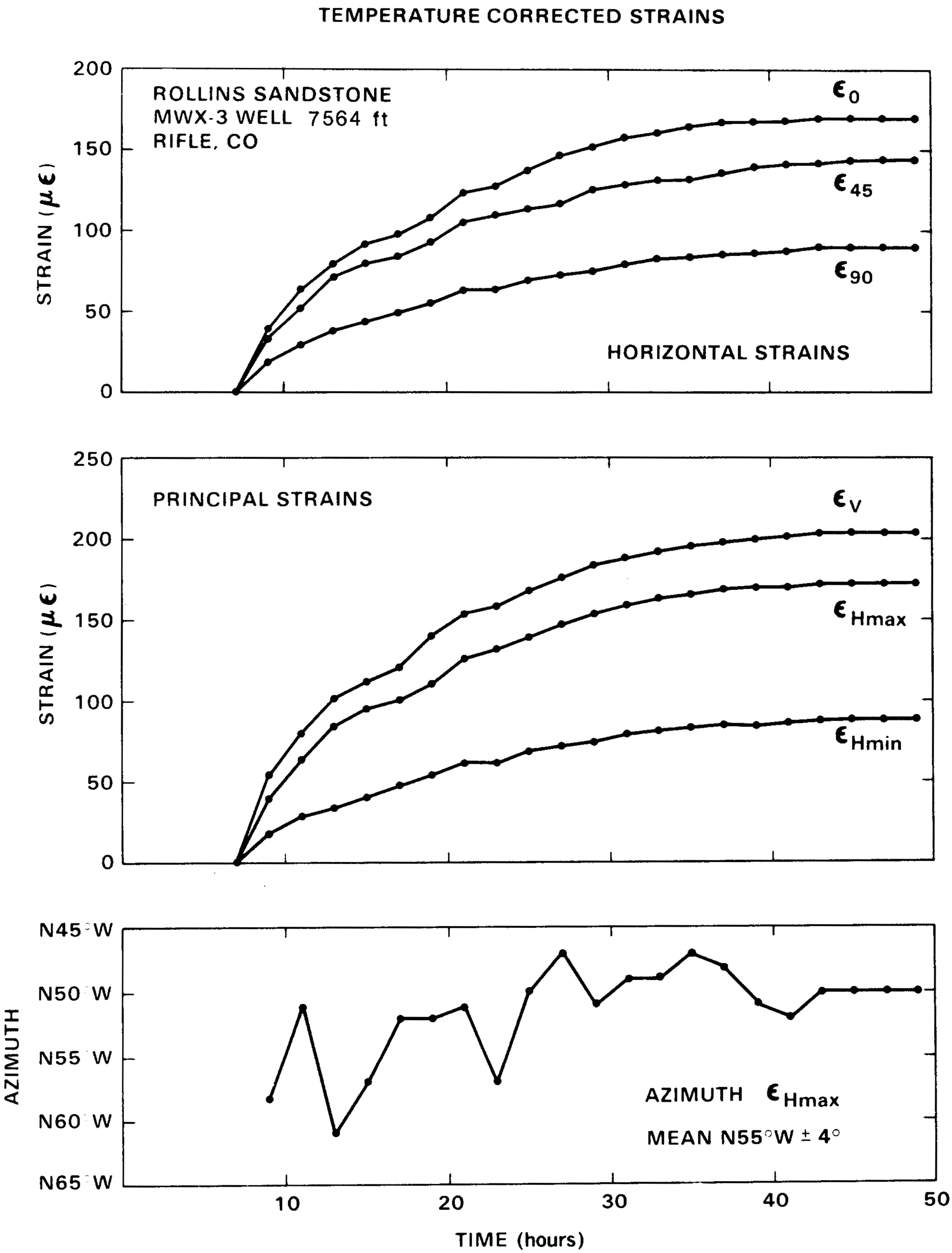

Figure 6.13 Example ASR Data for Rollins Sandstone

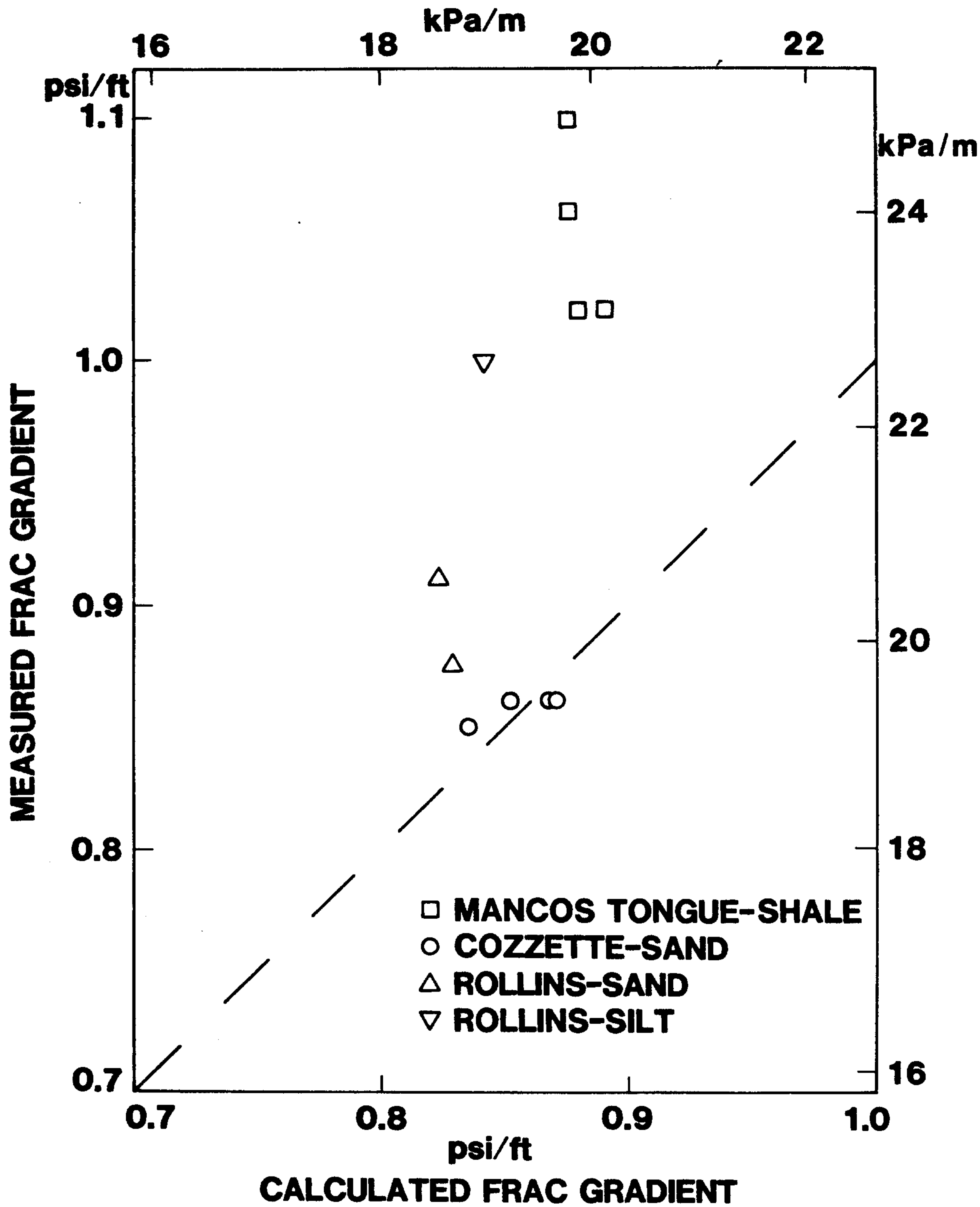

Figure 6.14 Calculated versus Measured Stresses

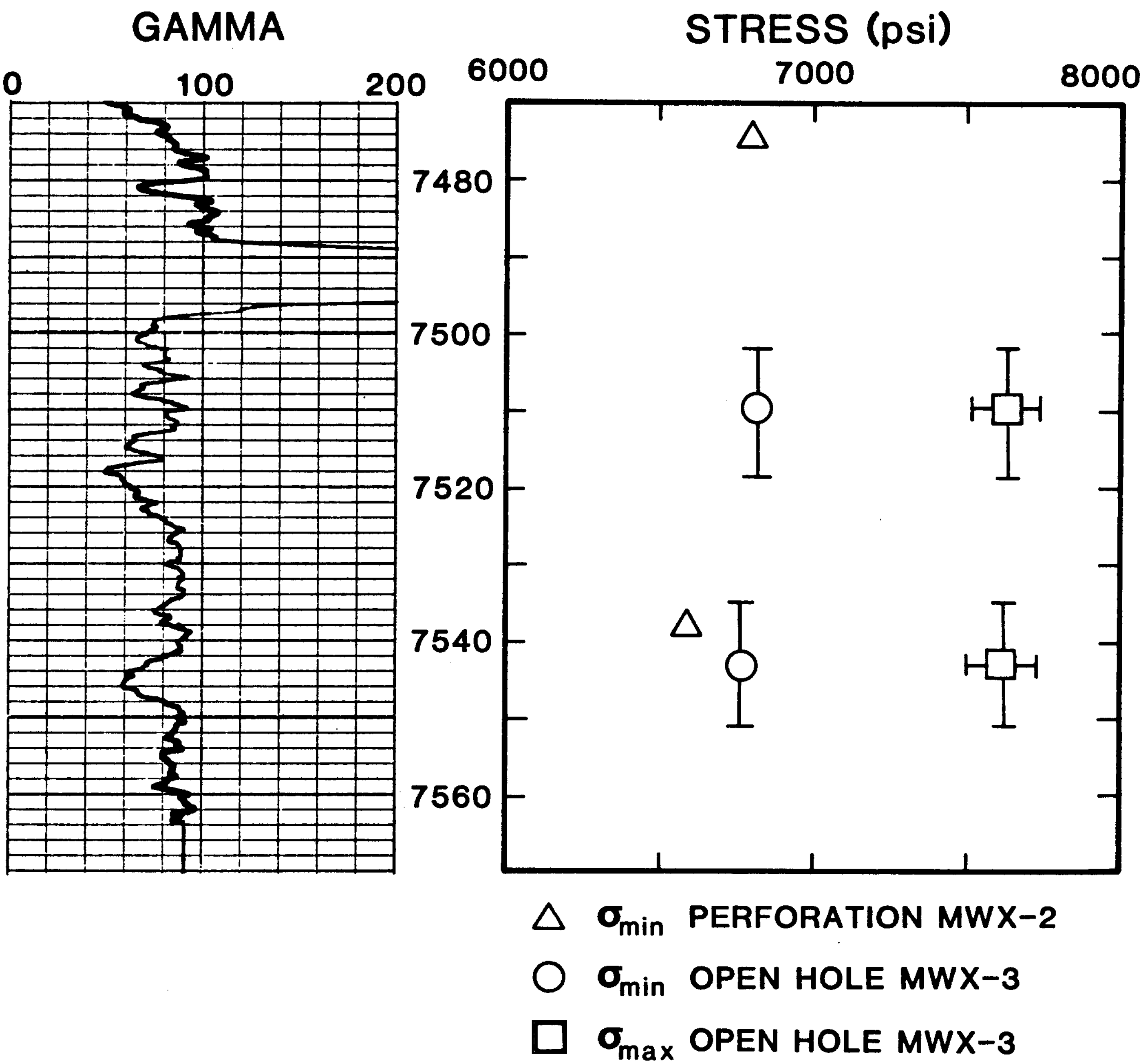

Figure 6.15 Comparison of Open Hole and Cased Hole Tests

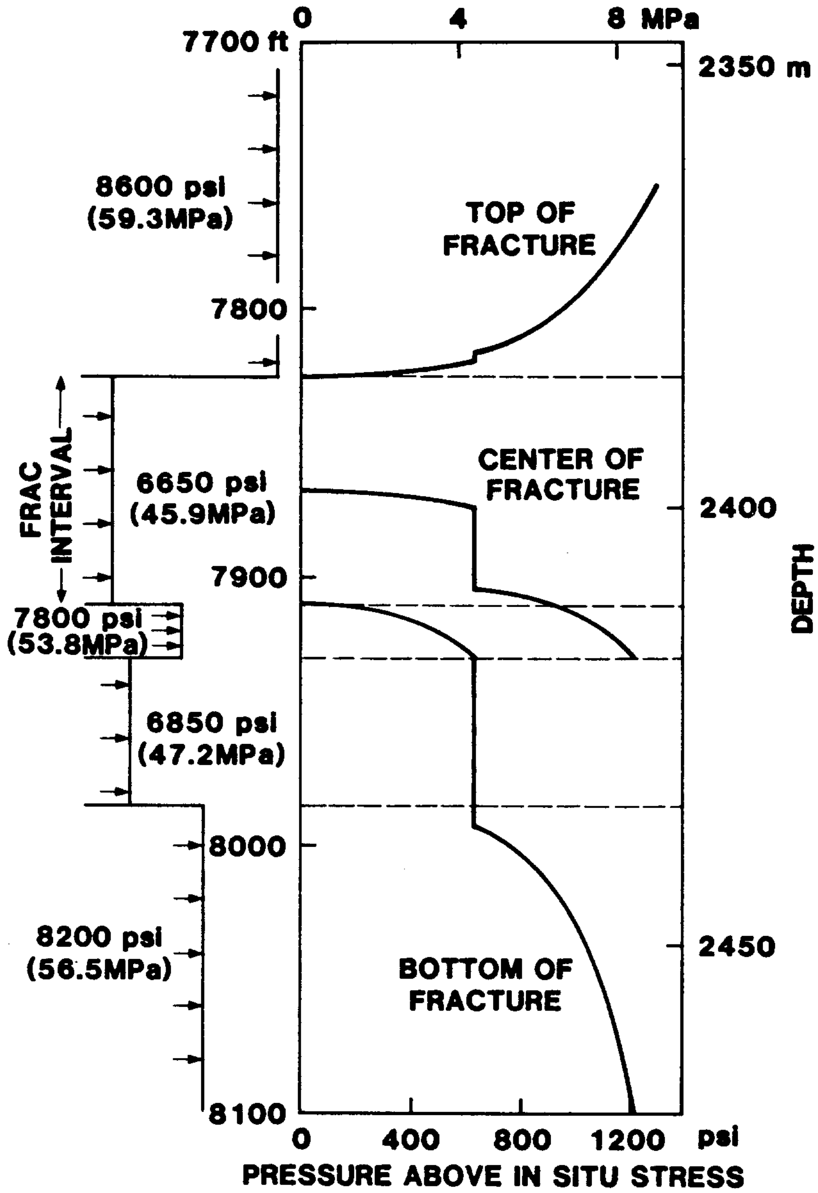

Figure 6.16 Calculated Fracture Height

INTENTIONALLY LEFT BLANK

7.0 WELL TESTING, ANALYSIS AND RESERVOIR EVALUATION

Paul T. Branagan
CER Corporation

7.1 INTRODUCTION

This section presents details from well testing and analysis of the Corcoran and Cozzette sandstones. These are the more continuous, "blanket" sandstones which are at the base of the Mesaverde Group at the MWX site. The geology of this interval and the reservoir properties derived from log and core analyses can be found in other sections of this final report and in References 1 through 9.

Several well tests were performed in the Corcoran and Cozzette sandstones. A short production test of the Corcoran was conducted in order to establish baseline production capacity. Some of the experiments conducted within the Cozzette included several short drawdown and buildup tests, as well as a more sustained interference and pulse test that utilized two of the MWX wells. The surface and subsurface location of wells MWX-1 and MWX-2 are shown in Figure 7.1 along with their separation at the depth of the Cozzette. Since the tests performed in the Corcoran were minimal, the emphasis of this section is placed on the Cozzette data and their analysis.

During test periods, bottomhole pressure, bottomhole temperature, surface tubing and casing pressures, fluid flow rates, and other pertinent information were acquired, manipulated and stored using a PDP-11/34 computer system. This field computer, interfacing hardware, accompanying calibration instrumentation, and repair facility are all housed within the DOE Western Gas Sands Program's Well Testing Trailer located at the MWX site. Most of the subsequent analytic and numerical analysis was performed on the DOE Nevada Operation's Cyber 76 computer and CER Corporation's VAX 730.

These marine blanket sandstones characteristically exhibit gas permeabilities on the order of 10 microdarcies (μd) or less in core. However, the production and test data from the MWX site along with subsequent analytic methods require an average reservoir permeability on the order of 100's of microdarcies. Data obtained from the observation well during the interference test of the Cozzette suggest that the pressure distribution from the production well was not radially symmetric, and thus, the reservoir was modeled as an anisotropic, naturally fractured reservoir. Numerical modeling techniques including a dual porosity reservoir model were used to stimulate this naturally fractured tight reservoir. Included in our analysis was a parametric sensitivity study for a number of salient well and reservoir parameters such as wellbore skin and/or damage, the potential effects of nearby boundaries, and exact placement of the observation well in a fractured tight matrix block. Several months of sustained winter pipeline production from the Upper Cozzette attests to the fact that the natural fracture system within the Cozzette extended over a large area.

Tests described in this report were to establish the productivity level and behavior of the reservoirs known to be of a continuous, more "blanket" nature than the lenticular sands found at shallower depth. It was thought that comparisons of the behavior of the two types of reservoirs would enable better evaluation of the degree of improvement in production rates obtained from hydraulic fracturing treatments in the lenticular types. Tests of the Corcoran and Cozzette sands indicated their production rates to be higher than their matrix permeabilities would support; thus, they are influenced by natural fracture systems. This condition reduces the validity of the desired comparisons.

7.2 CORCORAN WELL TESTS

7.2.1 Well Test Procedures

Preparation for production testing of the Corcoran marine blanket sandstone began August 13, 1982, in MWX-1. Prior to perforating the 7-in. diameter casing, the fresh water in the hole was displaced with water containing 3 percent KCl. The 7-in. casing was then perforated with 17-gram charges at one shot per foot over the interval 8110 to 8230 ft. Two-and-three-eighths-in. external upset end tubing equipped with a Baker model R-3 packer and seating nipple was run to 8069 ft. The well's configuration is shown in Figure 7.2.

Initially, the surface tubing shut-in pressure was 1160 psi and increased to 2580 psi after 45.5 hours. Assuming a full column of liquid within the tubing, the corresponding bottomhole pressures would be 6100 psi.

On August 17, 1982, attempts to flow the well were unsuccessful because of insufficient gas production to unload the liquid column in the tubing. However, a number of attempts to swab the well for two days revealed that the well was incapable of any continuous gas production. The initial gas production rate was 1 MCFD. On August 19, 1982, a wireline bottomhole gauge was run for a short pressure buildup survey. However, the well was flowed periodically for short periods, 5 to 15 minutes, to clean up. During these flow periods, the well surface tubing pressure was around 5600 psi which declined to 100 psi, while the bottomhole shut-in pressure was 6685 psi at a pressure gradient of 0.82 psi/ft.

On August 28, 1982, the well was filled with water containing 3 percent KCl for perforation breakdown. A 221 bbl mixture of 3 percent KCl water, surfactants, and benzoic acid flakes was pumped at an average injection rate of 6 barrels per minute at a surface treating pressure of 5000 psi. The benzoic acid flakes were utilized as a fluid diverting agent to assure even distribution of breakdown fluid in each set of perforations.

The perforations were flushed with 46 bbl of KCl water. The measured instantaneous shut-in pressure at the surface was 3500 psi. With a full liquid column, the shut-in bottomhole pressure would be 7025 psi or a pressure gradient of 0.87 psi/ft.

On August 29, 1982, the MWX-1 well was placed on production. Initially, it produced breakdown fluid and then produced gas at a rate of 200 MCFD. Surface tubing pressure during the early flowing period was 154 psi. Two days later, the flowing tubing pressure declined to about 100 psi with sporadic flow rates of 260 MCFD.

The well was then shut in for bottomhole pressure testing. After 12 hours of shut-in, the tubing pressure had risen to 5600 psi, while the measured bottomhole pressure was 6300 psi. Gas production resumed September 1, with the initial flow during wellbore storage depletion of 500 to 900 MCFD.

At 0700 hours on September 3, the well was flowing through a 0.5-in. choke at rates of 500 MCFD, with a corresponding flowing tubing pressure of 250 psi. The well continued to flow at 492 MCFD with an initial surface tubing pressure of 225 ± psi for the next four days. On September 7, the casing or annulus was then pressurized to 1000 psi, and the well was shut in at 1700 hours. Flow was resumed at 1930 hours at rates estimated at greater than 400 MCFD. At 0600 hours September 8, the well was shut in and the shut-in tubing pressure was 65 psi.

A modified isochronal test began at 1010 hours September 8. The first flow rate was selected to be between 125 and 135 MCFD. The surface flowing pressure was 5250 psi, which stabilized at 5230 psi after two hours. The second flow rate was 210 MCFD with a stable pressure of 5190 psi after two hours. The rate for the last period started at 310 MCFD, increasing to 420 MCFD after 1.5 hours. Figure 7.3 shows the average daily flow rate obtained from the Corcoran well test.

7.2.2 Corcoran Analysis

Interpretation of test results was difficult because the productivity of the well was found to be increasing with time. Figure 7.4 is a deliverability curve showing the estimated absolute open hole flow (AOF) for this zone to be 620 MCFD. Only two transient points were used to determine the type or mode of flow, laminar or turbulent. The slope of 1.0 between these two points indicated that the formation was producing in a laminar flow regime. However, as the productivity was continually increasing, the production mode was clearly subject to change.

During the early production period, September 2-8, the maximum flow rate achieved was 500 MCFD. Thus, the absolute open flow potential at that time would have been estimated at approximately 510 MCFD, and is below the value of 620 MCFD derived during the latter portion of the test. If the lower limit for deliverability is then assumed to be 620 MCFD, and if the entire 120 ft of perforations produced gas, an estimate of permeability for a homogeneous reservoir would be 30-60 μd. These results clearly indicate that production from this interval is not solely dependent on matrix permeability. It is most probably dominated by an extensive natural fracture system that greatly enhances the surface area of source rock that freely communicates with the wellbore and substantially increases production.

7.3 TRANSIENT PRESSURE TESTING AND ANALYSIS OF THE LOWER COZZETTE

One of the MWX program objectives was the experimental stimulation of the Upper Cozzette. In situ stress testing of the Upper and Lower Cozzette, as well as the intervening siltstone, indicated that a hydraulic fracture/stimulation initiated in the Upper Cozzette would probably extend downward and interconnect both the Upper and Lower Cozzette.[9] Thus, unless the production capacities of the Upper and Lower Cozzette were independently known prior to stimulation, the enhancing effects of the stimulation might never be fully understood due to the commingling of the two separate zones that would occur somewhere along the induced fracture. As a consequence, the Upper and Lower Cozzette were tested separately.

Well testing of the Lower Cozzette sandstone occurred in the MWX-1 perforated zone between 7940 and 7954 ft, which includes an 8-in. coal layer. The interval was perforated September 12 with 4 jet shots per foot. Figure 7.5 is a gamma-ray/neutron log showing the perforated Lower Cozzette interval. Note that only the apparent net pay of the lower sand interval was perforated.

A perforation breakdown was performed September 18. Fifty-eight rubber diverting balls were dropped and 65 bbl of 3 percent KCl water were injected before ball-out occurred. The measured surface ISIP was 3750 psi, but declined to 3400 psi after five minutes and remained unchanged for an additional 15 minutes. On September 19, the well was flowed at 100 MCFD with a surface pressure of 50 psi.

Figure 7.6 is a plot of the flow rate during the cleanup period. The bottomhole pressure during the last 100 hours was essentially constant at 600 psi, and it is evident from the increase in flow rate that the relative gas permeability was increasing during that period. Several swabbing runs were made over a 12-hour period on September 27 which produced approximately 20 barrels of gas-cut liquids. Then the well was shut-in for a bottomhole pressure buildup test on October 3. Figure 7.7 is a Horner plot of the pressure buildup data.[10] Several Horner slopes indicating various possible average reservoir permeabilities are superimposed on the data. These are primarily to aid in assessing the magnitude of the permeability as compared to the core data. Note that the value of 0.006 md fits the data during the latter part of the buildup.

On October 6, an additional flow test of the Lower Cozzette began. Figure 7.8 is a plot of the flow rates and bottomhole pressure vs time for this well test. A constant flow rate of approximately 95 MCFD was maintained between the second and sixth day, at which time the rate was increased to 150 MCFD for the remaining three days of drawdown. The upper portion of Figure 7.8 is a plot of bottomhole pressures obtained from a quartz pressure gauge during this drawdown period. Note that although the bottomhole pressure decreased from 4500 to 2200 psi during the rate change (95 to 150 MCFD), it then proceeded to increase for the last two days of constant gas production, thus indicating further enhancement in relative gas permeability.

The quartz pressure gauge was pulled for service on October 14, and a replacement was run in the hole in preparation for a buildup test. The well was shut in at 0800 hours on October 15. Figure 7.9 is a Horner plot of that bottomhole pressure buildup data. The Horner slope during the last usable 10 hours of bottomhole buildup pressure data yields an average gas permeability of 0.4 md, which is substantially in excess of the previously measured 0.006 md. The latter portion of the buildup is essentially unusable due to a small surface leak. The effects of the leak are observed on the Horner plot as a small pressure offset.

The CER/DOE tight gas reservoir model was utilized to history match both the drawdown and buildup periods where the average relative gas permeability was taken to be 0.4 md. A constant beta factor was used to account for the effects of nondarcy flow during the 95 MCFD flow period. A decrease in the nondarcy beta factor was then introduced during the transition to the 150 MCFD flow period to account for the apparent change in reservoir permeability that occurred during these two flow periods. The permeability or production capacity of the reservoir appeared to be flow-dependent, and therefore, using a variation in beta factor during the flow transition appeared warranted. Although additional stimulation and modeling could have been performed using the dual porosity or naturally fractured reservoir model, the continued increase in production capacity would have made such an effort no more reliable than assuming a homogeneous reservoir with an increased average permeability that would account for the existence of natural fractures. Neither the Horner plot nor linear flow analysis showed any sign that production into the well was occurring linearly, i.e., along one singular high permeability conduit such as a fault or fracture. Figure 7.10 is a composite graph showing the drawdown and buildup bottomhole pressure data along with the finalized version of the reservoir model. The basic values of reservoir parameters are given in Table 7.1. Note that the model data fit the measured values extremely well during both the drawdown and buildup periods.

Additional model runs confirmed a higher average reservoir permeability from buildup data than could be accounted for during the drawdown, and thus the permeability from drawdown data established the minimum average permeability. For instance, attempts were made to model the early production using a homogeneous reservoir with a gas permeability of 0.04 to 0.045 md. However, this value was inconsistent with the final buildup data and made a total history match impossible. Thus, it appears from these well tests and the analysis that the average reservoir gas permeability of the Lower Cozzette is about 0.4 md. If the gas permeability of the reservoir matrix is on the order of microdarcies, or less, as indicated by the core analysis, then these well testing results clearly indicate that the reservoir contains a significant number of natural fractures. The pressure signatures during well testing, however, do not indicate the presence of long singular fractures. This would imply that although the fractures need to be contiguous, they may be homogeneous in a macroscopic sense, thus giving the behavior of a system with a relatively high average permeability.

In conclusion, it can be seen that the very tight Lower Cozzette sandstone matrix acts as the source of gas and that the existence of a rather extensive interconnected system of natural fractures provides a high permeability conduit to transport gas from remote portions of the reservoir to the wellbore. The average relative gas permeability that best fits this scenario and the field data is 0.4 md. Furthermore, if the initial well test data, as shown in Figure 7.6 and 7.7, were all that was available for use in the analysis, then it would have been difficult to come close in estimating the real productive potential of this reservoir. The early test data showed a relative permeability of only 0.006 md and a maximum flow of about 75 MCFD. However, after further testing and clean up, the well was able to naturally produce significantly more gas, >150 MCFD, and indicated the much more permeable system of 0.4 md. This latter finding is clearly of significance to industry, particularly if the effects of a stimulation are derived from a ratio of production capacity before and after stimulation.

7.4 INTERFERENCE TESTING OF THE UPPER COZZETTE

7.4.1 Well and Reservoir History

Analysis of the Upper Cozzette cores revealed that the relative gas permeability of the sandstone matrix at in situ reservoir conditions was very tight, about 0.1 μd.

Substantial gas kicks during drilling and coring operations, however, indicated that the Cozzette might be capable of significant production rates. No indications of natural fracturing were noted during the field inspection of the core nor in subsequent laboratory analysis.

The mud weight during the initial penetration of the Cozzette was increased to about 14 lbs/gal which translates to a pressure gradient of 0.73 psi/ft. This is well above the normal gradient of 0.43 psi/ft and represents a substantially overpressured reservoir. Although the core analysis indicated a very tight matrix sandstone with no indication of fractures, the Cozzette at the MWX site was still considered a candidate for base case testing.

The 7-in. diameter casing in MWX-1 was perforated using 14 gm charges at a shot density of 2 shots per foot over the Cozzette interval 7855 to 7892 ft. The corresponding Cozzette interval in MWX-2 (123 ft away) was perforated in a similar manner. Both wells had 2-1/2-in. tubing set on a packer. Following several unsuccessful attempts to produce MWX-1 (including wireline swabbing), it was decided to perform a breakdown or small stimulation. The breakdown consisted of injecting 55 bbl of 2 percent KCl water at 3500 psi surface pumping pressure. As a result of the successful treatment, MWX-1 unloaded the tubing and began to produce.

Quartz bottomhole pressure gauges were run in MWX-1 and MWX-2, and to minimize the detrimental effects caused by wellbore storage, the pressure gauge in the observation well, MWX-2, was isolated from the bulk of the tubing (7800 ft) using the CER downhole shut-in tool. The pressure gauge is held in the tool seat using the high-pressure stress test pump that provides a positive pressure differential in the tubing and thus seals the bottomhole tool in place.

7.4.2 Interference Testing: Production Well--MWX-1

At the beginning of the interference test, MWX-1 was produced at a relatively constant flow rate of 320 MCFD. Figure 7.11 shows bottomhole pressure and production data from MWX-1 during this drawdown period. Following two days of drawdown, MWX-1 began to sporadically produce liquids, a portion of which was suspected to be oil base drilling fluid. After five days of production from MWX-1, pressure interference was clearly discernible in the MWX-2 observation well, and it was then decided to perform a series of pulse tests. The series of pulses in MWX-1 consisted of a 24-hour shut-in, 20 hours of production at 500 MCFD, 21 hours of shut-in, 18 hours of production at 600 MCFD, 39 hours of shut-in and a final production of 1100 MCFD for 24 hours. The resulting interference data as measured in MWX-2 will be discussed in the next section. The lower portion of Figure 7.11 shows the gas production history as measured from MWX-1 during the pulse tests.

It is clear that these high production rates (500, 600 and 1100 MCFD) cannot be attributed to production from the submicrodarcy sandstone matrix alone, but are most probably the result of an extensive natural fracture system. Neither log analysis, state-of-the-art core testing, nor the initial well testing revealed the enormous natural production capacity of this naturally fractured tight sandstone. Although a drill stem test (DST) was not performed at this particular interval during drilling, it probably would not have revealed the true nature of the reservoir.

A number of possible scenarios could be introduced to account for the inability, at least in early times, to readily distinguish this area of the Cozzette as a naturally fractured reservoir. For instance, the fracture spacing might be large compared to the diameter of the wellbore, and therefore the probability of penetrating a natural fracture would be low. Production from the reservoir would by necessity be throttled through the submicrodarcy matrix rock. Therefore, with no traces of fractures in the core nor a clear indication from logging that fractures existed, it would only lead to the conclusion that the system was as tight as the core analysis predicted, 0.0001 md. As a further example, damage to the natural fractures, the matrix or the combination could occur during the drilling or completion processes.

To explain the effects caused by damage to the fracture system, or reservoir, which were observed even during the relatively good production periods, it is necessary to compare data gathered early in the test with data obtained during the last period of pulses. Figure 7.12 shows the bottomhole pressure data acquired from MWX-1 along with the flow rate early in the test. Semilog analysis of this drawdown data yields an average permeability, $k_g = 75$ μd with a skin damage, $s = 2.6$. Similar data shown in Figure 7.13 were gathered during one of the last pulses and occurred approximately 10 days later and after over 3000 MCF of production. Semilog analysis of both the drawdown and buildup portions yields as average permeability, k_g = 225 μd and a skin, s = 0.04. Although the reservoir may be neither homogeneous nor producing in a radial model, the analysis indicates that in a relative sense, the system permeability has substantially increased.

None of the pressure buildup data, including some of extended 10-day periods, displayed slope changes that might indicate production from a dual porosity system. Thus, the analytic techniques of Warren and Root[11] and Kazemi[12] were not considered applicable in this case. Odeh[13] suggests that such behavior is not rare and cites field data to support a model where fractured reservoirs behave, on the average, as homogeneous systems.

7.4.3 Interference Testing: Observation Well--MWX 2

On the surface, the MWX-2 observation well is located 139 ft to the southwest of the MWX-1 production well. However, the subsurface depths of the top of the Cozzette sand in both MWX-1 and MWX-2 are 123 ft apart, as shown in Figure 7.1. Special analysis of the MWX-2 Cozzette cores showed good agreement with previous data from the MWX-1 core. That is, matrix relative gas permeabilities of about 0.1 μd or less at in situ reservoir conditions. Log and core derived water saturation and porosity values were also consistent between wells, as expected.

Figure 7.14 shows the downhole tool completion in MWX-2. Note that the pressure gauge becomes isolated within a small volume when the nipple and mandrel are seated.

As previously described, several pressure transients were introduced into the reservoir by alternately producing and shutting in MWX-1. The lower section of Figure 7.15 shows the flow rates as measured in the production well, MWX-1. The upper portion of Figure 7.15 displays the measured bottomhole pressure from MWX-2. Note that the amplitude of the corresponding pressure pulses at MWX-2 are only several psi, and that the corresponding time lag is about 2.5 hours.

To study the effects of selected relevant well, natural fracture, and reservoir parameters on this data set, several different analytic solutions[14] and numeric reservoir simulators were considered. One of the more appropriate methods for analyzing pressure interference data from anisotropic reservoirs was taken from Elkins and Skov.[15] The Elkins and Skov method assumes anisotropic permeability and considers that the pressure reduction caused by production of a well expands in elliptical form, with length/width varying as the square root of the ratio permeability along and at right angles to the fracture trend. The method allows calculation of fracture orientation by solving the equation,

$$P_i - P_{x,y} = -70.6 \frac{q\mu B}{\sqrt{k_x k_y}} \text{ Ei } -948 \frac{\phi\mu c}{t}\left[\frac{x^2}{k_x} + \frac{y^2}{k_y}\right] \qquad (1)$$

where:

P_i	=	initial pressure, psia
$P_{x,y}$	=	pressure at x, y at time, t, psi
q	=	production rate, MCFD
μ	=	viscosity of gas, cps
B	=	formation volume factor
t	=	time, hrs
c	=	compressibility of gas, 1/psi
ϕ	=	porosity
k_x	=	effective permeability in x direction, md
k_y	=	effective permeability in y direction, md
x	=	distance from producing well to observation well in x direction, ft
y	=	distance from producing well to observation well in y direction, ft

This equation is solved on a trial and error basis by assuming the permeabilities in the x and y directions until a "good match" between calculated and measured pressure is obtained. Note that the observation well effectively measures properties of the natural fracture system; it is unlikely that transients would be observed for the very tight matrix blocks.

The x and y directions for the anisotropic natural fracture permeabilities were taken to be parallel to the direction of maximum horizontal stress (N75°W) and the normal (S15°W) to that stress direction, respectively, as shown in Figure 7.1. The pressure drop measured in the observation well was 2.8 psi when the flow rate in the production well, MWX-1, was 600 MCFD and approximately 10 psi when 1100 MCFD was produced, as seen in Figure 7.15. A number of directional permeability values were tried in an attempt to find the best match to these data points. Although a range of anisotropic fracture permeabilities could be found that can provide acceptable pressure variations at the observation well, the best match occurred around the values of 120 md/0.4 md. It was therefore concluded that the ratio of k_x to k_y was large, about 100 to 400, and that the average natural fracture system permeability was about 7 md.

The CER/DOE tight gas reservoir model was used to study the relative effects and sensitivity of permeability, wellbore damage, boundaries, nondarcy flow and other reservoir and well parameters on the history match. Since the reservoir was found to be naturally fractured and producing anisotropically, this 3-D, single-phase model was run in cartesian coordinates. Appropriate well data were utilized at the corresponding block locations to simulate the wellbores of MWX-1 and MWX-2. At the areas of interest, the block sizes were made small to obtain good resolution. Figure 7.16 is a three-dimensional pictorial and Figure 7.17 is a plan view that describes the grid system and well locations used in the model to simulate the MWX Cozzette configuration.

Initially detailed in the simulator was a homogeneous reservoir varying only in permeability between computer runs. It is not surprising that a homogeneous reservoir system could not entirely history match the observation well, MWX-2, while still grossly satisfying the constraints imposed on pressure and flow rates at MWX-1. Nevertheless, it did provide a clear set of boundaries for certain parameters. Figure 7.18 is a composite graph of the simulated pressure response for the MWX-2 location with the variable being permeability. Homogeneous reservoir permeabilities shown are 100 μd, 200 μd, 300 μd, and 400 μd. In all cases, the amplitude of the pulse is about an order of magnitude larger than the measured data, and the transient time lag is excessive. (Refer to Figures 7.15 and 7.18.) It is evident from Figure 7.18 that, although a decrease in permeability will affect a decrease in the pressure pulse at MWX-2, that because the time lag is also directly dependent on permeability, a decrease in permeability would make the time lag further in error. Furthermore, in the case of the lowest permeability, 100 μd, the model showed that the production well was just barely able to sustain the required flow rates and thus using smaller permeabilities would obviously not meet the flow rate criteria imposed on MWX-1.

To decrease the amplitude of the pressure pulse at the observation well, MWX-2, while maintaining sufficient permeability to affect a transient time response in 2.5 hours, it was decided to try lowering the effective permeability around the observation well. This reduction in near-wellbore permeability was done in an effort to simulate either the effects of damage surrounding MWX-2 or the condition that the wellbore might not have a high conductivity path connecting it to the natural fracture network.

A number of variations were attempted, including different spatially reduced areas of permeability. In this set of scenarios, the entire reservoir permeability was maintained at 400 μd except for selected areas surrounding the MWX-2 wellbore where the permeability was reduced to the matrix value of about 0.4 μd. Figure 7.19 shows the results for only two of many cases of spatially reduced permeability simulations; the first has a radius of reduced permeability of 3 ft, while the radius for the second case was set equal to 11 ft. The nondamaged case is also shown as a reference. Reduction in pulse amplitude was achieved, but substantial time lag was introduced with larger reduced permeability areas. Thus, a reduced area of permeability may have existed around the observation well, but it was not totally responsible for the reduction in pulse amplitude that was observed.

To determine the sensitivity of directional or anisotropic permeability, the model values were varied in the x and y directions in a manner previously described. The larger value of reservoir permeability was taken to be in the direction of maximum horizontal stress, and the smaller value in a direction normal to the maximum horizontal stress (minimum horizontal stress). (Refer to Figure 7.1.) The results of several simulation runs are shown in Figure 7.20 and represent four different sets of anisotropic permeabilities, 80 md/400 μd, 20 md/400 μd, 4 md/400 μd and 1 md/400 μd. The homogeneous case 400 μd/400 μd is shown as a reference. The pulse amplitudes for the cases above 20 md/400 μd are in the range of the observed field data, and thus the ratio of the normal values of permeabilities is again seen to be large.

Additional simulation runs were performed to study the effects of no-flow boundaries or loss of natural fracture permeability within the reservoir. Only the largest of the directional permeability cases, 80 md/400 μd and 40 md/400 μd, were considered. The results showed that when boundaries of 1000 ft or larger were included, no perceptible changes in the transient pressure pulses at the observation well would occur, and, therefore, the area of the Cozzette that contains natural fractures that communicate with the MWX-1 wellbore probably extends at least a distance of 1000 ft.

The final investigation of fracture criteria and matrix values was performed using a modified version of a dual porosity model developed for the DOE Morgantown Energy Technology Center (METC). The model, "SUGARMD," is a 2-dimensional, 2-porosity, single-phase cartesian coordinate reservoir simulator.[16] Flow into the well occurs through the fracture network while the matrix or source rock acts as a uniformly distributed gas source that feeds the fractures. In this study an unsteady state option was involved in which a radial simulation is performed to solve for the pressure distribution within the matrix elements. The bulk of this effort was concentrated on matching the pressure data taken during the pulse testing. Transients introduced by prior production were replicated by the superposition of a general 1-psi-per-day reservoir rise. Although a wide range of fracture spacing was evaluated, there is evidence from outcrop studies to suggest a spacing of about 20 feet. Therefore, the emphasis was placed on 20-ft spacing throughout most of this analysis.

A wide range of anisotropic natural fracture permeabilities was investigated. However, the matrix permeability was confined to the values derived from the core analyses (0.1 μd). A good match was found for anisotropic fracture permeabilities of 100 md/100 μd with a matrix permeability of 0.1 μd. Figure 7.21 is a composite of this simulated data and the observed field data.

7.4.4 Pipeline Production

Following the interference test, MWX-1 was connected to the local pipeline gathering system. Sporadic production into the pipeline occurred between March and June, 1983. During this period, the average gas production rate was about 550 MCFD, and the cumulative volume of gas produced amounted to about 35 MMSCF. Figure 7.22 details the MWX-1 monthly production performance into the pipeline and flared testing periods. Surface pressure measurements made during this production period did not indicate that the reservoir had reached a boundary, and thus revealed that the areal extent of the natural fractures was considerable.

7.4.5 Post-Production Testing of the Upper Cozzette

Post-production reservoir testing of the Upper Cozzette included two relatively short tests that were conducted during May and June, 1983. These tests were performed following sustained winter production into the sales pipeline that included gas production in excess of 30 MMCF. The test objective was to provide additional data that could be compared with the information previously obtained during the Upper Cozzette interference tests conducted in the fall of 1982 as a means of assessing the impact this substantial gas production may have had on reservoir production capacity.

The first test in this series involved an attempt to observe the pressure transients in MWX-2 from production and pulses initiated in MWX-1. A packer leak in the observation well, however, obscured the pressure transients and thus analyzable interference data were not obtained. Bottomhole pressure buildup data were recorded from the production well, MWX-1, and subsequently analyzed.

The second test provided excellent bottomhole pressure data from MWX-1. The analysis of these data, combined with the results of the fall 1982 buildup test, provided clear evidence that a significant increase in relative gas permeability had occurred between the test period of 1982 and this test in 1983. This permeability increase is most probably the result of dewatering of the matrix, natural fractures, or both, and/or a general reduction in skin.

The first test in this series, conducted in early May 1983, included an interference test that was hampered by sporadic pressure fluctuations in the observation well. The source of these spurious signals was found to be the result of fluid leaks within the bottomhole packers. Following several unsuccessful attempts to stop fluid communication between the bottomhole and the wellbore annulus of the observation well, MWX-2, further efforts to observe interference were terminated and the production well was returned to the sales pipeline.

A second test was initiated during mid-June, and once again, small pressure perturbations in the observation well obscured the pressure transients occurring within the reservoir. MWX-1 was shut-in on June 25 to acquire bottomhole pressure buildup data.

Figure 7.23 is a Horner plot of the resultant data. The calculated relative gas permeability, k_g, was 382 μd and represents an increase of about 70 percent over the value of 225 μd derived during the fall/winter testing period of 1982; again, the trend of continued cleanup with production is observed.

Data gathered during the buildup of the production well provided valuable information concerning the relative changes that occurred during the course of winter pipeline production. This information showed that the reservoir gas production capacity had increased and that there was no indication of the presence of boundaries or a decrease in the ability of the natural fracture system to provide gas from distant locations within the reservoir to the wellbore. These data are significant in general and of great importance to producers within this basin and other tight gas sand areas whose production is dominated by the existence of natural fractures.

7.4.6 Summary of Upper Cozzette Interference Testing

Analysis of the blanket marine Cozzette sandstone at the DOE MWX site incorporated test data from logging, core analyses, geologic and sedimentologic assessments and well testing.

Although detailed laboratory core analysis indicated the matrix permeability at in situ reservoir conditions to be very tight, about 0.1 μd, well testing and pipeline production data from MWX-1 showed that the Cozzette was capable of sustained productive rates that require a minimum system permeability of 200 to 400 μd. This evidence implies an enhanced mode of production which, for this case, was taken to be the result of production through a rather extensive natural fracture network. Wellbore damage around the production well, MWX-1, was evident early in the test but diminished considerably in about 10 days. Continual production increases suggest that well cleanup continues for long periods, perhaps months, and significantly improves well production.

Analysis of pressure interference data from the observation well, MWX-2, revealed that the reservoir's natural fracture permeability was considerably anisotropic. This suggests that the distribution of natural fractures provides asymmetric conductivity paths to the production well which would result in an elliptical pressure distribution surrounding the production well.

The composite effects on the pressure disturbances at MWX-2 that would result from variations in fracture permeability, wellbore damage, nearby boundaries and other phenomena were simulated using reservoir models. The results of this modeling sensitivity analysis suggest the following scenario for the Cozzette at MWX:

- A natural fracture system with an average permeability of 7 md, a large permeability ratio (>100:1), aligned in the maximum stress direction, within a very tight sandstone matrix.

- Good pressure communication between the observation well and the naturally fractured reservoir, i.e., not much damage surrounding the well.

- Large areal extent of the fracture system with no apparent boundaries closer than 1000 ft.

These results also show that stimulation techniques, including a propped hydraulic fracture, would have little, if any, effect on enhancing production and may be counterproductive.

7.5 MARINE WELL TESTING AND ANALYSIS CONCLUSIONS

An extensive research-oriented field and laboratory investigation was conducted in the marine blanket sandstones at the MWX site. The results of this investigation provide a number of significant conclusions that can be applied both to this specific location and to other fractured tight marine sandstones in general. The conclusions are:

- Unstimulated production rates from very tight matrix sandstones of approximately 0.1 μd can be substantial, providing there exists an extensive, interconnected natural fracture system that is connected to the well.

- Damage surrounding the wellbore, principally in the natural fractures, can mask the productive capacity of highly overpressured reservoirs such as those found at MWX.

- Average values for reservoir permeability obtained from the MWX-1 production well (200 to 400 μd) do not reveal the severe anisotropy of the natural fracture system or its high flow capacity.

- Well test data from the production well may indicate conventional production history and not exhibit, as some[11,12] would suggest, a slope change on a semilog plot that might result from a dual porosity system.

- Continued cleanup of these zones suggests prefrac testing be extended and carefully monitored and analyzed before considering any stimulation techniques.

One of the most significant elements of this DOE-sponsored experiment is the assemblage and distribution of a rather large and comprehensive set of geologic, geophysical, and well test data that ultimately becomes public information.

7.6 REFERENCES

1. Lorenz, J. C., "Sedimentology of the Mesaverde Formation at Rifle Gap, Colorado and Implications for Gas-Bearing Intervals in the Subsurface," Sandia Report, SAND82-0604, March 1982.

2. Heinze, David M., "Mineralogy and Petrology Aspects of the Mesaverde Formation at Rifle Gap, Colorado, Specific to the Sedimentology and Gas-Bearing Intervals in the Subsurface," Sandia Report, SAND83-0287, March 1983.

3. Kukal, G. C., "Log Analysis of the Corcoran/Cozzette Sandstone," Report by CER Corporation, for Sandia National Laboratories, October 1984.

4. Randolph, P. L., "Porosity and Permeability of Mesaverde Sandstone Core from the DOE Multi-Well Experiment," SPE Preprint 11765, 1983 SPE/DOE Symposium on Low Permeability Gas Reservoirs, Denver, Colorado, March 14-16, 1983.

5. Submittal of the Special Core Analysis Study for Sandia National Laboratories from Core Laboratories, Inc., Document Number 61-4863, 1983.

6. Verbeek, E. R. and Grout, M. A., "Fracture Studies in Cretaceous and Paleocene Strata in and Around the Piceance Basin, Colorado: Preliminary Results and Their Bearing on a Fracture Controlled Natural-Gas Reservoir at the MWX Site," Draft Copy, USGS, Denver, Colorado, 1984.

7. Clark, J. A.: "The Prediction of Hydraulic Fracture Azimuth through Geological, Core and Analytical Studies," SPE/DOE 11611, 1983 SPE/DOE Low Permeability Symposium, Denver, Colorado, March 14-16, 1983.

8. "Multi-Well Experiment Differential Strain Curve Analysis on MWX-1 Cores," The Dowell Rock Mechanics Research Laboratory, August 1982.

9. Warpinski, N. R., et al, "In Situ Stress Measurements at DOE's Multi-Well Experiment Site, Mesaverde Group, Rifle, Colorado," SPE/DOE 12142, 58th Annual Technical Conference and Exhibition, San Francisco, California, October 5-8, 1983.

10. Matthews, C. S. and Russell, D. G., "Pressure Buildup and Flow Tests in Wells," SPE Monograph, Volume 1, 1967.

11. Warren, J. E. and Root, P.J., "The Behavior of Naturally Fractured Reservoirs," Soc. Pet. Eng. J., September 1963, pp. 245-255.

12. Kazemi, H., "Pressure Transient Analysis of Naturally Fractured Reservoirs with Uniform Fracture Distribution," Soc. Pet. Eng. J., December 1969, pp. 451-462.

13. Odeh, A. S., "Unsteady State Behavior of Naturally Fractured Reservoirs," Soc. Pet. Eng. J., March 1965, pp. 60-66.

14. Earlougher, R. C. Jr., "Advance in Well Test Analysis," Monograph Series, Society of Petroleum Engineers of AIME, Dallas, Vol. 5, 1977.

15. Elkins, L. F. and Skov, A. M.: "Determination of Fracture Orientation from Pressure Interference," Trans. AIME, 1960, 219, 301-304.

16. Science Applications, Inc., "Simulator for Unconventional Gas Resources Multidimensional Model 'SUGAR-MD'," Volumes I and II, DOE/MC/08216-1440, September 1983.

Table 7.1

Base Set of Reservoir and Well Parameters Derived from Log, Core, Sedimentological and Other Data that were used as Initial Values in History Matching the Cozzette

Formation Height, h		30 feet
Formation Porosity, ϕ		6.9%
Formation Water Saturation, S_w		40%
Reservoir Temperature, T		230°F
Gas Viscosity, μ		0.018 cp
Initial Reservoir Pressure, P_i		6,300 psi
Dry Klinkenberg Permeability, k		1.0 μd
In Situ Klinkenberg Permeability, k_g		0.08 μd
Wellbore Radius, r_w		3.5 in.
Perforated Intervals	MWX-1	7855-7892 ft
	MWX-2	7830-7840 ft
		7850-7860 ft
		7874-7884 ft
Tubing Length	MWX-1	7820 ft
	MWX-2	7820 ft

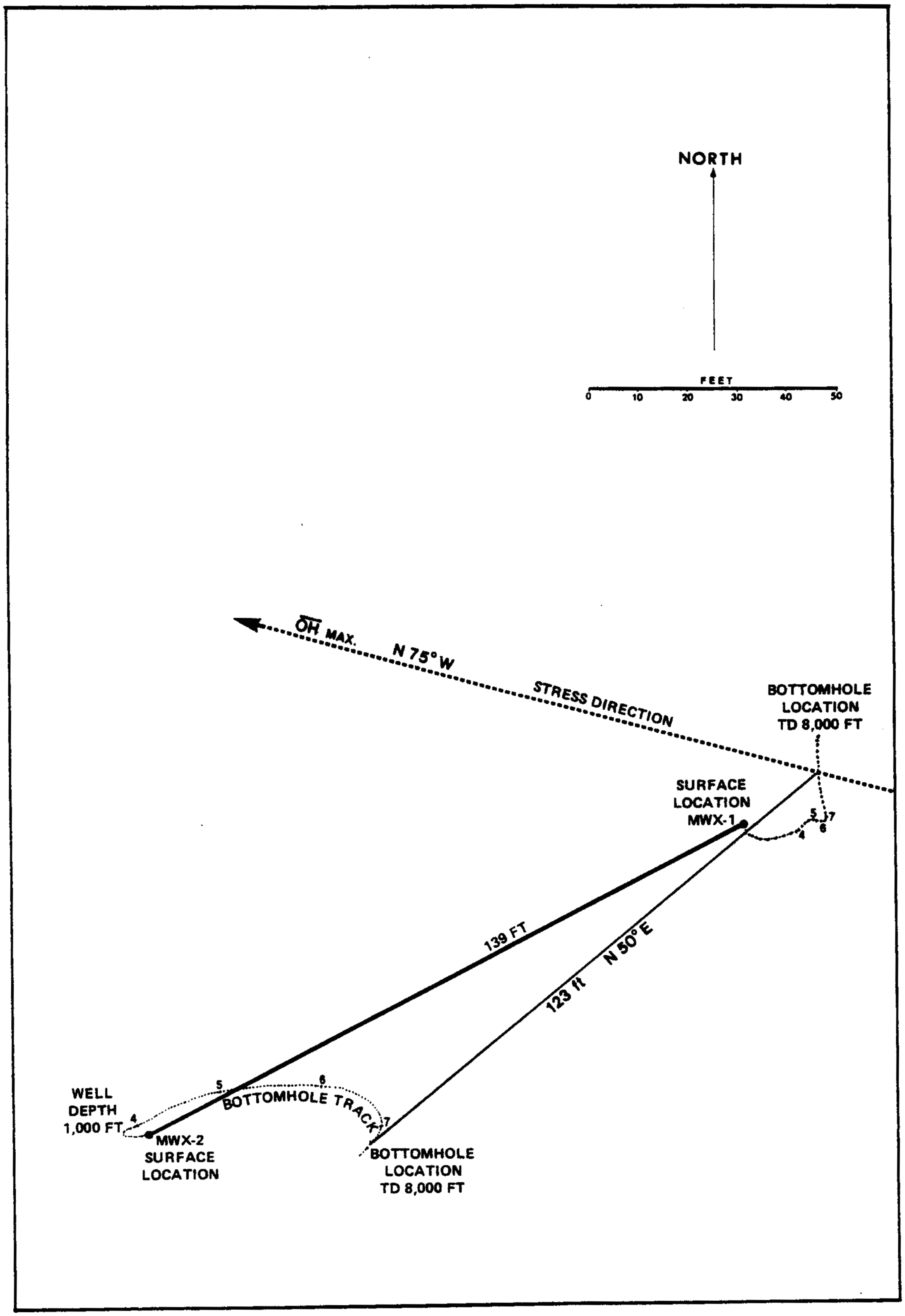

Fig. 7.1 Relative Surface and Subsurface Location of the MWX Wells, Showing Distance Between Wells 1 and 2 at the Cozzette Depth Along with the Derived Direction of Maximum Horizontal In Situ Stress

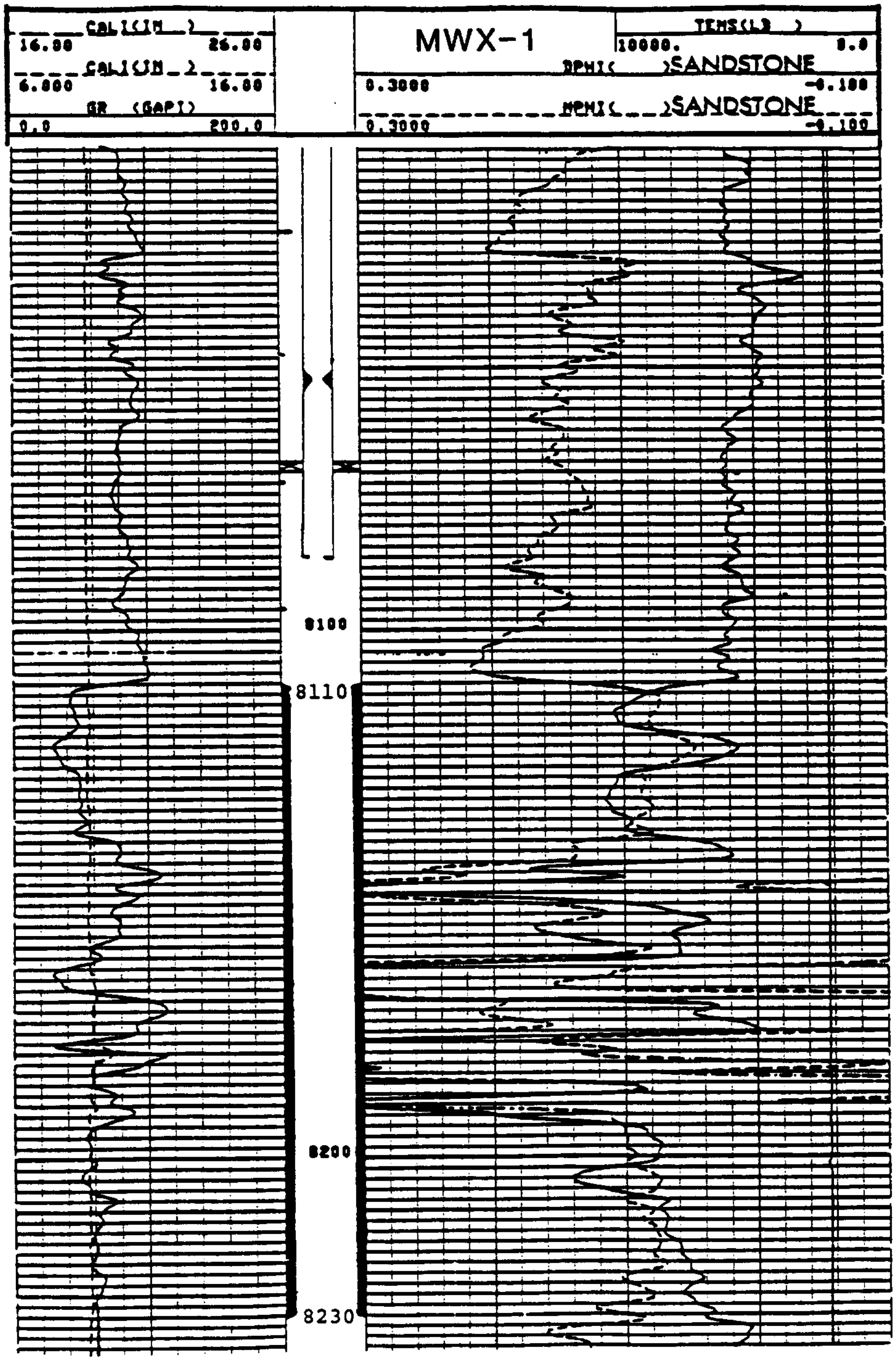

Fig. 7.2 MWX-1 Well Completion for Testing Corcoran Sand

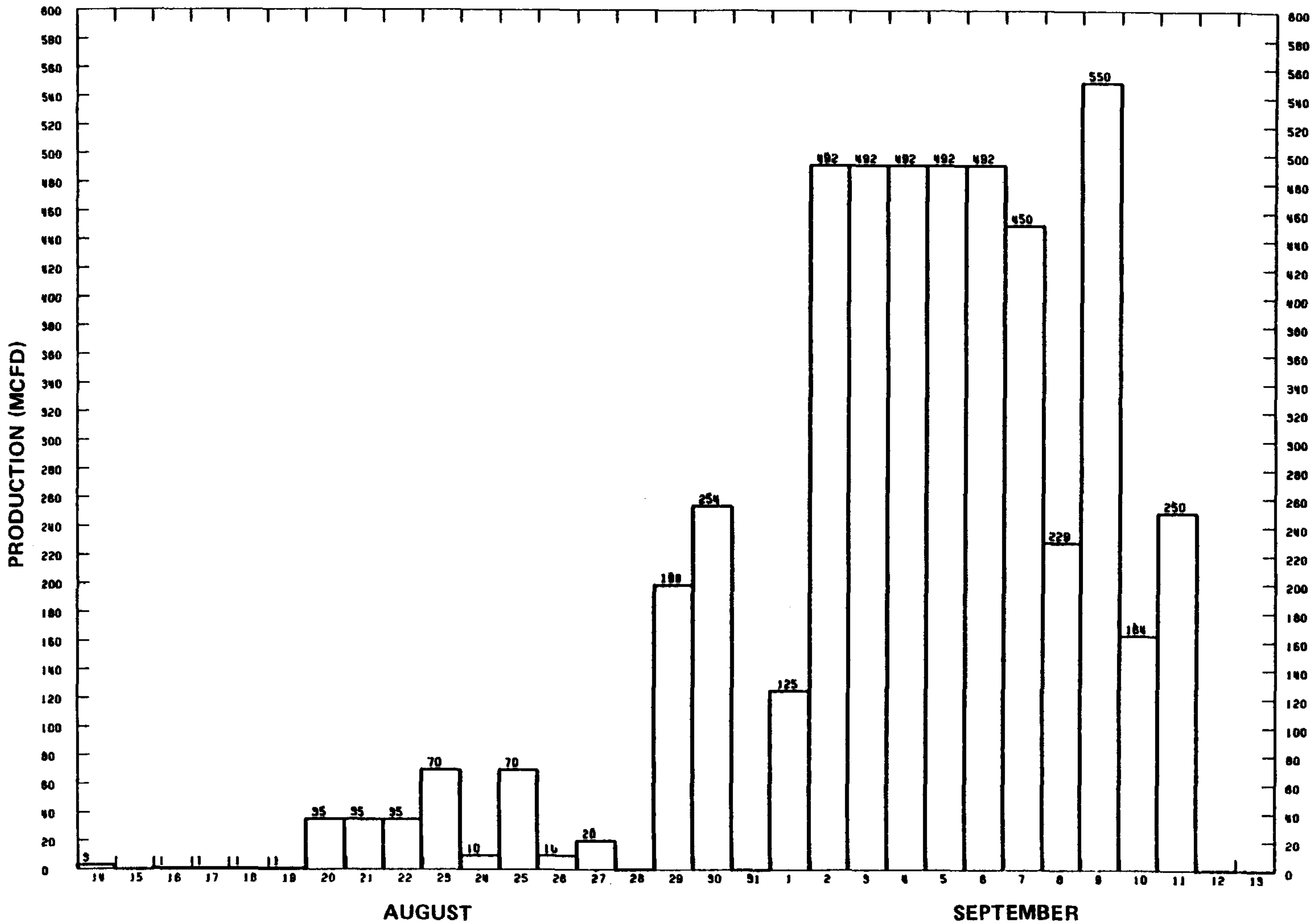

Fig. 7.3 Average Daily Flow Rate for the Corcoran Well Test

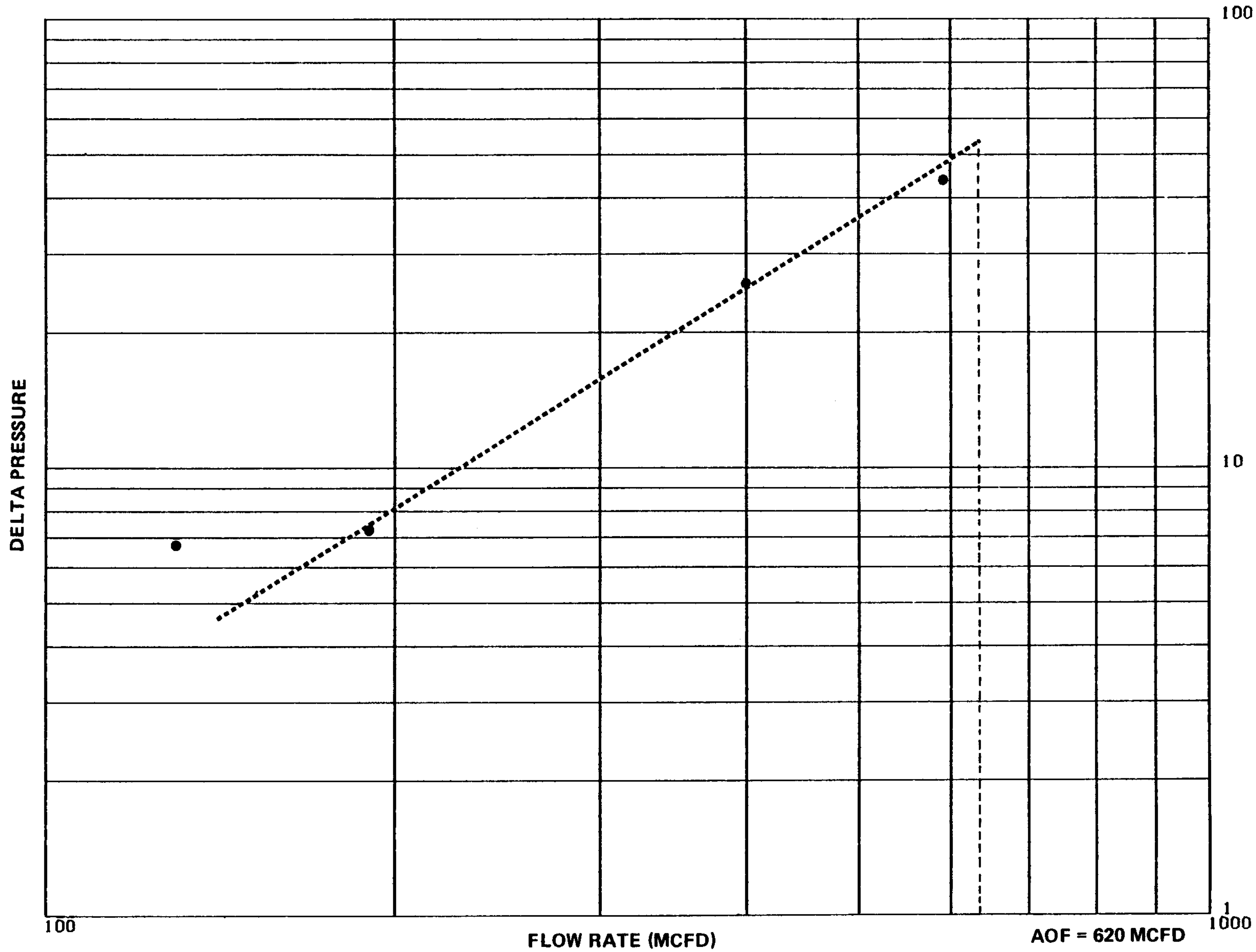

Fig. 7.4 Deliverability Curve from a Modified Isocronal Test of the Corcoran Sandstone

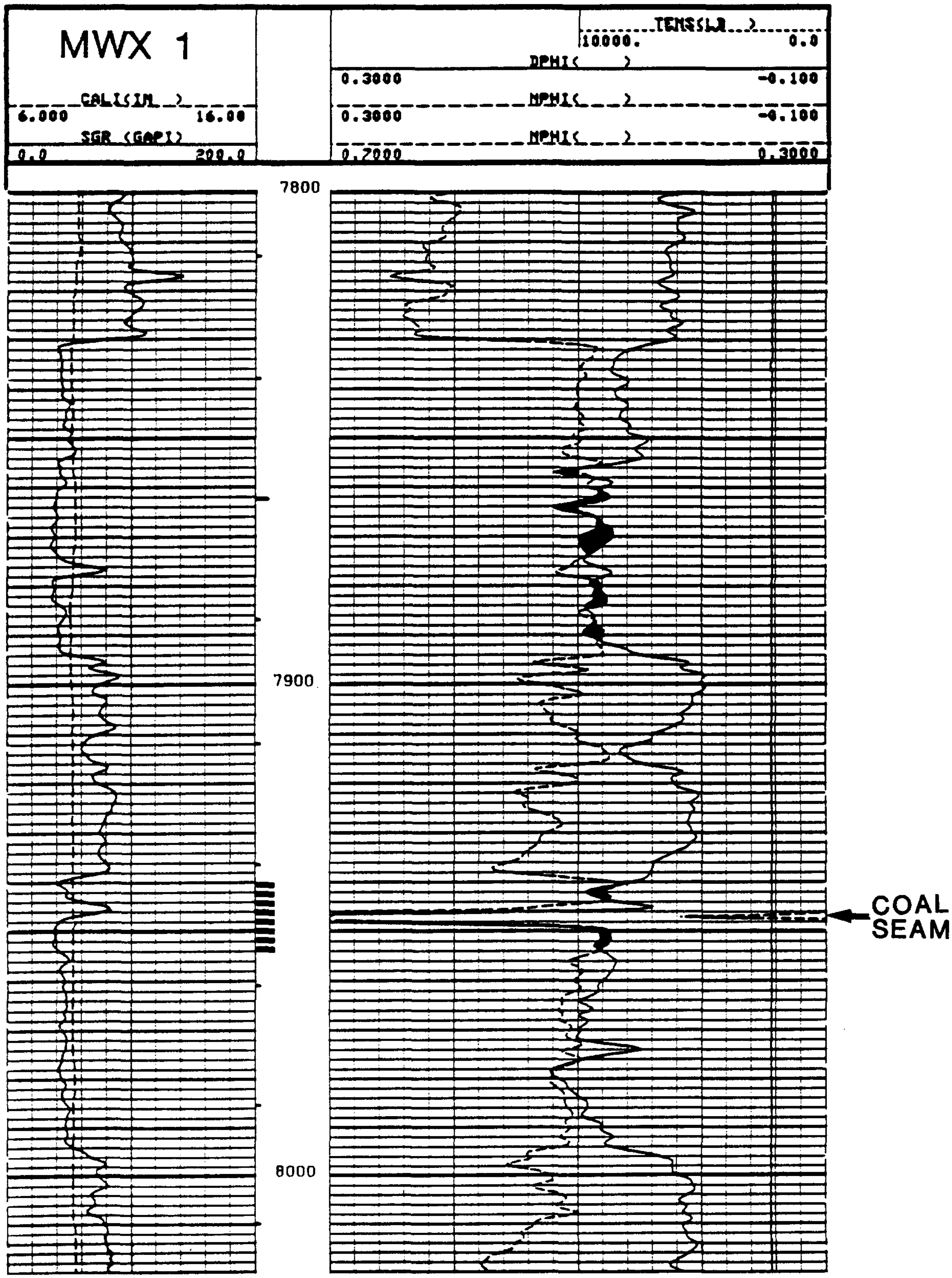

Fig. 7.5 Gamma Ray/Neutron Log Showing Location of the Perforated Interval of Lower Cozzette in MWX-1

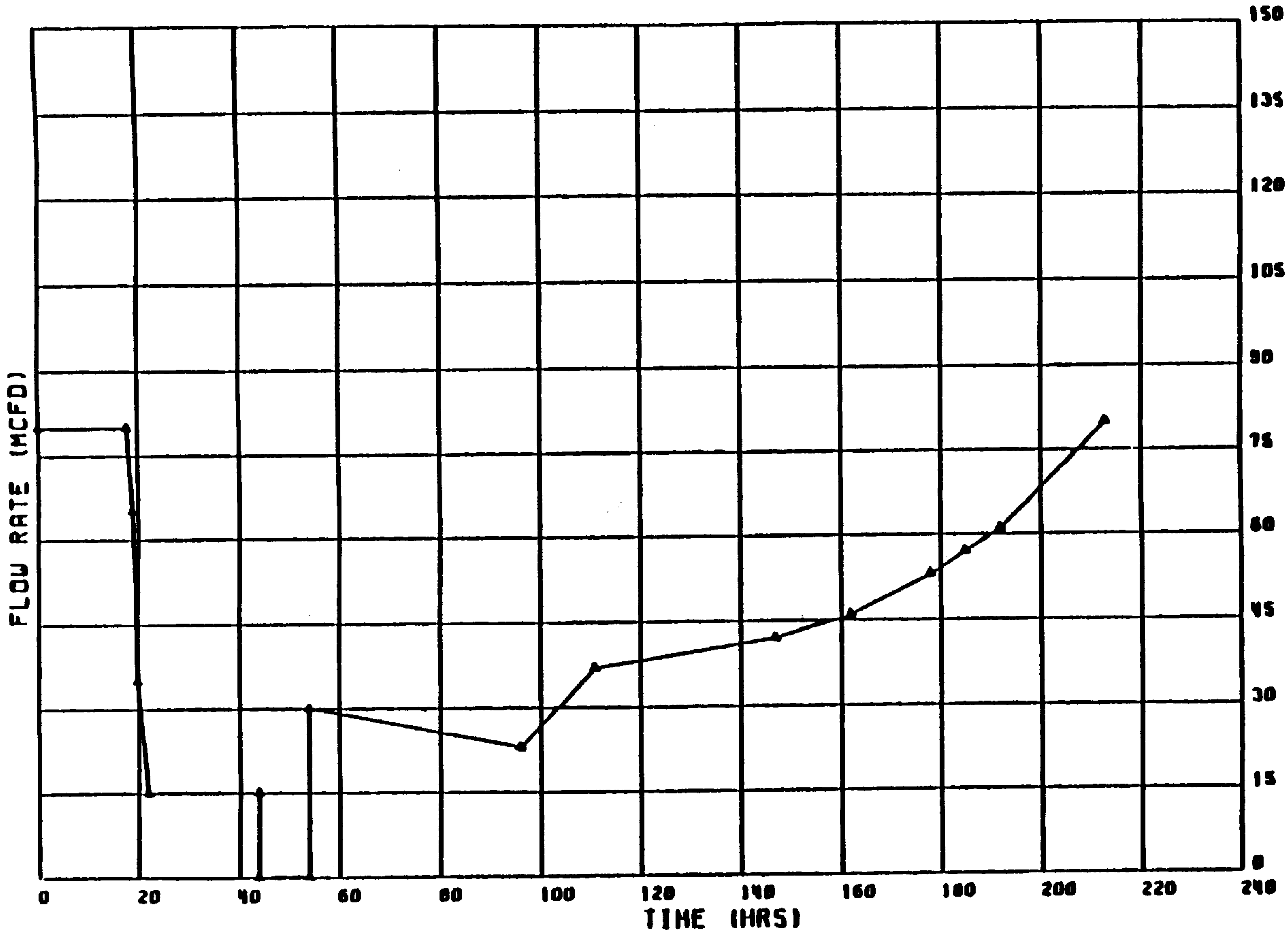

Fig. 7.6 Flow Rate from the Lower Cozzette During Cleanup Period, Sept. 24-Oct. 3, 1982

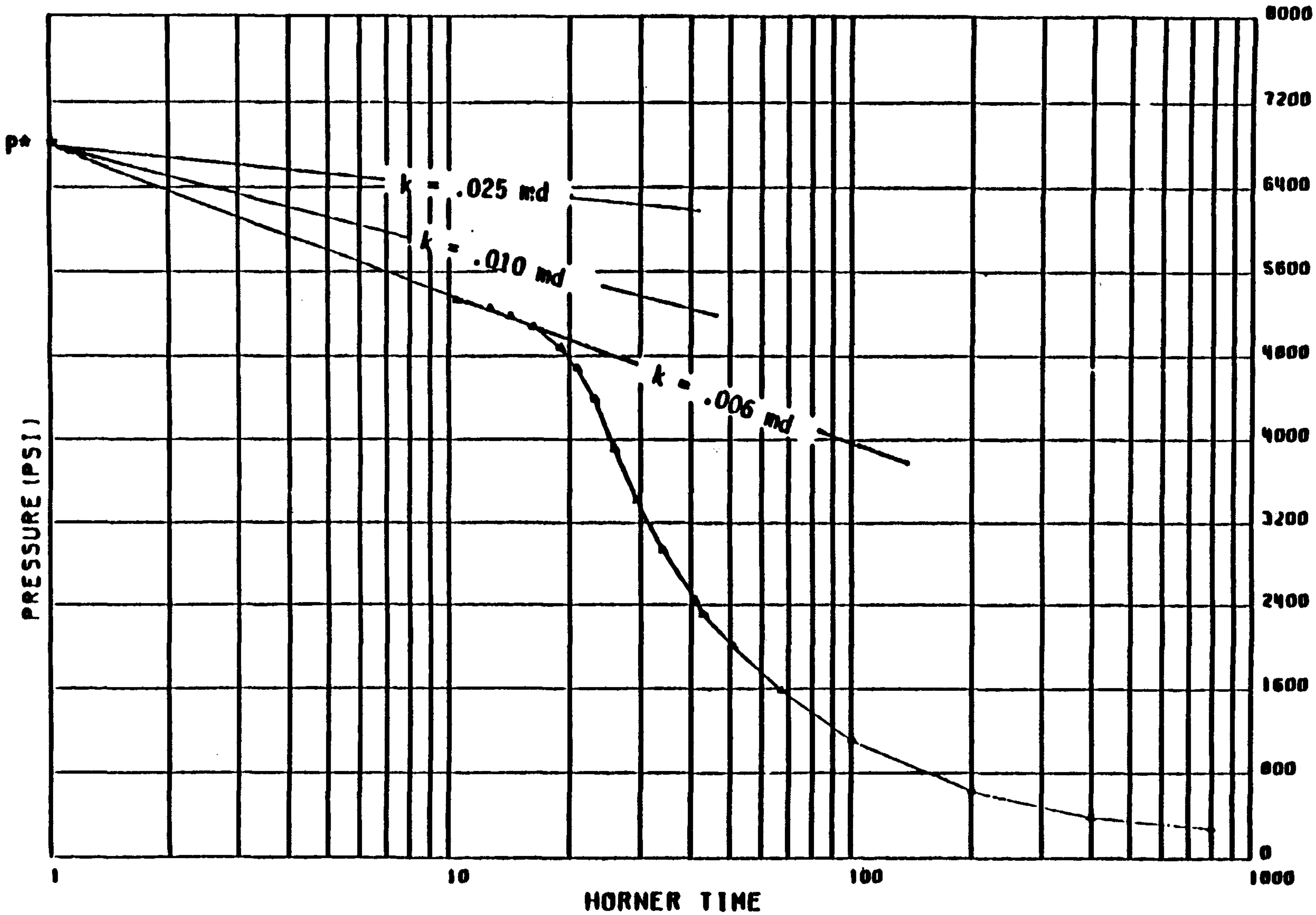

Fig. 7.7 Bottomhole Pressure Buildup Data Following Cleanup, Oct. 3-4, 1982 (note several Horner Slopes indicating potential value of permeability for a P* = 6,800 psi)

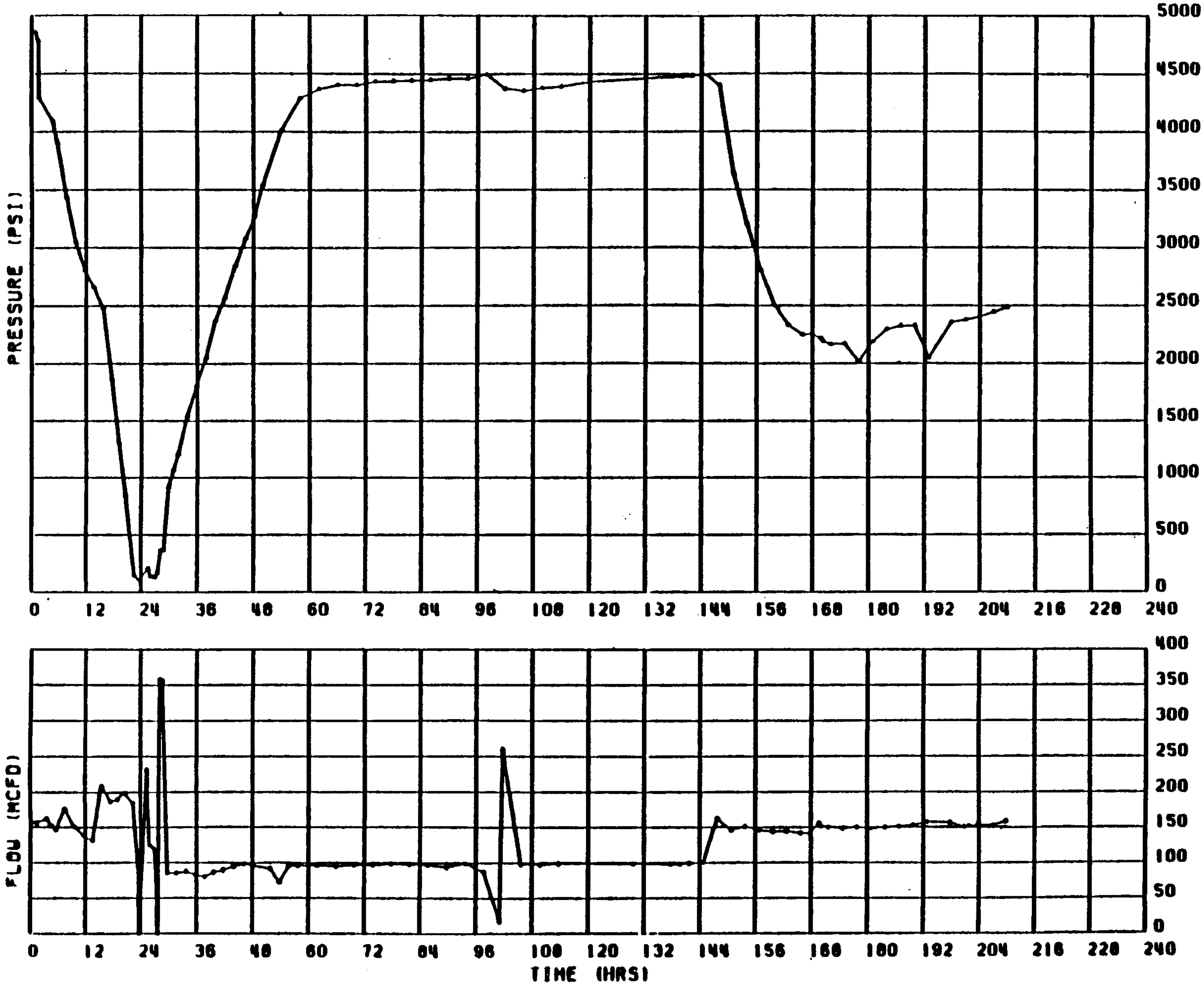

Fig. 7.8 Bottomhole Pressure and Flow Rates During Testing of the Lower Cozzette, Oct. 6-15, 1982

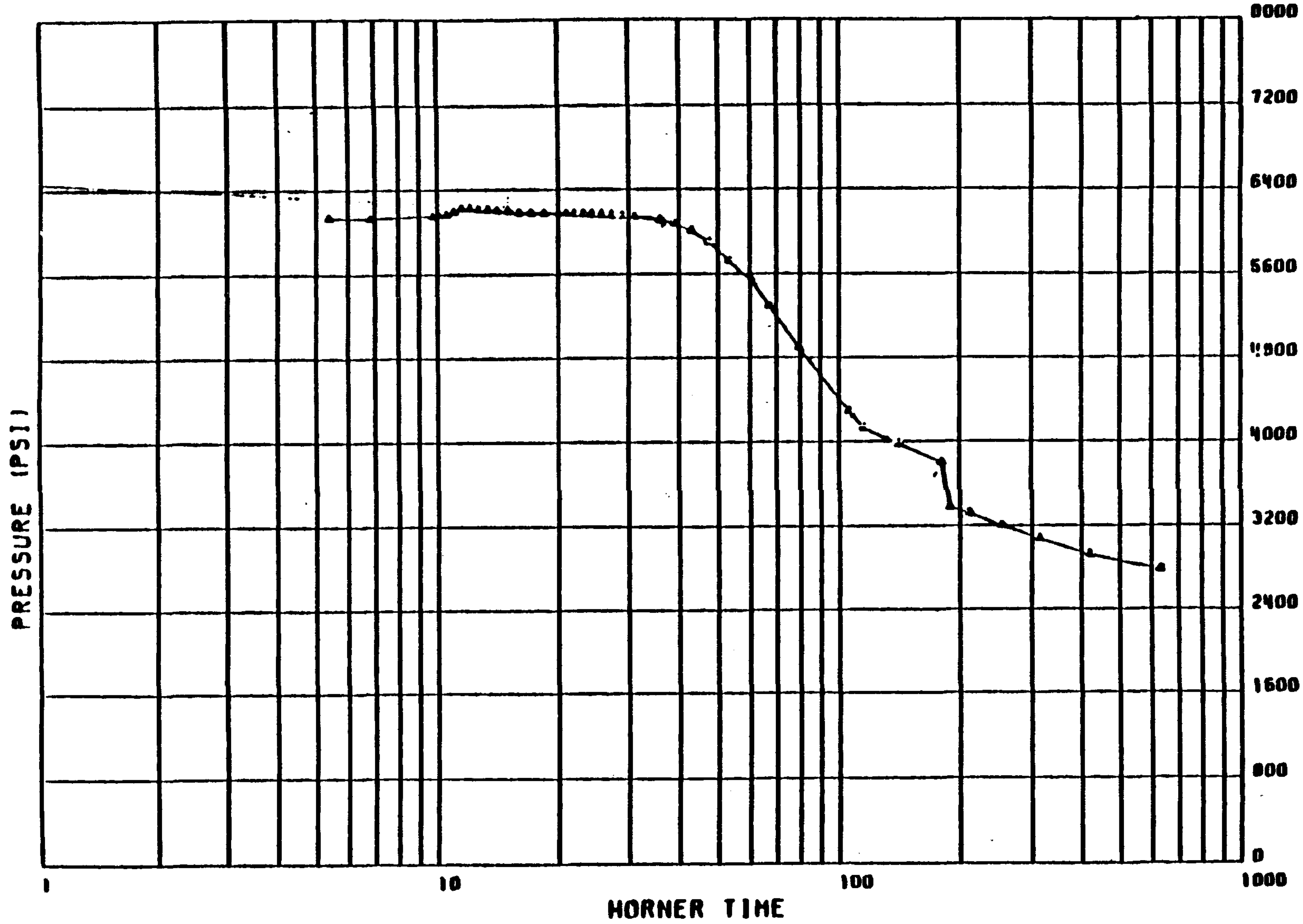

Fig. 7.9 Horner Plot of Bottomhole Pressure Data for the Final Buildup in the Lower Cozzette, Oct. 15-16, 1982

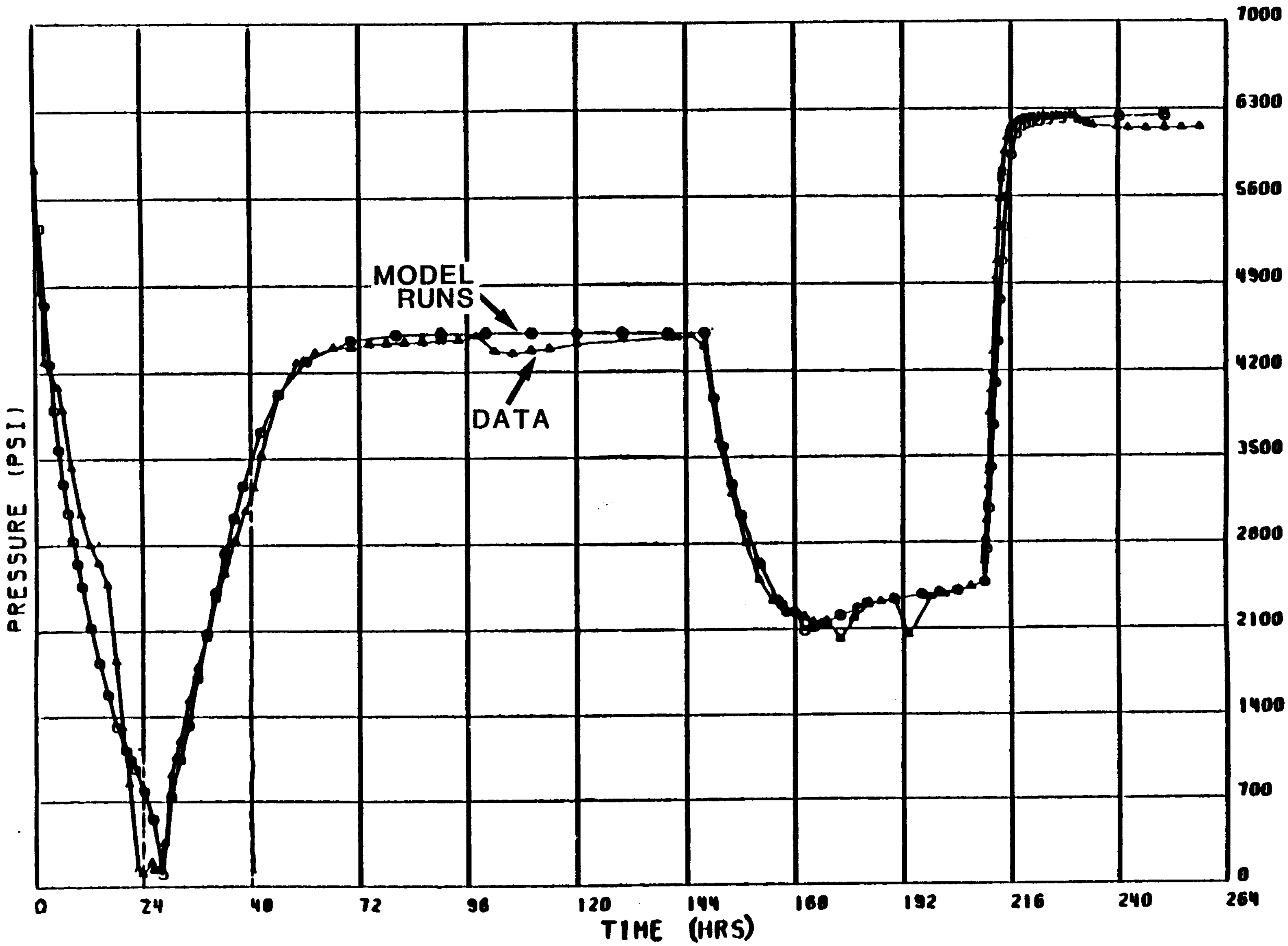

Fig. 7.10 Bottomhole Pressure Data and Reservoir Model Simulated Data for the Lower Cozzette Tests

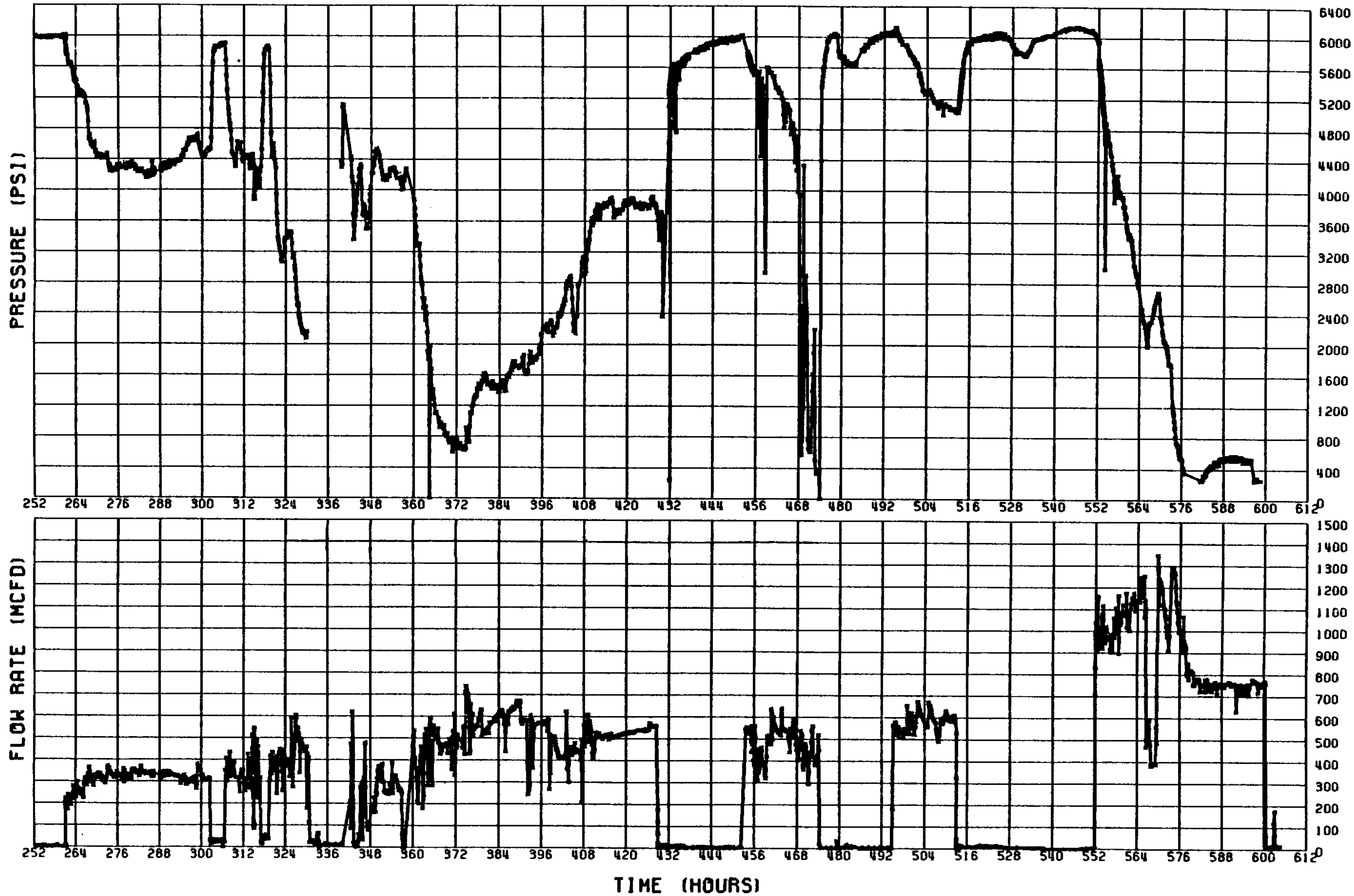

Fig. 7.11 MWX-1 Pressure and Flow Rate Measurements During the Testing of the Upper Cozzette Beginning Nov. 29, 1982

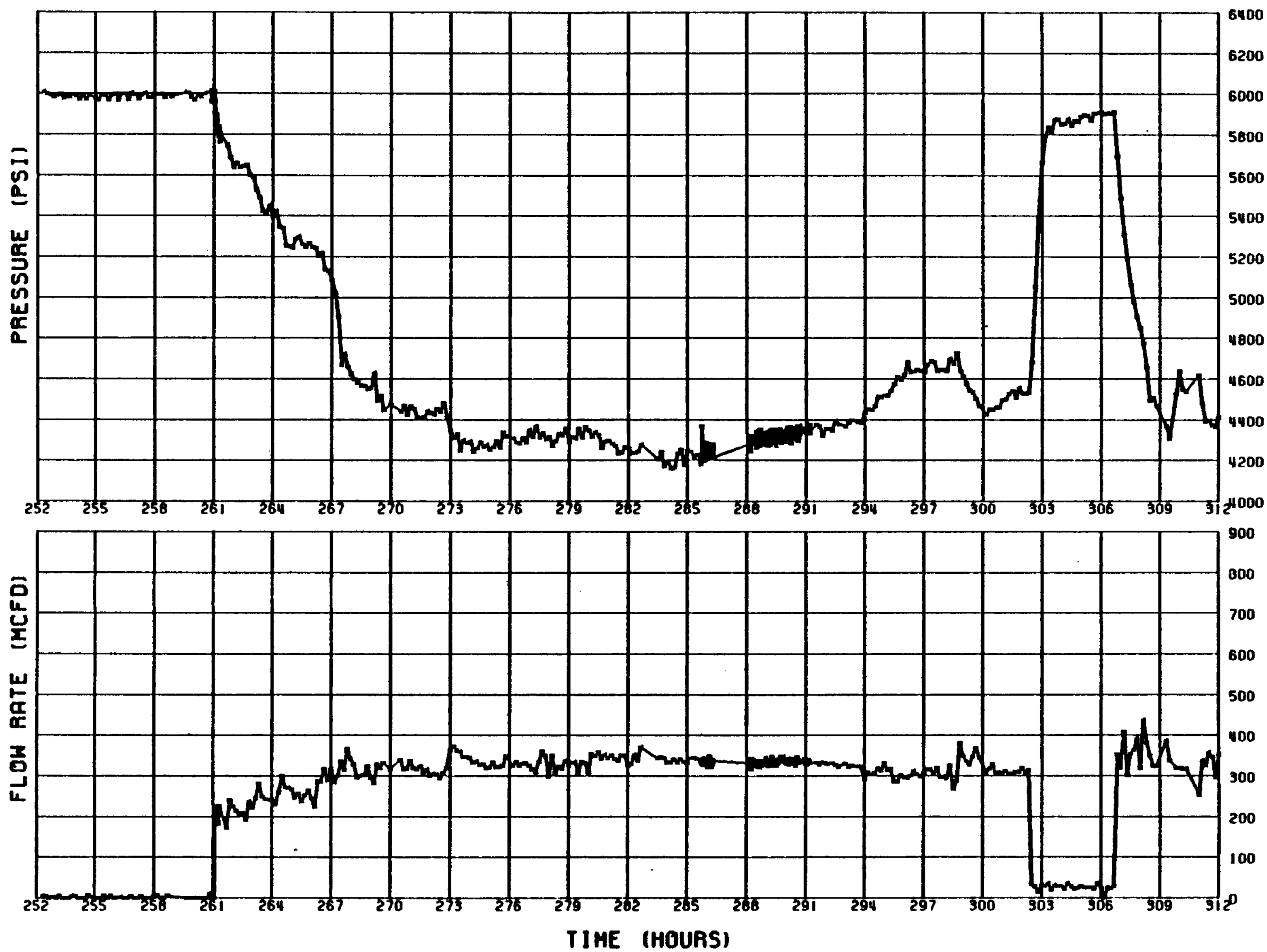

Fig. 7.12 Early Time Gas Production Rate and Bottomhole Pressure from MWX-1 Interference Test of the Cozzette Sandstone

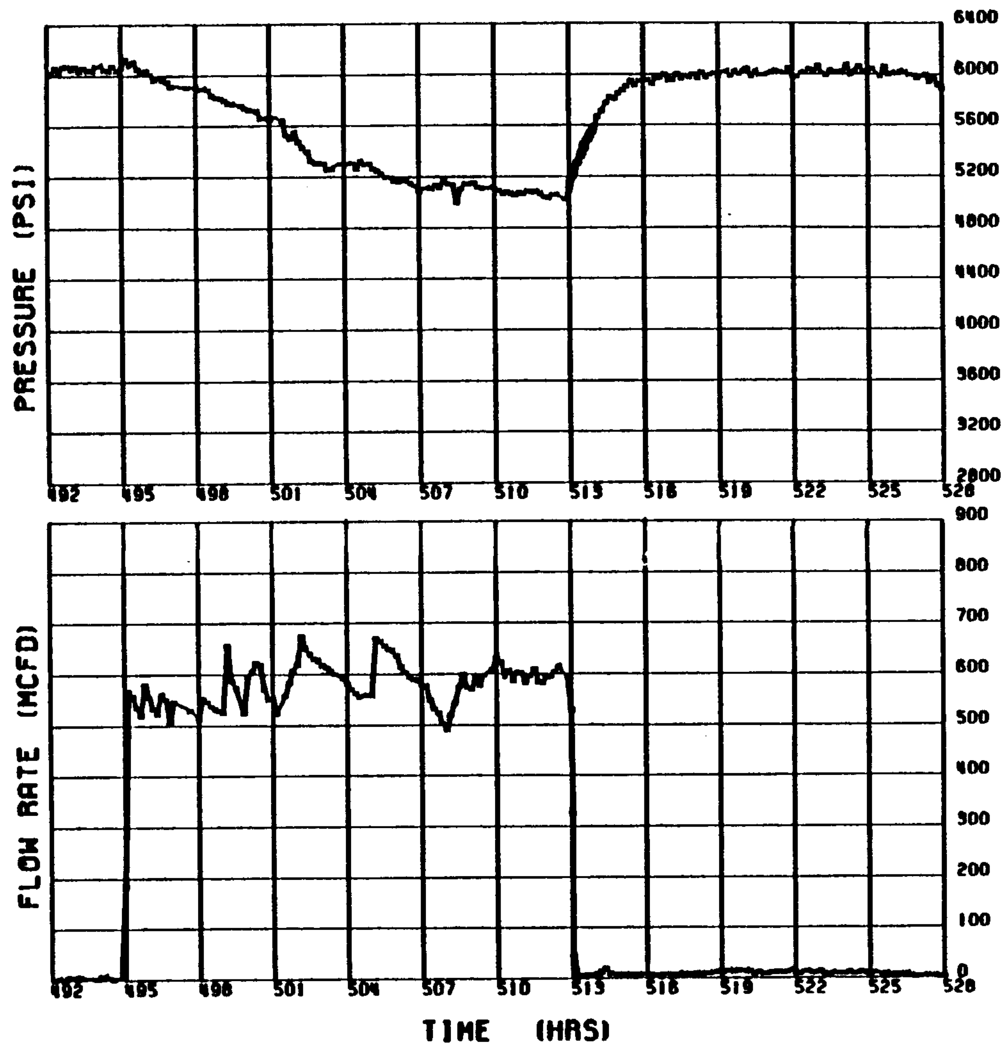

Fig. 7.13 Pressure History and Production Flow Rate at MWX-1 During the Second Pulse in the Interference Test of the Cozzette

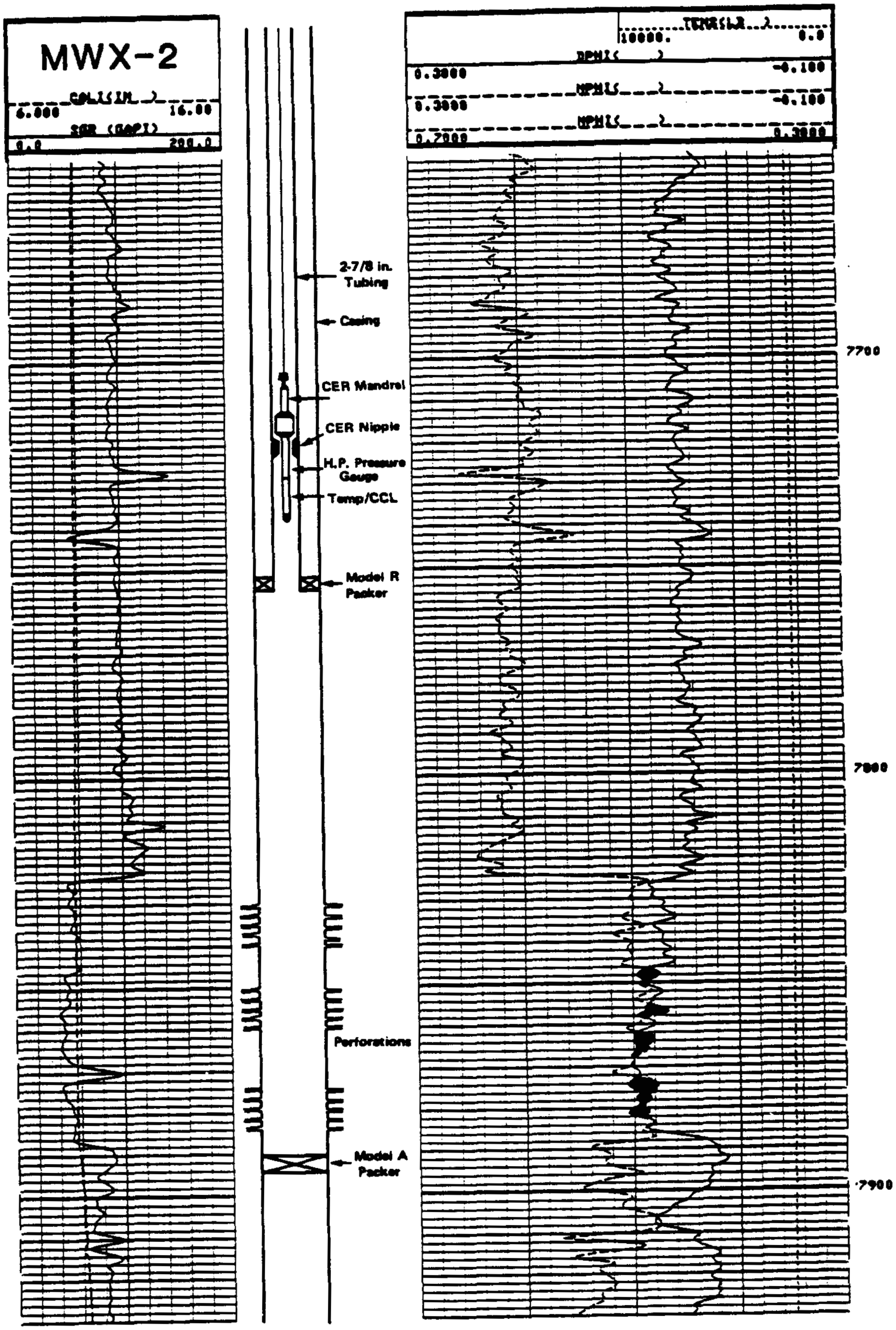

Fig. 7.14 Bottomhole Tool Configuration in the Observation Well, MWX-2 During Interference Testing of the Upper Cozzette

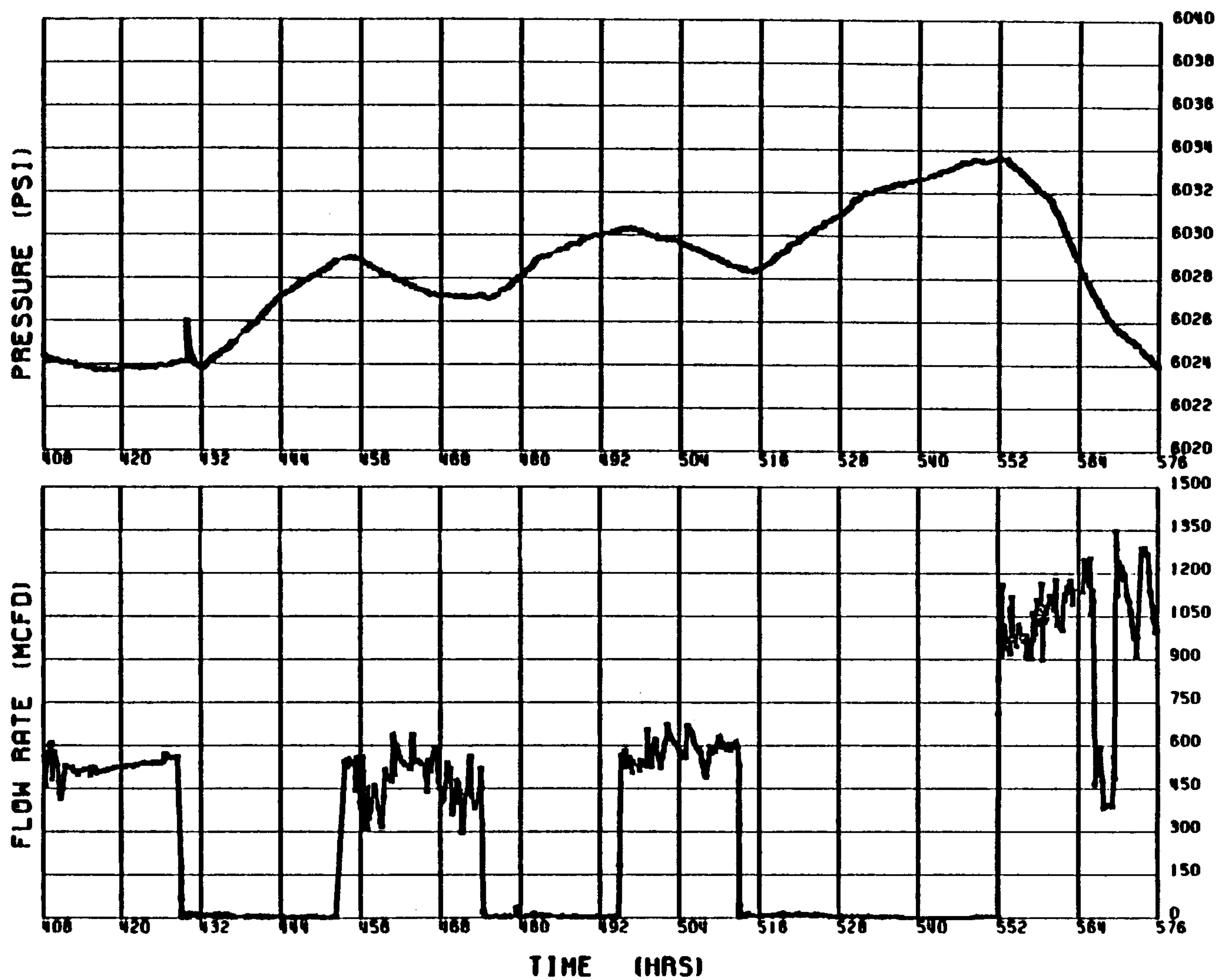

Fig. 7.15 Pressure History at MWX-2 and Production Flow Rates at MWX-1 for the Pulsing Period of Interference Testing of the Cozzette

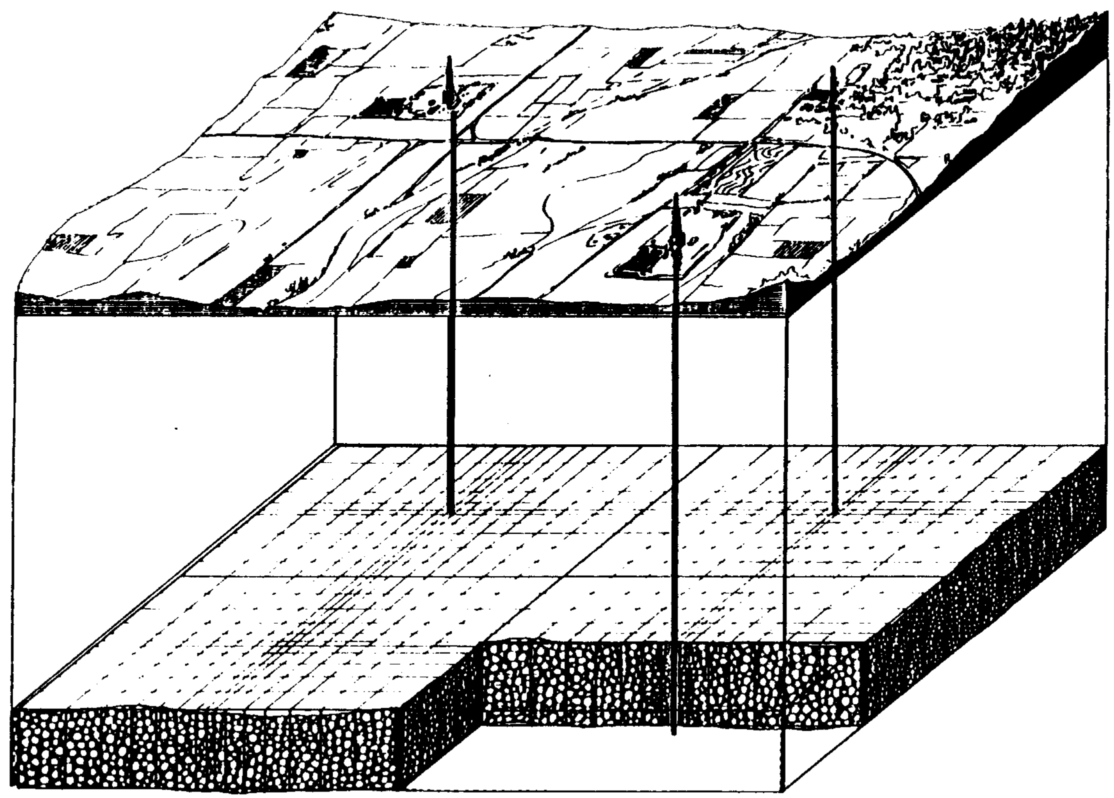

Fig. 7.16 DOE/CER Tight Gas Reservoir Model Grid System Used to Simulate Interference Testing of the Cozzette Sandstone at the MWX Site

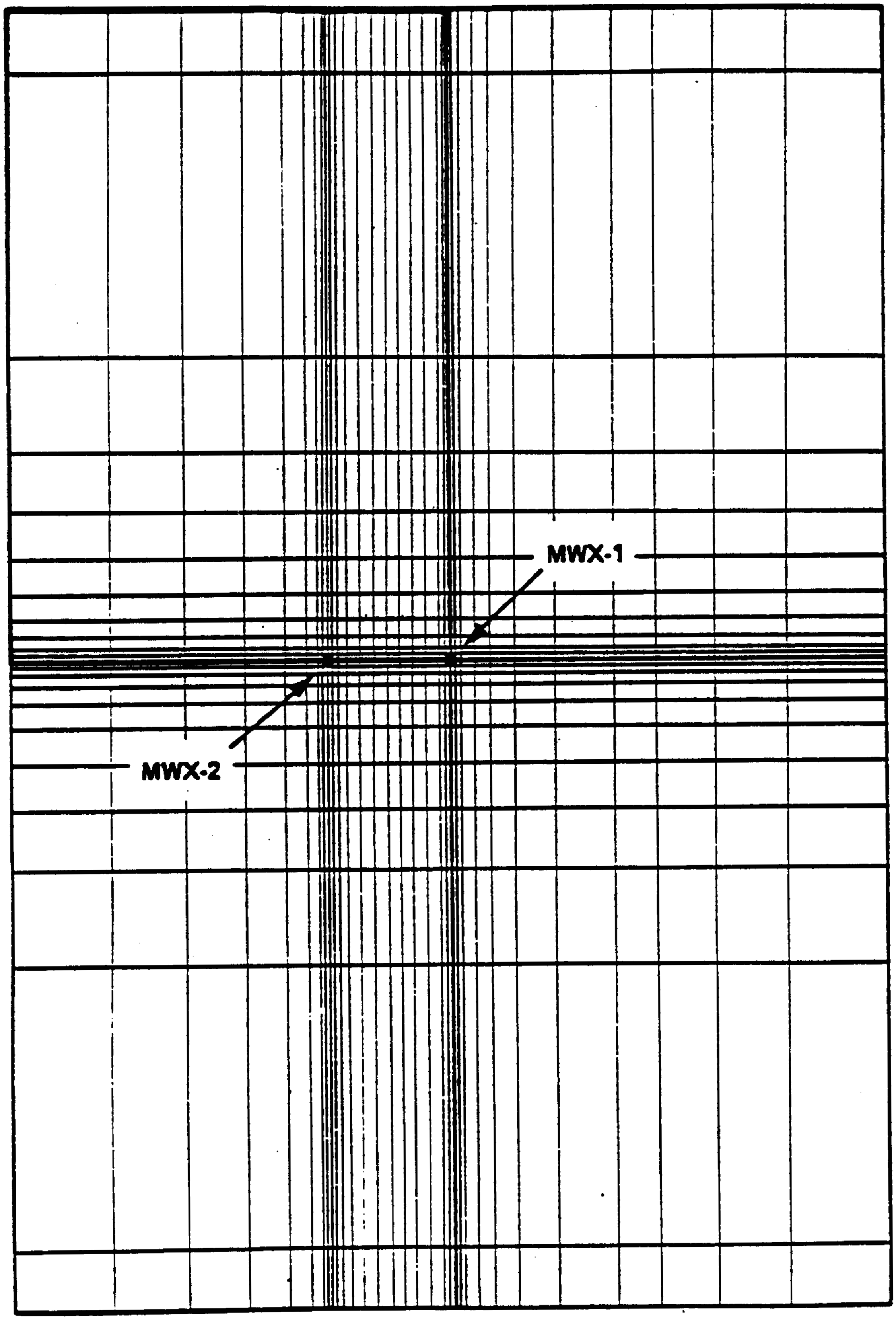

Fig. 7.17 Plan View of the Reservoir Model Grid Pattern Used to Analyze the Upper Cozzette Interference Well Testing

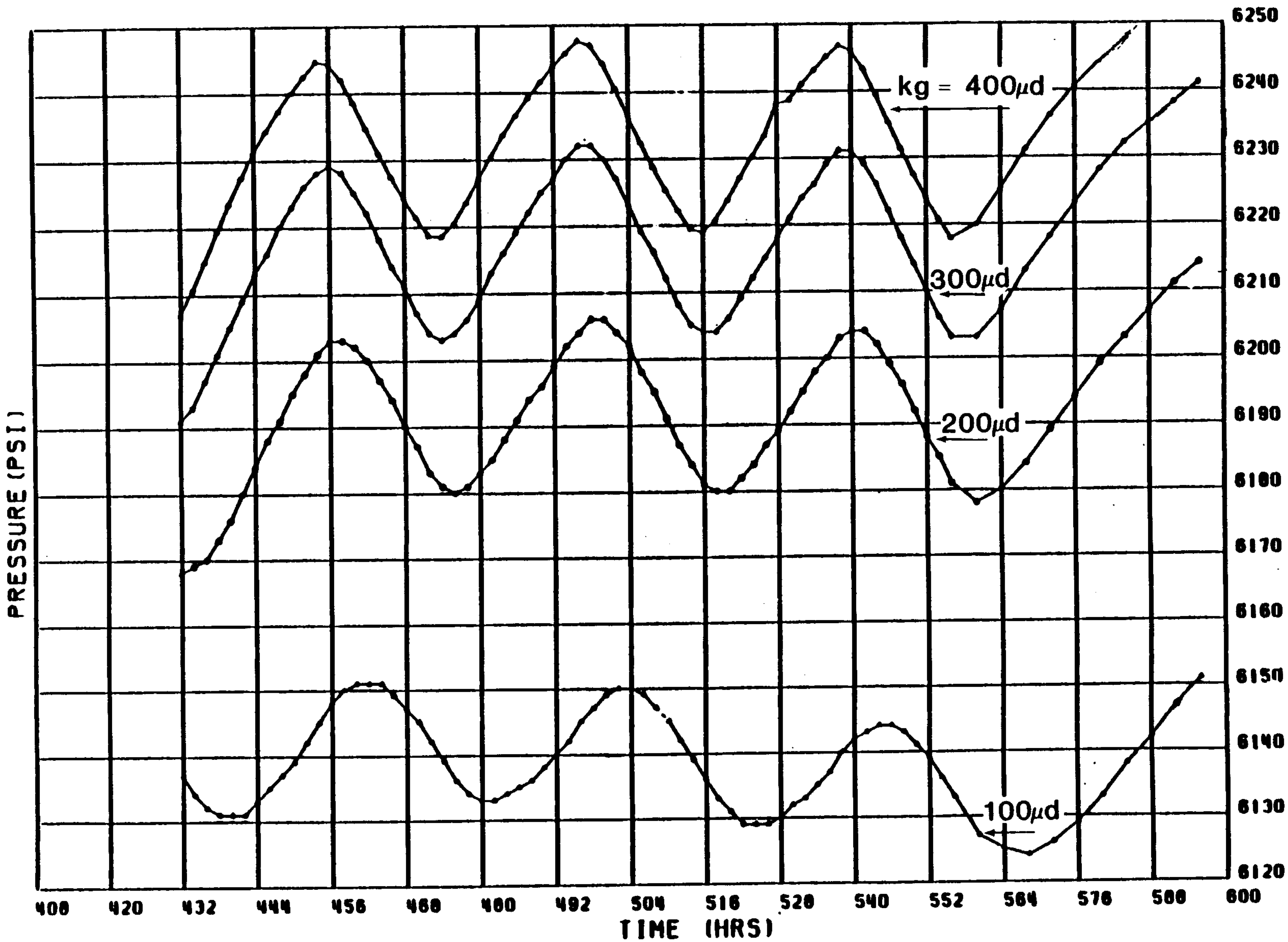

Fig. 7.18 Model Derived Pressure Histories for the Pulses Expected at the Observation Well, MWX-2, with Homogeneous Reservoirs of 100μd, 200μd, 300μd and 400μd

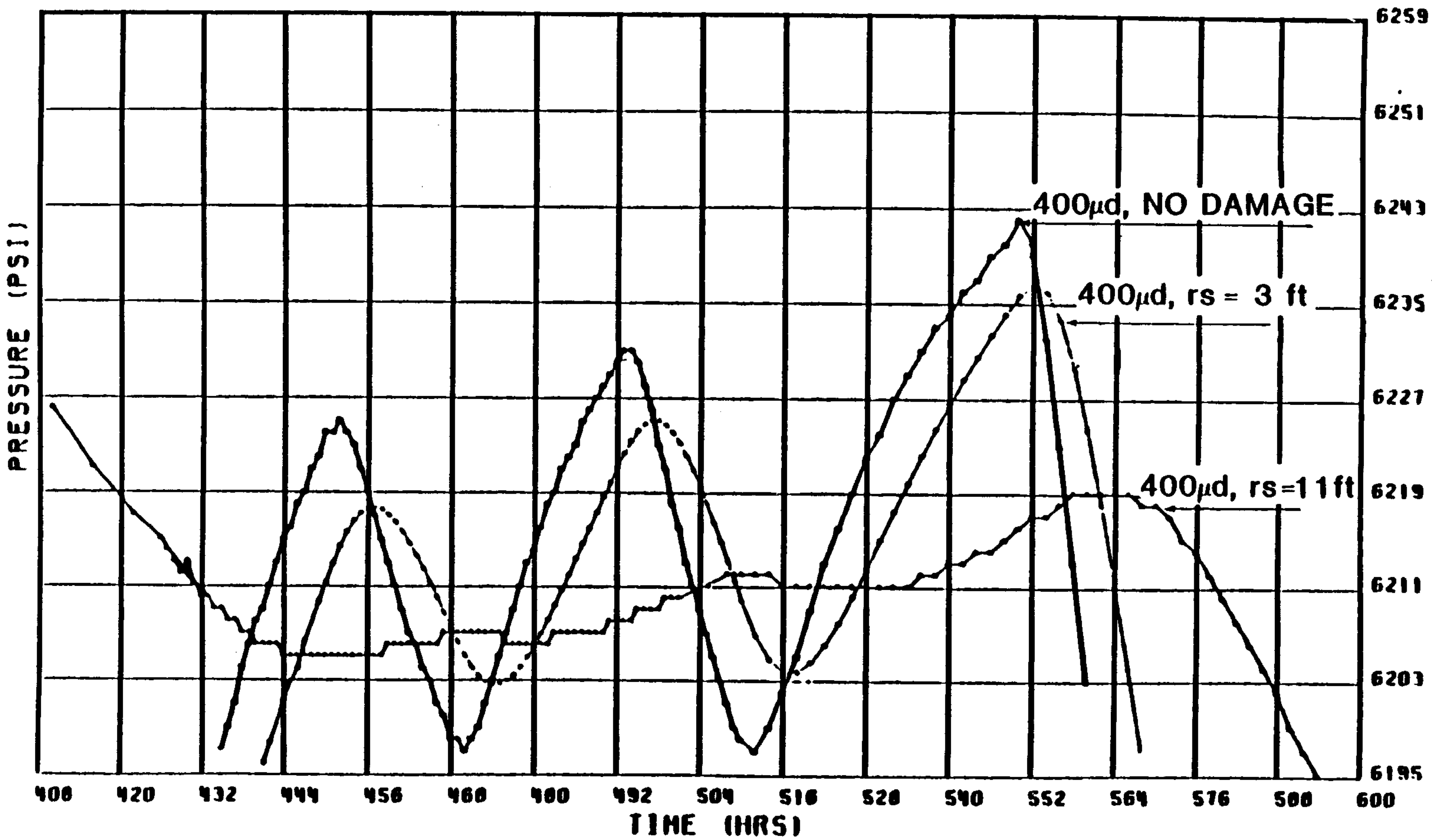

Fig. 7.19 Pressure Histories for a Homogeneous Reservoir Permeability of k=400μd, with a Reduction in Permeability to k=0.4μd, Around the Observation Well (the two cases are reduced permeability areas with radii of 3 and 11 ft)

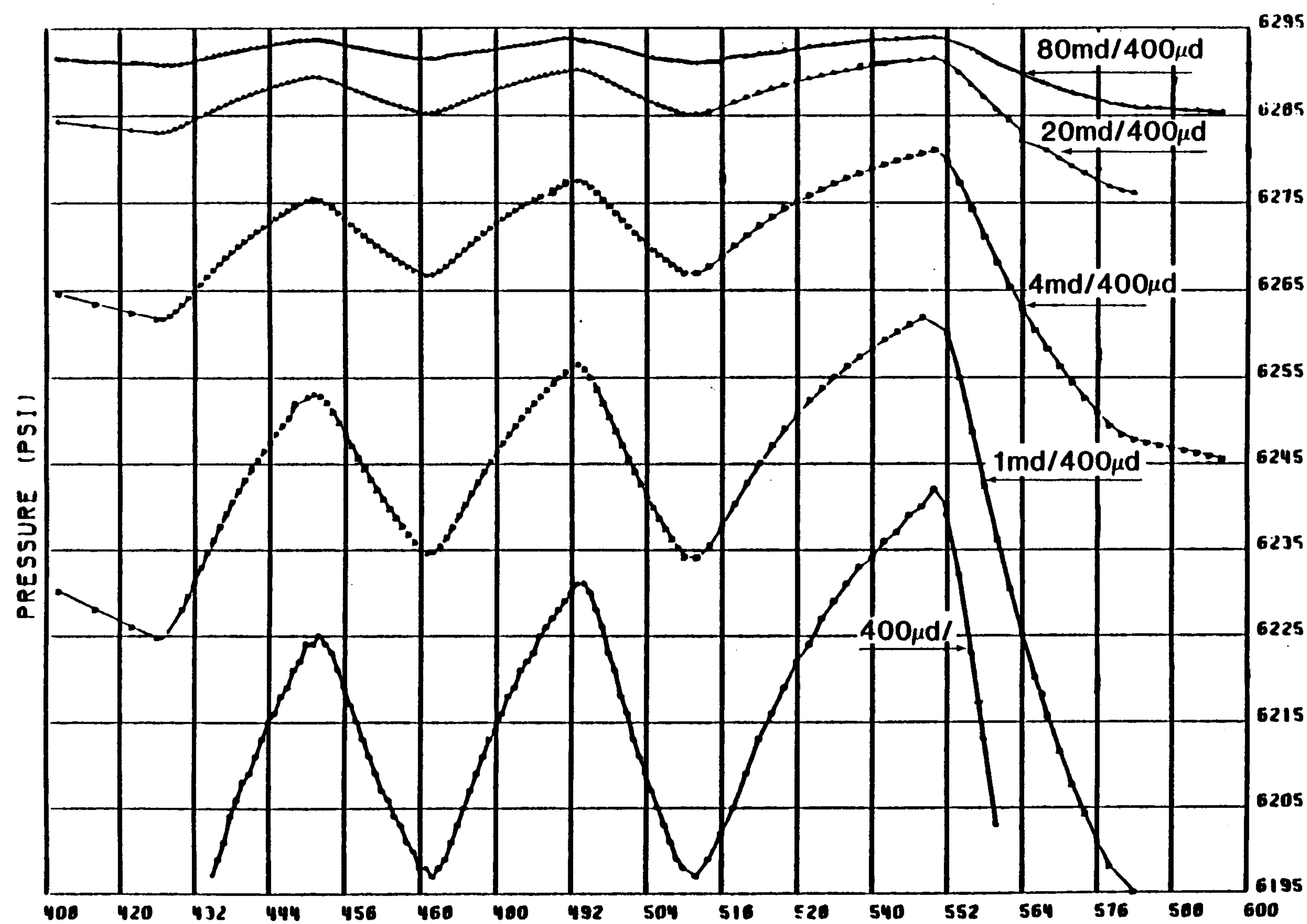

Fig. 7.20 Various TIGHTGAS Simulated Pressure Histories for Anisotropic Reservoir Permeabilities, 80md/400μd, 20md/400μd, 1md/400μd, and as a Reference, a Homogeneous Reservoir of 400μd

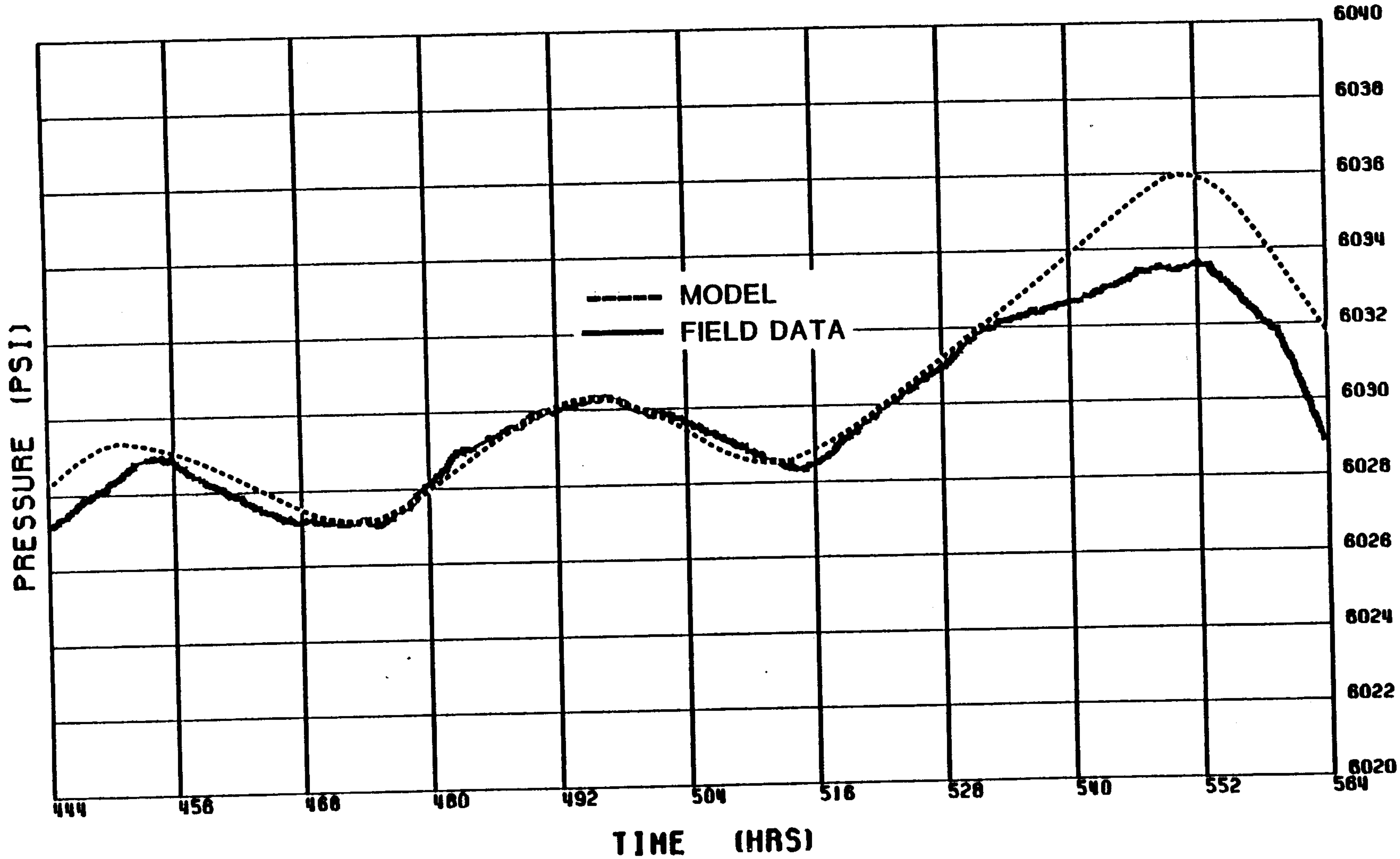

Fig. 7.21 Fractured Reservoir Model "SUGARMD" Pressure History Superimposed on the Field Data from the Observation Well, MWX-2, Using Anisotropic Fracture Permeabilities of 100md/0.1md, Along with 20 ft Matrix Blocks of 0.1μd

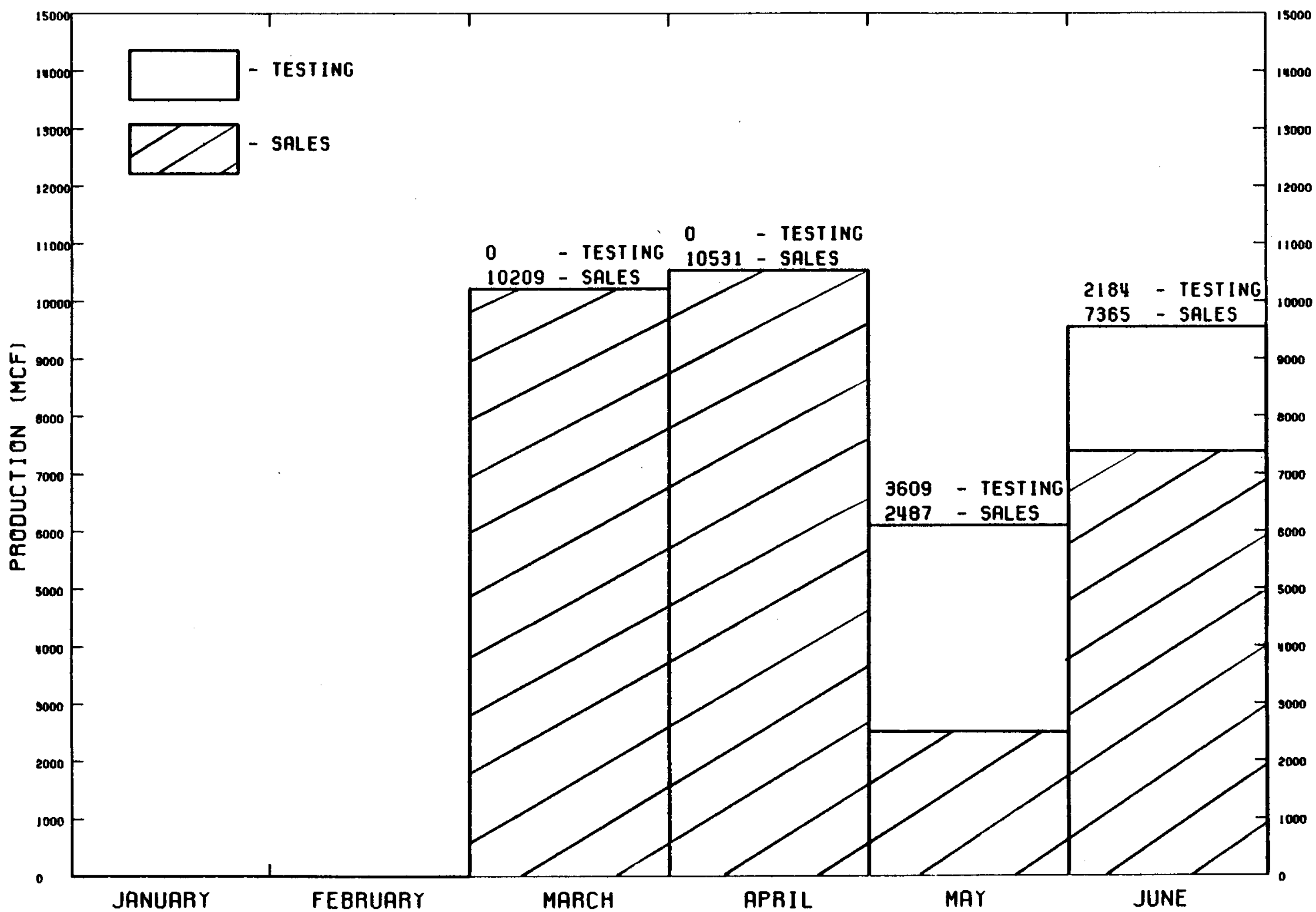

Fig. 7.22 Monthly Gas Production from the Upper Cozzette in MWX-1, Showing the Values for Pipeline Sales and Flared Testing Periods

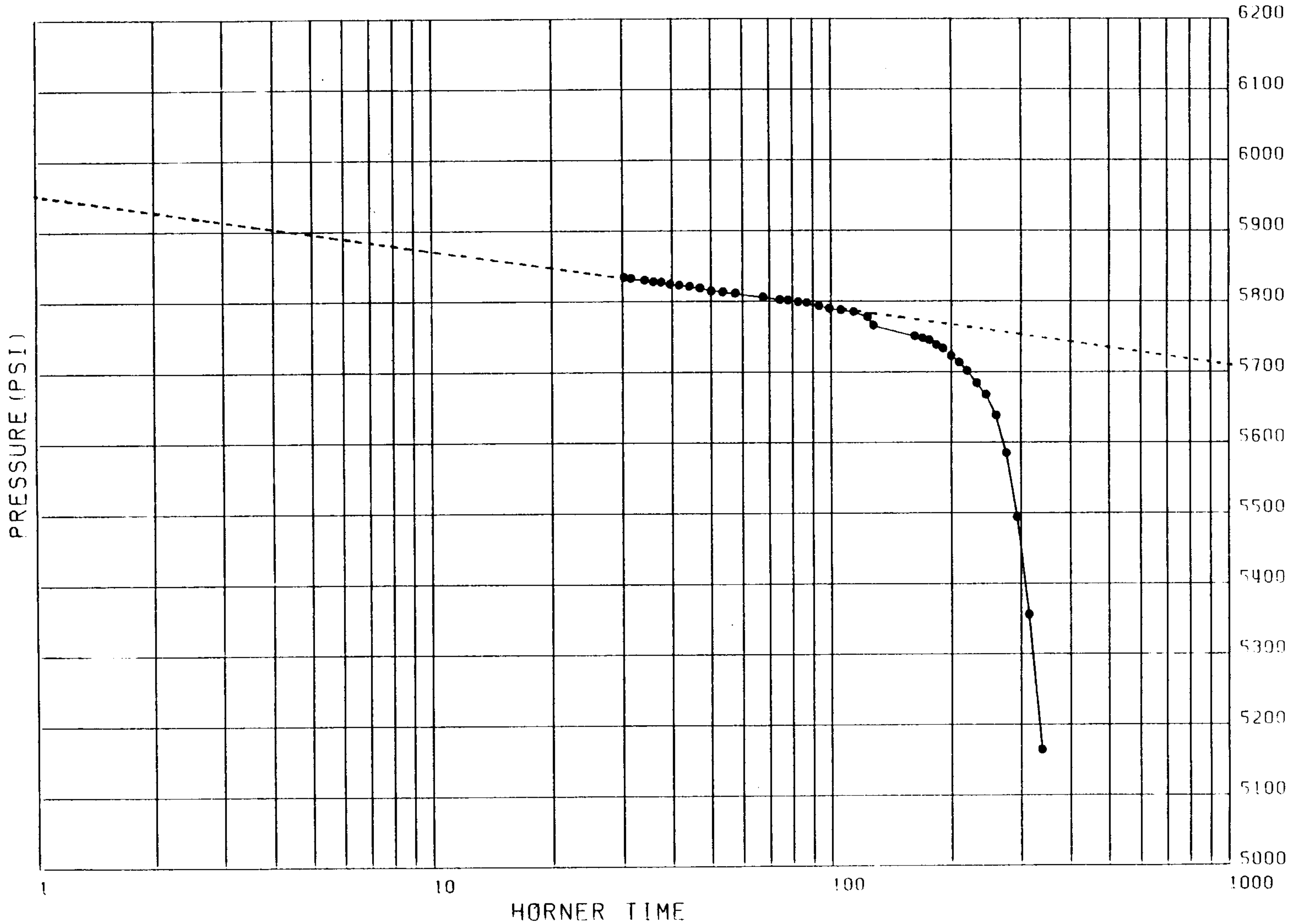

Fig. 7.23 Horner Plot from MWX-1 Bottomhole Pressure Buildup Data Gathered after a Sustained Period of Gas Pipeline Production, June 1983

8.0 BIBLIOGRAPHY

S. J. Finley
Sandia National Laboratories

The technical output from the Multiwell Experiment resides in an MWX Data File which is maintained in the project's office at Sandia National Laboratories in Albuquerque, NM.

The MWX Data File is intended to be "results-oriented." Thus, it includes such entries as (1) data reports from contractors and others, (2) memoranda, informal reports and compilations of results and analyses, (3) formal publications and reports, and (4) in some cases, planning documents, review meeting summaries, etc. It is not intended to include every sheet of paper ever written on MWX or every bit of data taken. In general, these are entries which are referenceable and which convey data.

The MWX Data File has the following overall organization:

1.0 Well data by well
1.1 Well logs by well and logging program; analyses
1.2 Core and fluid analyses by type and performer
1.3 Core-log correlation
1.4 Geology by topic
1.5 Environmental
1.6 Geophysics by type
1.7 Stress testing by interval
1.8 Well testing by interval
1.9 Stimulation and fracture diagnostics by interval
3.1 General reviews and status reports
3.3 Quarterly reports
3.5 Topical meetings, displays and workshops
3.7 Technical Review Panel
3.8 Plans

A computer-based index to the MWX Data File is also maintained in which each entry is indexed by accession number, data file number, author(s), title, company, date, alternate report number, key word(s), and comments/notes. Thus, searches, retrieval, and summaries of various types can be made readily. Two listings from this index are presented:

(A) A listing is given in this section of publications and formal reports which include information on the marine interval. (These are selected from the index through the key words "formal" and "marine.")

(B) A listing of the complete MWX Data File index data is given in Appendix 9.7 for those entries which contain results for the marine interval.

MARINE FORMAL REPORTS

****
ACCES NUM N00327
REPORT NUM 1.8.0.008
AUTHOR BRANAGAN,P
AUTHOR COTNER,G
AUTHOR LEE,SJ
AUTHOR WILMER,R
TITLE INTERFERENCE TESTING OF THE NATURALLY FRACTURED COZZETTE: A CASE STUDY AT THE DOE MWX SITE
CORP AUTH CER
DATE 840500
ALT NUMBER SPE12869
NOTES PRESENTED AT THE UNCONVENTIONAL GAS RECOVERY SYMPOSIUM IN PITTSBURGH, PA, MAY 13-15, 1984
****
ACCES NUM N00318
REPORT NUM 1.8.0.007
AUTHOR BRANAGAN,P
AUTHOR LEE,SJ
AUTHOR WILMER,R
TITLE WELL TESTING AND RESERVOIR EVALUATION (2.16)
CORP AUTH CER
DATE 831018
ALT NUMBER DOEMETC843
NOTES TECHNICAL PROCEEDINGS OF THE WESTERN GAS SANDS SUBPROGRAM REVIEW, MORGANTOWN, WV, OCTOBER 18-19, 1983
****
ACCES NUM N00301
REPORT NUM 1.4.2.012
AUTHOR EATOUGH,MO
TITLE MINERALOGIC AND PETROLOGIC OVERVIEW OF CORE SAMPLES FROM THE DEPT. OF ENERGY'S WESTERN GAS SANDS PROJECT MULTIWELL EXPERIMENT, PICEANCE BASIN, COLORADO
CORP AUTH BENDIX
DATE 830300
ALT NUMBER SPEDOE11764
NOTES THIS PAPER WAS PRESENTED AT THE 1983 SPE/DOE SYMPOSIUM ON LOW PERMEABILITY HELD IN DENVER, COLORADO, MARCH 14-16, 1983
****
ACCES NUM N00308
REPORT NUM 1.4.2.013
AUTHOR HEINZE,DM
TITLE MINERALOGY AND PETROLOGY ASPECTS OF THE MESAVERDE FORMATION AT RIFLE GAP, COLORADO, SPECIFIC TO THE SEDIMENTOLOGY AND GAS-BEARING INTERVALS IN THE SUBSURFACE
DATE 830300
ALT NUMBER SAND830287
****

ACCES NUM N00575
REPORT NUM 1.1.4.012
AUTHOR **KUKAL,GC**
TITLE *A SYSTEMATIC APPROACH FOR THE EFFECTIVE LOG ANALYSIS OF TIGHT GAS SANDS*
CORP AUTH CER
DATE 840500
ALT NUMBER SPEDOE12851
NOTES PRESENTED AT SPE/DOE/GRI UNCONVENTIONAL GAS RECOVERY SYMPOSIUM, MAY 13-15, 1984, PITTSBURGH PA

****

ACCES NUM N00576
REPORT NUM 1.1.4.013
AUTHOR **KUKAL,GC**
TITLE *LOG ANALYSIS IN LOW PERMEABILITY GAS SAND SEQUENCES - CORRECTING FOR VARIABLE UNFLUSHED GAS SATURATION*
CORP AUTH CER
DATE 830600
NOTES PRESENTED AT SPWLA 24TH ANNUAL LOGGING SYMPOSIUM, CALGARY ALBERTA, CANADA JUNE 27-30, 1983

****

ACCES NUM N00636
REPORT NUM 1.3.010
AUTHOR **KUKAL,GC**
AUTHOR **HILL,RE**
TITLE *LOG ANALYSIS OF CLAY VOLUME: AN EVALUATION OF TECHNIQUES AND ASSUMPTIONS USED IN AN UPPER CRETACEOUS SAND-SHALE SEQUENCE*
CORP AUTH CER
DATE 860000
NOTES TO BE PRESENTED AT THE 1986 SOCIETY OF PROF. WELL LOG ANALYSTS MEETING, HOUSTON, TEXAS

****

ACCES NUM N00574
REPORT NUM 1.1.4.011
AUTHOR **KUKAL,GC**
AUTHOR **SIMONS,KE**
TITLE *LOG ANALYSIS TECHNIQUES FOR QUANTIFYING THE PERMEABILITY OF SUB-MILLIDARCY SANDSTONE RESERVOIRS*
CORP AUTH CER
DATE 850500
ALT NUMBER SPEDOE13880
NOTES PRESENTED AT THE SPE/DOE 1985 LOW PERMEABILITY GAS RESERVOIR SYMPOSIUM DENVER, COLORADO, MAY 19-22 1985.

****

ACCES NUM N00160
REPORT NUM 1.6.2.002
AUTHOR **LEE,MW**
TITLE *VERTICAL SEISMIC PROFILES AT MULTI-WELL EXPERIMENT SITE, GARFIELD COUNTY, COLORADO*
CORP AUTH USGS
DATE 831100
ALT NUMBER USGS OPEN FILE REPORT 84-168

****
ACCES NUM N00294
REPORT NUM 1.4.3.033
AUTHOR **LORENZ,JC**
TITLE *SEDIMENTOLOGY OF THE MESAVERDE FORMATION AT RIFLE GAP, COLORADO AND IMPLICATIONS FOR GAS-BEARING INTERVALS IN THE SUBSURFACE*
DATE 820300
ALT NUMBER SAND820604
****
ACCES NUM N00298
REPORT NUM 1.4.3.036
AUTHOR **LORENZ,JC**
TITLE *LATERAL VARIABILITY IN THE CORCORAN AND COZZETTE BLANKET SANDSTONES AND ASSOCIATED MESAVERDE ROCKS, PICEANCE CREEK BASIN, NORTHWESTERN COLORADO*
CORP AUTH SAND
DATE 830300
ALT NUMBER SPEDOE11608
NOTES THIS PAPER WAS PRESENTED AT THE 1983 SPE/DOE SYMPOSIUM ON LOW PERMEABILITY HELD IN DENVER, COLORADO, MARCH 14-16, 1983
****
ACCES NUM N00309
REPORT NUM 1.4.3.037
AUTHOR **LORENZ,JC**
TITLE *RESERVOIR SEDIMENTOLOGY IN MESAVERDE ROCKS AT THE MULTI-WELL EXPERIMENT SITE*
DATE 830600
ALT NUMBER SAND83-1078
****
ACCES NUM N00671
REPORT NUM 1.4.5.013
AUTHOR **LORENZ,JC**
AUTHOR **BRANAGAN,P**
AUTHOR **WARPINSKI,NR**
AUTHOR **SATTLER,AR**
TITLE *FRACTURE CHARACTERISTICS AND RESERVOIR BEHAVIOR OF STRESS-SENSITIVE FRACTURE SYSTEMS IN FLAT-LYING LENTICULAR FORMATIONS*
CORP AUTH SAND
CORP AUTH CER
DATE 860518
ALT NUMBER SPE 15244
NOTES PRESENTED AT THE UNCONVENTIONAL GAS TECHNOLOGY SYMPOSIUM OF THE SOCIETY OF PETROLEUM ENGINEERS, LOUISVILLE, KY, MAY 18-21,1986
****
ACCES NUM N00328
REPORT NUM 1.2.55.005
AUTHOR **MORROW,NR**
TITLE *RELATIONSHIP OF PORE STRUCTURE TO FLUID BEHAVIOR IN LOW PERMEABILITY GAS SANDS*
CORP AUTH NMPRRC
DATE 840500
ALT NUMBER NMERDI2703303

****
ACCES NUM N00705
REPORT NUM 1.2.55.012
AUTHOR MORROW,NR
TITLE RELATIONSHIP OF PORE STRUCTURE TO FLUID BEHAVIOR IN LOW PERMEABILITY GAS SANDS: YEAR THREE
CORP AUTH NMPRRC
DATE 850200
ALT NUMBER NMERDI 2-72-4309
****
ACCES NUM N00447
REPORT NUM 1.2.55.004
AUTHOR MORROW,NR
AUTHOR BROWER,KR
AUTHOR KILMER,NH
TITLE RELATIONSHIP OF PORE STRUCTURE TO FLUID BEHAVIOR IN LOW PERMEABILITY GAS SANDS
CORP AUTH NMPRRC
DATE 820000
ALT NUMBER DOE BC 10216-14
****
ACCES NUM N00704
REPORT NUM 1.2.55.011
AUTHOR MORROW,NR
AUTHOR BROWER,KR
AUTHOR KILMER,NH
TITLE RELATIONSHIP OF PORE STRUCTURE TO FLUID BEHAVIOR IN LOW PERMEABILITY GAS SANDS, 1984 FINAL REPORT
CORP AUTH NMPRRC
DATE 840900
ALT NUMBER DOEBC10216-13
****
ACCES NUM N00669
REPORT NUM 1.2.55.009
AUTHOR MORROW,NR
AUTHOR WARD,J
AUTHOR BROWER,KR
TITLE ROCK MATRIX AND FRACTURE ANALYSIS OF FLOW IN TIGHT GAS SANDS, 1985 ANNUAL REPORT
CORP AUTH NMPRRC
DATE 860200
ALT NUMBER DOEMC21179-2032
****
ACCES NUM N00300
REPORT NUM 1.2.12.020
AUTHOR RANDOLPH,PL
TITLE POROSITY AND PERMEABILITY OF MESAVERDE SANDSTONE CORE FROM THE U.S. DOE MULTIWELL EXPERIMENT, GARFIELD COUNTRY, COLORADO
CORP AUTH IGT
DATE 830300
ALT NUMBER SPEDOE11765
NOTES THIS PAPER WAS PRESENTED AT THE 1983 SPE/DOE SYMPOSIUM ON LOW PERMEABILITY HELD IN DENVER, COLORADO, MARCH 14-16, 1983

****
ACCES NUM   N00326
REPORT NUM 1.2.12.021
AUTHOR   RANDOLPH,PL
AUTHOR   SOEDER,DJ
AUTHOR   CHOWDIAH,P
TITLE   POROSITY AND PERMEABILITY OF TIGHT SANDS
CORP AUTH   IGT
DATE   840513
ALT NUMBER SPEDOEGRI12836
NOTES   PRESENTED AT THE 1984 SPE/DOE/GRI UNCONVENTIONAL GAS RECOVERY SYMPOSIUM, PITTSBURGH, PENNSYLVANIA, MAY 13-15, 1984
****
ACCES NUM   N00572
REPORT NUM 1.6.4.002
AUTHOR   SEARLS,CA
TITLE   THE MULTIWELL EXPERIMENT GEOPHYSICS PROGRAM FINAL REPORT
CORP AUTH   SAND
DATE   850900
ALT NUMBER SAND 85-1013
****
ACCES NUM   N00297
REPORT NUM 1.6.4.003
AUTHOR   SEARLS,CA
AUTHOR   LEE,MW
AUTHOR   MILLER,JJ
AUTHOR   ALBRIGHT,JN
AUTHOR   FRIED,J
AUTHOR   APPLEGATE,JK
TITLE   A COORDINATED SEISMIC STUDY OF THE MULTI-WELL EXPERIMENT SITE
CORP AUTH   SAND
CORP AUTH   USGS
CORP AUTH   LANL
CORP AUTH   CSM
DATE   830300
ALT NUMBER SPEDOE11613
NOTES   THIS PAPER WAS PRESENTED AT THE 1983 SPE/DOE SYMPOSIUM ON LOW PERMEABILITY HELD IN DENVER, COLORADO, MARCH 14-16, 1983
****
ACCES NUM   N00329
REPORT NUM 1.2.12.022
AUTHOR   SOEDER,DJ
AUTHOR   RANDOLPH,PL
TITLE   POROSITY, PERMEABILITY AND PORE STRUCTURE OF THE TIGHT MESA VERDE SANDSTONE, PICEANCE BASIN, COLORADO
CORP AUTH   IGT
DATE   840916
ALT NUMBER SPE13134
NOTES   PRESENTED AT THE 59TH ANNUAL TECHNICAL CONFERENCE AND EXHIBITION HELD IN HOUSTON, TEXAS, SEPTEMBER 16-19, 1984

****
ACCES NUM   N00474
REPORT NUM 1.4.5.003
AUTHOR **SPENCER,CW**
AUTHOR **KEIGHIN,CW**
TITLE *GEOLOGIC STUDIES IN SUPPORT OF THE U.S. DOE'S MULTI-WELL EXPERIMENT,GARFIELD COUNTY, COLORADO.*
CORP AUTH   USGS
DATE   841100
ALT NUMBER OFR 84757
NOTES   SUMMARY OF USGS WORK ON MWX
****
ACCES NUM   N00513
REPORT NUM 1.9.5.004
AUTHOR **TEUFEL,LW**
AUTHOR **HART,CM**
AUTHOR **SATTLER,AR**
AUTHOR **CLARK,JA**
TITLE *DETERMINATION OF HYDRAULIC FRACTURE AZIMUTH BY GEOPHYSICAL, GEOLOGICAL, AND ORIENTED CORE METHODS AT THE MULTI-WELL EXPERIMENT SITE, RIFLE, CO.*
CORP AUTH   SAND
DATE   840916
ALT NUMBER SPE 13226
NOTES   PRESENTED AT THE 59TH ANNUAL SPE MEETING HOUSTON TX, SEPTEMBER,1984
****
ACCES NUM   N00269
REPORT NUM 1.7.0.006
AUTHOR **TEUFEL,LW**
AUTHOR **WARPINSKI,NR**
TITLE *DETERMINATION OF IN SITU STRESS FROM ANELASTIC STRAIN RECOVERY MEASUREMENTS OF ORIENTED CORE: COMPARISON TO HYDRAULIC FRACTURE STRESS MEASUREMENTS IN THE ROLLINS SANDSTONE, PICEANCE BASIN, COLORADO*
CORP AUTH   SAND
DATE   840600
ALT NUMBER SAND840512C
NOTES   PRESENTED AT THE 25TH U.S. SYMPOSIUM ON ROCK MECHANICS, EVANSTON,ILL. JUNE 25-27,1984.
****
ACCES NUM   N00271
REPORT NUM 1.7.0.007
AUTHOR **WARPINSKI,NR**
TITLE *INVESTIGATION OF THE ACCURACY AND RELIABILITY OF IN SITU STRESS MEASUREMENTS USING HYDRAULIC FRACTURING IN PERFORATED CASED HOLES*
CORP AUTH   SAND
DATE   830600
NOTES   24TH US SYMPOSIUM ON ROCK MECHANICS, JUNE 1983
****

ACCES NUM   N00649
REPORT NUM 1.4.5.012
AUTHOR   **WARPINSKI,NR**
TITLE   *ELASTIC AND VISCOELASTIC MODEL OF THE STRESS HISTORY OF SEDIMENTARY ROCKS*
CORP AUTH   SAND
DATE   860400
ALT NUMBER SAND86-0238
****
ACCES NUM   N00701
REPORT NUM 1.7.5.001
AUTHOR   **WARPINSKI,NR**
TITLE   *ELASTIC AND VISCOELASTIC CALCULATIONS OF STRESSES IN SEDIMENTARY BASINS*
CORP AUTH   SAND
DATE   860518
ALT NUMBER SPE 15243
NOTES   PRESENTED AT THE UNCONVENTIONAL GAS TECHNOLOGY SYMPOSIUM OF THE SOCIETY OF PETROLEUM ENGINEERS HELD IN LOUISVILLE, KY, MAY 18-21,1986
****
ACCES NUM   N00267
REPORT NUM 1.7.0.004
AUTHOR   **WARPINSKI,NR**
AUTHOR   **BRANAGAN,P**
AUTHOR   **WILMER,R**
TITLE   *IN SITU STRESS MEASUREMENTS AT DOE'S MULTI-WELL EXPERIMENT*
CORP AUTH   CER
CORP AUTH   SAND
DATE   840100
NOTES   WESTERN GAS SANDS SUBPROGRAM REVIEW TECHNICAL PROCEEDINGS DOE/METC/84-3, JANUARY 1984
****
ACCES NUM   N00311
REPORT NUM 1.7.0.008
AUTHOR   **WARPINSKI,NR**
AUTHOR   **BRANAGAN,P**
AUTHOR   **WILMER,R**
TITLE   *IN-SITU STRESS MEASUREMENTS AT DOE'S MULTIWELL EXPERIMENT SITE, MESAVERDE GROUP, RIFLE, COLORADO*
CORP AUTH   CER
CORP AUTH   SAND
DATE   831005
ALT NUMBER SPE12142
NOTES   PRESENTED AT THE 58TH ANNUAL TECHNICAL CONFERENCE AND EXHIBITION HELD IN SAN FRANCISCO, CA, OCTOBER 5-8, 1983.

INTENTIONALLY LEFT BLANK

DISTRIBUTION:

M. J. Singer
Deputy Assistant Secretary for Oil, Gas,
Shale, and Special Technologies
US Department of Energy
D-119, FE-30 (GTN)
Washington, DC 20545

D. B. Uthus
Office of Oil, Gas and Shale Technologies
US Department of Energy
D-122, FE-33 (GTN)
Washington, DC 20545

J. R. White
Office of Oil, Gas and Shale Technologies
US Department of Energy
D-129 FE-33 (GTN)
Washington, DC 20545

US Department of Energy (7)
Morgantown Energy Technology Center
Box 880 Collins Ferry Road
Morgantown, WV 26505
Attn: A. A. Pitrolo
C. A. Komar
K-H. Frohne (3)
A. Layne
J. K. Westhusing

US Department of Energy (2)
Bartlesville Project Office
PO Box 1398
Bartlesville, OK 74005
Attn: R. Folstein
A. Crawley

F. Heuze
Lawrence Livermore National Laboratory
MS L200
Livermore, CA 94550

J. A. Albright
Earth & Space Science Division
ESS-4
Los Alamos National Laboratory
Los Alamos, NM 87545

US Geological Survey (2)
Box 25046
Denver Federal Center
Denver, CO 80225
Attn: B. E. Law, MS 971
C. W. Spencer, MS 940

CER Corporation (30)
PO Box 15090
Las Vegas, NV 89114
Attn: R. L. Mann (25)
F. R. Myal
P. T. Branagan
G. C. Kukal
W. H. Mathis
C. Cipolla

L. F. Elkins
3412 N. Preston
Oklahoma City, OK 71322

J. L. Fitch
6034 Walnut Hill Circle
Dallas, TX 75230

T. Kirst
Mobil Oil Corp.
25737 Foothills Drive North
Golden, CO 80401

F. G. Martin
907 Glendell Drive
Irving, TX 75061

D. E. Nierode
Exxon Production Research Co.
PO Box 2189
Houston, TX 77001

R. J. Saucier
Shell Western E&P
Suite No. 7560
PO Box 576
Houston, TX 77001

Mobil Research and Development Corp. (3)
PO Box 819047
Dallas, TX 75381
Attn: M. Strubhar
L. Medlin
E. Sprunt

R. W. Veatch
Amoco Production Co.
Research Department
PO Box 3385
Tulsa, OK 74102

R. Veghte
Chandler & Associates
Suite 1400
1860 Lincoln Street
Denver, CO 80203

National Institute for Petroleum and Energy Research (3)
PO Box 2128
Bartlesville, OK 74005
Attn: H. B. Carroll
C. J. Raible
B. L. Gall

Smith Energy Services (2)
R. D. Timberline Building
Junction Hwys 58 & 93
Golden, CO 80403
Attn: D. Holcomb
W. Holcomb

L. Harrington
The Western Company
PO Box 186
Fort Worth, TX 76101

J. Elbel
Dowell-Schlumberger Research Center
PO Box 2710
Tulsa, OK 74101

J. McLennan
Dowell-Schlumberger
PO Box 5818
Denver, CO 80217

M. Conway
Halliburton Services
PO Box 1431
Duncan, OK 73536-0426

M. Brugler
Core Laboratories, Inc.
7304 E 38th Street
Tulsa, OK 74145

Core Laboratories, Inc. (2)
10703 E. Bethany Drive
Aurora, CO 80014
Attn: S. Leeds
H. Hunt

R. E. Jenkins
Core Laboratories, Inc.
7501 Stemmons Freeway
Box 47547
Dallas, TX 75247

P. Senseny
RE/SPEC, INC.
PO Box 725
Rapid City, SD 57701

L. Fukui
United Nuclear Services
PO Box 1569
Grand Junction, CO 81501

Institute of Gas Technology (2)
3424 S. State Street
Chicago, IL 60616
Attn: P. L. Randolph
D. J. Soeder

Petroleum Recovery Research Center (2)
NM Institute of Mining and Technology
Socorro, NM 87801
Attn: J. J. Taber
N. R. Morrow

J. Walls
Dallas Petrophysics Laboratory
Core Laboratories, Inc.
1300 East Rochelle Bvld.
Irving, TX 75062

R. A. Plumb
Schlumberger-Doll Research
Old Quarry Road
PO Box 307
Ridgefield, CT 06877

R. Kry
Esso Resources Canada Limited
Research Department
339 50th Avenue SE
Calgary, Alberta T2G 2B3
CANADA

Union Oil Company of California
Research Department (2)
PO Box 76
Brea, CA 92621
Attn: C. Allen
J. Smith

K. Hansen
Shell Development Co.
Bellaire Research Center
PO Box 481
Houston, TX 77001

C. Ossian
ARCO Oil & Gas
PRC G118
Research & Technical Services
2300 West Plano Parkway
Plano, TX 75075

R. Wright
Department of Geology
University of New Mexico
Albuquerque, NM 87131

J. Johnson
Department of Geology
Mesa College
Grand Junction, CO 81501

B. Kelso
Colorado Geological Survey
Department of Natural Resources
1313 Sherman Street, Rm 715
Denver, CO 80203

R. Hunter
Bureau of Land Management
Horizon Drive
Grand Junction, CO 81505

W. Hansen
Amoco Production Co.
1670 Broadway
Denver, CO 80202

M. Krey
133 N. 8th Street
Grand Junction, CO 81505

R. B. Chancellor
Rio Blanco Natural Gas Company
621 17th Street
Suite 1255
Denver, CO 80293

W. J. Barrett
Barrett Energy Company
1125 17th Street, Suite 2100
Denver, CO 80202

R. Martin
Coors Energy Company
PO Box 467
Golden, CO 80402

J. N. Burkhalter
Burkhalter Engineering Inc.
715 Horizon Drive
Suite 330
Grand Junction, CO 81506

W. H. Pease, Jr.
Willard Pease Oil and Gas Company
PO Box 1874
Grand Junction, CO 81502

B. L. Sampson
Coseka Resources (USA) Ltd.
200 Writer Square
1512 Larimer Street
Denver, CO 80202-1602

D. O. Cox
Angus Petrotech Corp.
14062 Denver West Parkway
Suite 200
Golden, CO 80401

Gas Research Institute (3)
8600 West Bryn Mawr Avenue
Chicago, IL 60631
Attn: P. A. O'Shea
I. A. Salehi
C. F. Brandenberg

S. A. Holditch
S. A. Holditch and Assoc. Inc.
Suite 200, 3833 Texas Avenue
Bryan, TX 77801

T. Logan
Resource Enterprises, Inc.
743 Horizon Court, Suite 203
Grand Junction, CO 81506

J. Schwoebel
Resource Enterprises, Inc.
400 Wakara Way
Salt Lake, City, UT 84108

A. Jones
Terra Tek, Inc.
420 Wakara Way
Salt Lake City, UT 84108

Colorado Oil & Gas Commission
1580 Logan Street, Suite 380
Denver, CO 80203

Petroleum Information Services
PO Box 2610
Denver, CO 80201-2612

1540	W. C. Luth
1542	W. R. Wawersik
1542	L. W. Teufel
6000	D. L. Hartley
6200	V. L. Dugan
6201	D. Engi
6240	R. K. Traeger
6242	J. C. Dunn
6250	B. W. Marshall
6253	D. A. Northrop (30)
6253	S. J. Finley
6253	J. C. Lorenz (5)
6253	A. R. Sattler (5)
6253	N. R. Warpinski (5)
6253	MWX File
6254	B. Granoff
6257	J. K. Linn
6257	C. A. Searls
6258	P. J. Hommert
8024	P. W. Dean
3141	D. K. Brown (5)
3151	W. L. Garner (3)
3154-1	C. H. Dalin for DOE/OSTI (28)